THE UNIVERSITY OF HULL

Development of an electro-kinetically driven integrated DNA profile separation and detection system

being a Thesis submitted for the Degree of

Doctor of Philosophy

in the University of Hull

by

Jennifer Ann Oakley M.Chem

July 2010

ABSTRACT

Described in current literature is the methodology of different aspects of creating a DNA profile which has been successfully performed within a micro-fluidic environment; however integration of each of the different procedures onto a single device has not been documented. This thesis presents briefly the application of a gel supported reagent matrix to aid in the integration of DNA extraction, PCR amplification, and the injection, separation and detection of a DNA sample onto one single micro-fluidic device. The gel supported system was designed to provide greater stability to the reagents during the analysis process and also during long periods of dormancy, enabling the mass production of one use micro-fluidic device, encapsulating all required reagents at time of manufacturing.

Described is the application of electro-osmotic pumping through a gel supported reagent matrix, where a silica monolith was used to support both the electro-osmotic pumping mechanism and the extraction of DNA from cellular debris. The gel supported system also enabled the delivery of a precise and accurate sample plug by an electro-kinetic pinched injection across a gel-to-gel interface, contributing to the improvement and optimisation of the separation of the DNA by capillary electrophoresis. The approach taken in this thesis and the results documented suggest several advantages of integration, including simplification of instrumentation with no need for moving parts and reduction of macro to micro interfacing and power requirements.

ACKNOWLEDGEMENTS

The author would like to acknowledge the help and guidance provided by her supervisors Professor Gillian M. Greenway and Professor Stephen J. Haswell. In addition, the author would like to acknowledge the support and assistance of Professor John Greenman, Doctor Charlotte Dyer, Doctor Antony Walmsley, Doctor Howard V. Snelling and Doctor Abigail Webster. Finally, the author would like to thank her family and friends for supporting her during the undertaking of this work.

DECLARATION

The work documented in this thesis was carried out in the Department of Chemistry, University of Hull, under the supervision of Professor Gillian M. Greenway and Professor Stephen J. Haswell between July 2006 and July 2009. Except where indicated, this work is original and has not been submitted for any other degree.

PUBLICATIONS AND CONFERENCE PAPERS

Oakley, J. *et al. Development of a gel to gel electro-kinetic pinched injection method for an integrated micro-fluidic based DNA analyser,* Analytica Chimica Acta, 2009, 652(1-2), 239-244.

Oakley, J. *et al. A gel based integrated device for DNA profiling*. Analytical Research Forum, Kent, 2009.

Oakley, J. *et al. Development of a bi-functional silica monolith for electro-osmotic pumping and DNA clean-up/extraction using gel-supported reagents in a microfluidic device*, Lab on a Chip, 2009, 9, 1596-1600.

Shaw, K. Oakley, J. et al. Micro TAS, San Diego, 2008.

Oakley, J. *et al. An Integrated Separation And Detection System For On-Chip DNA Analysis Of Forensic Samples.* MicroScale Bioseparations, Methods for Systems Biology, Berlin, 2008.

Oakley, J. *et al. Integrated sample preparation and separation for on-chip DNA analysis of forensic samples.* Analytical Research Forum, Glasgow, 2007.

CONTENTS

ABBREVIATIONS and ACRONYMS

AC	Alternating current
ACM	Asymmetric capitance modulation
APS	Ammonium persulphate
ATR	Attenuated total reflection
BSA	Bovine serum albumin
CAD	Computer assisted data
CAE	Capillary array electrophoresis
CCD	Charged coupled device
CE	Capillary electrophoresis
CEC	Capillary electro chromatography
CGE	Capillary gel electrophoresis
DC	Direct current
DCM	Dichloromethane
DEP	Dielectrophoresis
DHA	Dihexyl acrylamide
DNA	Deoxyribose nucleic acid
dNTP's	Deoxyribonucleotide triphosphates
dsDNA	double stranded DNA
EC	Electrochemical
EDTA	Ethylenediaminetetraacetic acid
EDTA	Ethylenediaminetetra-acetate
EK	Electrokinetic
EOF	Electro-osmotic flow
EOP	Electro-osmotic pumping
EtOH	Ethanol

FASS	Field amplified sample stacking
FSS	Forensic Science Service
FT	Fourier transformation
HEC	Hydroxy ethyl cellulose
HF	High frequency
HPC	Hydroxypropylcellulose
HPLC	High performance liquid chromatography
HPMC	Hydroxypropylmethylcellulose
IR	Infra red
ITP	Isotachophoresis
LCW	Liquid core waveguide
LED	Light emitting diode
LIF	Laser induced fluorescence
LPA	Linear poly acrylamide
LUM	Lower upper middle
MDD	Magneto hydrodynamic
NIR	Near Infra red
PAM	Polyacrylamide
PCR	Polymerase chain reaction
PDMA	Polydimethylacrylamide
PDMS	Poly(dimethylsiloxane)
PEO	Poly(ethylene) oxide
PEO	Polyethylene oxide
PMMA	Poly(methyl methacrylate)
PNIPAM	Poly (N-isopropylarylamide
PRESS	Predicted error sum of squares
RNA	Ribonucleic acid

RSD	Relative standard deviation
SDS	Sodium dodecyl sulphate
SGM	Second generation multiplex
ssDNA	single stranded DNA
STRs	Short tandem repeats
TBE	Tris(hydroxymethyl) aninomethane base, boric acid and EDTA
TE	Tris EDTA
TEMED	N,N,N',N'- tetramethylyene-diamine
TIR	Total internal reflection
TMAPS	Trimethylammoniopropane sulfonate
Tris	Tris(hydroxymethyl) aminomethane
UV	Ultra violet
VNTRs	Variable number tandem repeats

Chapter 1: Introduction

1 Aim

The aim of this chapter is to provide a comprehensive introduction to the concepts and ideas investigated throughout this thesis, including an extensive review of the latest literature relevant to these topics.

1.1 At 'scene of crime' DNA analysis – A larger project

The global aim of the project, as stated in the original brief was as follows;

> *"To develop a portable integrated DNA processing/analysis instrument for 'at scene of crime' use with remote operational capability."*

The research was to focus on system design and the optimisation of DNA extraction, PCR amplification, and separation and characterisation based on micro fluidic and lab-on-a-chip technology.

1.1.1 The project at a glance

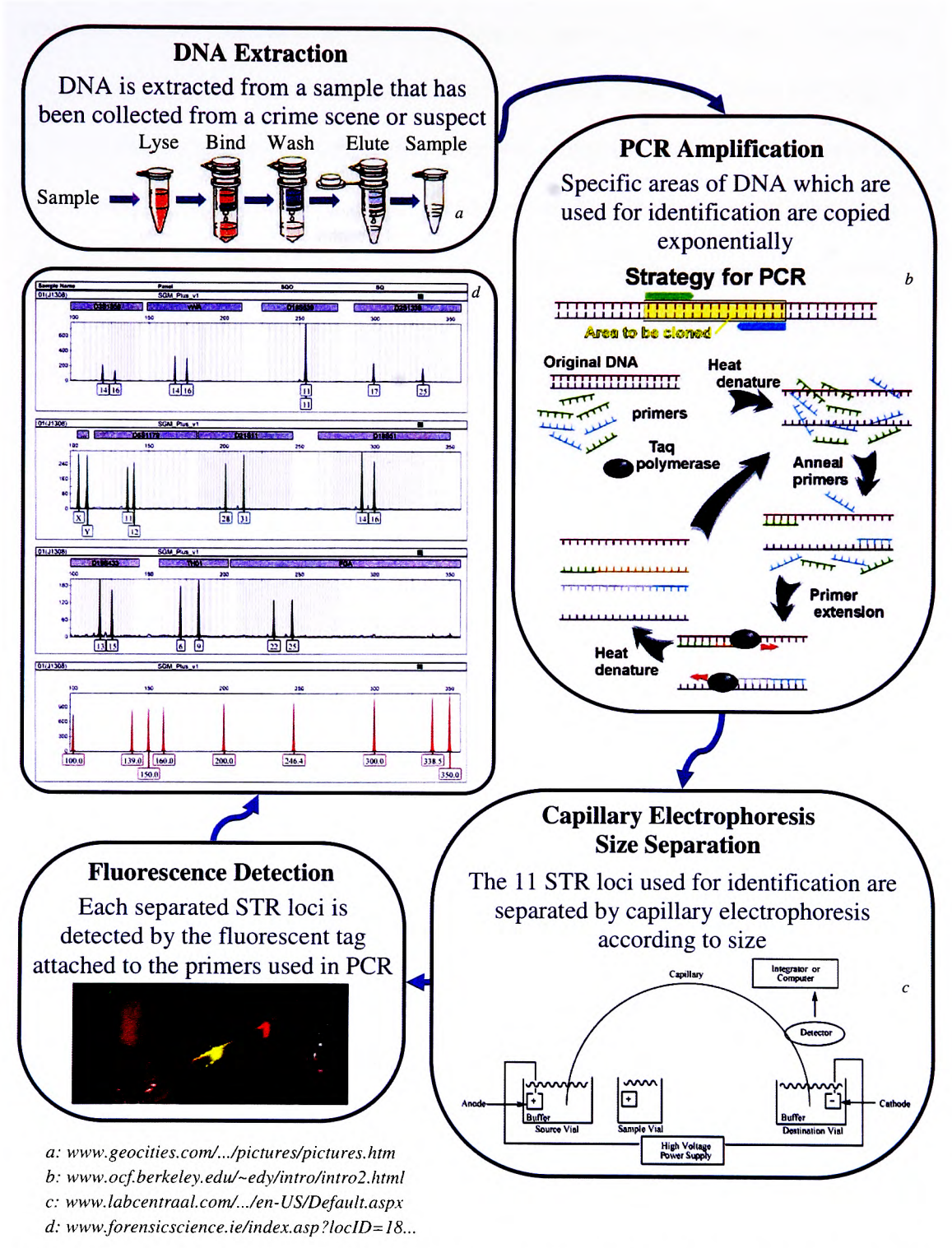

a: www.geocities.com/.../pictures/pictures.htm
b: www.ocf.berkeley.edu/~edy/intro/intro2.html
c: www.labcentraal.com/.../en-US/Default.aspx
d: www.forensicscience.ie/index.asp?locID=18...

Figure 1-1 Flow diagram depicting each stage of the process of DNA analysis, including extraction, PCR amplification, separation by capillary electrophoresis, fluorescence detection and an example of a final analysis.

1.1.2 The importance of the 'DNA profile' to society

DNA profiling is a uniquely powerful tool that is capable of providing an association between an individual and a piece of biological evidence found at a scene of crime or incident. The technique has many useful functions, including the inclusion or exclusion of a suspect in a criminal investigation, the identification of disaster victims, or paternal identification. In criminal investigations alone, 3500 matches are made to a sample taken from a scene of crime alone in a single month[1], indicating the importance of this technique to today's society. The biological sample could take a number of forms, such as fingerprints, hairs, blood, semen, saliva, urine, skin flakes, etc. The many different possible forms a biological sample can take increases the durability and usability of the technique.

1.2 Introduction to 'DNA fingerprinting'

The definition of 'DNA fingerprinting' is,

> *"the obtaining or comparing of genetic fingerprints for identification; specifically, the comparison of DNA in a person's blood with that identified in matter found at the scene of a crime, etc."(Oxford English Dictionary)*

Alec Jeffreys, who originally coined the above phrase, first published the idea of using multiple hyper-variable DNA fragments as a means to give a unique positive identification of an individual in the paper ***Forensic application of DNA 'fingerprints'***.[2]

The theories and techniques first described by Jeffreys have progressed significantly since then, but the basic principles are the same. DNA is combined into chromosomes;

there are 23 matched pairs of chromosomes in the human genome, of each of the chromosome pairs one of the chromosomes is inherited from the mother and one from the father. Contained within each of the chromosomes is DNA classed as coding or non-coding regions, the coding regions contain the information necessary for each cell to function properly. Non-coding DNA is often referred to as 'junk' DNA, and contains repeated DNA sequences of different lengths that, as far as we know, serve no real biological purpose. However, the junk DNA does have some useful properties that have been utilised in the process of human identification via DNA analysis.

This junk DNA can be characterised as satellites, which are long repeated sequences of DNA bases pairs, where the 'repeated sequence' is as long as several thousand bases in length. Minisatellites are shorter repeated sequences, where the 'repeated sequence' is approximately 10 to 100 bases in length; these are also referred to as VNTR (variable number tandem repeat). The 'repeated sequence' in a microsatellite or STR (short tandem repeat) is approximately 2 to 6 base pairs in length.

VNTRs and STRs are present in specific locations within the chromosome, called a locus or loci (plural). As each chromosome is one of a matching pair, there is also a matching locus at the same position on each of the chromosome pair. The repeated sequence of base pairs that comprise of a VNTR or a STR are vulnerable to mutation, which can occur over time and affect the length of the repeated sequence. The different possible lengths in sequence that can develop at a specific locus are called alleles, and it is the analysis of the different possibilities of alleles at multiple loci that constitutes a DNA profile.

In the earlier stages of the work, DNA profiling involved the identification, isolation and analysis of VNTRs, the original technique was difficult, time consuming and

required highly trained personnel to produce a credible DNA profile. But with the invention of the polymerase chain reaction (PCR) which allows for the rapid and effective amplification of STRs, the analysis of DNA is a much simpler, faster and accurate tool.

1.2.1 DNA fingerprinting today

The Forensic Science Service (FSS) completed a population study in the early 90s to document the allele variation of a loci within the population, from this they developed the first multiplex kit of four loci used in forensic casework. The second generation multiplex (SGM) system was quickly followed by the SGM Plus kit in 1999, based on 11 core loci. The UK and much of Europe use 10 core STR loci as identifying genetic markers in DNA analysis, plus the gender marker Amelogenin, 8 of these overlap with the 13 core loci used in America, which provides the possibility of information sharing between forces or authorities.[3] All the profiles of importance that have been collected in the UK are held in the UK national DNA database, established in 1995, the database currently contains approximately 4.5 million profiles.

Generally two samples are compared in order to match a piece of evidence with a reference sample of a suspect, the evidence is considered strong if the combination of characteristics within the profile is rare. The determination of the probability of a match between the samples occurring is determined by the Product Rule, which simply, is determined by multiplying together the frequencies of the individual alleles, incorporating the fact there are two alleles at each locus inherited from each parent.

Presently, samples are collected at a crime scene by an experienced trained individual, bagged and labelled. The sample is then transported to one of several forensic

laboratories around the country to be analysed, once there it is sorted, removed from the evidence bag and prepared according to the media it is in, or found on (i.e. a blood sample, cigarette butt). The DNA is extracted from the sample by many different means depending on the media and type of sample, the extracted DNA then undergoes amplification by PCR.[4]

Once amplified, the DNA sample is loaded on an instrument such as the ABI 310 Genetic Analyzer or the Beckman P/ACE MDQ. The standard method of separation in these instruments is capillary electrophoresis in a specifically designed separation matrix, for example the ABI prism 310 has a standard 47 cm capillary electrophoresis separation column filled with POP-4. The detection systems are a multi-dye system, where fluorescent tags are attached to the primers used in the amplification process.

The ABI prism 310 utilises 4 dyes: 5-carboxyfluorescein, succinimidyl ester (5-FAM, SE) *single isomer*, 6-carboxy-4',5'-dichloro-2',7'-dimethoxyfluorescein, succinimidyl ester (6-JOE, SE), 6-carboxytetramethylrhodamine, succinimidyl ester (6-TAMRA, SE) *single isomer* or the trademarked version developed by *Applied Biosystems,* NED™, and 6-carboxy-X-rhodamine, succinimidyl ester (6-ROX, SE) *single isomer*, (blue, green, yellow and red successively).

Table 1-1: SGM Plus™ loci breakdown

Dye	Loci
Blue	D3S1358
	vWA
	D16S539
	D2S1338
Green	D8S1179
	D21S11
	D18S51
	Amelogenin
Yellow	D19S433
	TH01
	FGA
Red	Allelic ladder

The loci are identified as they pass the detector by the colour of the dye, computer assisted data (CAD) analysis is used to estimate the DNA fragment size and distinguish between the alleles of the STR loci.[5] The profile produced is then checked for possible errors, stutters or anomalies before being compared with the profiles in the database or with a known profile obtained from a case.

For routine samples each stage of the laborious process involved in producing a DNA 'fingerprint' is performed at a different station by different technicians, during which the chain of custody must be maintained throughout. The system, whilst being very effective, is susceptible to problems, the total travelling time the sample takes between when it is first detected and collected to the point where a comparison can be made can take as much as 10 to 11 days. During this time, which in itself can delay the

progression of an investigation considerably, there is also a risk of misplacement or contamination of the sample, thus affecting the reliability of the results in court. A device capable of performing all these processes in a completely integrated system at a scene of crime will eliminate many of these problems, speeding up the detection of a possible profile match and eradicate the possibility of doubt in the system.[6]

1.3 Introduction to micro-fluidics and Lab on a Chip

Micro-fluidic devices refer to a glass or polymer device, where a chemical or bio-analytical reaction takes place in volumes as little as a few micro-litres. Different structures such as channels or chambers are created on the surface of a single wafer, and a second wafer with positioned access points is bonded on top of the first, creating a micro-litre reaction vessel sandwiched between the two wafers.

Micro-fluidic devices have the benefits of high sample throughput and high sample volume efficiency, they require smaller sample volumes, allow for the possibility to perform parallel analysis at the same time, they are portable and allow the integration of different processes onto one device.[7] Reaction times are faster due to the short transport times of sample from different components through the chip, as is the time for dissipation of heat through the sample to occur and therefore because of the high surface-to-volume ratio, achieving the temperature required at any given time is much quicker.[8] Also due to their relatively low cost they allow for the choice of disposability, which there is a great demand for especially with point of care devices to guarantee against cross contamination, in addition time, money and effort is saved on preparation and clean up procedures with throw away chips.[9]

1.3.1 Fabrication considerations

Typically the main medium used to fabricate micro-fluidic devices are polymer materials, such as poly(methyl methacrylate) (PMMA) or poly(dimethylsiloxane) (PDMS), or silica (glass) as they are both transparent with good surface properties.[10] Glass supports electro-kinetic movement, and has a high thermal tolerance which facilitates its suitability for integration of other features into the system, such as PCR for example. It is also considered the superior medium for a higher quality separation by electrophoresis and sensitive fluorescence detection as it allows particular control of the surface chemistry of the channel.[11]

Polymer devices, (PMMA, PDMS, etc.) are inexpensive, strong, easier to form channels in, and some forms can allow the transmission of more light into the channel than glass. Polymer devices require a different approach to the fabrication of the geometry; soft lithography, injection moulding, hot embossing, and casting are typical fabrication methods for polymer devices. These fabrication methods are simpler than the complicated photolithography and wet/dry etching used in the fabrication of glass chips, enabling a rapid production rate. However polymer devices do not have very good surface chemistry properties and the fabrication of the polymer chips is less reliable as the fabrication process can distort the media, reducing the uniformity of the channels. Therefore polymer devices are only really cost effective for high volume production, i.e. mass produced throw away chips.[10, 12]

1.3.2 'Lab on a chip' – Integrating different processes onto one device

The integration of each process step required for a complete analytical function on to one micro-fluidic device is the ultimate goal of micro-fluidic applications, but can also

prove to be the most elusive. A fully automated system would reduce the amount of human intervention and thus increasing the integrity of the sample,[13] which is essential for micro bio-analytical applications.

The reason integration can prove to be difficult to implement is the high degree of complexity required to successfully move a sample from one area to another on a single device and in operating each process without interfering with one another. Using the example discussed previously, a device capable of DNA analysis used for identification purposes, the DNA template must be extracted from any other cellular debris and washed with an alcohol to remove any components that would interfere with the polymerase chain reaction (PCR), but the alcohol itself inhibits PCR. Once extracted and washed the DNA template is amplified to increase the concentration of the sample to allow detection which requires a cyclic heating process to be performed, temperatures required can exceed 90°C which will chemically alter and physically damage the polymer based separation matrix required to separate the DNA sample after amplification. Finally, the geometries most suited to an efficient separation require the channel to be as small as possible to minimise diffusion and band broadening, however to increase the detection capability of the system a longer path length, i.e. channel depth, would be preferable. In addition, the method requires the sample to be moved to three separate sections of the chip in order to perform each one of the processes.

A portable system is only as small and portable as its largest component, therefore an integrated system with many components such as pumps, voltage power supplies, heaters/coolers, detection systems (including the excitation source, the detector and any other optics required) can result in a fairly large system. Furthermore, the computer equipment to control the system and/or collect data all needs to be miniaturized as well,

not to mention a power source to power all these components, all these factors should be considered when designing a micro-fluidic device capable of complete sample analysis.

The work discussed in this thesis is my contribution to the project as a whole, and is focussed on the movement of the reagents and products within an integrated device as part of reagent placement and product separation and analysis.

1.3.3 Common pumping mechanism utilised in micro-fluidic devices

Controlling the fluidic movement in an integrated system can be problematic; the difference in depths and widths of channels and chambers for example, can cause changes in the hydrodynamic pressure and alter the fluidic flow profile. Introducing a system of valves and barriers can control the fluidic movement in the system, controlling these problems.[11, 14, 15] There are numerous hydrodynamic driven pumps available that can be externally attached to an integrated device via tubing and connectors, however generally the size of these components make them unsuitable for a potentially portable device.

Grover *et al.* discussed the problems associated with using valves and micro pumps in integrated systems, and commented on some of the different options available for both.[11]

Vilkner *et al.* compiled a review discussing the recent developments in micro total analysis systems (μTAS), including methods of non-mechanical micropumping.[16] Other novel methods to control the flow of an integrated PCR device were reviewed by Zhang *et al.*[17] This subject was expanded a year later by Zhang *et al.* in a second review

discussing advances and trends in micro pumps, micro valves and micro mixers within PCR micro-fluidic chips, covering the last decade.[18]

There are two main types of fluid driving micro pumps, mechanical and non mechanical (no moving parts) based micro-pumps.[18] To induce fluidic movement in a micro-fluidic system, pressure or hydrodynamic driven flow tends to be used. Generally this would involve a certain number of external controls, pumps and valves, and this is referred to as mechanical pumping, as some form of external equipment is required to initiate the movement. Non-mechanical pumping refers to micro fluidic movement generated from inside the chip without the aid of an external valve or pump; the most common form of non-mechanical pumping is electro-kinetic movement, where only electrodes imbedded in the device have any contact with the macro world. The different variations of mechanical and non-mechanical micro pumps will be discussed in more detail in the following section.

1.3.3.1 Mechanical micro pumps

Mechanical pumping refers to the method of fluidic movement around the micro-fluidic device that relies on an (usually) external device that requires moving parts to generate or control the momentum of flow.

1.3.3.1.1 Piezoelectric Actuation Micro-pumping

Piezoelectric actuation micro pumps are formed due to the fact that the piezoelectric material has the ability to alter shape when an electric field is applied. The chip is fabricated with a layered design where the piezoelectric material is sandwiched between the polymer medium (such as polydimethylacrylamide (PDMA)). When an electric current is applied the piezoelectric material alters the inner dimensions of the channel.

The advantages of a piezoelectric micro-pump are they have a fast mechanical response, a high actuation force and a comparatively high stroke volume.[19]

1.3.3.1.2 Pneumatic Peristaltic Micro-pumping

Pneumatic peristaltic micro pumps are formed when a series of on/off actuation sequences are applied to active pneumatic micro valves. The advantages of pneumatic micro-pumps are that they are simple, effective and relatively small, but still larger than most actuator micro-pumps. Jeong *et al.* developed a PDMS micro pump consisting of three cascading actuators in a micro-fluidic channel connecting two inlet and outlet ports creating a series of dynamic valves. The pump, 5 mm x 5 mm, was capable of affecting 85% of the volume of the liquid chamber and demonstrated a flow rate of 73.9 nl min^{-1} without the problem of back pressure interfering with the flow rate.[20]

1.3.3.1.3 Thermo-Pneumatic Peristaltic Micro-pumping

Thermo-pneumatic micro pumps were first reported in 1990 by Van de Pol *et al.*[21] An air filled chamber with an internal heat resistor was incorporated on top of the pump diaphragm. The heat resulted in the expansion of the air in the chamber which pushed the solution from the storage chamber into the downstream channels and chambers, the design was updated in 2004 by Liu *et al.*[22] Thermo-pneumatic pumps have the advantage that the movement is predictable as air expansion has a linear relationship to temperature, however the temperature response time is limited by heat transfer resulting in low pump rates and the need for a membrane complicates the fabrication design and increasing the cost.

1.3.3.2 Non-mechanical micro pumps

Non mechanical pumping refers to mechanisms that do not require external mechanical components to generate the movement within a micro-fluidic device.

1.3.3.2.1 Magneto Hydrodynamic Micro-pumping

Magneto hydrodynamic (MHD) micro pumps are created when a transversal ionic current in a channel is subjected to a magnetic field at a 90° angle to the current direction; Lorentz force acting on the ionic current induces flow in the channel direction. However, electrolysis can be a problem with MHD micro-pumps, as bubble formation occurs even at low voltages and miniaturization is difficult.[23]

1.3.3.2.2 Electrochemical Micro-pumping

Electrochemical micro pumps work by electrochemically generating bubbles in the system and using these bubbles as an actuation force to push the fluid in the direction required. They are efficient and have a low power consumption (less than 150mW), however they are difficult to control, complicated to incorporate into a complex system and generally generate short burst movement so therefore pro-longed movement in one direction cannot be sustained.[24]

1.3.3.2.3 Acoustic-wave Micro-pumping

Acoustic-wave micro pumps incorporate an inter-digitised transducer connected to a high radio frequency power source to produce a surface acoustic wave, the fast alternating electric field generates a displacement on the channel surface which moves at the speed of sound. When the sample is put onto the surface, this momentum is transferred to the sample, moving the droplet the same direction as the wave. This method provides fast movement and fast analysis, the ability to move very small

volumes and can be utilised not only for movement but also for mixing and dispensing of small droplets.[25] However, the equipment required substantially complicates the fabrication of the micro-fluidic device; in addition it is difficult to prevent the unwanted movement of other liquids contained within the system.

1.3.3.2.4 Surface Tension and Capillary Micro-pumping

There are a number of different approaches to surface tension and capillary micro pumps:

Thermo capillary micro-pumps use temperature gradients on the surface to direct the flow.

Electro capillary micro-pumps use electro wetting to direct the flow, electro wetting refers to a localised potential difference on the capillary surface that alters the surface contact angle of a fluidic droplet, if the contact angle is higher one side of the droplet than the other the difference can be used to lead the direction of the flow.

Passive capillary micro-pumps use the channel or chamber geometries, or the surface properties of the capillary surface to direct the flow.

1.3.3.2.5 Ferro-fluidic Magnetic Micro-pumping

Ferro-fluidic magnetic micro-pumps use ferromagnetic particles supported in a carrier fluid to form a solid plug which can then be directed by an external magnetic field to manipulate the fluidic movement around the channel. The advantage of using the particles is that they conform to any channel shape when the magnetic field is applied therefore always forming a good seal within the channel, and they are also very easy to manipulate.

1.3.3.2.6 Electro-kinetic Micro-pumping

Electro-kinetic micro-pumps refer to the movement of ions due to their electric charge. There are two types of electro-kinetic movement; electrophoresis and electro-osmosis (described in greater detail in Section1.4). The advantages of electro-kinetic micro-pumps are they have a flat flow profile which results in less sample dispersion, there are no moving parts, they allow good control of flow and they are simple to operate and to integrate. However, the flow rate is slower than that achieved with pressure driven flow, and electro-mixing can occur as a uniform flow of all species within a sample cannot be achieved with electro-kinetic movement and certain components or additives in a sample can modify the potential which can have an adverse effect on the flow profile.

Electro-osmotic micro-pumping (EOP) works as electro-osmotic flow is induced across a parallel silica based monolith which prevents the solution pumped across the monolith from flowing backwards due to hydrodynamic forces, generating a flow of approximately 0.6 $\mu l min^{-1}$.[26]

Gui *et al.* utilised electro-osmotic pumping in an electro-kinetic based continuous flow PCR chip, but found the presence of proteins and other impurities altered the potential of the system affecting the electro-osmotic flow, however the system was easy to operate and showed greater potential for integration over hydrodynamic pumping.[27] Kim *et al.* used a borosilicate glass and low ion density liquids to achieve much higher flow rates. Reichmuth *et al.* describe the use of zwitterionic additives, trimethylammoniopropane sulfonate (TMAPS), to enhance the performance of the electro-osmotic pumping and reported a three-fold increase in flow rate. This increase in performance allows for the potential of reduction in voltage and power requirements, thus lending itself to portable hand held integrated micro total analytical systems.[28]

Kuo *et al.* describe a novel micro-fluidic driver using AC electro kinetics which they claim achieves bubble free micro pumping, where asymmetric capacitance modulation (ACM) was used to operate the AC current at a higher frequency, thus hindering the production of bubbles.[29] Advantages of field induced flow based micro pumps over membrane displacement based micro pumps is that they are simpler in design, there are no moving parts, and no special fabrication process is needed which makes it easier to integrate. But in a field induced micro pump the conductivity is a limiting factor.

1.4 Theory of electro-kinetic movement

1.4.1 Electro-osmotic flow (EOF)

EOF describes the bulk flow of solution along a channel as an electric field is applied; a cation rich electric double layer forms at the surface of the channel, when an external field is applied the double layer migrates towards the cathode carrying the bulk solution with it.

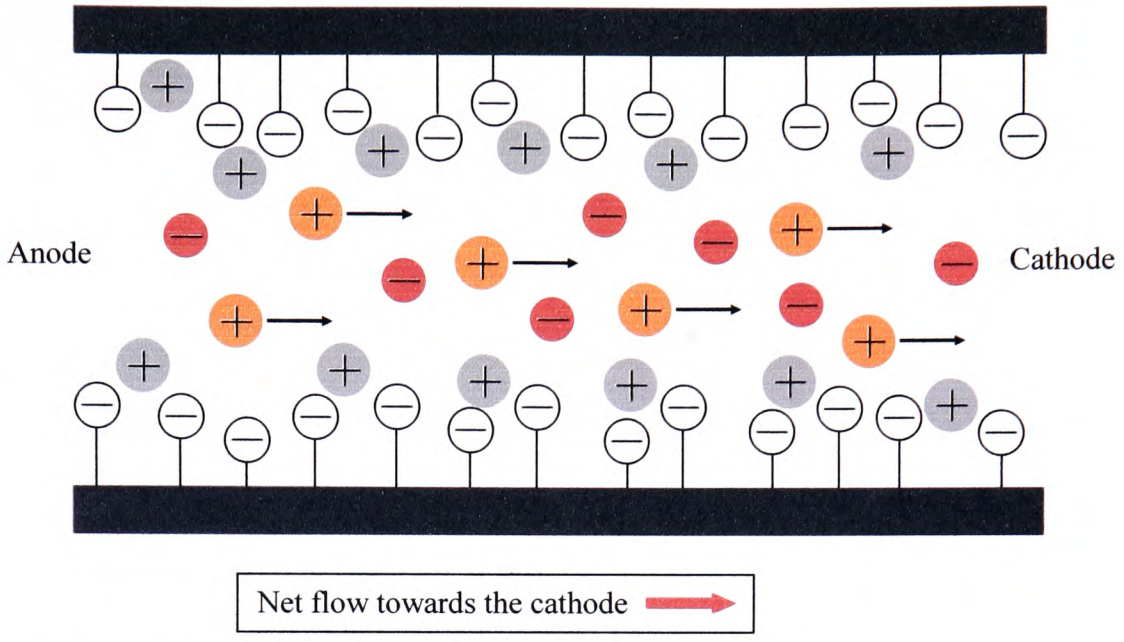

Figure 1-2 Illustration of electro-osmosis flow in a silica capillary

The electro-osmotic mobility (μ_{os}) describes the velocity of the EOF through a channel when an electric field is applied and can be described by Equation 1-1.[30]

$$\mu_{os} = \frac{v_{os}}{E} \equiv \frac{LL_{tot}}{t_{os}V}$$ **Equation 1-1**

Where v_{os} is the electro-osmotic velocity (ms^{-1}), E (Vm^{-1}) is the electric field, L (m) is the length from the point of sample injection to the detection region, L_{tot} (m) is the total length of capillary between electrodes, t_{os} (s) is the migration time to the detector, and V is voltage (V) applied across the capillary.

1.4.2 Electrophoresis

Electrophoresis refers to the migration of ions in solution under influence of an electric field; different solutes have different mobilities and therefore migrate at different speeds. The electrophoretic mobility (μ_{ep}) of an ion is constant of proportionality

between the speed of the ion and strength of electric field, and can be calculated by Equation 1-2.[30]

$$\mu_{ep} = \frac{q}{f} = \frac{v}{E}$$ **Equation 1-2**

Where q is the net charge, f is the translational friction coefficient, v is the migration velocity of the component and E is the electric field.

1.4.3 Electrolysis and Joule heating

When an electric field is applied to a small volume of solution, two phenomena can occur, electrolysis and Joule heating, both can have a severe affect on the operation of the micro-fluidic system.

Electrolysis is a problem that can be highly underestimated, the two most common reactions to occur at the electrodes are described in Equation 1-3 and Equation 1-4, characterising electron transfer at the cathode and anode respectively, but other reactions can occur depending on the conditions.

$$2H_2O + 2e^- \rightarrow 2OH^- + H_2$$ **Equation 1-3**

$$2H_2O + 4H^+ \rightarrow 4e^- + O_2$$ **Equation 1-4**

Electrolysis can affect the pH of the system, but more importantly it can generate bubbles in the system. The injection point is the most likely source for bubble formation and debris build up in micro-fluidic system.[31] Bubbles in a gel based system can cause numerous problems, including diminished separation resolution which will result in a

decreased current during operation altering the mobility and changing the separation pattern, in addition the lifetime of the gel filled capillary can be significantly reduced.[32]

Joule heating is an inevitable phenomenon for electro-kinetic movement in micro-fluidic devices as it requires a high voltage difference to be applied to small volumes of liquids which can generate a large quantity of heat in the liquid, however the problem can be reduced or negated by the use of buffers or by chip design.[33] In some cases the Joule heating effect has been used to advantage, Hu *et al.* describe a process where the Joule heating effect was successfully shown to precisely control the thermal cycling in a PCR reaction.[34] A Taq polymerase, TaqMan, capable of performing a PCR reaction which cycles through only two temperatures (95 and 61°C), and the PCR reagents were electro-kinetically pumped thorough the micro channel back and forth, with a higher current used for the higher temperature and a lower current used for the lower temperature.

1.5 Sample introduction in capillary electrophoresis systems

A clean reproducible injection is important as it has a beneficial effect on the validity of the analysis, it is critical for accurate, reproducible separations with microchip capillary electrophoresis.[35] An increased sample volume is preferable for detection purposes, but will result in an increase in band broadening and a reduction in the resolution of the sample.[36] The volume of the injected sample is also dependent on the efficiency of the extraction and sample processing as well as the sensitivity of the detection system.[37] Controlling accurately the introduction of sample into a micro-fluidic device is difficult to accomplish, common forms of sample introduction involve hydro-dynamic, pneumatic or electro-kinetic control.[38]

Hydrodynamic injections are controlled by altering the pressure difference between the two ends of the capillary, this can be achieved using external pumps and/or valves, but successful injections have also been achieved using pressure pulse applied to a membrane on a reservoir via a mechanical actuator. A pressure pinched injection was achieved with a multipart injection valve and three syringe pumps. Easley *et al.* used a pressure injection in an integrated micro-fluidic genetic analysis system,[39] capable of multiple injections due to small sample volume. The advantages of pressure injections are no electro-kinetic bias is present and the mechanism is insensitive to the channel surface.

Huang *et al.* described a novel method for the injection of precise amounts of DNA sample in an integrated DNA and RNA amplification, separation and detection system, involving a combination of a pneumatically driven and electro-kinetically driven transportation mechanism.[13] The pneumatic approach was also used by Leach *et al.*; they developed a flow injection analysis system that mimicked the operation of a standard six port two way valve used in liquid chromatography. The device consisted of a two-layer polydimethylsiloxane (PDMS) monolith and multiple pneumatically driven peristaltic pumps.[40]

Another combination method of sample introduction was described by Zhang *et al.* as a negative pressure pinched injection. A combination of negative pressure, electro-kinetic, and hydrostatic forces, this method has shown to provide controlled, well defined and non-biased sample plug. However, the constant voltage applied to the separation channel during the injection results in EOF occurring, this affects the hydrostatic forces and the performance of the pinched injection.[41]

1.5.1.1 The importance of chip design on the injection process

The design of the micro-fluidic device is important when considering the injection mechanism with a capillary (Figure 1-3), as it affects the diffusion properties and the likelihood of leakage occurring down the separation channel. Also when considering different injection mechanisms, it is important to match the geometries.

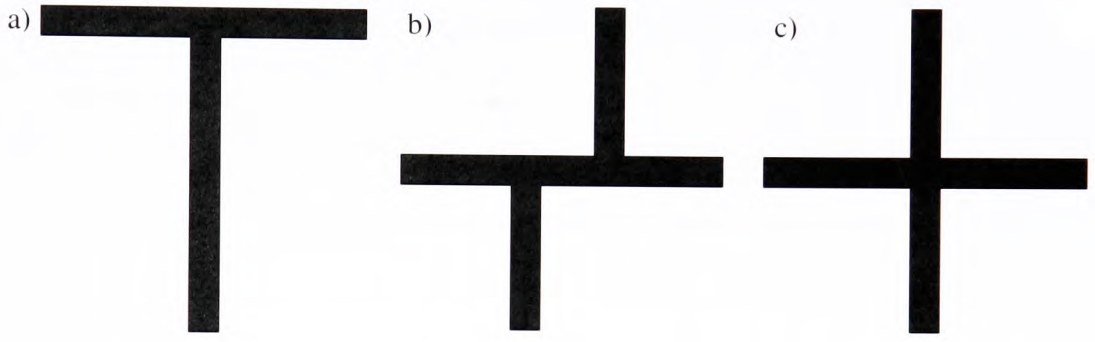

Figure 1-3 Three different T geometries for injection, a) the standard T, b) the double-T and c) the cross.

In addition to the standard channel geometry used for the injection of a sample plug in a micro-fluidic device, more involved designs have been developed to optimise the efficiency and precision of an injection, in-order to increase the resolution of the separation and detection. Leong *et al.* discussed how the shape of the sample plug can have a large effect on the resolution of its separation, and they described an integrated system incorporating a cross form injection geometry with an expansion chamber at the inlet of the separation chamber.[42]

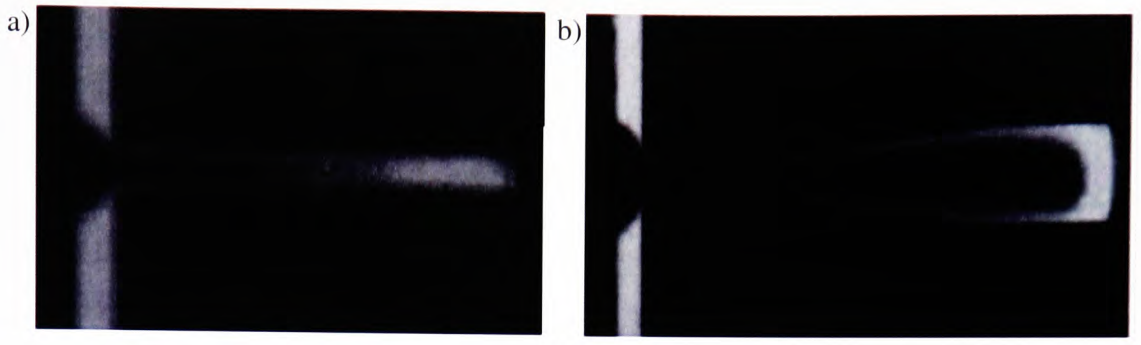

Figure 1-4 Comparison of sample plug shape achieved in a micro-fluidic device, for a capillary electrophoretic separation, a) traditional cross from pinched injection, b) use of expansion chamber.[42]

The expansion chamber, effectively a coned increase of the width of the separation channel to its final width, encouraged the pinched injected sample plug to stack in the separation chamber altering its shape from a long diffuse plug to a narrow band ready for separation (Figure 1-4).

1.5.2 Electro-kinetic controlled sample introduction

When considering an electro-kinetic injection for efficient separation there are two main issues to address. Firstly, the increase of plug length caused by dispersion of the sample plug into the separation channel during loading; as diffusion is the biggest problem when trying to achieve a good separation resolution.[43] The second issue with electro-kinetic injection is the possibility of continuous sample leakage into the separation channel during the separation, causing peak tailing and increased sample background.

One of the earlier groups to accomplish DNA fragment sizing and separation also used an electro-kinetic injection, the sample was introduced via a cross channel into a 5cm long separation channel, 100μm width, the injection process was completed in 120 seconds.[44, 45] Schmalzing *et al.* credit the ultra fast separation capabilities of their

system to the extremely short injection plugs achieved by an electro-kinetic injection across a suitably designed geometry.[46]

1.5.2.1.1 Negative pressure pinched injection

Negative pressure pinched injection is achieved by a combination of negative pressure, electro-kinetic, and hydrostatic forces; the quantity of the sample injected is geometrically defined by the intersection of the channel. An example of the pressure pinched injection, as described by Zhang *et al.*[41], can be seen in Figure 1-5.

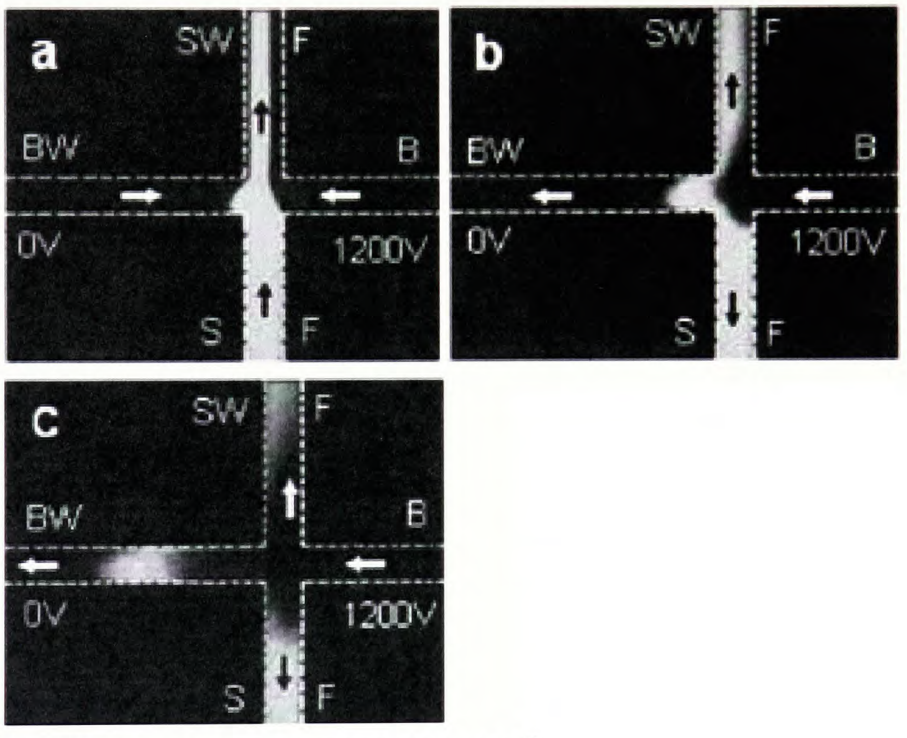

Figure 1-5 A negative pressure pinched injection.[41]

This method has shown to provide controlled, well defined and non-biased sample plug in a much shorter loading time compared to a normal electro-kinetic injection, however the constant voltage applied to the separation channel during the injection results in EOF occurring, this affects the hydrostatic forces and the performance of the pinched injection.

1.5.2.1.2 Gated electro-kinetic injection

In a gated electro-kinetic injection, a continuous stream of sample is electro-kinetically driven along a set path by an electric field applied to the sample channel. For a brief period a positive charge is also applied to the separation channel, creating a second electric field in the perpendicular direction which causes a small volume of sample to divert from the continuous stream into the separation channel. When a suitable sample plug has been injected, a negative charge is applied to the cross channel perpendicular to the separation channel creating a gate which directs the continuous sample stream away from the separation channel and into the sample channel only. The continuous sample stream continues in its original path, whilst the sample plug continues down the separation channel (Figure 1-6).[47]

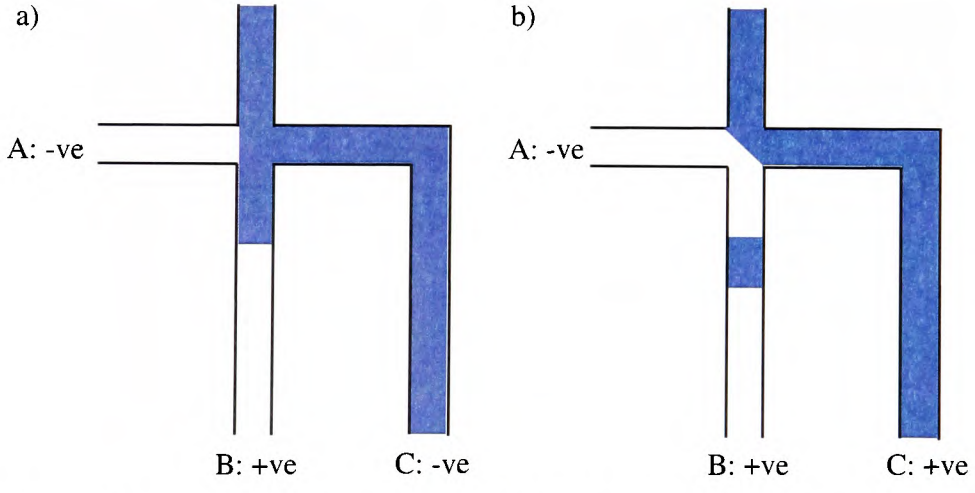

Figure 1-6 Visualisation of the mechanism of the gated electro-kinetic injection, a) the electric field is applied to both the separation (channel B) and the sample (channel A) channels to induce a plug into the separation channel, b) a second negative voltage is applied perpendicular to the separation channel (channel C) creating the 'gate' affect.[47]

The gated injection successfully avoids the pitfalls of electro-kinetic injection described in Section 1.5, while the continuous movement of the sample in the sample channel

allows for very little sample dispersion into the separation channel, allowing the length of the sample plug to be strictly controlled. Also the gated effect created by the negative voltage applied perpendicular to the separation channel significantly reduces the leakage of the sample during the separation process, reducing the degree of peak tailing and the sample background during separation.

The disadvantage of a gated electro-kinetic injection is similar to the pinched injection, in which it suffers from an electro-kinetic bias, where the injection favours components with a lower negative electrophoretic mobility, therefore in a mixed solution the components with a higher negative charge will move in a higher volume into the separation channel.

A variation to the gated injection was discussed by Wenclawiak *et al.* for the application of capillary electrophoresis. A high powered laser was used to bleach sections of the sample stream creating a succession of very short sample plugs in the channel; this method is referred to as optically gated injection. The main advantage of this method is the incredibly small sample volume achievable, around the pico-litre range, which are highly reproducible allowing for separations with a very small deviation in retention times and peak areas.[48]

1.5.2.1.3 The double-L injection

The double L injection[49] is only feasible when using the double T channel geometry (Figure 1-3b); instead of the standard mechanism where the sample flow is across the separation channel the sample flow is now at a right angle (Figure 1-7).

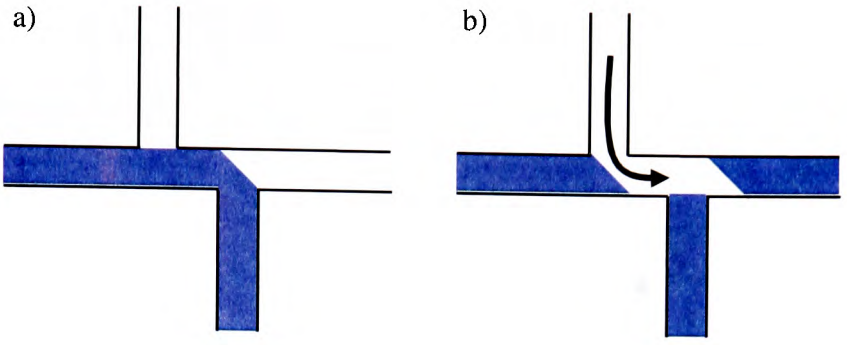

Figure 1-7 Visualisation of the mechanism of the double-L electro-kinetic injection, a) firstly the sample flow is directed around the first right angle of the double T channel, b) the first flow is stopped and a second reagent flow is directed around the second right angle of the double T. The sample trapped in the void between the two right angles of the double T is the injected sample plug.[49]

This method can be controlled by electro-kinetic movement or by hydrodynamic pumping, and is reported in the literature to produce highly accurate and precise injections resulting in high resolution and high throughput analysis. However, the size of the injected plug is entirely dependent on the length of channel between the two right angles of the double T, significantly reducing the flexibility of the system.

1.5.2.1.4 Pinched electro-kinetic injection

The principle of the pinched electro-kinetic injection is that a plug of a controllable size is pulled into the separation channel, from a stream of sample moving past the entrance.[48] Once a plug of controlled size is contained in the separation channel, the remaining sample in the cross bar is prevented from following down the separation channel by an applied voltage between electrodes B and D, this mechanism is illustrated in Figure 1-8.

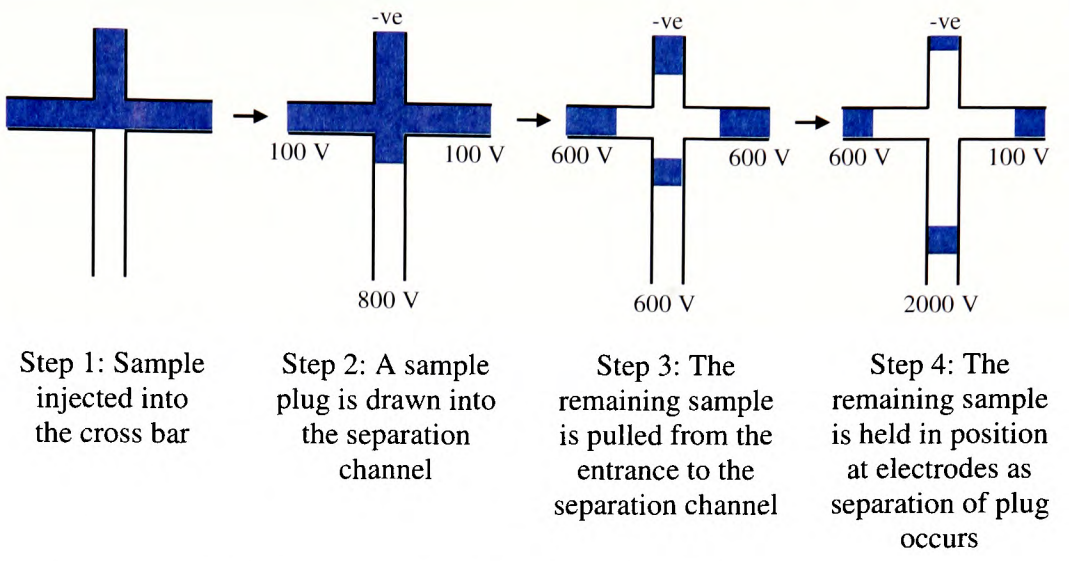

Figure 1-8 The mechanism of a pinched electro-kinetic injection.

The advantage of the pinched injection is that the problem of continuous sample leakage during the separation process is addressed; the pull back of the remaining sample efficiently prevents leakage of excess sample further down the process, reducing the peak tailing and the sample background. However, to avoid sample dispersion and increased sample plug length, the sample injection and pull back must be performed at a very fast rate. To allow this process to happen efficiently the control of the voltages must be very precise and therefore a degree of automation is required. Also another disadvantage of a pinched injection is a small degree of electro-kinetic bias can affect the volume of the injected sample, for example the same injection will result in a larger volume of a sample of neutral components compared to a sample of anionic components.

1.5.2.2 Sample pre-concentration and focusing

Stacking is a form of sample pre-concentration performed in an electric field, if a sample plug of 5mm is injected into a channel, when the analyte band passes the detector it cannot be any smaller than 5mm and in some cases will probably grow in size due to band broadening. Field amplified sample stacking (FASS) is the simplest and most common example, where the stacking effect occurs based on the interaction between the electric field and electrolyte solution present in the system either side of the sample zone. The electrolyte solution has a much higher conductance than the sample, the lower conductance sample zone has a much higher field strength causing ions to move faster through the zone and accumulate or 'stack' at the sample/electrolyte interface boundary, therefore concentrating all the sample in the original injection into a narrower band at the interface.[50]

Xu *et al.* describes a sub second iso-electric focusing technique in free flow electrophoresis, which overcame problems with Joule heating by enlarging the surface area of the chamber or the channel by the addition of posts to the system.[51] Iso-electric is often confused in literature when discussing focusing of other components in an electric field, as it implies the focusing of a component to one point by the application of an electric field alone.

Isotachophoresis (ITP) is a non mechanical method to pre concentrate DNA ready for the injection of the sample, where a binary buffer system is used to focus the sample constituents between a leading and terminating buffer. Hydroxide ions were directly electro-kinetically injected between the buffers, lowering the conductivity zone, inducing field focusing, known as base stacking.[52]

Zalewski *et al.* describe a method of electro-kinetic sorting and collection of different fractions of a sample by an automated system which uses fluorescence detection at a voltage controlled entrance, if a separated fraction is detected the necessary voltage is applied that will manipulate the fraction down the desired channel.[53]

The moveable wall concept described by Lee *et al.* is an alternative method for sample focusing, an active micro channel width controller was constructed using pneumatic side chambers adjacent to the channel wall and a micro chopper, the device was made from PDMS to accommodate the flexibility required in the channel. The width of the channel was attenuated using the constructed channel width controller in order to focus the hydro-dynamically pre-focused stream and generate focused micro droplets of sample.[54]

1.6 Separation by capillary electrophoresis

In column chromatography, the components are dissolved in a mobile phase which is passed through a stationary phase, different interactions between the components and the stationary phase result in a difference in the retention time of each component along the column. For a miniaturized system, column chromatography would be difficult to achieve, due to the relatively low efficiency for molecules of a high molecular weight, that characteristically have low diffusion rates and back pressure problems. This problem is not experienced in electrophoresis, as an expensive stationary phase is not required, and the development from the slab gel electrophoresis to capillary electrophoresis on chip has increased the usability of this method, allowing the design and development of many different portable analytical devices.

1.6.1 Separation of DNA

There are many different types of separation available that have been utilized for the application of separating DNA fragments according to size. Goedecke *et al.*[55] used capillary array electrophoresis (CAE) for the separation of forensic DNA samples, the design involved 16 channels that allowed a tandem repeat method to be implemented. Whilst Kang *et al.*[56] developed a direct current - dielectrophoresis (DC-DEP) method for the separation of micro-particles. Soper *et al.*[57] fabricated a polymer micro-system for DNA sequencing based upon capillary electro-chromatography (CEC – a hybrid of capillary electrophoresis (CE) and high performance liquid chromatography (HPLC)) where the mobile phase and the analyte are electro-pumped through a separation bed consisting of micro-post supports coated with a hydrophobic phase. Free flow electrophoresis has also been utilized as a separation technique,[51, 58] but due to the fact that DNA cannot actually be separated by size with free flow electrophoresis as it has a constant charge to size ratio, without certain modifications it is not widely used for the application of DNA analysis.

Currently, the standard method for the separation of single stranded DNA is capillary electrophoresis, sometimes referred to as capillary gel electrophoresis (CGE) when a gel matrix is used to aid separation.[59] Its superiority to other methods is born out of its ability to provide a higher resolution, its compatibility with many forms of detection, and with the possibility for automation and portability.[43]

There are two main theories describing the separation mechanism of DNA in capillary gel electrophoresis, there are the sieving mechanism and the biased reptation (a specific thermal motion of very long linear macromolecules, polymer chains, in a concentrated solution of polymers) with fluctuations mechanism (BRF).[60] The sieving mechanism is

self explanatory, the entangled gel/polymer consisting of cross linked branches creating pores acting like sieves, the larger DNA fragments get caught up in the pores and are slowed considerably compared to the smaller fragments. When the DNA fragments are actually larger than the pore size of the gel/polymer, then it holds that the sieving mechanism is no longer appropriate, instead the BRF theory is applied.[43] In the BRF mechanism, being too large to force itself into a pore, it is assumed the DNA is forced to deform and thread itself through a mesh-like tube system. As it moves through the gel it has to choose new 'tube' sections to move into, the electric forces control this choice to a degree by organizing the tubes in a manner that reduces the potential energy of the system.[61] The 11 loci used in the STR plus kits that will be analysed are between 100 and 400 base pairs in length, the separation mechanism that is more likely to apply is the sieving mechanism, however the larger fragments may utilize the BRF mechanism.

Although some people have attempted to separate DNA fragments by electrophoresis without the use of a traditional gel or polymer separation matrix, Duong *et al.*[62] for example, described a free gel system where the separation was aided instead by topographically structured channels which were designed with cavities periodically placed along the channel. In addition, Minc *et al.*,[63] developing an earlier idea published by Doyle *et al.*,[64] described a system they called '*Ephesia*' consisting of a self assembling magnetic bead matrix, which forms columns when a constant homogeneous magnetic field is applied. The DNA becomes entangled around the columns in much the same principal as with the gel and polymer matrix, the benefit of such a system is the reproducibility of the matrix, allowing accurate comparison between experiments, and investigation of the affects of other factors. However, it is difficult and complex to create, and is generally more suited to the separation of larger DNA fragments. The

different separation matrices available, and their associated properties, are discussed in the following section.

1.6.2 Factors to consider when optimising CE separation

There are many factors that could affect the optimisation of separation, the peak shape and spacing or resolution.

1.6.2.1 The choice of gel or polymer

A cross linked polymer gel consists of polymer chains interwoven creating pores to which the DNA molecule travels through, the larger a molecule is the more difficulty encountered when attempting to move through the polymer matrix. Different polymers with different chain lengths can create different pore size properties in the polymer, a smaller pore size will result in more difficulty experienced by the DNA molecule to travel through the matrix, slowing it down, however this can result in peak broadening. A compromise has to be made between the pore size required for satisfactory resolution, without adverse band broadening, also taking into consideration viscosity properties and the self coating abilities of the solution. A detailed discussion of the different matrices suitable for the size separation of DNA STR's can be found in section 1.6.3.

1.6.2.2 Polymer concentration

An increase in polymer concentration will result in an increased resolution, this will affect the mobility and increase the time taken for the separation. The increase in resolution seen with the increase in polymer concentration is limited to the DNA

fragment length, i.e. longer fragments will not experience the same improvement in resolution as the shorter fragments.[65] Also, an increase in concentration will also increase band broadening due to diffusion, if peak spacing and band broadening increase at the same rate, there is no benefit to an increase in polymer concentration.

1.6.2.3 pH of polymer

pH has been shown to have an effect on the separation, a lower pH (closer to neutral, pH 7.5) resulted in a quicker migration time for the DNA and a better resolution.[66]

1.6.2.4 Injection volume

As previously stated in section 1.5, the volume of sample injected into the capillary can have a large effect on not only the accuracy and reproducibility of the separation, but also on the resolution of the sample. Large volume injections, whilst being preferable in terms of detection, can lead to a large amount of diffusion and band broadening occurring during the separation, resulting in a detrimental effect on the resolution of the separation.

1.6.2.5 Capillary length

Increasing the capillary length will also increase the resolution of the separation, but can also result in an increase in band broadening. As mentioned above, the increases in resolution is limited to DNA fragment length, and there is no benefit to an increase in the separation length if the peak spacing and band broadening increase at the same rate.

1.6.2.6 Capillary diameter

An increase in capillary diameter does not directly affect resolution, but will cause an increase in diffusion and therefore peak width, which will hence result in some degree of loss to resolution.

1.6.2.7 DNA protonation

DNA is susceptible to protonation which can cause a mobility shift,[67] the migration of DNA fragments along a separation channel with the same parameters can vary in time between successive separations, this drift in migration time is the reason why an internal standard DNA marker is required in the commercial systems.[12]

1.6.2.8 Electric field strength

The effect of electric field strength on separation is as you would predict, an increased field strength will result in an increased mobility, but the difference in mobility between differently sized DNA fragments decreases with increased field strength, therefore resulting in a poorer resolution.[68] Optimal field strengths that have been utilized to separate single stranded DNA are variable, depending not only on channel dimensions and geometries, but also on the separation matrices, so it follows the values stated in the literature vary considerably. Some insist $300Vcm^{-1}$ is high,[15] but it is generally believed using an applied voltage of higher than 4000V regardless of the channel length, can be problematic as this can lead to Joule heating at the electrodes. Bubbles are created inside the channels and once present, these can be very difficult to remove and have unpredictable adverse effects on the electric field. Methods to combat Joule heating include increasing the surface area of the channel. Xu *et al.* utilized a support system by

constructing a series of posts within the channel, not only increasing the surface to volume ratio but also aiding the direction of the fluidic movement through the channel as required, it was reported the increase in volume to surface ratio could dissipate Joule heating by as much as 30 $mWcm^{-1}$.[51]

1.6.3 Different separation matrices

To achieve the size separation resolution required for a DNA 'fingerprint' analysis, some form of separation or 'sieving' matrix will be required. There are many different matrices to choose from, and as discussed in section 1.6.2.1, the choice of polymer separation matrix can have a large impact on the resolution of the separation. The ideal separation matrix should have the following properties: a high sieving ability, dynamic coating abilities (i.e. coats the walls of the channel to prevent DNA-wall interactions and EOF) and have a low viscosity so it is easier to load into the channel. Unfortunately, for the first to be true the last has to be sacrificed, and vice versa, therefore a compromise has to be reached.

Linear poly-acrylamide (LPA) is a cross-linked polymer gel solution, and is widely used for high resolution separations due to its high sieving capability. However, it has a very high viscosity and is therefore difficult to load into a channel, and the high pressure required could damage the capillary channels. In addition, there are accounts in the literature claiming that when LPA is used as the separation matrix, the channel surface needs to be coated beforehand with a dynamic coating to prevent EOF and DNA-wall interactions.[69] Schmalzing *et al.*[46] utilized poly-acrylamide in the analysis of STRs, achieving a separation of single locus STR samples in 30 seconds in a 26 mm separation length at 200 Vcm^{-1}, in this case there was no coating applied.

Other polymers include poly(ethylene oxide) (PEO), a low viscosity entangled polymer that is commonly used for the separation of DNA fragments when a replaceable, stable, and easier to handle solution is required.[70] Cellulosic polymers, including hydroxyethylcellulose (HEC), hydroxypropylcellulose (HPC) and hydroxypropylmethylcellulose (HPMC), are also useful matrices acting either as a separation matrix or an adsorptive coating for DNA separations performed on acrylic polymer chips.[12] Zhou *et al.*[69] described a new matrix, poly (*N*-isopropylarylamide) (PNIPAM), the group reported that the addition of an additive, mannitol, dramatically increased the sieving capability of the polymer, whilst still retaining a low viscosity. PNIPAM was designed to have the dynamic coating and loading abilities of PDMA and the sieving capability of LPA, however the resulting solution is temperature sensitive above 32°C where the resolution decreases dramatically.

Thermo-responsive polymers were designed to alleviate some of the compromises made when choosing a suitable polymer for capillary electrophoresis separation, temperature dependent viscosity transitions allow easy loading of the gel at low temperatures where the viscosity is low, and at higher temperatures the sieving ability increases as the viscosity of the solution increases.[68, 71] Thermo-responsive polymers tend to be mixes utilizing the best properties of each, for example; poly(N,N-dimethylacrylamide) grafted to poly(methyl methacrylate) (PDMA-g-PMMA), poly(isopropylacrylamide) grafted to poly(ethylene oxide) (PNIPAM-g-PEO), polyacrylamide grafted to PNIPAM (PAM-g-PNIPAM),[72] HPC and HEC blends.

Copolymers have the advantage that the cross-linkages are less flexible due to the side chain obstructions naturally present, which reduce slippage of the entangled chains and stabilise the polymer. With polymer blends however, it is difficult to control vital

aspects of the final polymer, i.e. the molecular weight, the grafted chain length and density, therefore reproducing the polymer and optimizing the polymers performance is difficult. Also the differences in each polymer could lead to uneven mixing and therefore, concentration and density differences throughout the polymer.[73]

1.6.4 EOF interference with capillary electrophoresis

During electrophoresis, if suitable conditions are present EOF can also occur and as such EOF has been documented as being problematic during DNA separation, as DNA is negatively charged and migrates towards the anode whilst EOF travels in the opposite direction towards the cathode, this can lead to distorted peaks and low resolution.[15] A common practice to combat this problem is to apply a coating or 'modification' to the surface of the capillary. One of the first surface modification techniques was devised by Hjertén and is termed the 'Hjertén coating', the coating works by neutralizing the charge on the channel surface with a covalently bonded silane linker which then polymerises with the linear polyacrylamide.[74] Other approaches to alter the surface chemistry of the capillary include: localized surface modification, selective hydrophobic coatings,[75] modification of the native surface with plasma techniques including chlorinated gases and oxygen plasma.[76] Another approach to remove interference from EOF was described by Badal *et al.*,[77] he suggests that the addition of anionic or cationic surfactants could be used to control EOF.

1.7 Detection

There are many detection methods that are able to be implemented in a DNA detection system: Electrochemical detection (EC) was been utilized by Ertl *et al.*[78] due to its

suitability for integration into the chip and in a portable device however EC has a low sensitivity compared to other techniques available and have encountered problems with interference from the electrophoresis potentials. Chemiluminescence is an extremely sensitive detection method used in many different techniques; it has also been utilized in the determination of ultra micro DNA in conjunction with free flow injection. Chemiluminescence is sensitive with good detection limits, it is a rapid process, reproducible, simple instrumentally and can be used with on-line analysis.[79] However, fluorescence detection is more suitable for this application as it is highly sensitive, and fluorophores can be excited and detected selectively permitting a lot of flexibility in the system.[8] It is also a detection system that benefits from being miniaturized as the background interference signal is also greatly reduced.

Fluorescence is a form of luminescence, an electron reaches an excited singlet state when irradiated by an external source, when the electron returns to the electronic ground state the substance loses the excess energy as a photon, emitting light (see Figure 1-9).

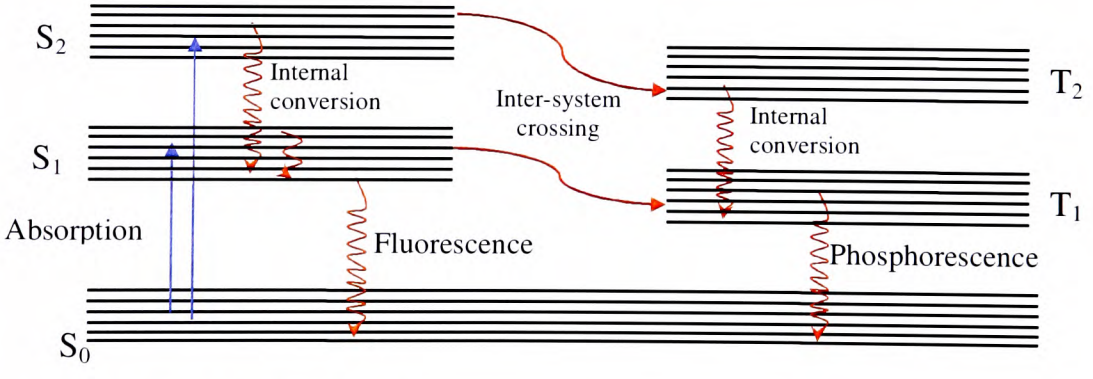

Figure 1-9 The Jablonski diagram

1.7.1 Fluorescence detection

As described in Section 1.2.1, fluorescent dye bound to the 5'-end labelled oligonucleotide primers[80] are used in the PCR reaction in order that detection of the amplified DNA can be achieved. There are a number of dyes available that have been used to tag the primers with, altering the specifications of the detection system accordingly.

The basic concept of a fluorescence detection system can be seen in Figure 1-10;[83]

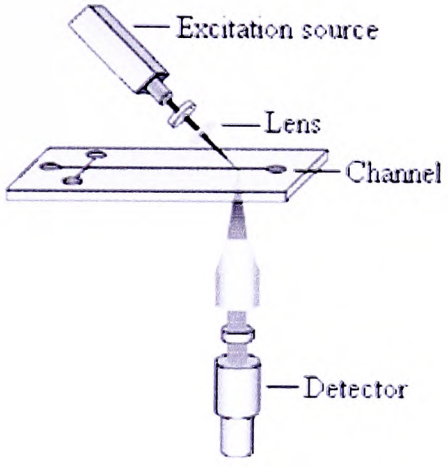

Figure 1-10 The concept of a fluorescent detection system

Zhu *et al.*[81, 82] for example created a time resolved detection scheme using four dyes that were excited and emitted in the Near-Infrared range, IRD700, IRD800, AlexaFluor680 and NIR-Br (a near-IR bromine-modified tricarbocyanine dye), and the detection system therefore involved near-infrared fluorescence with two pulsed-diode lasers (680 and 780 nm) and two avalanche photodiodes.

1.7.2 Excitation sources

An excitation source is required to excite the fluorescent tags that label the oglionucleotides, and make them fluoresce so they can be detected. There are many different excitation sources available with differing advantages and disadvantages;

Light-Emitting Diodes (LEDs) are a good possibility as an excitation source for an integrated system; they are very cheap, easily operated, portable and have small power consumption compared to many other sources available. However, they are not very powerful, efficiency quoted for standard devices is as low as 20%, and a lot of the emission is lost due to the difficulty in focusing the source down on to the narrow channel, the emission spectrum from a LED is also much broader and not monochromatic like the laser diode.[84]

LEDs are still an attractive option as a possible excitation source for the inclusion in the proposed end 'box', as the advantages of the LEDs over the laser diodes are a lower power requirement and a lower cost. However, these advantages are tempered with the many sensitivity issues within the detection system as a whole.

A variation to the LED is the Organic Light-Emitting Diodes (OLEDs),[85] where the photoresist layer is coated in an organic film, but their use has been more directed towards general space illumination as they emit less light per unit area than normal LEDs and the use in an integrated micro-fluidic device will be affected accordingly.

An alternative excitation source is a laser (known as laser induced fluorescence, LIF) which can offer high sensitivity and selectivity in the detection system, and is commonly used for detection in DNA sequencing machines.[86] Also the development of high quality laser diodes, small devices that are portable and capable of being operated

from a battery but with the same region of intensity as the bench top version (efficiency ranging from 50-80% depending on the device), makes them a credible option for a portable system. However, laser diodes are expensive compared to the other devices available.

1.7.3 Detectors

The photodetector is an important component of any optical detection system, and again the choice of which to use from the many available, is dependent on what compromises can be made within the integrated system;

Photodiodes are inexpensive and robust, have a good working linear range, experience low noise, and have a high quantum efficiency (approximately 80%), however, they have no internal gain, the response time is slow, and they have a small area of collection. Overall, the sensitivity of the photodiodes is low, and to improve the sensitivity requires integration of the signal.

Photo multiplier tubes (PMTs) have high bandwidth, good sensitivity, fast response times, a high gain and low noise capacity, they also have a large area of collection, capable of multiplying the signal produced by incident light by a factor of $10,^{9}$ and therefore do not require any form of integration of the signal. Nevertheless, compared to other detectors available they have low quantum efficiency.

Charge coupled device's (CCDs) are generally thought of as image sensors, they have improved wavelength selectivity and sensitivity compared to other PMTs allowing real time, multiplex analysis of the sample and have a high quantum efficiency

(approximately 90%).[87, 88] They have low light level detection and high signal to noise ratio.

The choice of detector used has implications on the type of filter system that will be required, as some devices are more sophisticated than others, but most devices cannot distinguish between the emission wavelengths of the coloured dyes, they only read the photon signal intensity. As described in Section 1.2.1, the dye system incorporates multiple dyes; in order to distinguish each of the dye colours, and therefore the alleles, a filter system may be required. Filter systems can be quite complex, especially in real time detection systems. Delivery methods exist such as rotating filter wheels, which are fitted with discreet narrow band filters in between the 'spokes', which allow the system to distinguish between the wavelength emissions. Lee et al. developed a system that contains an adaptive filter with a lower-upper-middle (LUM) algorithm, which eliminates any optical noise from the fluorescence information.[88]

Once the signal has been filtered, dichromatic mirrors are used to split the signal into its respective emission wavelengths which are sent in the direction of the right detection channel. The optical path of a detection system can lead to a degradation of the final signal by as much as 50% depending on the number of filters, mirrors, etc. are involved.

The sensitivity of the detection system can be a problem, especially on chip, aligning the optics in such a way that the excitation source and the detector both have sufficient access to the usually very narrow channel, whilst not interfering with each other is difficult; when filters are also needed the problem is compounded. Hanning *et al.*[86] achieved a high sensitivity total internal reflection (TIR) system by utilizing a Liquid Core Waveguide (LCW) to optimise the collection of the laser-induced fluorescence in a DNA sequencing system. The exterior of the separation capillary was coated with a

refractive index fluoropolymer (a lower refractive index than the separation medium), so the florescence emitted travelled down the LCW and was collected at the end of the capillary. Wang *et al.*[84] used the same principal to increase the sensitivity of a light-emitting diode detection system, using a Teflon AF coating to convert the separation capillary into a LCW.

There is also the possibility of using a commercial spectrometer, incorporating the optics and the detection, such as an *Ocean Optics spectrometer*, measuring light emitted across a specific wavelength range through a complete detection/capture system such as a fibre optic delivery directly into the spectrometer. The new generation spectrometers are small and portable; they are highly efficient and are already designed to be compatible with many forms of capture methods, such as fibre, negating the need to incorporate features such as filters, dichromatic mirrors, etc., reducing the amount of engineering that the integrated system will require.

1.8 Conclusions

Utilising the lab on a chip approach allows the possibility to develop a fully integrated system for DNA analysis. The system would be designed to utilise the same 11 core loci as used in the SGM Plus kit. The fluorescence detection system would also be based on the same multiplex approach of the four dyes to ensure rapid separation and detection.

The particular aspects of developing the system that were studied in this thesis are the parameters for system integration, which include;

1. Use of electro-kinetic movement for washing/elution, loading and injecting and separation

2. Electrophoresis in polymer matrices

3. Characterisation of dyes for detection in the optical system

Chapter 2: Reagents and Instrumentation

2 Aim

The aim of this chapter was to provide a detailed account of the reagents and instrumentation utilised as part of the experimental procedure undertaken in this thesis.

2.1 Reagents

Table 2-1 provides a list of the main chemicals used throughout the course of this thesis.

Table 2-1 Table of chemical reagents and the suppliers

Reagents	Supplying company
Acryloyl chloride	Sigma Aldrich (Poole, Dorset, UK)
Agarose gel - Low gelling point (36°C)	Sigma Aldrich (Poole, Dorset, UK)
Agarose gel – Standard	Bioline Ltd (The Edge Business Centre, London, UK)
Ammonium buffer (NH_4)	Bioline Ltd (The Edge Business Centre, London, UK)
Ammonium persulfate, 98% (APS)	Sigma Aldrich (Poole, Dorset, UK)
Azobiz(4-cyanopentenoic acid)	Sigma Aldrich (Poole, Dorset, UK)
Boric acid	Sigma Aldrich (Poole, Dorset, UK)
Bovine serum albumin (BSA)	Bioline Ltd (The Edge Business Centre, London, UK)
Bromophenol blue	MBI Fermentas UK (Sheriff Hutton, York, UK)
Dichloromethane (DCM)	Sigma Aldrich (Poole, Dorset, UK)
Dihexylamine	Sigma Aldrich (Poole, Dorset, UK)

Reagents	Supplying company
dNTP's	Bioline Ltd (The Edge Business Centre, London, UK)
Ethylenediaminetetra-acetate (EDTA)	Sigma Aldrich (Poole, Dorset, UK)
Ethidium bromide	Sigma Aldrich (Poole, Dorset, UK)
Formamide, 98%	Avocado Research Chemicals Ltd (Morecambe, UK)
GoTaq® (Hot start Taq DNA polymerase)	Promega (Hampshire, UK)
Guanidine hydrochloride	Sigma Aldrich (Poole, Dorset, UK)
Hydrochloric acid (HCl)	Sigma Aldrich (Poole, Dorset, UK)
Hydroxyethyl cellulose (HEC)	Sigma Aldrich (Poole, Dorset, UK)
Loading dye	MBI Fermentas (Sheriff Hutton, York, UK)
Magnesium chloride (MCl_2)	Bioline Ltd (The Edge Business Centre, London, UK)
Milli-Q water	Milli-Q-column (Millipore Ltd, Livingston, UK)
N,N dimethylacrylamide solution, 40%	Sigma Aldrich (Poole, Dorset, UK)
N,N,N',N'- tetramethylyene-diamine, 99% (TEMED)	Sigma Aldrich (Poole, Dorset, UK)
NN',-methylenebisacylamide solution, 2%	Sigma Aldrich (Poole, Dorset, UK)
Oligonucleotide primers (see Table 2-2)	Ordered to specification from MWG Biotech (Ebserberg, Germany)
Polyethylene oxide (PEO), Average Mv ~ 600,000 powder	Sigma Aldrich (Poole, Dorset, UK)
Polyethylene oxide (PEO), Average Mv ~ 8,000,000 powder	Sigma Aldrich (Poole, Dorset, UK)
Potassium silicate, 9% K_2O, 21% SiO_2	Prolabo (Merck, supplied by VWR International Ltd, Lutterworth, Leicestershire, UK)
QIAamp® DNA Micro Kit	Qiagen (Qiagen House, West Sussex, UK)

Reagents	Supplying company
Quant-iT™ PicoGreen® dsDNA Assay kit	Invitrogen Ltd (Paisley, Scotland, UK)
REAX™ MASTERMIX 25 PCR Beads	Q Chip Life Science, Q Chip Ltd, (Cardiff, Wales, UK)
Sodium dodecyl sulphate (SDS)	Sigma Aldrich (Poole, Dorset, UK)
Sodium Hydroxide (NaOH)	Sigma Aldrich (Poole, Dorset, UK)
Triethylamine	Sigma Aldrich (Poole, Dorset, UK)
Tris(hydroxymethyl) aminomethane (Tris)	Fisher Scientific UK Ltd (Loughborough, Leicestershire, UK)

Table 2-2 Table of the oglionucleotide primers used throughout the experimental procedure, supplied by *MWG Biotech* (Ebersberg, Germany)

Amelogenin	Forward	5′-CCCTGGGCTCTGTAAAGAATAGTG-3′
	Reverse	5′-ATCAGAGCTTAAACTGGGAAGCTG-3′
D16S539	Forward	5′-ACTCTCAGTCCTGCCGAGGT-3′
	Reverse	5′-TGTGTGTGCATCTGTAAGCATG-3′
vWA	Forward	5′-GGACAGATGATAAATACATAGGATGGATGG-3′
	Reverse	5′-GCCCTAGTGGATGATAAGAATAATCAGTATGTG-3′
FGA	Forward	5′-GGCTGCAGGGCATAACATTA-3′
	Reverse	5′-ATTCTATGACTTTGCGCTTCAGGA-3′
THO1	Forward	5′-GTGATTCCCATTGGCCTGTTC-3′
	Reverse	5′-ATTCCTGTGGGCTGAAAAGCTC-3′
D8S1179	Forward	5′-ACCAAATTGTGTTCATGAGTATAGTTTC-3′
	Reverse	5′-ATTGCAACTTATATGTATTTTTGTATTTCATG-3′

2.1.1 Preparation of reagents

2.1.1.1 0.5 M ethylenediaminetetraacetate solution

Ethylenediaminetetraacetate (EDTA) (Figure 2-1) is a polyamino carboxylic acid commonly used as a chelating agent, binding to metal cation's present in the solution and reducing the reactivity, EDTA also inactivates enzymes that require the metal ions for functionality.

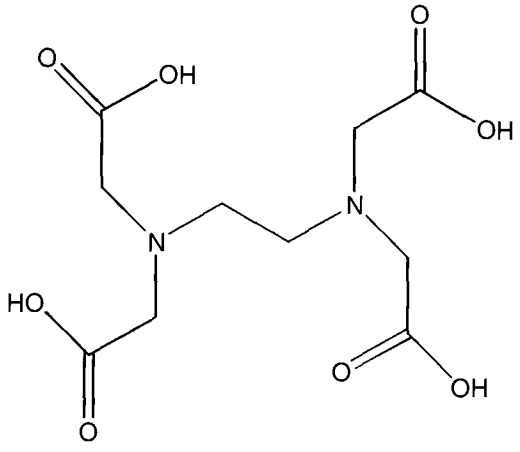

Figure 2-1 Chemical structure of ethylenediaminetetraacetate (EDTA)

A 0.5 M solution of EDTA was prepared in a 1000 ml volumetric flask, 186.1 g of EDTA was dissolved in 900 ml of Milli-Q water. The pH of the solution was then adjusted to a pH of 8 by drop-wise addition of 1 M NaOH, the flask was then filled to the mark, of 1000 ml.

2.1.1.2 1 M Tris(hydroxymethyl) aminomethane solution

Tris(hydroxymethyl) aminomethane (Tris) (Figure 2-2) is a common component of many biological buffer solutions, with a pK_a of 8.06 and a effective pH range between approximately 7 and 9.

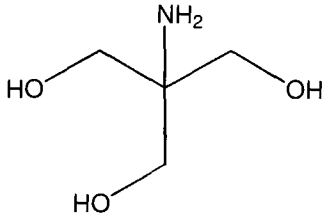

Figure 2-2 Chemical structure of Tris(hydroxymethyl) aminomethane (Tris)

A 1 M solution of Tris was prepared in a 500 ml volumetric flask, 60.47 g of Tris was dissolved in 450 ml of Milli-Q water. The pH of the solution was then adjusted to a pH of 7.5 by drop-wise addition of 1 M HCl, the flask was then filled to the mark, of 500 ml.

2.1.1.3 Tris-EDTA buffer solution

Tris-EDTA buffer (TE buffer) is a common biological buffer typically used to protect DNA or RNA from degradation, it can be utilised at either pH 7.5 or pH 8 depending on if used in conjunction with RNA or DNA respectively.

A 10 X solution of TE buffer was prepared in a 500 ml beaker, where 400 ml of 1 M Tris(hydroxymethyl) aninomethane and 80 ml of 0.5 M EDTA were mixed in the beaker, the pH of the solution was then adjusted to a pH of 8 by drop-wise addition of 1 M NaOH.

2.1.1.4 5 x TBE buffer

Tris(hydroxymethyl) aminomethane base, boric acid and EDTA make up the common biological buffer TBE buffer. TBE buffer is used most frequently with nucleic acids, specifically as the buffer used in the separation matrix for electrophoresis.

A 5 X solution of TBE buffer was prepared in a 1000 ml volumetric flask, 54 g of tris(hydroxymethyl) aminomethane and 27.5 g boric acid were dissolved in 900 ml of deionised water, to which 20 ml of 0.5 M EDTA was added, deionised water was added to adjust the final volume of the solution to 1000 ml.

2.1.1.5 Guanidine hydrochloride

Guanidine is a strong base which is naturally found in urine as a product of protein metabolism. Guanidine hydrochloride is a common guanidine salt notable for its chaotropic properties and can be used to denature proteins (Figure 2-3).

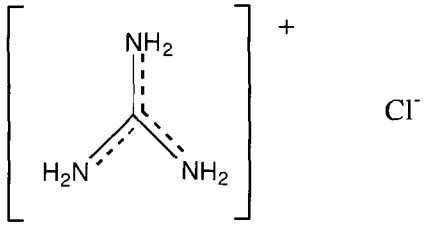

Figure 2-3 Chemical structure of guanidine hydrochloride

A 5 M solution of guanidine hydrochloride was prepared in a 10 ml volumetric flask, 4.8 g of guanidine hydrochloride was dissolved in 9 ml of deionised water, when the crystalline solid was fully dissolved the flask was filled to the mark with deionised water.

2.1.1.6 PicoGreen for DNA analysis and quantification

Quant-iT™ PicoGreen® dsDNA reagent is a very sensitive fluorescent stain that binds to nucleic acids in DNA, however the fluorescence is only activated when the DNA is double stranded. Therefore, Quant-iT™ PicoGreen® dsDNA assay kit is a powerful tool for the quantification of double stranded DNA, allowing successful quantification of as little as 25 pg ml^{-1}.[89]

The PicoGreen fluorescent stain is prepared by adding 12 µl of stock solution in 5 ml of 1 X TE buffer, to quantify dsDNA, 2 µl of PicoGreen is added to 50 µl of sample. To successfully quantify DNA, a standard curve is required; several standards of DNA in serial concentration are provided with the assay kit against which measurement can be made.

2.1.2 Preparation of separation polymers

2.1.2.1 Poly(ethylene) oxide (PEO)

Polyethylene oxide (PEO) powder was dissolved in 1 x TBE buffer, and allowed to form by the prolonged stir method.[70] Simply, the polymer is slowly dissolved at a slow stir speed for several hours in order to reduce the amount of air introduced into the polymer. During this investigation a number of concentrations of the PEO polymer were investigated in the range of 2 to 3% (w/v).

2.1.2.2 Hydroxyethylcellulose (HEC)

Hydroxyethylcellulose (HEC) was made up to a concentration of 1% by two different methods,[90] the first and a standard method, in which 0.1007 g of HEC powder was dissolved in 10 ml of 1 x TBE buffer solution, the solution was stirred for two hours at 100 rpm then degassed for two hours. The second method based on prolonged stirring in which 0.1012 g of HEC powder was dissolved in 10 ml of 1 x TBE solution, and the solution was then stirred at 60 rpm for a minimum of 12 hours. This second method proved to be successful, producing a solution that was free of trapped air, and was less involved to prepare. A 2% HEC solution (0.2005 g in 10 ml of 1 x TBE) was also made by the prolonged stirring method.

2.1.2.3 Linear poly acrylamide (LPA)

Linear poly acrylamide (LPA) was prepared by pipetting 2.44 ml (± 1%) of 40% acrylamide solution, 1.30 ml of 2% NN',- methylenebisacrylamide solution, 4 ml 5 x TBE buffer and 12.045 ml deionised water into a sample tube. The solution was mixed and degassed with helium for 2 hours before being polymerised by adding 200 µl of ammonium persulfate (APS) and 20 µl of N,N,N',N'-tetramethlyene-diamine (TEMED), after which the solution was left to polymerise for several hours.

2.1.2.4 Linear poly acrylamide-co-Dihexylacrylamide (LPA-co-DHA)

LPA-co-DHA is a separation co-polymer described by Chiesl,[91] LPA forms a co-polymer with N,N-Dihexylacrylamide (DHA) (Figure 2-4) by micellular co-polymerisation. To make the DHA, an oven dried 500 ml round bottom flask was submerged into an ice bath, to 60 ml of dichloromethane (DCM) 618 µl of

dihexylamine and 603 µl triethylamine was added and mixed for 5 minutes. 625 µl acryloyl chloride was added to a further 60 ml of DCM, mixed and introduced to the round bottom flask and subjected to further mixing for a period of 5 minutes.

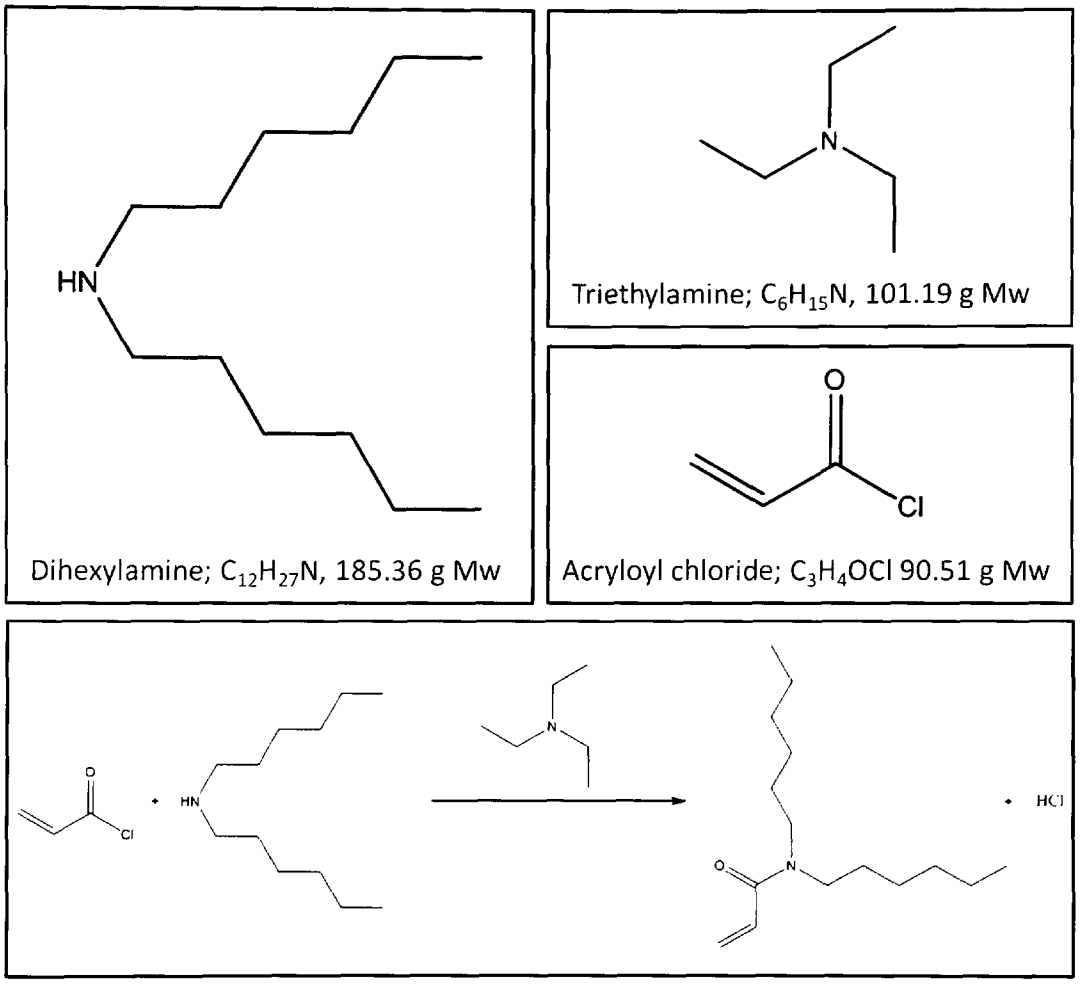

Figure 2-4: Primary chemical reactants, and reaction scheme of the formation of DHA

The resulting solution was washed repeatedly by first adding 50 ml of 0.1 M sodium hydroxide (NaOH) to the solution and mixed thoroughly before transferring to a separating funnel. The solution was allowed to settle and the bottom layer was siphoned off and transferred to a clean vessel, the drying agent magnesium sulphate was added to remove any traces of water present, and filtered out. The filtered solution was

transferred back to the separating funnel and the procedure repeated with 0.1 M hydrochloric acid (HCl) and finally distilled water. The solvent was removed from the solution by rotary evaporation; the remaining solution was proven to be DHA by analysis with head space mass spectrometry (see Figure 2-5 and Figure 2-6).

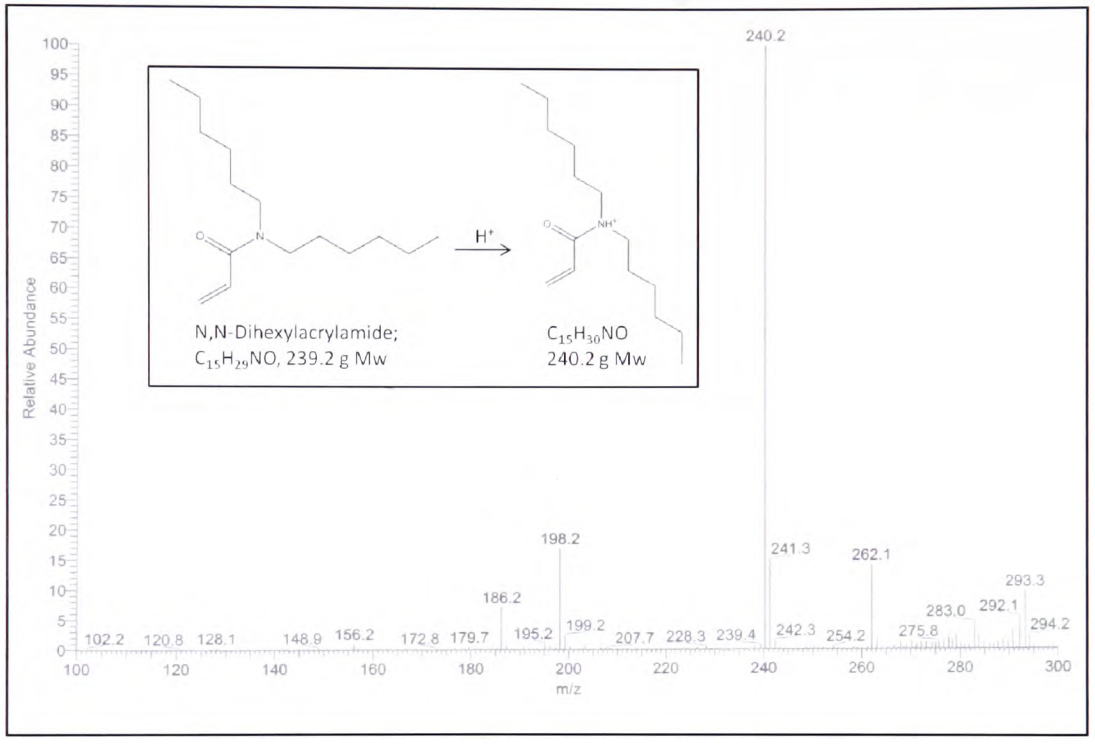

Figure 2-5: Mass spectrum of DHA, internal diagram illustrating molecular ionisation of DHA

The internal diagram shown in Figure 2-5 displays the molecular ionisation of DHA, the molecular formula and the molecular weight of 240.2 g, analysis of the mass spectrum shows the predominant peak to be at 240.2 m/z, strongly suggesting that the solution contained DHA.

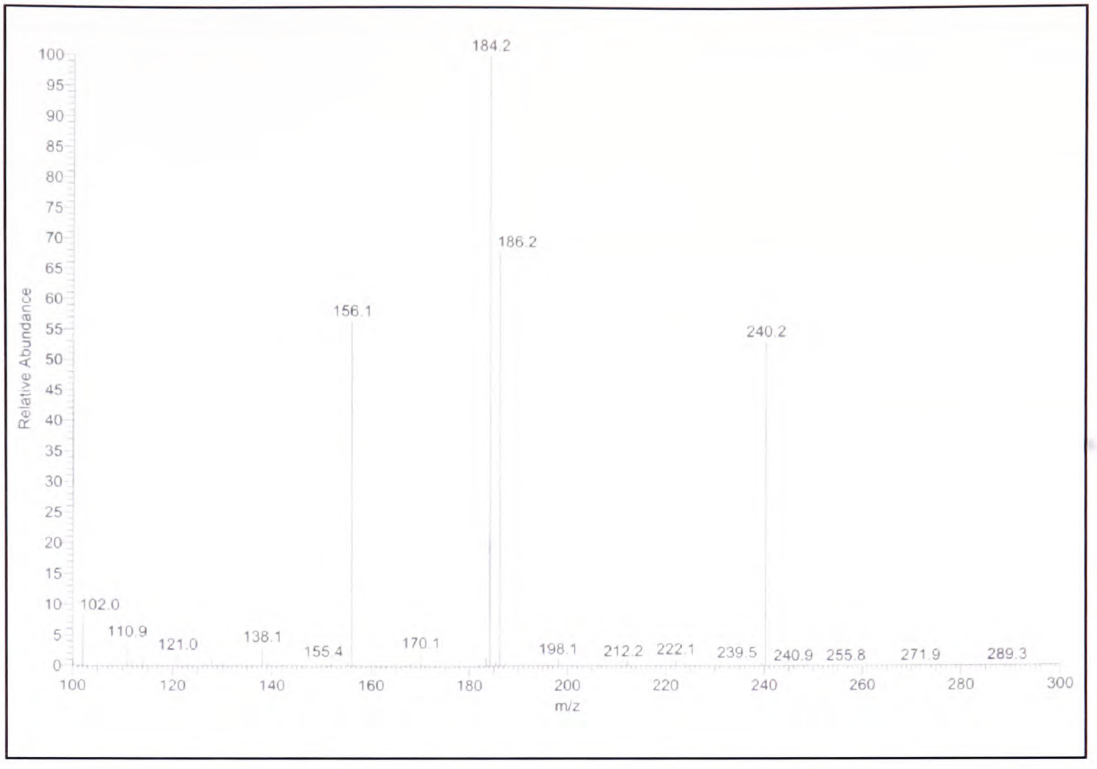

Figure 2-6: Mass spectrum of electron ionisation fragmentation of DHA

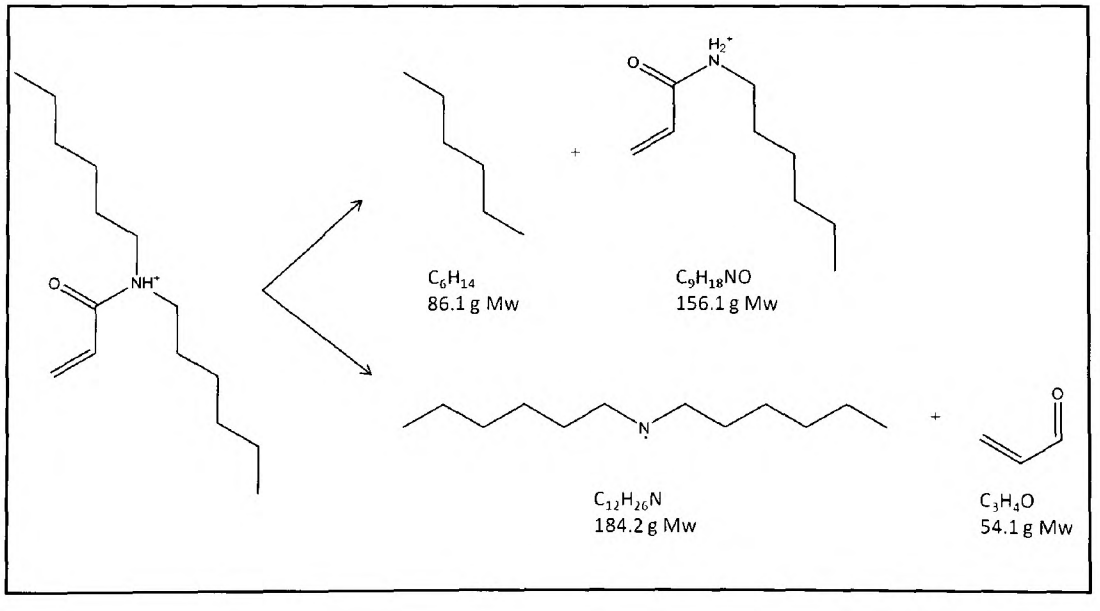

Figure 2-7: Corresponding fragmentation

Further analysis of the solution produced by electron ionisation fragmentation (Figure 2-6) indicates predominant peaks at 156.1 m/z, 184.2 m/z, 186.2 m/z and 240.2 m/z, Figure 2-7 displays the fragmentation of DHA, and the corresponding molecular weights of the derivatives. Again, the analysis strongly confirms the presence of DHA.

After the formation of the DHA, and subsequent analysis, the co-polymer was produced. The DHA was deposited into a clean an oven dried 250 ml round bottom flask, to which 2.5 g of sodium dodecyl sulphate (SDS) was added (Figure 2-8).

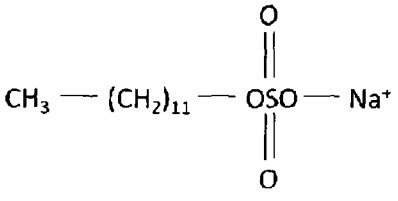

Figure 2-8: Sodium dodecyl sulfate

SDS is used to form micelles with the DHA molecule, the hydrocarbon side chains congregate in the centre of the micelle anchoring to the base, in this case the DHA molecule, and the carboxylate groups are exposed on the outside of the micelle, thus forming the basis of micellular polymerisation. The SDS and the DHA were mixed together at a slow speed with a metal stirrer, 100 ml of deionised water was added to the DHA and SDS reactants and stirred for 5 minutes. 7.5 ml of 40% acrylamide solution was added and mixed under nitrogen for 30 minutes. A water bath was prepared to a temperature of 50°C, in to which the round bottom flask was submerged, 0.045 g of azobis(4-cyanopentanoic acid) was added and the solution again sealed under a nitrogen atmosphere with a slow stir speed. The solution was monitored to observe when polymerisation had taken place, when it was established polymerisation had taken place

sufficiently; the flask was submerged into an ice solution in order to prevent further polymerisation.

The polymerised solution was then transferred to a dialysis membrane, and submerged in a covered beaker of deionised water for a period of several days. The membrane is designed so that molecules below a certain size will move out of the membrane into the beaker of water in order to control the size of the polymer; the water in the beaker was replaced periodically in order to ensure completion of this process.

To the polymerised co-polymer solution 200 ml of deionised water was added, this was then left to be absorbed into the polymer with the aid of gentle agitation. After 60 minutes the solution was poured into a 1 litre beaker, the co-polymer was drawn out of the solution by adding 5 ml aliquots of acetone and stirring, this was repeated until 100 ml of acetone was added and no more evidence of precipitation could be seen. The acetone was added in this manner in order to remove as much impurity from the co-polymer as possible. The precipitate was a white, slimy, foam like mass, which was filtered under vacuum to remove any residue of acetone, and then cut into small sections and freeze dried under vacuum using a Lyotrap freeze dryer. The freeze dried co-polymer was crushed into a fine powder by pestle and mortar, and then stored at 0°C until required.

The separation polymer was formed by dissolving the powder in 1 x TBE buffer according to weight per volume percentage.

2.1.2.5 Calculating the theoretical molar mass of LPA-co-DHA

The degree of polymerisation was calculated from Equation 2-1[92]

Equation 2-1

$$\textbf{Degree of polymerisation } (dp) = \frac{[monomer]}{[initiator]}$$

Equation 2-2

$$Theoretical\ molar\ mass = dp \times Mr$$

However, when considering a copolymer, the degree of polymerisation for each monomer must be first calculated. Therefore, when considering copolymer A_a-co-B_b, the molecular weight of the polymer can be determined by multiplying the degree of polymerisation with the molecular weight of the monomer;

Firstly, 0.045 g of the initiator, 4,4'-azobis(4-cyanopentanoic acid) (molecular mass of 280.29g), was added, which is 0.00016 moles.

In this case acrylamide was the monomer$_a$, 7.5 ml of acrylamide solution was added to the copolymer. The solution has a density of 0.4 gml^{-1}, therefore a weight of 3.0 g was added which equates to 0.0422 moles, the degree of polymerisation of monomer$_a$ is indicated in Equation 2-3.

Equation 2-3

$$dp_a = \frac{[monomer_a]}{[initiator]} = \frac{0.0422}{0.00016} = 262.97$$

Monomer$_b$ was the dihexylacrylamide, which was prepared by a 1:1 reaction between dihexylamine and acryoyl chloride in the presence of triethylamine. 0.618 ml of dihexylamine was pipetted into the reaction, it has a molecular weight of 185.36 g and a density of 0.795 gml^{-1}, therefore a mass of 0.491 g was added, equating to a 0.00265 moles. 0.625 ml of acryoyl chloride was added to the reaction, it has a molecular weight

of 90.51 g and a density of 1.114 gml^{-1}, therefore a mass of 0.696 g was added, equating to a 0.00769 moles.

$$dp_b = \frac{[monomer_b]}{[initiator]} = \frac{0.00265}{0.00016} = 16.51$$ **Equation 2-4**

As the reaction was 1:1, we can determine the acryolyl chloride was added to the reaction in excess, therefore the maximum theoretical number of moles of dihexylacrylamide was determined by the number of moles of dihexylamine.

$$Theoretical\ M = (dp_a \times Mr_a) + (dp_b \times Mr_b)$$ **Equation 2-5

$$= (262.97 \times 71.08) + (16.51 \times 239.20)$$

$$= 22641.76\ g$$

2.2 Instrumentation

2.2.1 The micro fluidic device

2.2.1.1 Fabrication of borosilicate micro-fluidic devices

Figure 2-9 outlines the fabrication process undertaken to produce all the micro-fluidic devices used in this study.[93] The borosilicate base plate is coated in a thin layer of chromium by vapour deposition, to which a photo-resist layer is spin coated on to the surface (supplied by TELIC 1631 (Santa Monica, California, USA)). The optical mask, a specific channel design drawn with the technical drawing package, AutoCAD (supplied by *Autodesk* (Farnborough, Hampshire, UK)) and produced by *JD Photo-Tools* (Oldham, UK), is then placed on the base plate. The surface is then exposed to

UV light, the photo-resist layer exposed through the optical mask is developed, and the exposed metal layer is removed. The base plate is then heated to harden the photo-resist layer and remove any residual solvents from the surface. The wet etching of the channel is performed using a solution of 1% HF and 5% NH_4F in water at 70 °C.[94] Once complete, the photo-resist and metal layers are removed the top plate, complete with wells drilled into position, is thermally bonded at a temperature of approximately 500 to 600 °C.

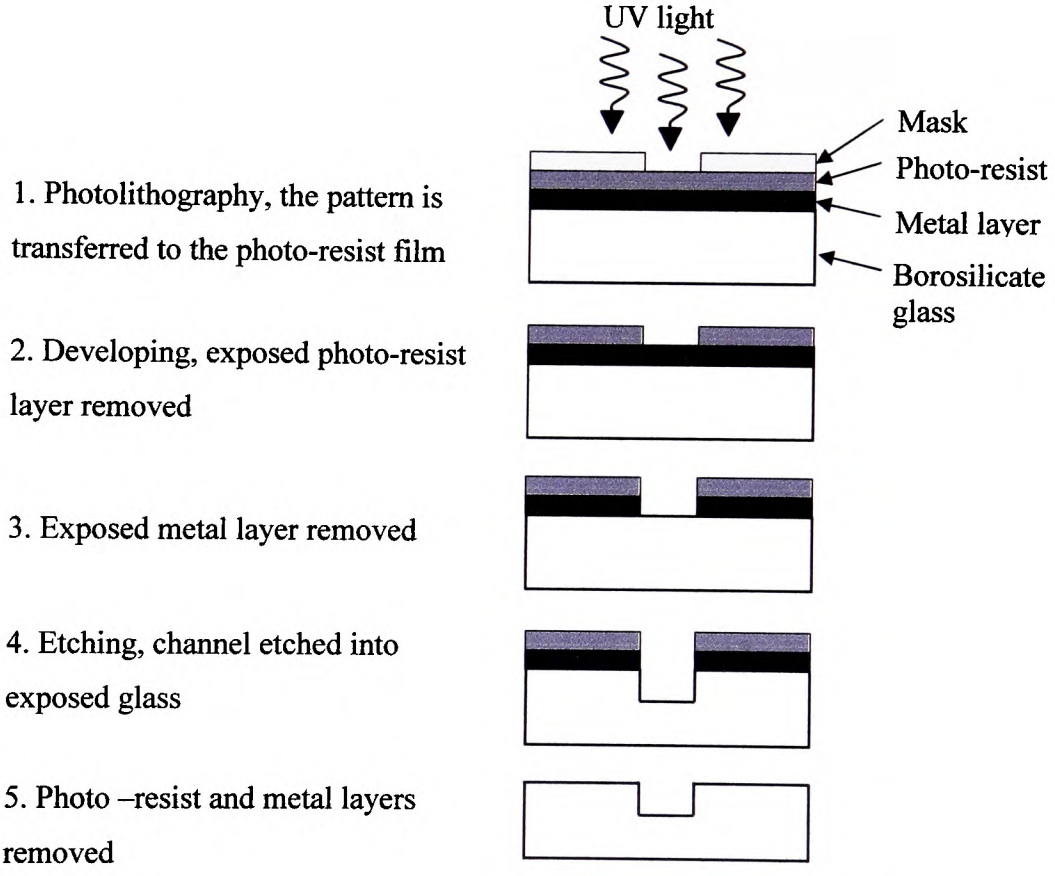

Figure 2-9 Schematic illustration of fabrication process of micro-fluidic devices

2.2.1.2 Base plate designs

The micro-fluidic device designs used in the work contributing to this thesis are shown in Figures 2-10 to 2-20.

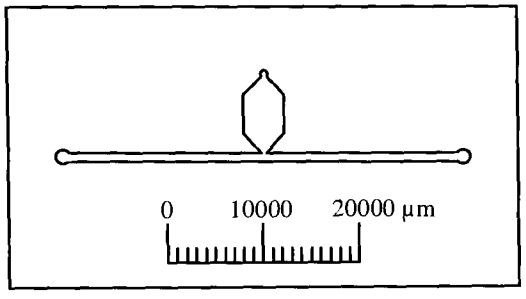

Figure 2-10 Micro-fluidic device design 1: Channels are etched to a depth of 80 µm and a width of 1000 µm, hexagonoal dimensions; 4000 by 8000 µm.

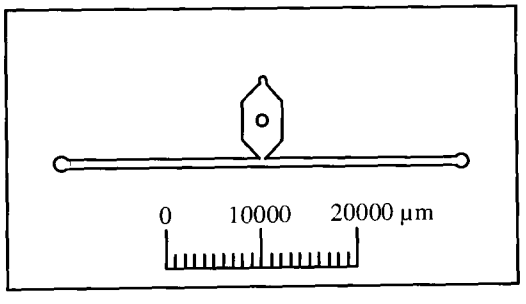

Figure 2-11 Micro-fluidic device design 2: Channels are etched to a depth of 80 µm and a width of 1000 µm, hexagonoal dimensions; 4000 by 8000 µm. A well is drilled into the top plate at the centre of the hexagonoal chamber.

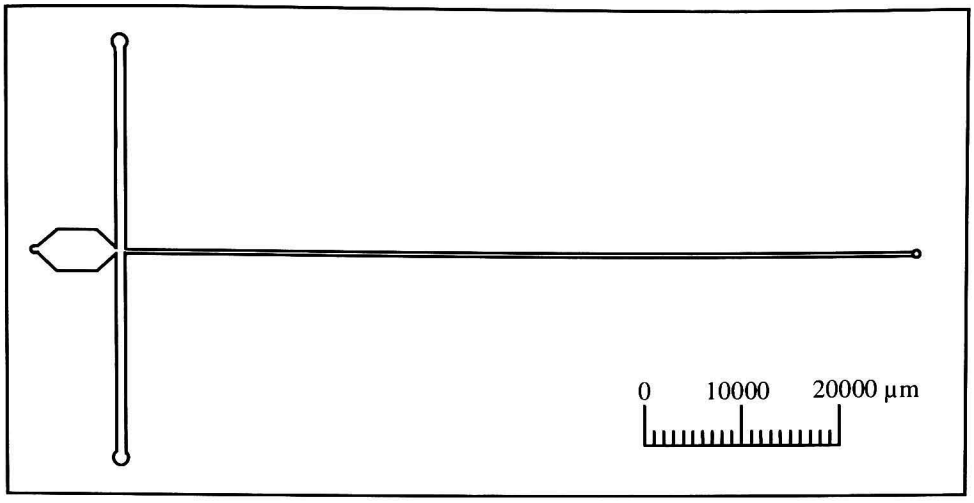

Figure 2-12 Micro-fluidic device design 3: Channels are etched to a depth of 80 µm and widths of 1000 and 200 µm, hexagonoal dimensions; 4000 by 8000 µm.

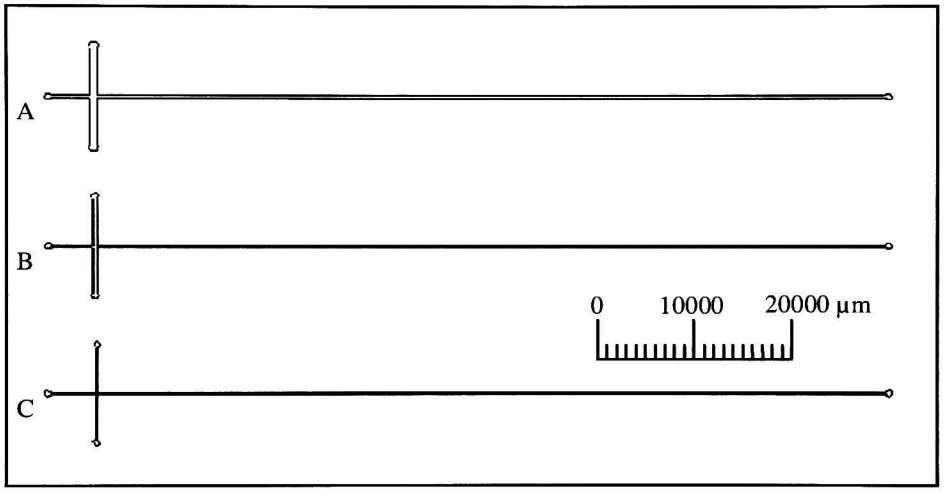

Figure 2-13 Micro-fluidic device design 4: All channels are etched to a depth of 40 µm. A channel widths; 300 µm and 900 µm. B channel widths; 200 µm and 600 µm, channel widths; 100 µm and 300 µm.

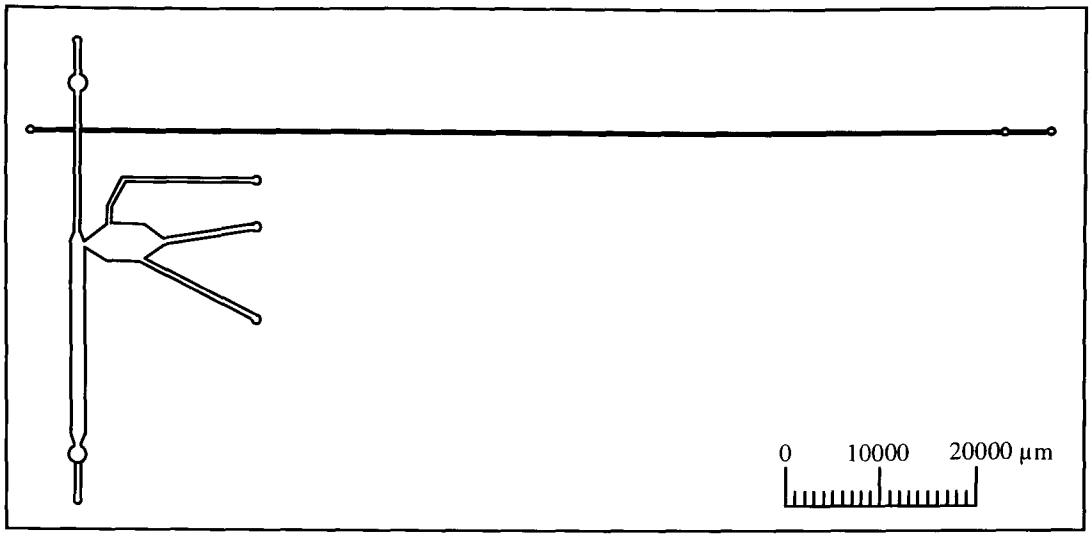

Figure 2-14 Micro-fluidic device design 5: The base plate is etched to a depth of 80 µm, the top plate is etched to a depth of 180 µm, all features except the separation channel are double etched. Vertical channel widths of 1500 and 600 µm, separation channel width of 200 µm, hexagonoal dimensions; 4000 by 8000 µm, channel widths from hexagonal chamber of 600 µm.

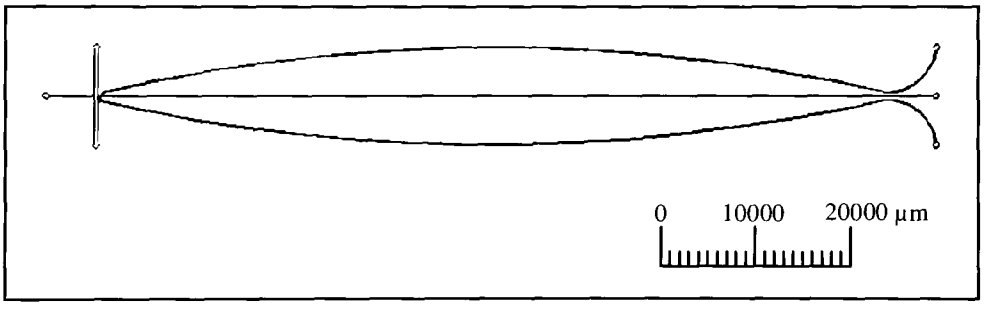

Figure 2-15 Micro-fluidic device design 6: Channels are etched to a depth of 50 µm, vertical channel widths of 600 µm and the separation channel has a width of 200 µm.

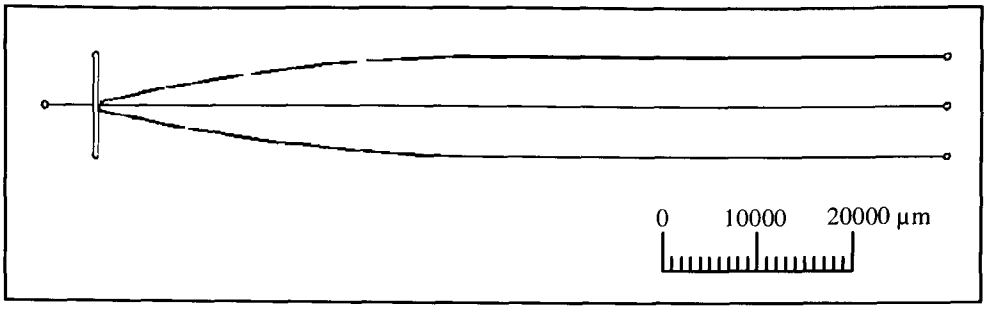

Figure 2-16 Micro-fluidic device design 7: Channels are etched to a depth of 50 µm, vertical channel widths of 600 µm and the separation channel has a width of 200 µm.

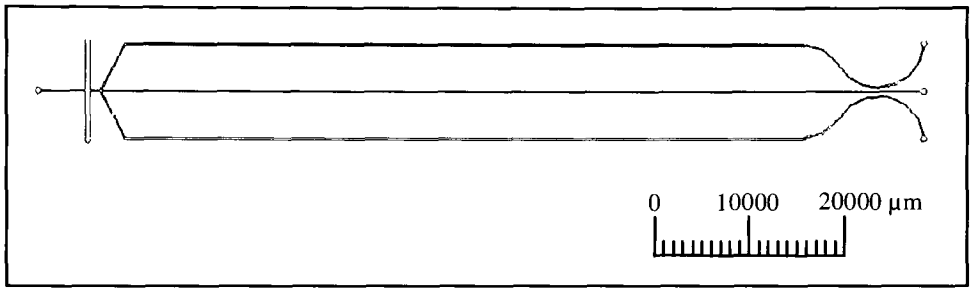

Figure 2-17 Micro-fluidic device design 8: Channels are etched to a depth of 50 µm, vertical channel widths of 600 µm and the separation channel has a width of 200 µm.

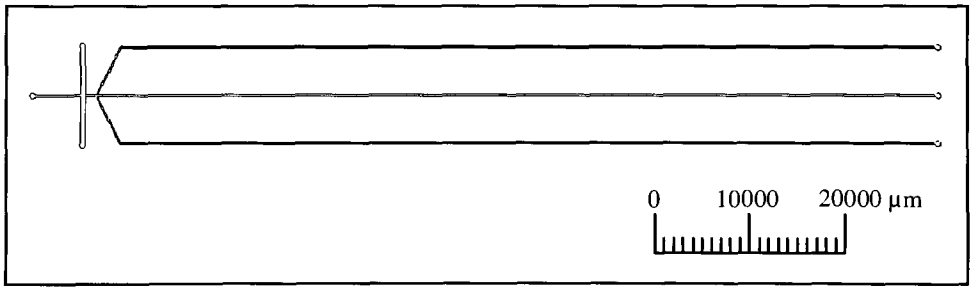

Figure 2-18 Micro-fluidic device design 9: Channels are etched to a depth of 50 µm, vertical channel widths of 600 µm and the separation channel has a width of 200 µm.

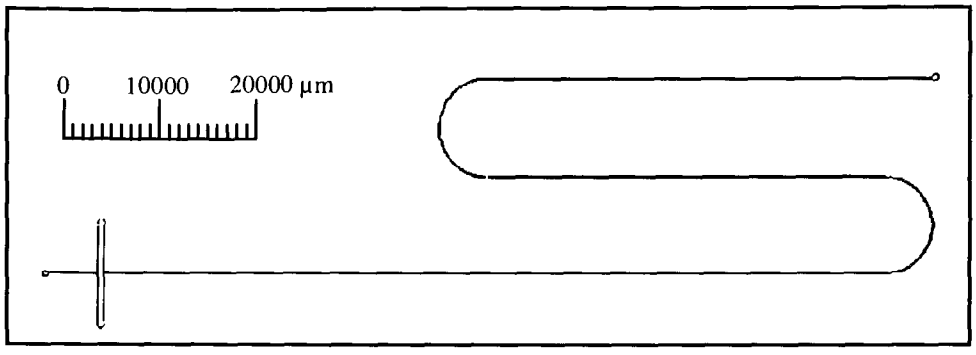

Figure 2-19 Micro-fluidic device design 10: Channels are etched to a depth of 50 µm, vertical channel widths of 600 µm and the separation channel has a width of 200 µm.

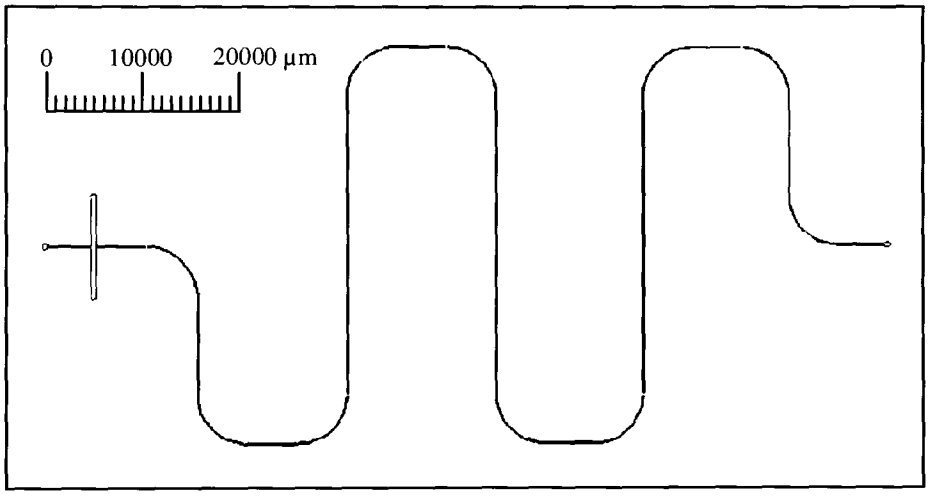

Figure 2-20 Micro-fluidic device design 11: Channels are etched to a depth of 50 µm, vertical channel widths of 600 µm and the separation channel has a width of 200 µm.

2.2.2 Electro-kinetic movement

A Paragon 3B power supply unit, containing input and output control of four separate 0-1000 V D.C. power supplies, custom built by *Kingfield Electronics Ltd* (Chesterfield, Derbyshire, UK) was utilised for the operation of EOF. For electrophoresis, a power supply capable of providing a higher voltage was required and an H Series compact, regulated power supply (0-10,000 V D.C.) was supplied by *EMCO High Voltage*

Corporation (Sutter Creek, California, USA). Both the Paragon 3B and the H Series power supply units were controlled using LabView software (version 5.0), written and supplied by *National Instruments Corporation Ltd* (Newbury, Berkshire, UK). Platinum wire, diameter 500 μm, acted as electrode contacts and was supplied by *Johnson Matthey* (London, UK). A voltmeter was required for external confirmation of data provide by LabView, and to monitor currents generated by the 10 kV H Series compact power supply, a 1906 Computing Multimeter was used, supplied by *Thurlby Thandar Instruments Ltd.* (Huntingdon, Cambridgeshire, UK).

2.2.3 Laser induced fluorescence detection

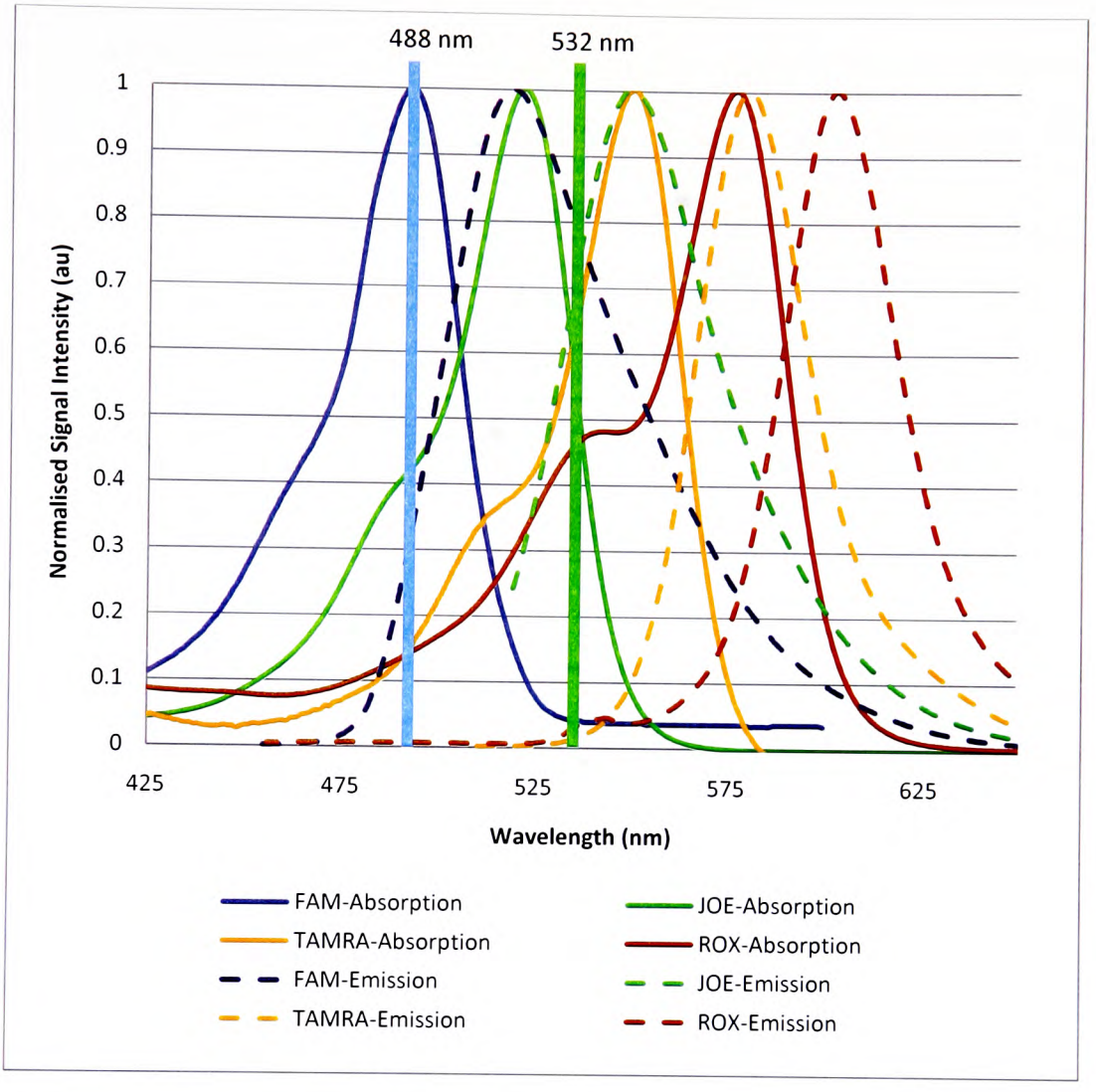

Figure 2-21 Absorption and Emission spectra of the four dyes commonly used to label the oglionucleotides, 5-carboxyfluorescein, succinimidyl ester (5-FAM, SE) *single isomer*, 6-carboxy-4',5'-dichloro-2',7'-dimethoxyfluorescein, succinimidyl ester (6-JOE, SE), 6-carboxytetramethylrhodamine, succinimidyl ester (6-TAMRA, SE) *single isomer*, and 6-carboxy-X-rhodamine, succinimidyl ester (6-ROX, SE) *single isomer*.

The laser induced fluorescence detection system included two lasers diodes; the blue laser was a continuous wave frequency-doubled solid state blue laser, Model number: FCD488, JDSU, supplied by *Photonic Products* (Hatfield Broad Oak, Hertfordshire,

UK). It had a wavelength of 490 ± 2 nm, a CW output power of 20 mW, a beam divergence of 0.3 mRad, and a beam diameter of 0.4 mm. The variable output power was computer controlled, by *HyperTerminal software*, *Hilgrave* (Monroe, Michigan, USA).

The green laser was a diode pumped green *CrystaLaser®*, *CrystaLaser®* (Reno, Nevada, USA). It had a wavelength of 532 nm, a CW output power of 10 mW, a beam divergence of 2 mrad, and a beam diameter of 0.36 mm. The lasers were chosen due to their ability to excite the four dyes, falling in the absorption spectrum of each at the most optimum point available.

The detection system that was utilised was an Ocean Optics S2000 fiber optic spectrometer, supported by 001Base32 Spectrometer Operating Software, *Ocean Optics Inc.* (Dunedin, Florida, USA). The spectrometer was utilised due to its suitability and adaptability within the detection box, the fibre optic allows for the angle of the detection to change according to what point of the device the detection point was determined to be, in addition the spectrometer was chosen due to its availability.

Additional specialised optical and photonic equipment was supplied by *Melles Griot* (Huntingdon, UK), and included various accurate positioning equipment and mirrors, which are indicated in Figure 2-22. The equipment was chosen by necessity to achieve the correct angle of excitation and detection.

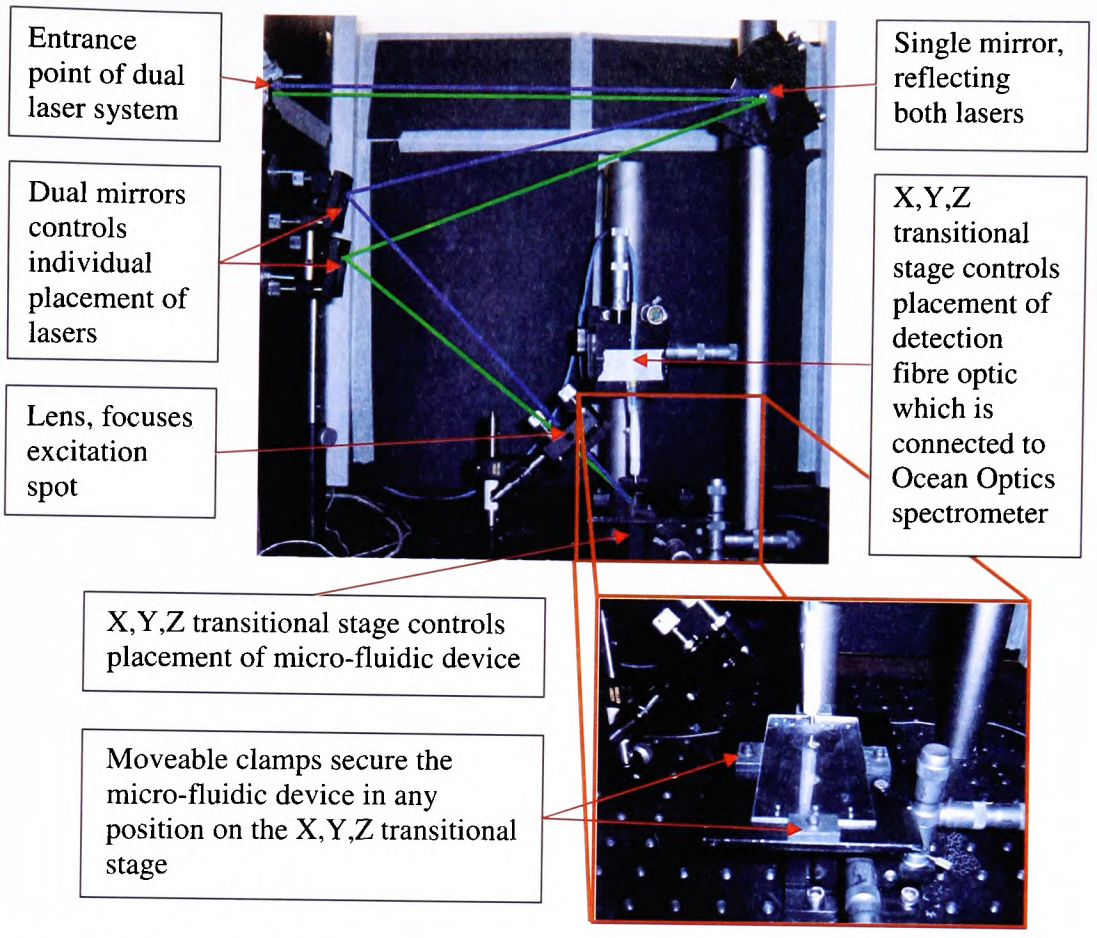

Figure 2-22 Fibre optic detection system used for all fluorescent detection work performed in a micro-fluidic device, incorporating a dual laser detection system. (Inset) Close up of micro-fluidic device clamped into position within the detection system.

Visualisation of the movement of the fluorescently labelled PCR products were recorded with a Zeiss Axiovert S 100 fluorescence microscope coupled to a Hamamatsu ORCA-ER digital camera, *Leeds Precision Instruments* (Boone Avenue North, Minneapolis, USA).

Characterisation of the fluorescent dyes was achieved using a Perkin Elmer Lambda 25 UV-Visible spectrometer, *Perkin Elmer Inc.* (Waltham, Massachusetts, USA).

2.2.4 Miscellaneous instrumentation

Hydrodynamic pumping was performed using a KDS200 Syringe Infusion Pump supplied by *Kd Scientific* (Holliston, Massachusetts, USA).

All PCR amplification was performed in a TECHNE TC-312 Thermal Cycler supplied by *Barloworld Scientific* (Bibby Scientific Ltd, Staffordshire UK).

'PCR plates' were first separated by agarose slab gel electrophoresis in which 115 V was applied for 45 min, using a Horizontal Electrophoresis tank, SCIE PLAS with MD-250N OmniPAC MIDI power supply (*SCIE PLAS*, Warwickshire, UK). After staining with 0.5 $\mu g ml^{-1}$ ethidium bromide the separated products were visualised using a UV transilluminator supplied by *Syngene* (Synoptics Ltd, Cambridge, UK).

Extracted DNA was quantified using a POLARStar OPTIMA plate reader supplied by *BMG LABTECH Ltd* (Aylesbury, UK), used in conjunction with the Quant-iT™ PicoGreen® dsDNA Assay kit.

The prepared co-polymer was freeze dried under vacuum using a Lyotrap freeze dryer, manufactured by *LTE Scientific Ltd* (Oldham, UK).

An MIX4150 Grant Vortex mixer PV1 supplied by *SLS* (Hull, East Yorkshire, UK) was used to appropriately mix the PCR reagents before the amplification and products before analysis.

The micro-tube used to connect syringe to the micro-fluidic device were supplied by *Anachem* (Luton, Bedfordshire, UK), and the micro-tubes connectors used to connect the sample syringes to the micro-tube were supplied by *Supelco, Sigma-Aldrich company Ltd.* (Poole, Dorset, UK).

Genetic sequence of DNA samples and size standards were performed on ABI PRISM® 310 Genetic Analyzer, *Applied Biosystems* (Foster city, California, USA).

2.3 Conclusions

This chapter described the general experimental details in terms of equipment and reagents for the research undertaken which is described in the following chapters. Specific experimental details for each experiment are described within the relevant chapters.

Chapter 3: Integration by electro-osmotic pumping

3 Aim

The chapter describes the development of a novel approach to introducing the reagents and sample for initial sample preparation into the micro-fluidic device and a method of manoeuvring reagents around the device.

After briefly investigating hydrodynamic pumping, the development of a novel extension to electro-osmotic micro-pumping (EOP) was investigated. The use of a gel supported matrix was also explored with the aim of increasing the stability of the reagents contained within a micro-fluidic device. This would allow the introduction of reagents at the time of manufacture, thus reducing the risk of contamination.

The intention of this chapter was to demonstrate the manner by which the three key sub components of the process could be integrated on to one device using the 'gel' approach, depicted in Figure 3-1 is the intended strategy to accomplish integration by electro-osmotic pumping on a single device including the following steps;

1. Removal of cellular debris and DNA clean up
2. Introduction of the sample to the PCR reagents in relation to the positioning of the thermal cycling device
3. Movement of the DNA products from where it is amplified to where it will be separated

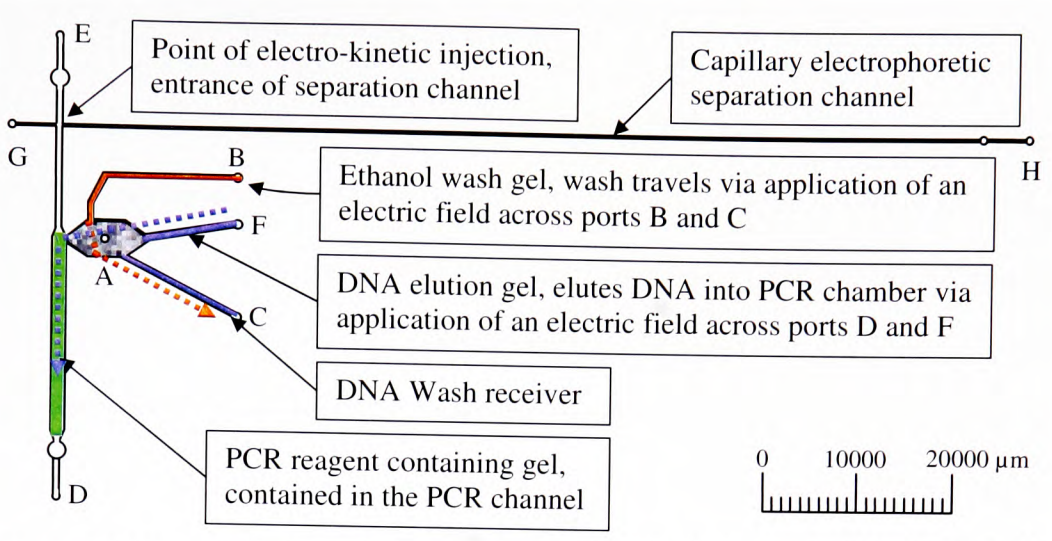

Figure 3-1 Micro-fluidic device design 5, with indication of gel placement within the device in preparation of the EOP approach to integration.

3.1 Preliminary investigation of integration of multiple processes onto one device

PCR amplification was performed in the PCR chamber (indicated in Figure 3-1), the design and development of the PCR process within the micro-fluidic device was not part of my sphere of activity. The work investigated in this thesis details the electro-kinetic movement around the device, including the movement of the DNA sample from the extraction chamber to the PCR amplification chamber, and the introduction of the PCR reagents into the micro-fluidic device at the required time.

After PCR amplification, the PCR products were then transported into the area where sample injection into the separation channel was performed, separation by capillary electrophoresis was detected at the end of the channel by laser induced fluorescent detection of the fluorescently labelled sample.

3.1.1 Experimental

As described in section 1.2 and illustrated in Figure 1-1, there are 4 main processes involved with producing a DNA profile, which are extraction of the DNA from other cellular debris (traditionally accomplished via hydrodynamic pumping), amplification of the specific multiple DNA loci, separation of multiple DNA loci according to their base pair length (traditionally accomplished via electrophoretic movement), which is fluorescently detected as they are separated, the movement of the reagents and products around the device could be accomplished through many different methods. However, hydrodynamic pumping, electro-osmotic and electrophoretic movement are very different methods of fluidic manipulation, and difficult to accommodate on a single micro-fluidic device.

As stated previously, in a micro-fluidic device, a common method of controlling the fluidic movement around the micro-fluidic device is by hydrodynamic pumping, using a syringe pump (KDS200 Syringe Infusion Pump).

DNA clean up and extraction involves priming the surface of the solid phase medium to accept the DNA by passing TE buffer across the surface, the DNA sample is passed across the separation medium, followed by an iso-propanol wash to remove any cellular debris, the cleaned DNA is eluted from the separation medium using water.

Hydro-dynamic pumping requires four syringes containing each one of the solutions, TE buffer, DNA sample, alcohol wash and DNA elution solution. The syringes were connected to the micro-fluidic device by micro-tubing, the tubing was glued into position on the chip and connected to the syringes via specialised connectors.

3.1.2 Results and Discussion

Experimentation showed that the addition of the multiple reagents meant an overly complicated set-up requiring multiple syringe pumps, which was difficult to engineer. In addition, there was a large volume of reagent waste that was travelling around the micro-fluidic device, the large volume of liquid, and the multiple introduction points made it difficult to control the exact movement of the solution. This became a problem when the iso-propanol wash was passed through the device, because if the iso-propanol found its way into the PCR amplification chamber, it would inhibit the PCR process.

During preliminary investigations it was found that due to the nature of the micro-fluidic device design, introduction of any reagents into the device resulted in displacement of the previous solution with the new reagents. This was meant to be achieved by introduction of reagents in successive processes; complicated timing and blockages had to be put into place in order to direct the fluidics where necessary, at the required time. Although this task was not impossible, it was considerably difficult; this problem was highlighted when the PCR amplification process was reached. Movement of the DNA sample into the PCR amplification by hydrodynamic pumping meant that the PCR reagents could not be added before the DNA, as they would be pushed out by the introduction of the eluted DNA. Therefore, the PCR reagents had to be introduced once the DNA was already in place, again this proved difficult as a large proportion of the DNA would be displaced at the introduction of the PCR reagents. This method required a large quantity of DNA to be eluted into the PCR chamber, to accommodate the lost volume due to displacement, so it was essential that good quality samples were used and maximum extraction efficiency was achieved.

An alternative approach was electro-kinetic movement of the PCR products from the PCR chamber to the point of electro-kinetic injection (indicated on Figure 3-1) which could be achieved by applying a straight voltage across electrodes D and E. A further problem to consider was there had to be a secondary reagent added to the PCR product sample before the injection takes place, the separating sizing ladder. It was also important to realise that the concentration of the PCR product could be controlled at the injection stage to increase the sensitivity of fluorescence detection as discussed in Chapter 4.

Many attempts were made to try and perform consecutive processes in succession, and the successive introduction of each of the reagents into the micro-fluidic device, but these were never successfully achieved.

The first generation of integrated micro-fluidic devices were designed on the premise that all reagent introductions would be performed via hydrodynamic pumping. This proved highly impractical when experimentation was undertaken, due to a number of reasons, firstly maintaining fluid integrity to the device was very difficult due to the number of reagent introduction points which created a large amount of pressure, and the numerous points at which leakage could occur. In initial experimentation involving hydrodynamic pumping, it was quickly seen that the device was so prone to leakage that it was necessary to pump excess volumes of reagents in-order to ensure that the correct volume of reagents required for the intended reaction was introduced.

Other problems that were highlighted during the initial integration experiments included observations which suggested that the number of hydrodynamic pumps required to introduce all the necessary reagents, were too many to engineer into the portable device successfully. It was decided electro-osmotic flow should be further investigated.

3.2 Proposed method of integration by EOP

Due to the difficulties observed with hydrodynamic pumping in the integrated micro-fluidic device, such as leakage and variable pressures, other forms of pumping were investigated.

Electro-kinetic movement within a micro-fluidic device is extremely common, via electro-osmotic flow or electrophoretic movement. Electro-osmosis allows for bulk flow of sample through the micro-fluidic device, however electro-osmosis is generally a weak force, often overpowered by hydrodynamic pressures within the device. The addition of the monolith in the pathway of the directional flow allows the electro-osmotically pumped solution to pass through and move in a continuous direction, preventing hydrodynamic forces pushing the solution back in the other direction.

The lengthy channels which characterised some of the earlier generations of integrated chips prevented movement by electro-kinetic means, as it would require electric field strength much greater than the micro-fluidic device would sustain. A new device was designed which included shorter channel lengths, which can be seen in Figure 3-2 (Micro-fluidic device design 5).

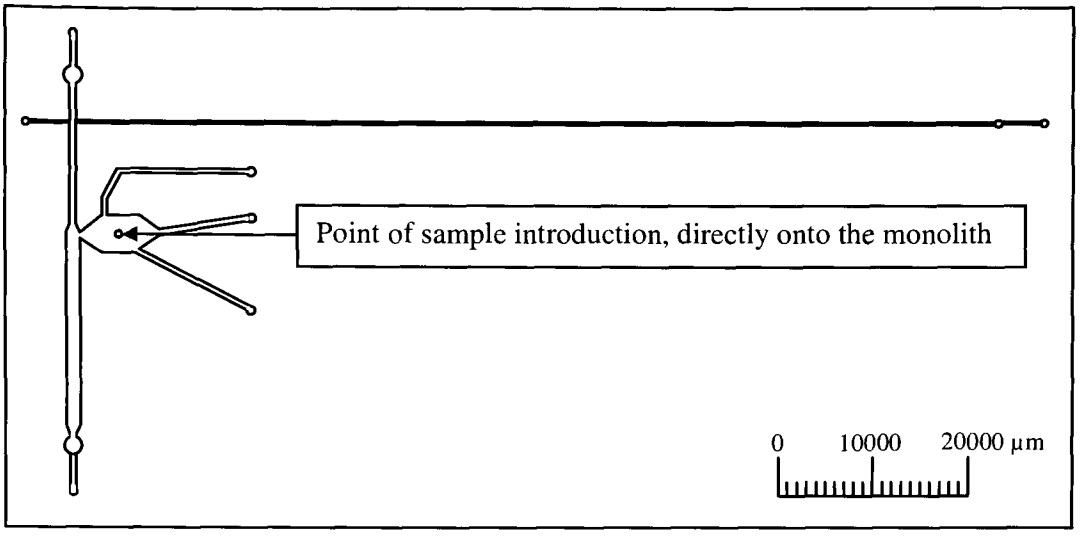

Figure 3-2 Micro-fluidic device design 5, the device designed to investigate the possibility of electro-kinetic pumping as a means to enable integration.

The schematic illustrations depicted in Figure 3-3 indicate the proposed directional flow of each of the solutions within the micro-fluidic device, to accomplish integration of the different processes by electro-kinetic movement.

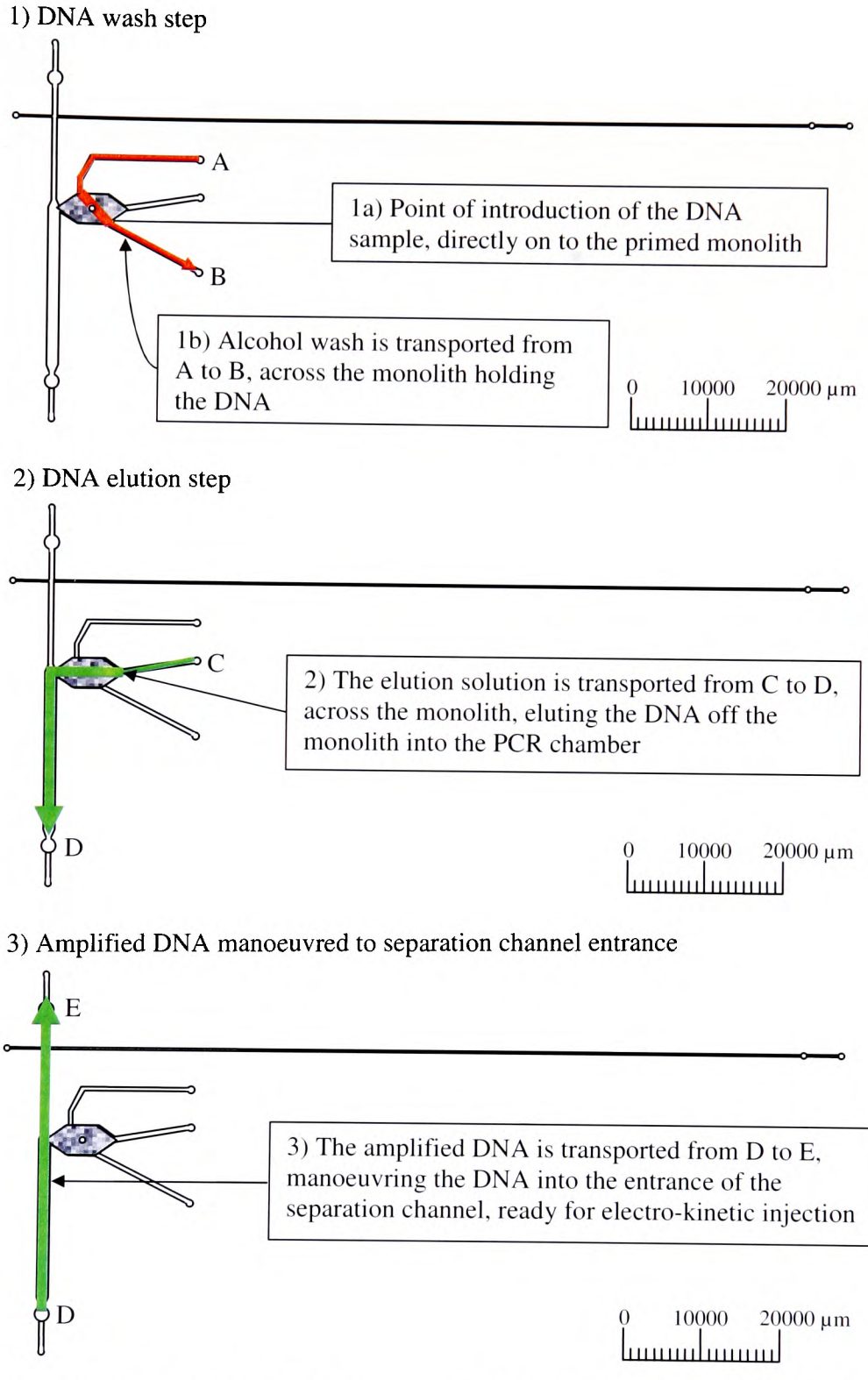

Figure 3-3 Schematic of electro-kinetic movement within the micro-fluidic device, 1) indicates the point where the DNA is added to the device, followed by the wash step. 2) DNA elution step. 3) Amplified DNA manoeuvred to separation channel entrance

3.3 Preparation of potassium silicate monolith

As described previously in Figure 1-1, solid phase extraction is one of the main methods used to extract DNA from a biological sample. Potassium silicate monoliths have previously been utilised within a micro-fluidic device for numerous processes, such as pressure control or as a separation medium.[26, 95, 96] In this case, the potassium silicate monolith which has a large number of silica bonds act as the solid phase extraction medium. The DNA is selectively adsorbed to the silica support in the presence of a chaotropic salt such as guanidine hydrochloride, the DNA can then be selectively eluted from the monolith altering the environment to an alkaline or a low salt concentration condition.

3.3.1 Experimental

The potassium silicate monolith was manufactured with a 10:1 ratio of potassium silicate to formamide, mixed into a paste and pressure injected into the micro-device. Controlled placement of the monolith was achieved using a hydroxyl-ethyl cellulose (HEC) gel made with glycerol (prepared by dissolving by 0.15 g of HEC into 5 ml of glycerol using the long stir method),[70] forming a highly viscous material that provides resistance to the potassium silicate/formamide paste. The HEC-glycerol gel was pressure injected into the sections where the monolith was not required; effectively masking off the area, the potassium silicate/formamide paste was injected against it and held in place. The micro-fluidic device was then put into an oven and allowed to cure at 95°C for 30 minutes, the HEC-glycerol gel could then be removed with water and the device placed back in the oven overnight.

When required for experimentation, the monolith was prepared by activating the silica surface with a 30 minute application of 1 x TE buffer, 5 µl of DNA template was then added to 120 µl of 5M guanidine hydrochloride and passed across the monolith.

3.3.2 Results and Discussion

Controlling the placement of the potassium silicate monolith was difficult; normally a photo initiated monolith is selected when accurate control of the placement of the monolith is required. However, previous reports have indicated that the monolith produced via the photo-initiated method proved ineffective at the extraction of DNA, providing very small extraction efficiencies.[96,97] By introducing the monolith solution in a more viscous state meant better placement of the monolith could be achieved, in addition the HEC gel provided a very clean means of masking of the channel where the monolith was required and was very straightforward to remove, as seen in Figure 3-4.

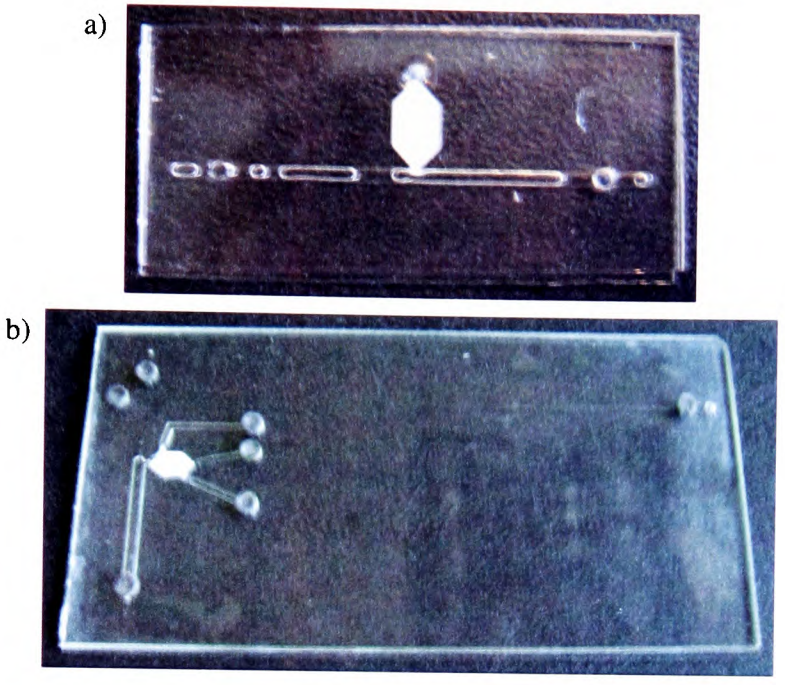

Figure 3-4 Thermally initiated potassium silicate monolith (as described in section 3.3), selectively placed in the extraction chamber of a) micro-fluidic device design 1 and b) micro-fluidic device design 5.

3.4 Preliminary investigation of electro-osmosis

3.4.1 Experimental

The preliminary electro-osmotic experimentation was performed with a 'goal post' system, consisting of two glass wells connected by a glass capillary containing a potassium silicate monolith prepared by the method previously described (see section 3.3). A schematic representation of the experimental set-up can be seen in Figure 3-5.

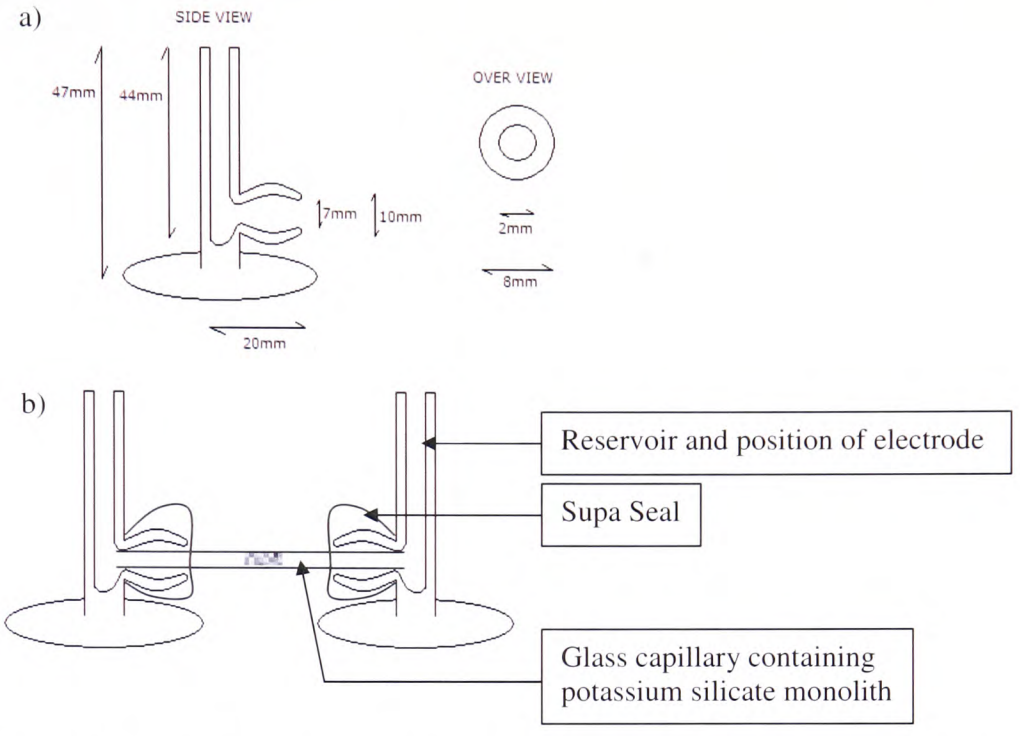

Figure 3-5 a) schematic diagram of the 'goal post', including internal measurements, b) representation of the 'goal post' electro-osmotic system

The goal post system allowed more accessible measurements of the electro-osmotic flow rate, by allowing measurement of the flow rate along the reservoir wall. The system was prepared by flushing the device with 1 M HCl for 5 minutes followed by 1 M NaOH in the same fashion, then a solution of TE buffer (Tris buffer containing EDTA), was passed through the system. Platinum electrodes were placed in the main channel of the goal posts, which were then filled up to a mark. A 1kV power supply was used to apply a voltage for a timed period before being switched off; the movement of flow was measured by removing the volume of liquid in the cathode goal post to the mark by syringe. The current during the experiment was measured at regular intervals with a voltmeter, in order to gauge how the current can alter when experimental changes

are made, and its effect on the bulk movement. The effect of voltage, capillary length, and the pH of the TE buffer were investigated within the system.

In addition the goal post system was utilised to investigate which of the reagents used in each of the processes could successfully be moved by electro-osmotic pumping, by filling the capillary with the solutions, pushed across the monolith, filling the wells also. Platinum electrodes were placed in the main channel of the goal posts as described previously, and a voltage applied for a timed period and the movement of flow measured. The solutions investigated were TE buffer, guanidine hydrochloride, iso-propanol, DNA/RNA free water and the PCR reagent solution.

3.4.2 Results and Discussion

During the investigation of the effect of applied voltage on the electro-osmotic flow rate, a capillary length of 40 mm was used, and the pH of the TE buffer working solution remained at pH 6.7 and a concentration of 10 mmol.

Table 3-1: Preliminary investigation of the effect of voltage on electro-osmotic flow rate

Voltage	50 Volts			100 Volts			200 Volts		
Flow rate (µl/min)	0.05	0.05	0.05	0.125	0.1	0.1	0.2	0.2	0.2
Average flow rate	0.05 µl/min			0.108 µl/min			0.2 µl/min		

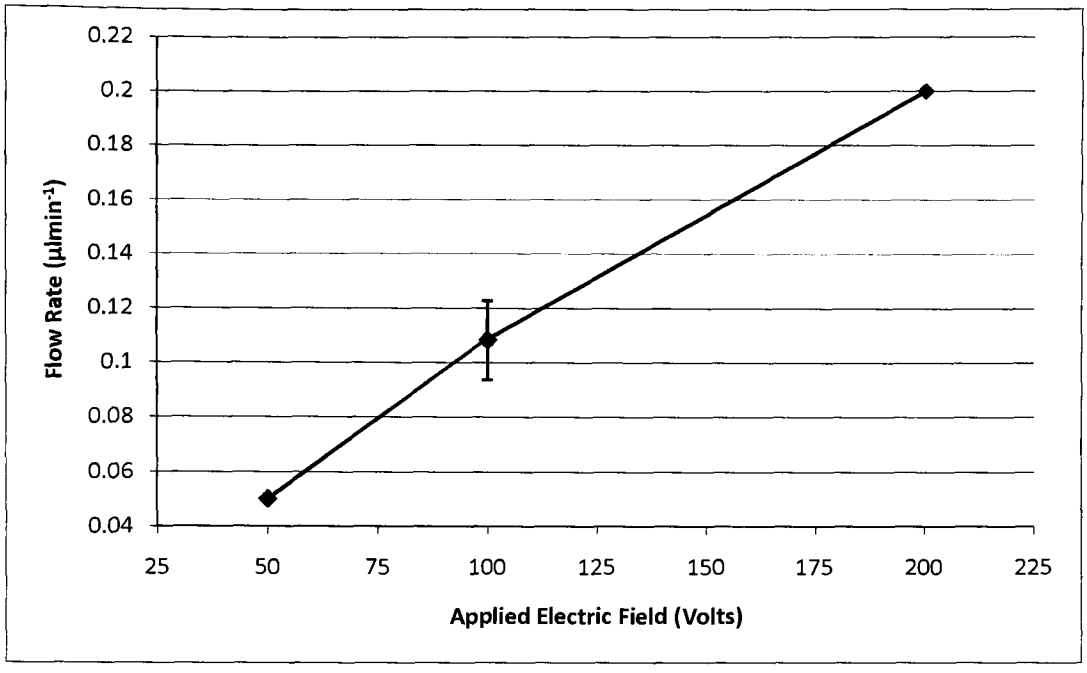

Figure 3-6 Electro-osmotic flow rates recorded for 10 mmol TE buffer, pH 6.7, in a 40 mm capillary, at varying applied electric fields.

During the experiment it became apparent that a trend had been established (see Table 3-1 and Figure 3-6), an increase in average flow rate occurred as the applied voltage was increased. The rate of increase suggested a linear relationship between applied voltage and the flow rate of the electro-osmotic flow.

For the investigation of the effect of capillary length on the electro-osmotic flow rate, an applied voltage of 200 Vcm^{-1} was used, and the pH of the TE buffer working solution was kept at pH 6.7 with a concentration of 10 mmol.

Table 3-2: Preliminary investigation of the effect of capillary length on electro-osmotic flow rate

Capillary length	30 mm			40 mm			50 mm		
Flow rate (µl/min)	0.8	0.8	0.7	0.4	0.3	0.35	0.03	0.025	0.027
Average flow rate	0.767 µl/min			0.35 µl/min			0.0275 µl/min		

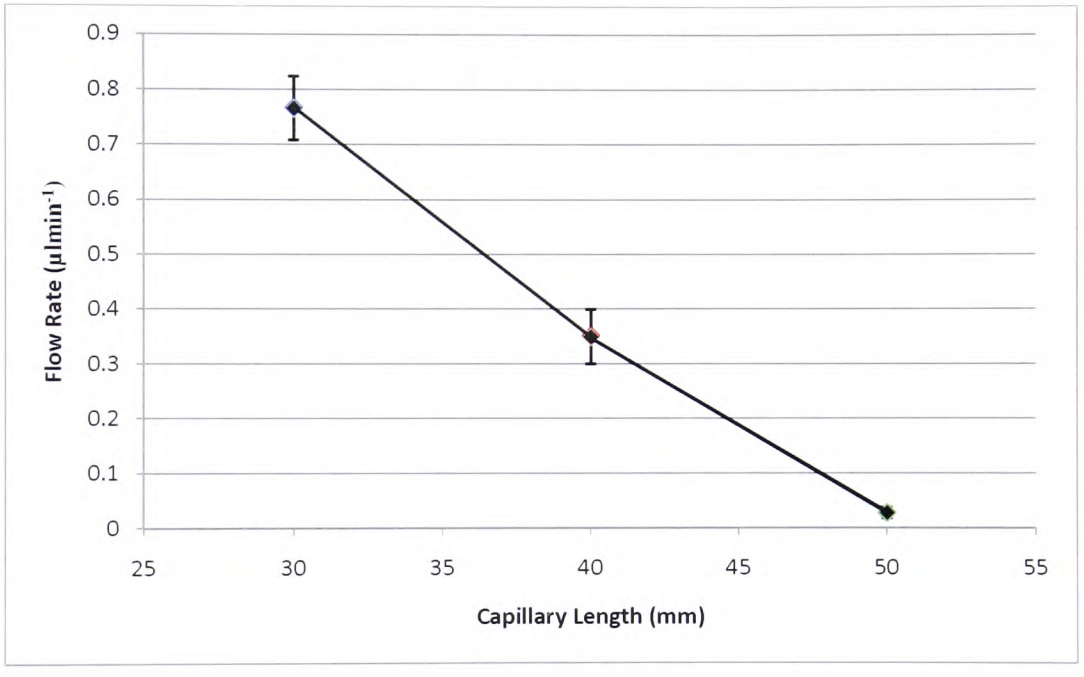

Figure 3-7 Electro-osmotic flow rates recorded for 10 mmol TE buffer, pH 6.7, at 200 Vcm^{-1}, at varying capillary lengths.

A relationship was identified in which the flow rate decreased as the capillary length increased (see Table 3-2 and Figure 3-7). The reduction in the flow rate increased noticeably until the point at which a threshold was reached, which appears to be close to 50 mm. Otherwise, initially the decrease in flow rate resulting from the increase of capillary length looked to be a linear relationship.

For the investigation of the effect of the pH of the TE buffer working solution, the constants within the experiment were the concentration of TE buffer working solution of 10 mmol, and an applied voltage of 200 Vcm^{-1} with a capillary length of 40 mm.

Table 3-3: Preliminary investigation of the effect of solution pH on electro-osmotic flow rate

pH of TE buffer	pH 6.7			pH 7.3			pH 8.8		
Flow rate (µl/min)	0.4	0.3	0.35	0.05	0.06	0.07	0.08	0.07	0.07
Average flow rate	0.35 µl/min			0.06 µl/min			0.073 µl/min		

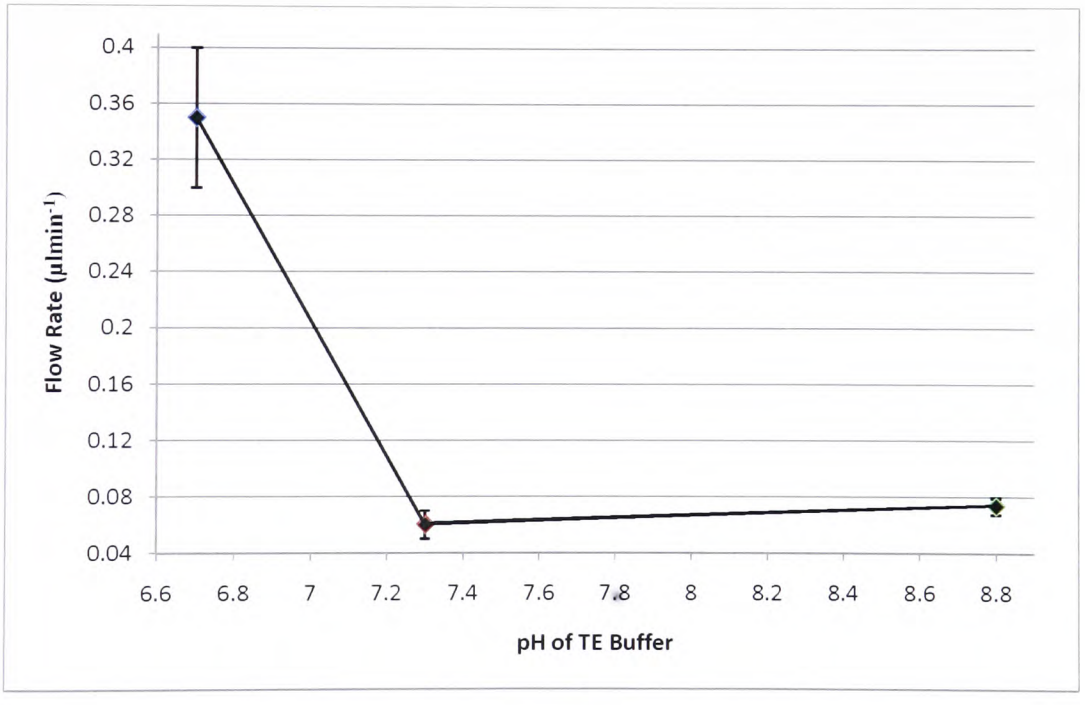

Figure 3-8 Electro-osmotic flow rates recorded in a 40 mm capillary, at an applied electric field of 200 Vcm-1, for 10 mmol TE buffer at varying pH's.

The results obtained (see Table 3-3 and Figure 3-8), suggested that the pH of the solution in which EOF occurs has an obvious effect on the average flow rate, with an increased flow being seen at the lower pH where an excess of hydrogen ions is found.

The investigation into the possibility of moving each of the reagent solutions by electro-osmotic pumping indicated that only iso-propanol would prove difficult to implement. Further investigation however identified that ethanol could be successfully manipulated by electro-osmotic pumping, and was still sufficient to clean the DNA appropriately.

3.5 DNA elution by electro-osmotic micro-pumping

If EOP was to be utilised to successfully elute DNA from the potassium silicate monolith, it was first necessary to prove a solution being pumped by the EOP method was capable of removing the DNA adsorbed to the silica surface of the monolith and carrying it to a designated area within a reasonable time frame.

3.5.1 Experimental

Micro-fluidic device design 1 (Figure 2-10) was prepared by flushing the device with 1 M HCl for 5 minutes followed by 1 M NaOH in the same fashion. A potassium silicate monolith was also prepared and loaded and positioned in the hexagonal chamber using the procedure described in section 3.3. The ethanol residue was removed from the channels and collected for later analysis, DNA and RNA free water was introduced into the channel, the electrodes secured into place and an electric field of 100 Vcm^{-1} applied across the monolith for 5 min. The solution pumped across the monolith was collected in fractions at the cathode. These fractions along with the remaining solution at the

anode and the ethanol wash solution were analysed for DNA, in order to capture a full insight into the amount of DNA eluted in relation to the amount added, illustrated in Figure 3-9.

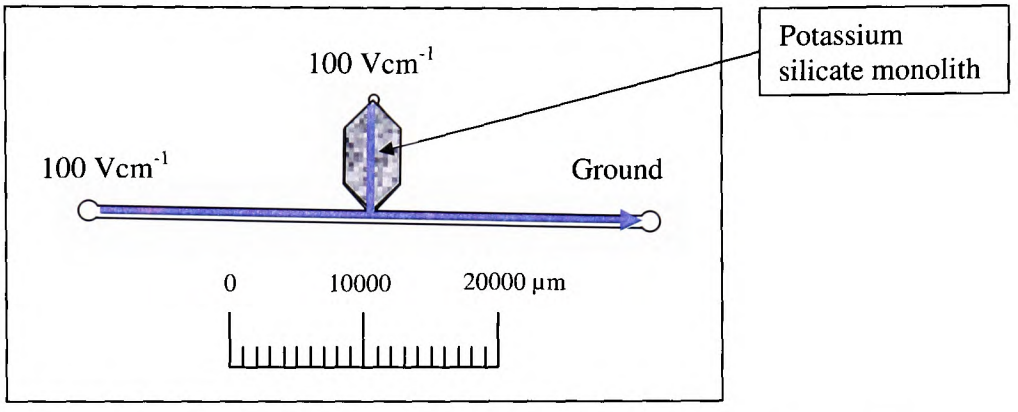

Figure 3-9 A schematic of the experiential procedure of DNA elution by EOP, using Micro-fluidic device 1, indicated on diagram is movement expected by application of electric field is shown by the directional arrow on the diagram.

3.5.2 Results and Discussion

During the application of the electric field, for both the ethanol wash and the elution steps, fractions of the solution were collected from both the cathode and the anode reservoirs. These fractions were then analysed using the POLARStar OPTIMA plate reader and the Quant-iT™ PicoGreen® dsDNA assay kit.

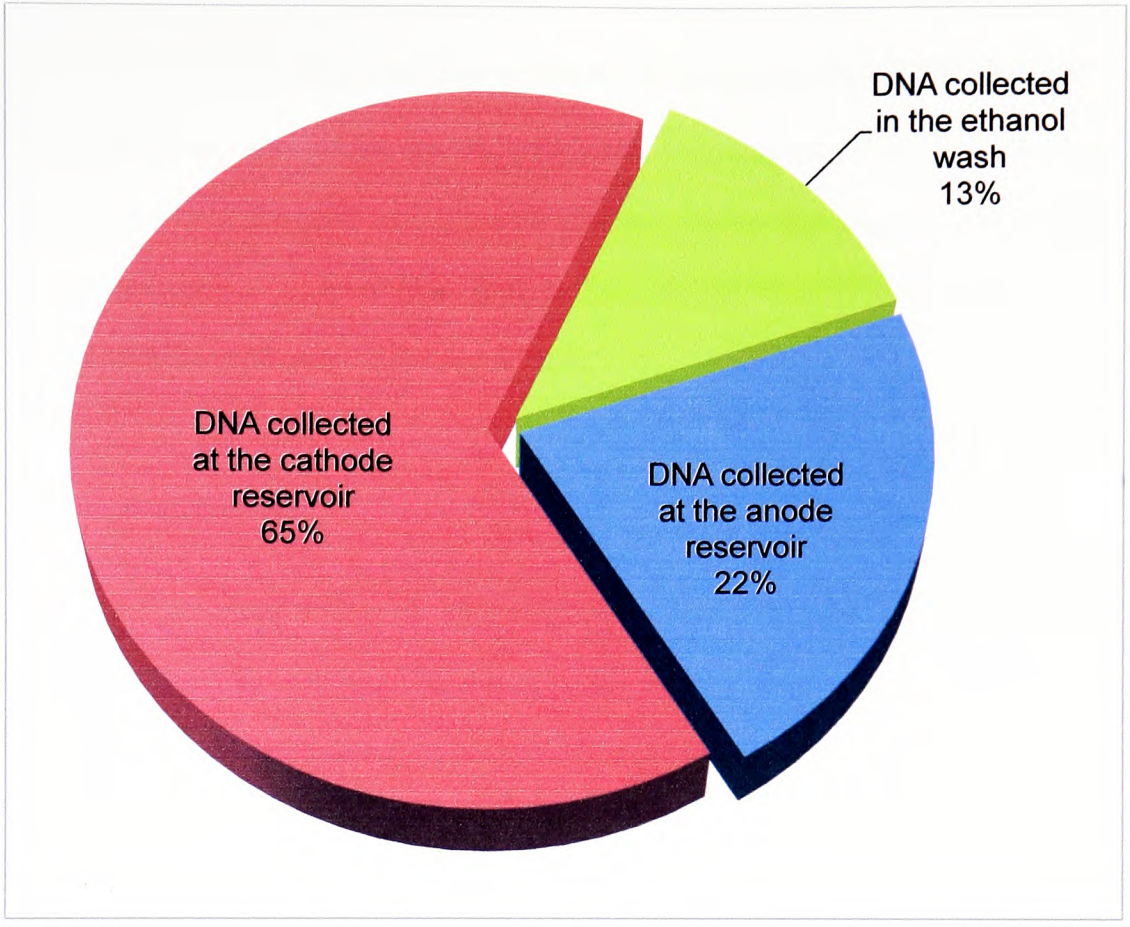

Figure 3-10 Pie chart conveying the results obtained from the analysis of DNA recovery during the investigation of DNA elution by EOP

As can be seen from the results displayed in Figure 3-10, the majority of DNA was found at the cathode, with an average DNA recovery of 65% being achieved. Whilst of the remaining 35% DNA, an average of 22% was recovered from the solution present at the anode, indicating some electrophoretic movement was also present. The remaining 13% of DNA was found in the ethanol wash solution; this was to be expected as the monolith was overloaded to ensure complete adsorption of the DNA on to the monolith surface.

3.6 Investigating the stability of the PCR reagents after EOP elution

It has previously been ascertained that EOP could be successfully utilised to wash and extract the DNA from the monolith, to the location of the PCR reagents (see Section 3.5). However, it was necessary to establish if the stability of the PCR reagents was still intact after the application of the electric field.

3.6.1 Experimental

The work described in Section 3.5 was expanded further in order to ascertain if the elution of DNA by EOP could be utilised within an integrated system that included the presence of reagents necessary for the functionality of the device. In particular, it was necessary to see if the integrity of the already sensitive reagents required for the PCR process had been compromised after the elution by EOP had been performed. The necessary reagents for PCR were prepared, these included 1 µl bovine serum albumin (BSA), 1 µl ammonium buffer (NH_4), 1 µl D16S539 forward primer, 1 µl D16S539 reverse primer, 0.5 µl dNTP's mixture, 0.2 µl $MgCl_2$ and 0.2 µl GoTaq® (Hot start Taq DNA polymerase). Micro-fluidic device design 1 (Figure 2-10) was prepared and loaded as described previously, after the device had been washed the elution solution was introduced into port A and the PCR reagent mix introduced into port B, see Figure 3-11

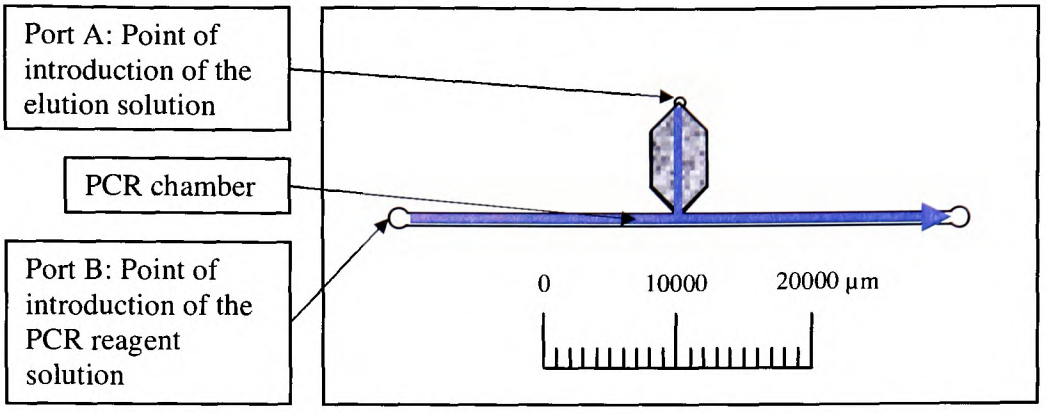

Figure 3-11 A schematic of the experiential procedure of DNA elution by EOP into a solution of PCR reagents, indicated on the diagram is the point of reagent introduction into the device and direction of movement expected by application of electric field.

The solution in the PCR chamber was collected, after mixing via vortex for 10 seconds the solution was amplified in a TECHNE TC-312 Thermal Cycler. After amplification, a DNA sizing ladder was added to the 'PCR products' which were separated by the slab gel electrophoresis method, applying a voltage of 115 V for 45 minutes. The gel plate was stained with ethidium bromide (1 drop in 50 ml) for 20 minutes before observation via a UV transilluminator.

3.6.2 Results and Discussion

Results seen in Figure 3-12, a UV transilluminator image of the DNA sample that had previously undergone the EOP process and was amplified and separated, indicated that after being exposed to the electric field the PCR reagents were no longer viable and the amplification process was unsuccessful.

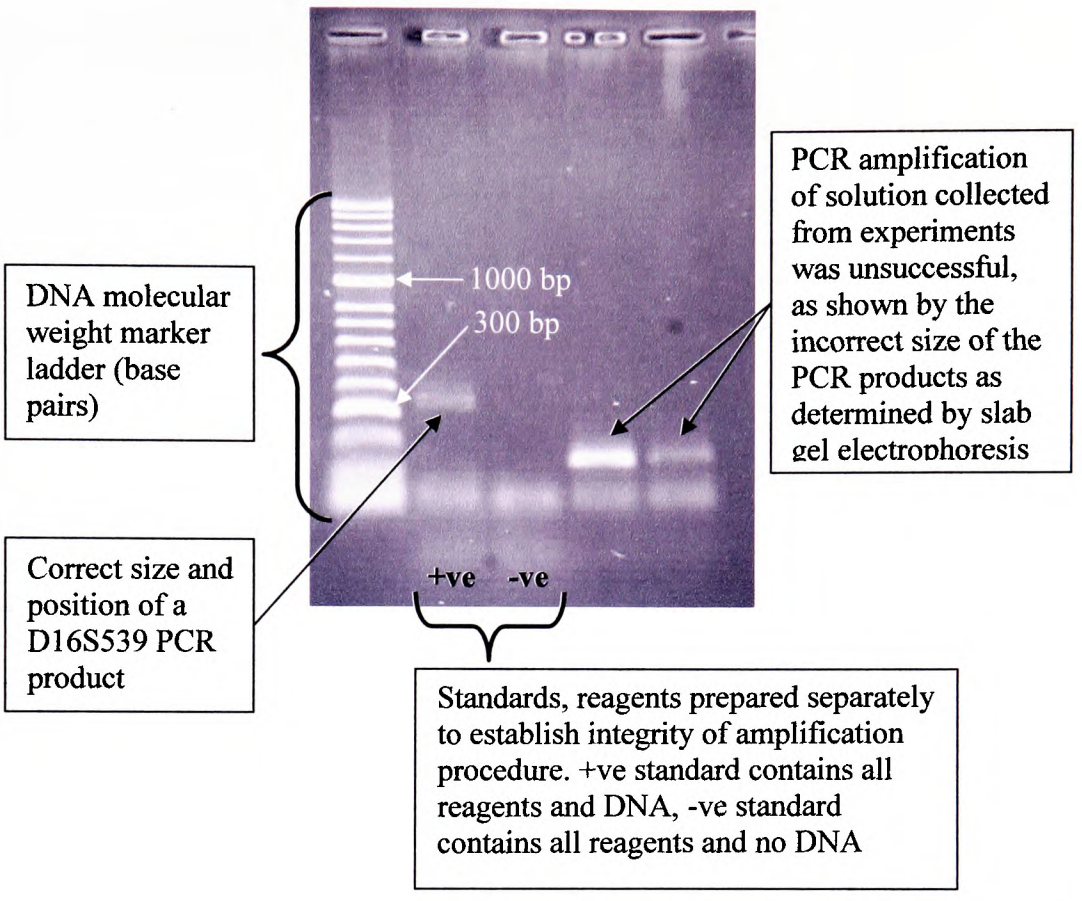

Figure 3-12 UV transilluminator image of D16S359 PCR products obtained from the elution of DNA by EOP into a solution containing PCR reagents.

Further investigation indicated it was in fact the electric field causing the loss of functionality of the PCR reagents, as proven when a replica experiment was performed where the DNA was added to the PCR reagents after the electric field had been applied to them. Results similar to Figure 3-12 were seen, where the amplification was proved unsuccessful by the incorrect sizing determined by the slab gel electrophoresis. These results indicated that although elution by EOP was possible, some means of protecting the PCR reagents from the electric field was required.

3.7 Development of gel encapsulated reagents

The negative effect the electric field posed to the stability of the PCR reagents resulted in the necessity to provide some form of protection while the reagents were in-situ, during the electro-osmotic pumping mechanism. The intention of the investigation into the encapsulation of the PCR reagents was to ascertain if the process would provide increased stability of the reagents when contained within the micro-fluidic device for extended periods of time. More importantly, to assess whether the encapsulation process would provide enough, if any, protection to the PCR reagents during the application of an electric field to ensure successful amplification was possible after the elution of DNA by electro-osmotic pumping had been performed.

It was also hypothesised, that if the encapsulation process was successful at protecting and providing greater stability to the PCR reagents, this approach could also be used to improve the stability of the other reagents required for a fully integrated DNA analysis device. This would include the encapsulation of the reagents required to wash the DNA, elute the DNA and also manoeuvre the DNA/PCR products to the correct analysis 'station' at the required time.

3.7.1 Experimental

A survey of commercial PCR reagents showed that the encapsulation of the PCR reagents in various polymer 'beads' already existed, including *PuReTaq Ready-To-Go™ PCR Beads* manufactured by GE Healthcare, *illustra™ PCR Beads* manufactured by Spartanbio and *REAX™ MASTERMIX 25 PCR Beads*, manufactured by Q Chip Ltd. to name a few.

The 'selling point' of the *PuReTaq Ready-To-Go™ PCR Beads* is that the system is designed to produce "robust and reliable amplification under pre-optimised reaction conditions" and "pre-formulated, pre-dispensed, single-dose, ambient-temperature-stable beads ensure greater reproducibility between reactions, minimize pipetting steps and reduce the potential for pipetting errors and contamination." [98] *Illustra™ PCR Beads* were designed for real-time PCR reactions, as with the *PuReTaq Ready-To-Go™ PCR Beads*, they are described as being "pre-mixed, pre-dispensed, single dose reactions that enable convenient set up of real-time PCR amplified cations on the Spartan DX™ ". The advantages include decreased reaction preparation time, decreased pipetting errors, stability of reagents at ambient temperatures and standardization of reagents.[99] *REAX™ MASTERMIX 25 PCR Beads* again encapsulates all the reagents that are needed for the PCR reaction in a single dose, which it is claimed, allows even untrained operators to perform PCR amplification in any thermal cycler, and increasing the potential for performing the reaction out of the laboratory environment. With advantages including; standardising and streamlining the set-up, producing robust and highly reproducible reactions, the beads can be stored and shipped at either 4°C or ambient temperature due to their highly stable nature, resulting in an overall reduction of test costs due to lower repeat rates and less reagent wastage.

As described, amongst the advantages of the PCR beads commercially sold, is the ability to provide greater stability for the reagents during experimentation and analysis, including at ambient temperature. It was hypothesised that if the encapsulation process could successfully shelter the reagents from adverse temperatures, it may also protect the reagents from other hostile environments, such as an electric field.

From the number of products available, REAX™ MASTERMIX 25 PCR Beads, manufactured by Q Chip Ltd were selected for investigation, due to the similar nature of the components to the existing reagents we had available to use and had used throughout this investigation. The REAX™ MASTERMIX PCR beads were analysed by attenuated total reflection (ATR) and components were confirmed by the manufacturer to be made from agarose gel.

3.7.2 Results and Discussion

ATR FT-IR analysis was performed on several different polymers and compared with the FT-IR analysis of the REAX™ MASTERMIX 25 PCR Beads, in order to establish which polymer was used in there manufacturing.

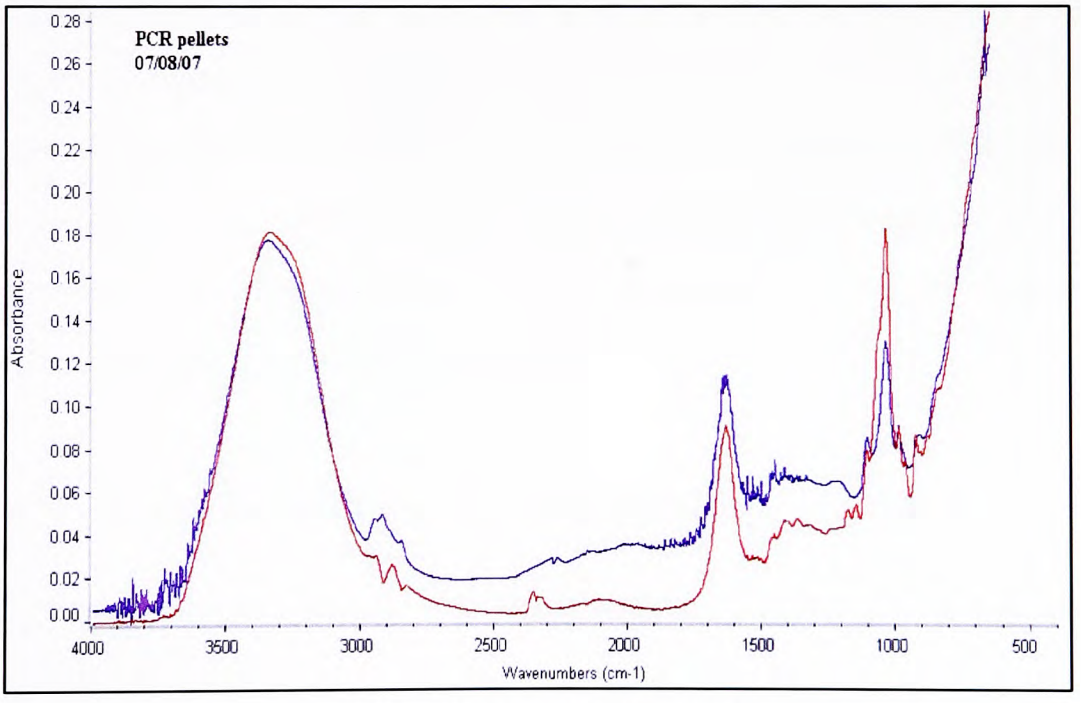

Figure 3-13 FT-IR analysis of REAX™ MASTERMIX PCR beads.

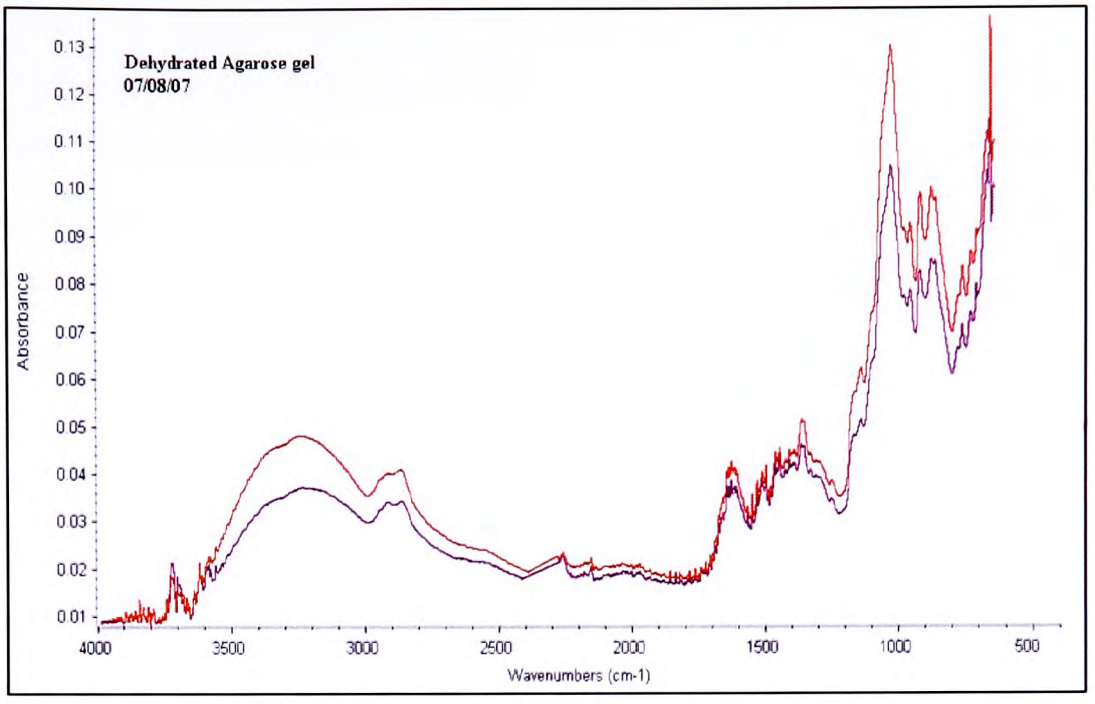

Figure 3-14 FT-IR analysis of agarose gel made up with DNA/RNA free water.

Comparison of the FT-IR spectra shown in Figure 3-13 (REAX™ MASTERMIX PCR beads) and Figure 3-14 (the agarose gel) clearly indicated that agarose was the main medium that encapsulated the PCR reagents in the REAX™ MASTERMIX PCR beads. Although, the spectra varied to a degree, there are a number of similarities between the spectra of the commercial bead and of agarose, suggesting that agarose was the most likely encapsulation media used for the commercial bead.

3.7.3 Investigation into the method of encapsulation

The polymer beads containing PCR reagents that are available commercially are generally designed for much larger reaction vessels, with the majority of reaction volumes being around 25 to 50 µl, which is much larger than the volume available in the micro-fluidic device so could not be used. Two methods of gel encapsulation were

investigated for the micro-fluidic system; the first method investigated was the encapsulation of the reagents in a micro sized polymer bead small enough to be contained within the channel, this would entail developing a methodology to create a bead of that size and volume. The second method investigated was full encapsulation, where the entire 'reaction' channel was filled with a polymer in which the reagents were trapped (see Figure 3-15).

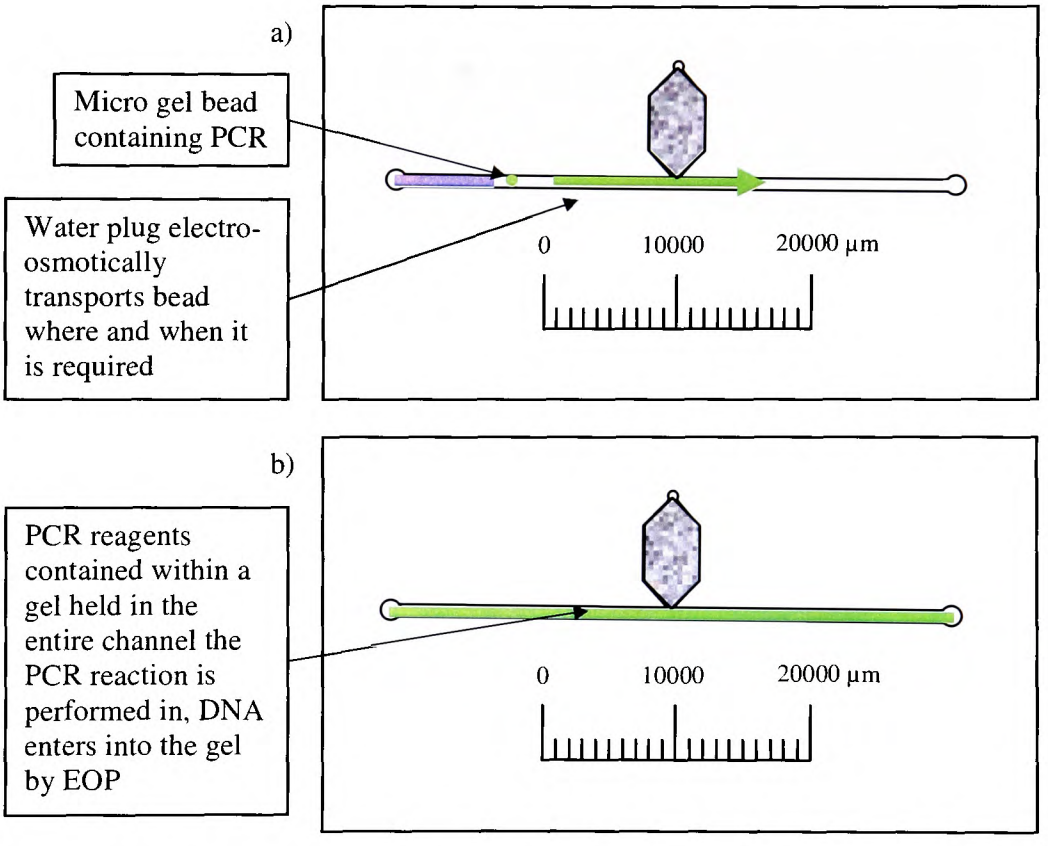

Figure 3-15 a) schematic representation of the gel bead approach to encapsulation, b) a schematic representation of the full encapsulation approach.

3.7.3.1 Experimental

Preliminary experiments were carried out in-order to investigate the best method to create a bead that was small enough to fit into the micro-fluidic device channels; however, further investigation deemed that the means to accurately divide the commercial beads into a size more applicable to the micro-fluidic reaction vessel were not feasible. This was considered unacceptable, as the accurate control of both the size and volume of the bead is crucial to ensure that the reactant proportions were correct, for the PCR reaction to be successful, especially when multiple loci were to be amplified. Each addition of a new primer to the solution increases the complexity of the reaction, and creates greater pressure on the precise balance of reagent concentrations that will prevent the possibility of reaction failure due to the formation of primer dimers.[100]

Therefore, experimentation was carried out to investigate the possibility of replicating the PCR reactants within a 'home-made' micro sized polymer bead.

The agarose gel was made to concentrations of 0.5, 0.75, 1.0, 1.25 and 1.5% with distilled water, by heating to 95°C in a water bath. While still in solution, a micro-pipette was used to pipette 1 µl of the gel onto a strip of parafilm and put into the fridge to cool, the gel bead produced was then introduced into the micro-fluidic device by depositing the bead into PCR water, which was then pipetted into a well in the micro-fluidic device with a wide bore pipette tip. The bead was forced into the channel by applying gentle pressure via a syringe, once the bead was in place, a voltage of 100 Vcm^{-1} was applied for 5 minutes.

An alternative encapsulation approach was then investigated, where the agarose gel solution was heated by the same method, but a syringe was used to introduce the gel into the entire channel of the micro-fluidic device while still in liquid phase. Agarose gel concentrations of 0.5, 0.75, 1.0 1.25 and 1.5% were investigated. A small volume of PCR water (5 μ) was placed into the well of each electrode point, this was to ensure contact could be ensured between the electrode and the agarose gel solution. Again a voltage of 100 Vcm^{-1} was applied across the channel for 5 minutes.

3.7.3.2 Results and Discussion

A bead of approximately 1μl volume could be created with the agarose gel, however, as mentioned previously (in Section 3.7.3.1) the accurate control of the size and volume of the bead was crucial to the experimental success, and could not be achieved sufficiently by this method either. Introducing the bead into the micro-fluidic device was also very difficult to achieve, and once in place and the voltage applied, it was found that controlling directionality and speed of the movement of the micro-bead was very difficult.

It was therefore necessary to alter the approach from utilising PCR reagent beads, to a full gel encapsulation approach. During the application of the electric field across the channel fully filled with the encapsulated gel, the volume of the water and agarose gel solution held in the cathode well noticeably increased, indicated that EOF had been established through the agarose gel medium.

3.7.4 Development of the DNA wash gel

3.7.4.1 Experimental

To remove any cellular debris introduced during the DNA sample loading process, which could potentially interfere or inhibit the PCR amplification process, a wash procedure was performed across the monolith. As described in section 3.4, typically iso-propanol is the reagent utilised to wash cellular debris away from the bound DNA prior to DNA elution, but is unable to be successfully manipulated by electro-osmotic pumping. Preliminary investigations involving trial and error indicated that a solution mixture of 80% ethanol and 20% sodium chloride (NaCl) could be successfully moved at a reasonable flow rate and was also capable of removing the problematic cellular debris, so this was therefore chosen for continuation throughout the investigation. (The ethanol solution was made up with 20% 1M sodium chloride solution in order to facilitate the electro-osmotic movement).

As part of the investigation into achieving encapsulation of all reagents required for an integrated DNA analysis micro-fluidic device, an attempt was made to encapsulate the ethanol-NaCl solution into an agarose gel. The agarose gel was made to a concentration of 3% (0.0030g agarose in 100 µl DNA/RNA water) and heated, once the gel was formed and whilst still in liquid form a 100 µl of 80 % ethanol and 20 % NaCl solution was added, the gel reformed capturing the ethanol solution inside.

The goal post system described in Section 3.4 was used for the investigation of the ethanol flow rates, which allows more accessible measurements of the electro-osmotic flow rate along the reservoir wall, and prepared in the same manner. A solution of 80 % ethanol and 20 % NaCl was passed through the system, and platinum electrodes placed

in the main channel of the goal posts, which were then filled up to a mark. A 1kV power supply was used to apply a voltage for a timed period before being switched off; the movement of flow was measured by removing the volume of liquid in the cathode goal post to the mark by syringe. The current during the experiment was again measured at regular intervals to assess the effect of the voltage. An electric potential of 100 Vcm^{-1} was applied across the monolith for a period of 5 minutes, after this time the electric field was terminated and the change in the fluidic level measured. This procedure was repeated with a systematic increase to the electric field, the voltages applied were 50, 100, 150, 175, 200 Vcm^{-1}, in order to establish a plot of flow rate vs. applied voltage for the ethanol solution. The experimental procedure described was then repeated in order to establish a similar flow rate graph for the ethanol solution gel, the only variation was the prior heating of the ethanol gel which enabled full injection throughout the system.

3.7.4.2 Results and Discussion

The electro-osmotic flow rate of the ethanol solution within agarose gel was established, and compared to the flow rate of ethanol in free solution and can be seen in Figure 3-16.

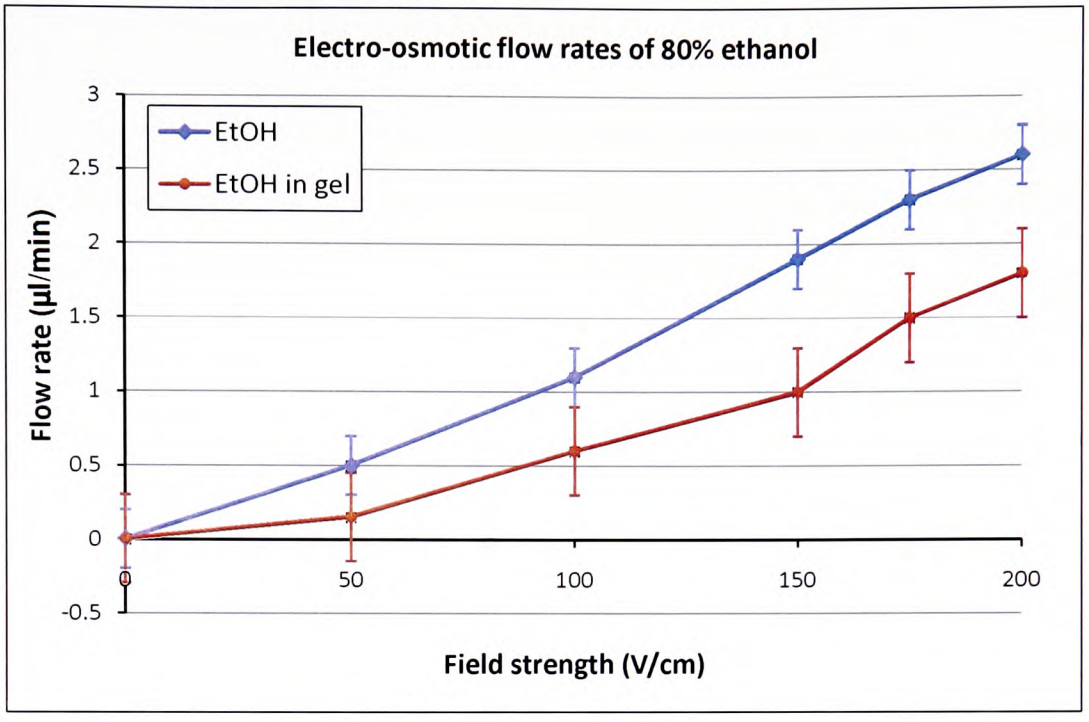

Figure 3-16 Flow rates achieved for EOP movement of ethanol wash solution in gel across a silica monolith at increasing field strengths, compared to that obtained for ethanol wash in free solution.

Although it can be clearly seen in Figure 3-16 that the electro-osmotic movement of the 80% ethanol solution in agarose gel produces a much slower flow rate than free ethanol and also a non-linear relationship between field strength and flow rate. This result was expected due to the interference effect of the cross polymer network on the bulk flow of liquid in electro-osmotic movement.

Further investigation is required in order to understand the nature of electro-osmotic movement in an agarose gel matrix. However, the agarose gel solution is clearly capable of supporting electro-osmotic pumping across a monolith towards a negative electrode at an acceptable flow rate for a micro-fluidic application.

3.7.5 Development of the DNA elution gel

It was established in Section 3.5 that DNA could be successfully eluted into solution from the potassium silicate monolith by EOP, however it was necessary to ascertain if the method could be transferred to the gel encapsulation system.

3.7.5.1 Experimental

Micro-fluidic device design 2 was prepared as described previously, (see Section 3.5), a potassium silicate monolith was loaded in to the end of a glass capillary, the loading of the DNA onto the monolith and wash steps were performed as described previously.

The DNA elution gel that was to be introduced into the extraction chamber, was prepared by dissolving 0.0015 g of low melting point agarose in 100 µl of DNA/RNA free water, the solution was then heated in a water bath at 75°C for 10 minutes to allow the gel to form. This composition was also duplicated for the ethanol was receiver gel.

The gel had to be reheated to reduce the viscosity, to enable the pressure injection of the gel into the micro-fluidic device channel. In order to visualise if any movement of DNA had occurred by EOP, DNA amplified by PCR using fluorescently labelled primers was loaded onto the monolith instead of standard DNA, the DNA was still quantified before use so a known quantity of DNA could be loaded.

The capillary was then placed into the well in the centre of the extraction chamber in the micro-fluidic device, and a voltage of 100 Vcm^{-1} was applied for 5 minutes, see Figure 3-17.

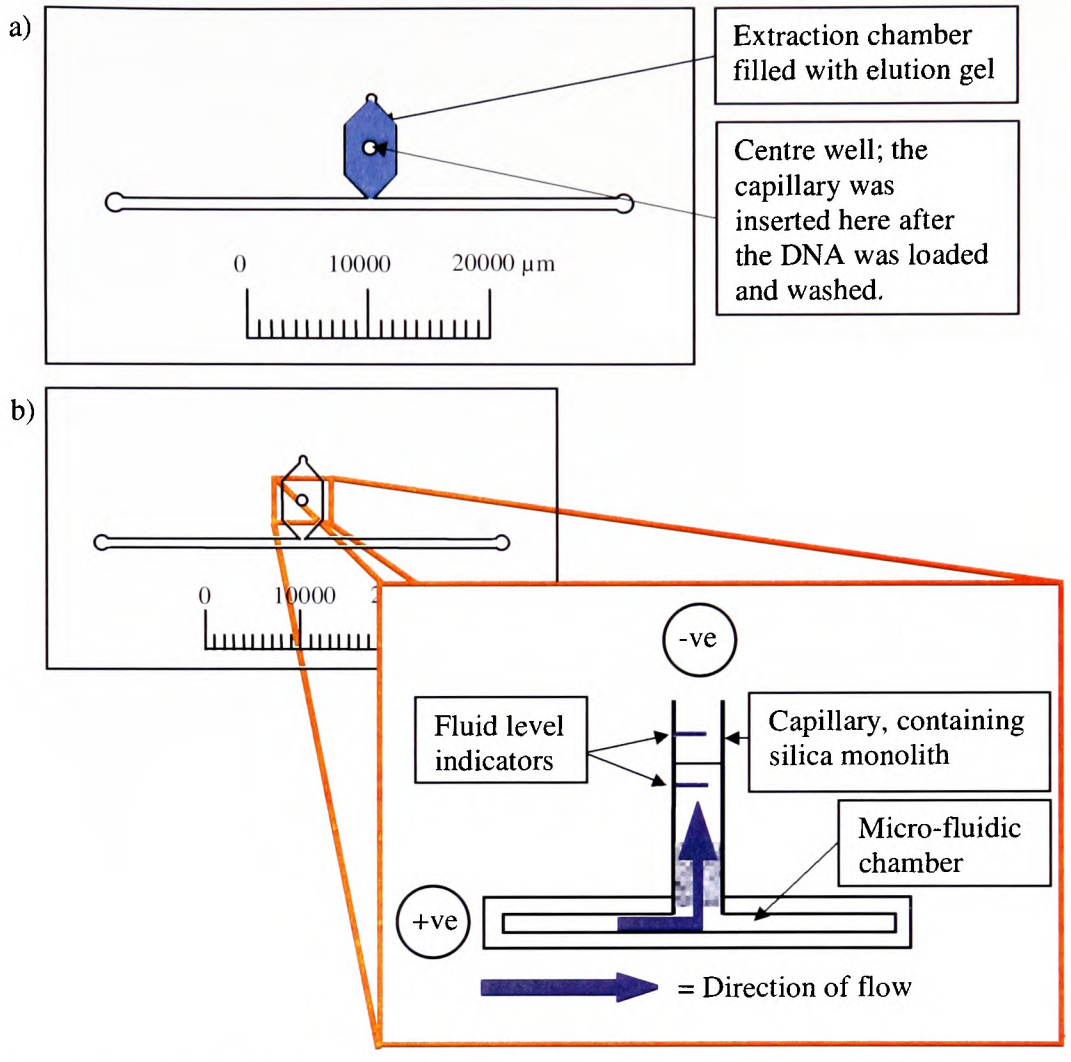

Figure 3-17 a) Micro-fluidic device design 2, extraction chamber and centre well that the capillary is inserted into are indicated. b) a schematic representation of how the capillary fits into the micro-fluidic chamber.

3.7.5.2 Results and Discussion

The DNA was loaded onto a monolith contained within a capillary, instead of a monolith inside the micro-fluidic device as it was thought that by loading and washing the DNA in a monolith, completely separate from the micro-fluidic device, would

further increase the probability that any DNA detected in the chamber was present due to EOP elution from off the monolith, and not leakage or contamination.

As the DNA sample loaded on the monolith had been labelled, this process was monitored using the florescence microscope.

It can be seen in Figure 3-18, that there is fluorescent 'debris' in the area surrounding the entrance of the extraction chamber where the monolith was inserted into the micro-fluidic device. This suggested that the DNA was successfully eluted from the monolith into the PCR reagent gel, by electro-osmotically pumping across the gel filled channel.

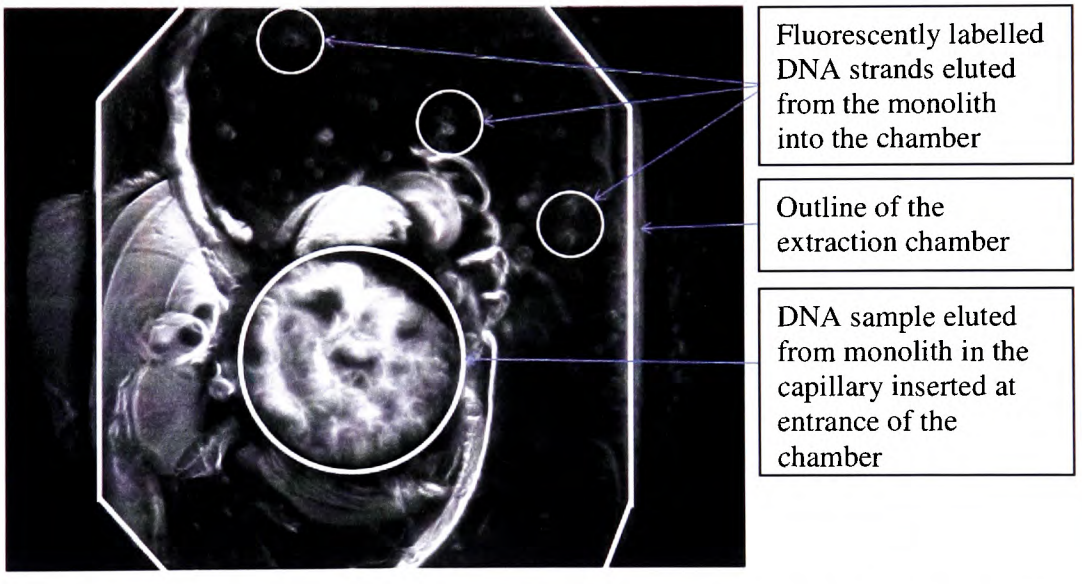

Figure 3-18 Microscope image of micro-fluidic chamber filled with agarose gel, the 'white dots' seen in the reservoir and the surrounding area are the fluorescently labelled DNA, which has been electro-kinetically transported from the monolith.

These results also confirm that the presence of DNA detected in the micro-fluidic device was due to EOP elution and no other means; a further experiment was then carried out to ensure the movement was not due to diffusion. A DNA loaded capillary

was inserted in to the reservoir, but an electric field was not applied, as can be seen in Figure 3-19.

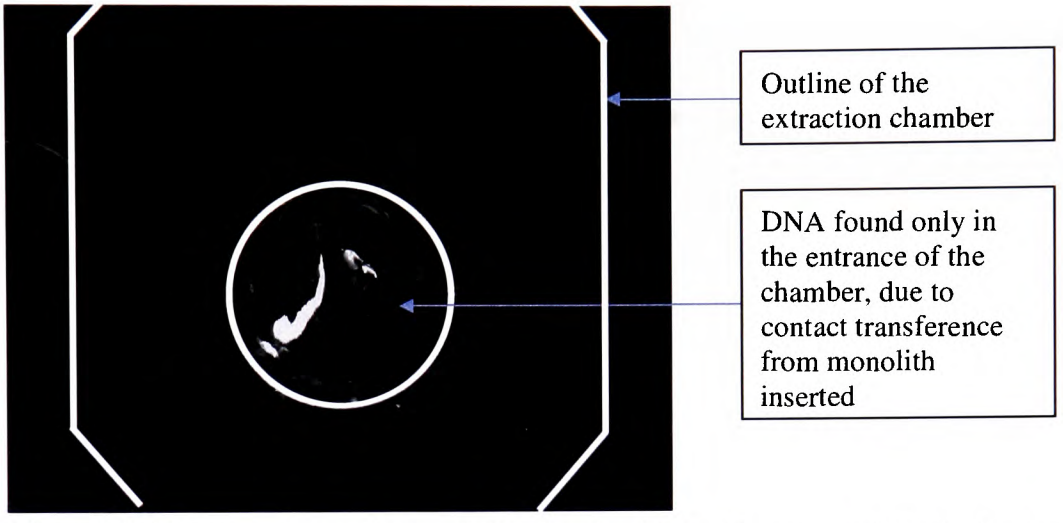

Figure 3-19 Microscope image of micro-fluidic chamber filled with agarose gel, illustrating how DNA was not transferred into the surrounding area of the chamber by diffusion.

After the same amount of time, the capillary was removed and the chamber inspected under the microscope. Only moderate evidence of florescence was detected in the actual chamber entrance where the monolith was inserted into the micro-fluidic device, and this was most likely due to contact transference from the monolith itself. However, in the area surrounding the entrance of the extraction chamber this time there was no evidence of fluorescence, confirming the movement observed in the surrounding area of the earlier experiment was not due to diffusion.

3.7.6 Investigation of electrode positions for EOP elution

In addition, to assess the versatility of the method in terms of how the experiment was set up and performed, and determine the optimum arrangement of electrode positions

from those available, alternative approaches were investigated for applying the electrical potential, incorporating different geometries for the electrodes.

3.7.6.1 Experimental

For this work, micro-fluidic device designs 1 and 3 were used, and variation of voltages, times and directional movements investigated. A schematic representation of the experimental design can be seen in Figure 3-20.

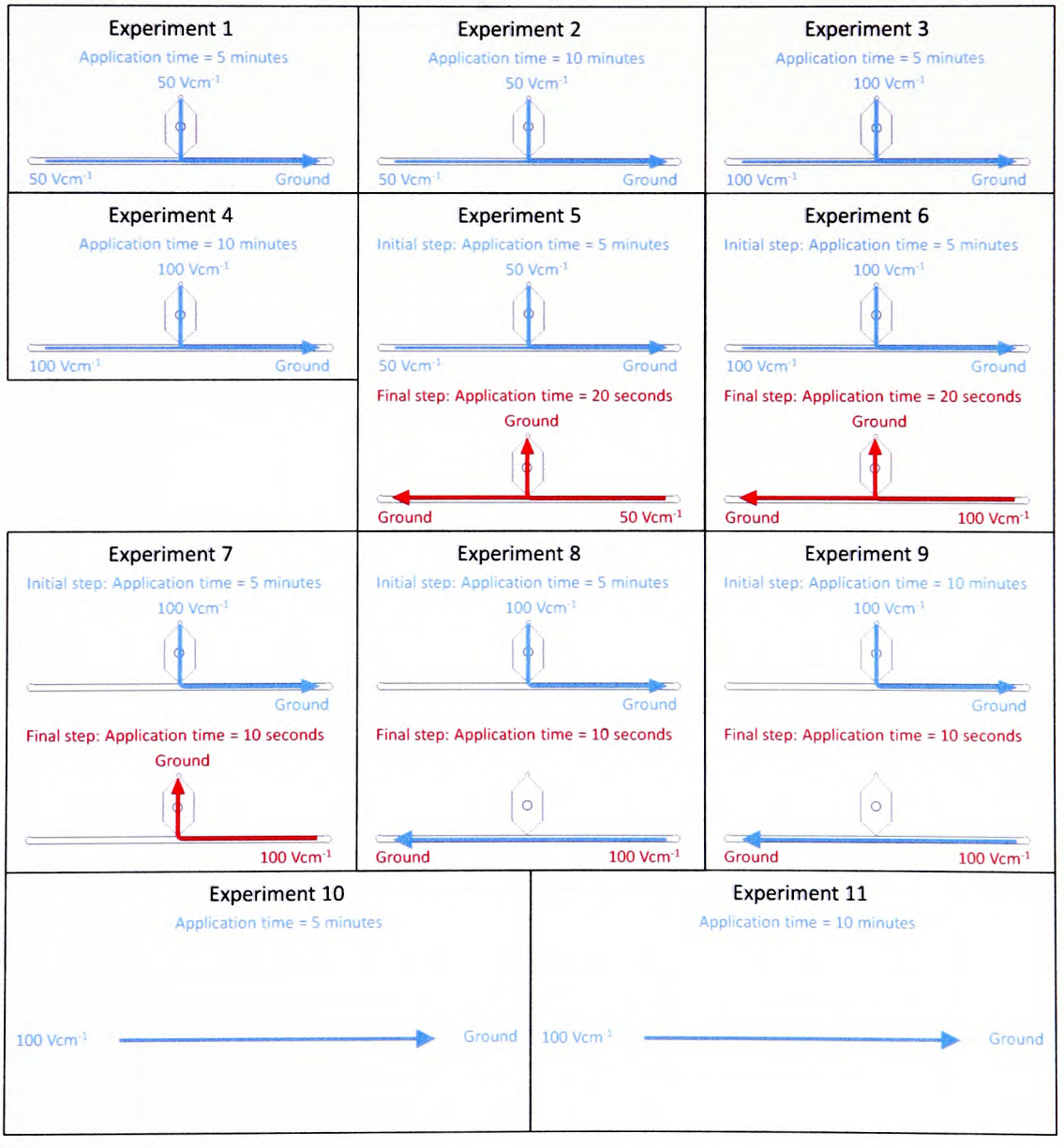

Figure 3-20 Schematic representation of the experimental plan to investigate the possible effect of variable change within the experiment.

3.7.6.2 Results and Discussion

The investigation of the different geometries and applied electric potentials (see Figure 3-20) indicated that the method is highly flexible, extraction efficiency results showed little variation between the different geometries, as seen in Table 3-4.

Table 3-4: DNA extraction efficiency achieved from the different experimental plans investigated

	Applied Voltage (Vcm^{-1})	Application Time	Extraction Efficiency (cathode)
Experiment 1	50	5 minutes	36 %
Experiment 2	50	10 minutes	38 %
Experiment 3	100	5 minutes	57 %
Experiment 4	100	10 minutes	49 %
Experiment 5	50	5 minutes	58 %
	50	20 seconds	
Experiment 6	100	5 minutes	56 %
	100	20 seconds	
Experiment 7	100	5 minutes	5 %
	100	10 seconds	
Experiment 8	100	5 minutes	65 %
	100	10 seconds	
Experiment 9	100	10 minutes	54 %
	100	10 seconds	
Experiment 10	100	5 minutes	51 %
Experiment 11	100	10 minutes	23 %

However, the results seen in Table 3-4 show Experiments 7 and 11 were highly unsuitable, several experimental plans vary little in their effectiveness (Experiments 3, 4, 5, 6 and 9), which indicates a high versatility of electrode positioning, suggesting the polymer medium based EOP process has high potential in other applications.

It was determined however, that the method is limited by the application of electric potential applied and the length of time of application, generally it was found that sufficient DNA could be collected from an application of 5 minutes, rendering a 10 minute application unnecessary as well as potentially damaging to the PCR gel. Whilst the investigation of the different applied electric fields showed a maximum electric field of 100 Vcm^{-1} could be successfully applied for a substantial time period without incurring damage to the gel, this field strength also proved to be the most efficient in terms of extraction efficiency.

To investigate possible movement of DNA by electrophoresis, the experiment was repeated with the electric potential reversed. The potential was reversed because with EOF, the DNA would be carried towards the cathode, but with electrophoresis the DNA itself would migrate towards the anode. The field strength was repeatedly increased until the increased field strengths resulted in considerable damage to the gel rendering it unusable, but only small volume of DNA movement was detected. This is most likely due to the fact that the electric field alone is not strong enough to elute the DNA attached to the monolith surface. In the case of elution by EOF, bulk flow of the solution occurs through the gel matrix and across the monolith, providing a more favourable environment for the DNA, allowing it to elute successfully.

3.7.7 Development of the PCR reagent containing gel

A series of agarose gel concentrations were investigated (10%, 5%, 3% 1.5%, 1% and 0.75%) to determine the concentration of gel that would facilitate the optimum PCR reaction to occur.

3.7.7.1 Experimental

The 'PCR gels' were prepared by dissolving differing weights of low melting point agarose in 100 µl of DNA/RNA free water, creating concentrated solutions of the agarose gel, the solution was then heated in a water bath at 75°C for 10 minutes to allow the gel to form. While the solution was still hot, a controlled volume of the gel solution was added to the PCR reagents (1 x NH_4 buffer, 1.5 µM BSA, 1 µM forward primer, 1 µM reverse primer, 200 µM dNTPs, 1.5 mM $MgCl_2$ and 1 Unit of GoTaq®) and mixed, providing the final gel solutions of concentrations of 10%, 5%, 3% 1.5%, 1% and 0.75%.

Micro-fluidic device design 2 was prepared and the DNA loaded as described previously, (see Section 3.5), the PCR reagent containing gel was pressure injected into the PCR channel. The platinum electrodes were attached and an electric potential of 100 Vcm^{-1} applied for 5 minutes, the experiment was performed on an ice block to maintain the integrity of the PCR reagents. Once the electro-kinetic movement was complete, the PCR gel was removed from the channel by pressure injection and collected. The resulting solution was then amplified in a PCR machine for 28 cycles. To introduce the sample to the slab gel electrophoresis (standard electrophoresis grade agarose gel at a concentration of 1.5%), the PCR product gel solution was heated to 75°C so it could then be injected into the wells. After amplification, the 'PCR products' were separated

by slab gel electrophoresis and visualised by ethidium bromide staining in conjunction with a transilluminator.

3.7.7.2 Results and Discussion

When performing the PCR reaction in a normal agarose gel solution, the PCR amplification proved unsuccessful. After monitoring the agarose gel consistency as the temperature cycle is applied, it was found that in the denaturing step (95°C) the gel was in liquid phase, but had a high viscosity. However, as the temperatures decreased in the extension step (72°C) and the annealing step (57°C), the viscosity of the solution greatly increased. It was thought that the high viscosity of the gel solution prevented the PCR reagents from mixing properly and reacting successfully at the annealing and extension steps.

To overcome this problem, low melting point agarose gel was investigated, it was hypothesised that the viscosity of the solution would remain sufficiently low at the extension and annealing steps, to allow the PCR reaction to be successful and this theory was proved to be correct. Further experimentation was performed to find the optimum gel concentration that would provide a suitable compromise between stability and usability, a higher viscosity would increase the stability of the reagents but would inhibit the PCR reaction; a lower viscosity would decrease the stability of the reagents but have less of an effect on the PCR reaction. Of the concentrations investigated, 0.75, 1, 1.5, 3, 5, and 10%, Figure 3-21 shows the visualisation of the results of solutions 0.75 to 3%.

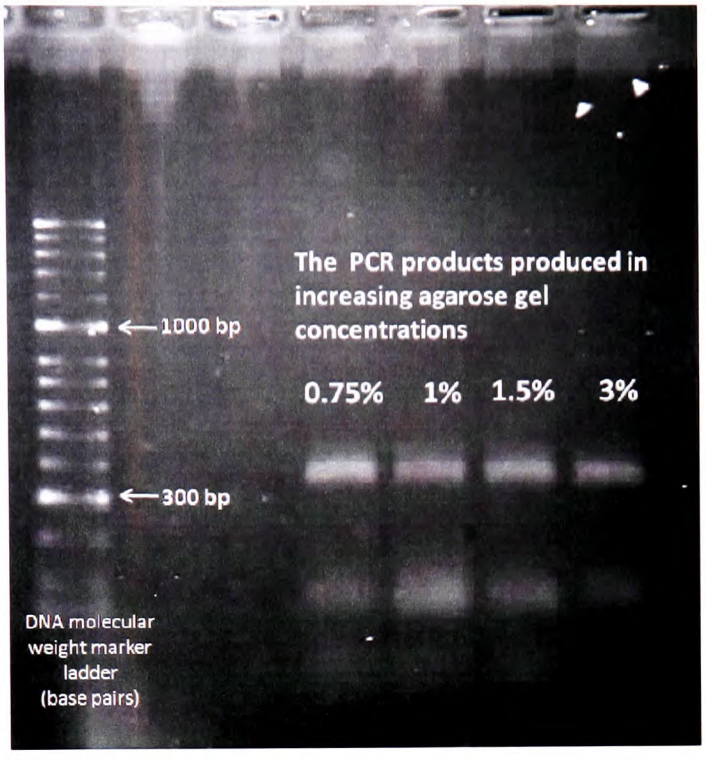

Figure 3-21 UV transilluminator image of D16S359 PCR products obtained from the stability testing of the concentration of reagent support gel.

The results from the experiment performed to determine the usability of the gels indicated that 1% and 1.5% were the easiest concentrations to manipulate and inject into the channel, below 1% and the gel formed had a very low viscosity and not all the PCR reagents were contained within the gel, above 1.5% and the gel was too difficult to re-melt and inject into the channel. These results were further supported by the PCR reaction experiments, 0.75% to 1.5% gel concentrations all provided a suitable environment for the reaction to occur. Although the 3% gel concentration enabled the reaction to occur the band was clearly of lower quality than the other concentrations investigated. The 5 and 10% gel concentrations could not be melted sufficiently to allow injection of the sample into the gel plate wells, however it is unlikely that the reaction would have been successful judging by the apparent trend. It was concluded

that a gel concentration of 1.5% was the optimum compromise between stability and usability.

It was then necessary to determine if there was sufficient DNA transported by electro-osmotic pumping for the PCR to proceed, and to establish if the PCR reagents contained in the gel were still viable after the application of the electric field. To do so, the eluted DNA and PCR reagents were amplified, separated and illuminated with a UV transilluminator, see Figure 3-22.

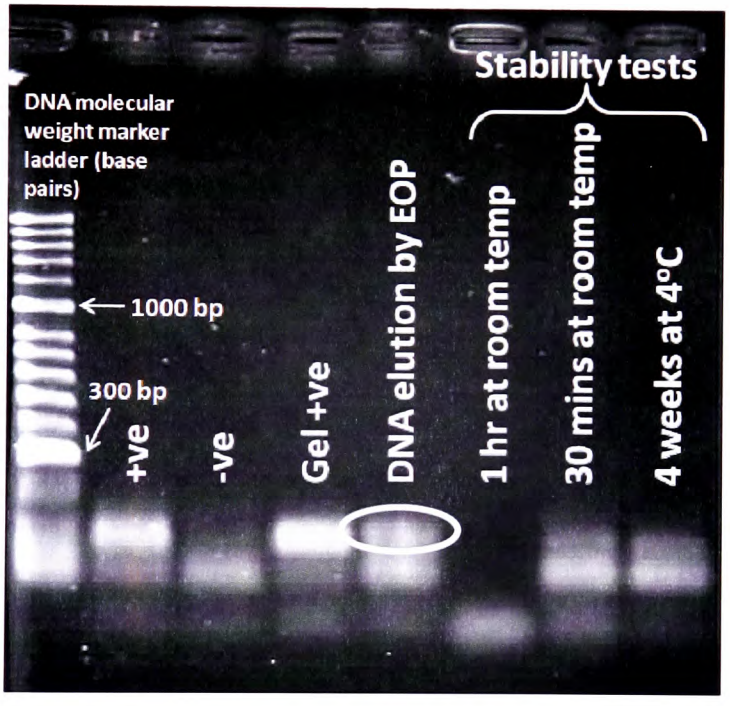

Figure 3-22 UV transilluminator image of Amelogenin PCR products following EOP of DNA into PCR reagents in gel. Positive and negative controls are samples of the PCR reagents with and without DNA template respectively. The 'gel positive' and 'DNA elution by EOP' are control samples of PCR reagents in gel and DNA, pre and post experimentation respectively. Stability tests; gel left at room temperature for 1 hour, gel left at room temperature for 30 minutes and gel stored at 4°C for four weeks.

The positive PCR band seen on the plate at approximately 100 base pairs indicated that DNA can be transported by electro kinetic movement in a sufficient concentration to allow PCR to occur, and also proved that the PCR reagents in gel solution were stable enough to withstand an applied electric potential. The stability tests indicated a trend of reducing stability of the PCR reagents when not kept refrigerated, at 30 minutes at room temperature there is evidence that the PCR reaction proceeded to some degree, however some mis-priming was evident, after 1 hour at room temperature the reagents were rendered completely unusable. The results indicated that the chip containing the PCR reagents must be kept refrigerated prior to use to maintain the stability of the reagents.

Further stability studies of the agarose gel was performed, where the agarose gel containing the PCR reagents was produced and stored at 5°C, at 1 week, 2 weeks, and 4 weeks, DNA was then added to the PCR reagent agarose gel and amplification by PCR was performed. The results indicated that the gel was still stable and viable after 4 weeks storage, demonstrating the suitability of the reagent gel for the intended stabilisation of reagent's which would enable pre-loading at time of manufacture.

Experimentations determined the optimum method of developing the PCR reagent containing gel as the following;

0.00294 g of low melting point agarose was dissolved in 100 µl of DNA/RNA free water creating a gel concentration of 2.94%, and heated in a 75°C water bath for 10 minutes. While the solution was still hot, 10.2 µl of the gel was added to the PCR reagents (1 x NH_4 buffer, 1.5 µM BSA, 1 µM forward primer, 1 µM reverse primer, 200 µM dNTPs, 1.5 mM $MgCl_2$ and 1 Unit of GoTaq®) and mixed, the concentration of the final gel solution was 1.59%.

3.7.8 Gel supported approach to integration of DNA analysis

Each step involved in the gel supported electro-osmotic pumping method has been previously described, however the integration of the different steps required a redesign of the chip that would allow the multiple introductions of the gel encapsulated reagents.

3.7.8.1 Experimental

Micro-fluidic device design 5 was prepared and the potassium silicate monolith added into the hexagonal structure as previously described (see Section 3.5), the differing reagent containing gels were separately prepared and loaded as follows:

The ethanol wash gel was made by dissolving low melting point agarose gel in deionised water to give a concentration of 3% (w/v) (0.0030 g agarose in 100 µl deionised water) and heated to 75°C. Once the gel was formed and still molten, 100 µl of 80% ethanol and 20% 1 M sodium chloride solution was added. The gel was then introduced into the wash delivery gel channel at port B where it solidified trapping the ethanol wash.

The DNA wash gel was prepared by dissolving low melting point agarose gel in deionised water to produce a concentration of 0.75% (w/v), and heated to 75°C for 10 minutes after which it was injected into the wash receiver gel channel through port C whilst still molten, then allowed to cool. A 0.75% (w/v) elution gel was similarly prepared and injected into the elution gel channel through port F whilst still molten, and allowed to cool.

The optimal PCR gel was prepared by dissolving low melting point agarose gel in deionised water to produce a concentration of 1.5% (w/v), and heated to 75°C for 10

minutes. Once the gel was formed and whilst still molten the PCR reagents were added (1 x NH_4 buffer, 1.5 μM BSA, 1 μM forward primer, 1 μM reverse primer, 200 μM dNTPs, 1.5 mM $MgCl_2$ and 1 Unit of GoTaq®) and mixed. The PCR gel was then injected into the PCR chamber through port D whilst still molten and on cooling the gel retained the PCR reagents.

A schematic illustration of how each of the reagent gels are contained within the micro-fluidic device can be seen in Figure 3-1. Once all channels were filled with gel-supported reagents platinum wire electrodes were secured in place at ports B-F and the chip was then ready for operational use. Firstly the loaded DNA was washed using the ethanol wash gel, of the electrodes placed in the device, ground was applied to electrode B whilst 400 Volts was applied to electrode C, an applied voltage of 100 Vcm^{-1}. This was followed by elution of the DNA from the monolith by applying a charge across electrodes D and F; ground was applied to electrode D whilst 600 Volts was applied to electrode F, an applied voltage of 100 Vcm^{-1}. At which point the PCR reaction was then initiated by applying a temperature of 95°C, followed by the PCR temperature cycles.

3.7.8.2 Results and Discussion

The gel supported electro-osmotic pumping approach to integration was investigated in continuous succession and the results can be seen in Figure 3-23;

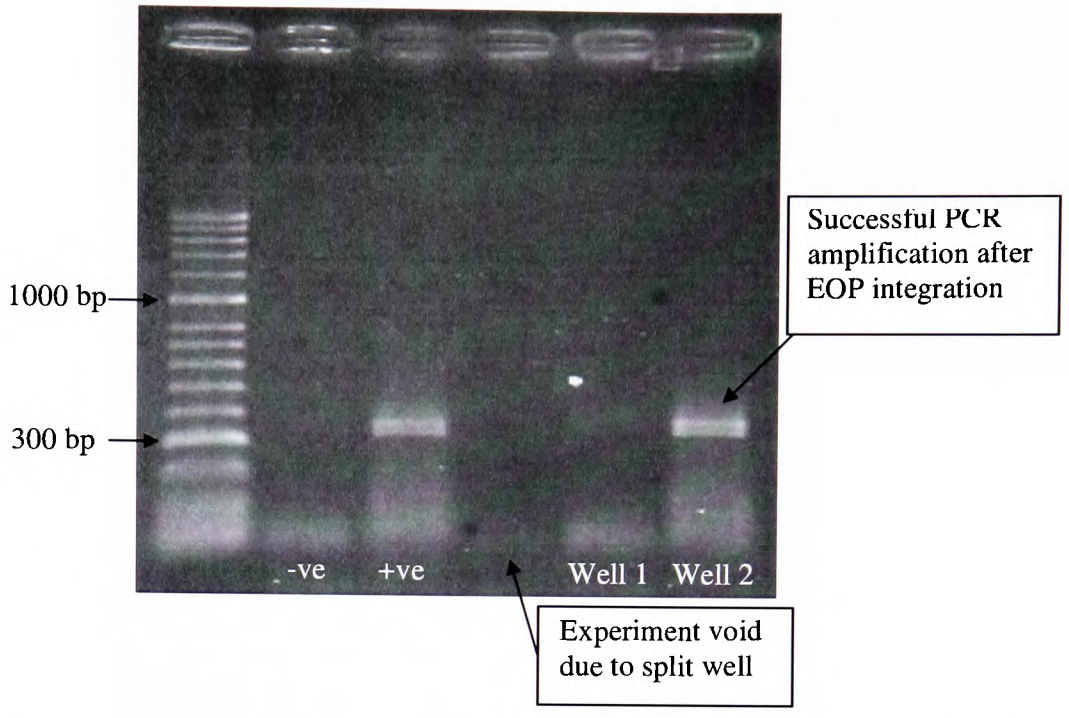

Figure 3-23: UV transilluminator image of D16S359 PCR products, that underwent the successive EOP procedure within the micro-fluidic device.

Results seen in Figure 3-23, show that the experiment was successful as indicated by the positive band located in line with the 300 bp marker on the sizing ladder, in Well 2.

3.8 Conclusions

This chapter has clearly shown how integration of each of the different processes onto a single device can be achieved by avoiding hydrodynamic pumping. By trapping reagents in a gel, and using EOP supported by a silica monolith, it is possible to have an integrated system with no moving parts. The sample once introduced on to the monolith can be washed, eluted and transported to the PCR chamber using the EOP approach in a continuous manner, without adverse effects from the electric field interfering with the subsequent reactions and processes.

Chapter 4: Development of electro-kinetic injection

4 Aim

The aim of the work described in this chapter was to identify the best method for injecting the PCR products into the CE channel of the integrated micro-fluidic device.

4.1 Development of electro-kinetic pinched injection of liquid into gel

4.1.1 Experimental

Micro-fluidic device design 4 (Figure 2-13) was cleaned and prepared by flushing through with 1M hydrochloric acid followed by 1M sodium hydroxide and deionised water before drying. The separation polymer was loaded into the separation channel by pressure injection into port D. Before performing a gel to gel injection, a voltage profile capable of performing a suitable EK injection of DNA products from solution into the separation gel was identified. The fluorescently labelled PCR product intended for injection was prepared in solution by diluting 9.8 µl of sample, into 10.2 µl of deionised water. The sample was then introduced into the micro-fluidic device by pressure injection into port A in order to ensure equal filling of sample matrix into both arms of the cross bar (B-C). The presence of the separation polymer provided enough resistance to ensure the PCR product sample was not introduced into the separation channel. Platinum wire electrodes were then secured into place in ports A-D (Figure 4-1).

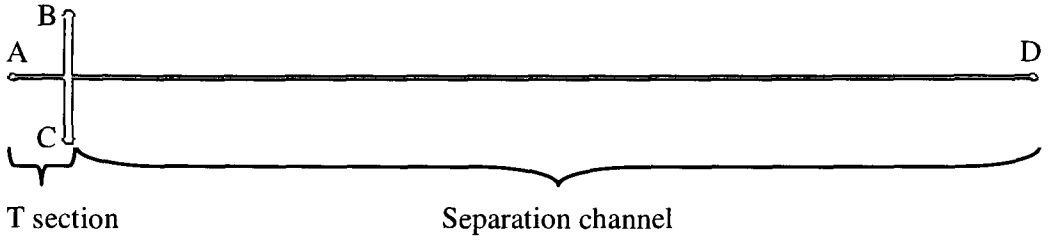

Figure 4-1 Diagram of micro-fluidic device used in this experiment, indicating well and electrode placement.

Once the micro-fluidic device was prepared the sample and separation matrices were inspected by eye to ensure no bubbles or debris, that could cause interruption to the applied electric field, had been introduced by the injection process. The voltage profile was automatically applied from a preset program entered through the LabView software. Systematic stepwise changes of voltages at the different electrodes were investigated with visual assessment of the results. The voltage profile selected (as given in Table 4-1) gave a reproducible plug injection approximately 5 seconds long with sample diffusion and tailing greatly reduced.

Table 4-1: The voltages and times required for the optimised electro-kinetic injection of sample contained within a solution, into PEO separation polymer.

	Applied voltage (V)			Applied time (seconds)
	Electrode A	Electrode B & C	Electrode D	
Step 1: Initial injection of sample	1	400	1100	5
Step 2: Concentration of sample and 'pull back' of excess	1	500	1237.5	10
Step 3: Clearance of excess from separation channel opening	1	600	1237.5	10
Step 4: Concentration of sample in separation channel	1	400	1237.5	5

Each of the injections was monitored via a fluorescent microscope, with a fluorescent image taken of the injection at multiple timed points throughout the experiment, allowing detailed measurements of the injected plug.

4.1.2 Results and Discussion

By making systematic stepwise changes to the voltages at electrodes placed in channels A-D and visually assessing the result on a fluorescent microscope a voltage profile was obtained that provided a satisfactory EK injection from solution to gel (injection of PCR product from the containing solution to the 'gel' based separation polymer) which gave a narrow plug of DNA products. These results were used as a comparison with the gel to gel injection process.

4.2 Development of electro-kinetic injection through a gel to gel interface

4.2.1 Experimental

Micro-fluidic device design 4 (Figure 2-13) was cleaned and prepared as described previously (see Section 4.1). The separation polymer was loaded into the separation channel by pressure injection into port D. The fluorescently labelled PCR product sample intended for injection was prepared in low melting point agarose gel, by dissolving 0.0029 g of low melting point agarose in 100 µl of DNA/RNA-free water, creating a gel concentration of 2.94% (w/v). The solution was then heated in a water bath at 75°C for 10 minutes to allow the gel to form, whilst the gel solution was still in the molten form, 10.2 µl of the gel was added to 9.8 µl of previously prepared PCR product (prepared in advance according to method described in Section 3.5). The final gel solution, which had a concentration of 1.5% (w/v), was injected into the micro-fluidic device whilst in molten form by pressure injection into port A and the electrodes secured into place.

The voltage profile was then modified from that used for the solution injection to identify a suitable profile that would perform a comparable EK injection in agarose gel (given in Table 4-2).

As stated previously, each of the injections was monitored via a fluorescent microscope, with a fluorescent image taken of the injection at multiple timed points throughout the experiment, allowing detailed measurements of the injected plug.

4.2.2 Results and Discussion

When the voltage profile optimised for solution based injection was applied to EK injection from the agarose gel in to the separation gel (PEO), the injection proved unsuccessful as no fluorescent PCR product was seen to move into the separation channel (Figure 4-2).

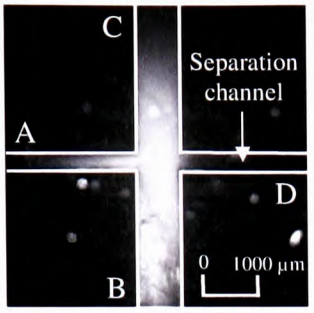

Step 1: Taken 5 seconds after start of injection

The PCR product should begin to move into the separation channel (i.e. towards D) upon the application of a 100 Vcm^{-1} electric field.

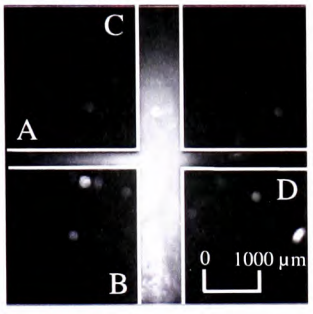

Step 2: Taken 15 seconds after start of injection

A small volume of PCR product can now be seen entering the separation channel, and the excess PCR product is beginning to be transported away from the entrance of the separation channel into the two side channels (B and C).

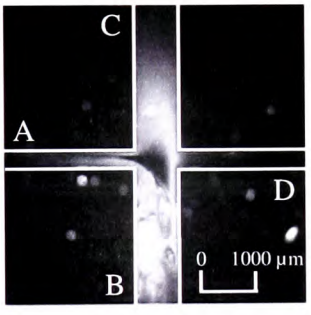

Step 3: Taken 25 seconds after start of injection

The PCR product that was beginning to enter the separation channel did not follow through. Instead the PCR product remains at the entrance of the separation channel and is not transported away with the rest of the excess PCR product into the two side channels.

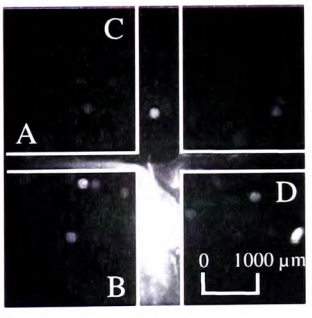

Step 4: Taken 30 seconds after start of injection

At this point the injection has completely failed, no PCR product was injected into the separation channel and the removal of the excess PCR product was also unsuccessful.

Figure 4-2: Visualisation of the un-successful electro-kinetic injection of fluorescent PCR product contained within agarose gel, illustrated by a series of fluorescent images taken at recorded times throughout the injection.

As can be seen in Step 1, in Figure 4-2, the PCR products were not pulled into the separation channel (i.e. towards D), furthermore, after the initial injection the excess sample is usually pulled away from the entrance to the separation channel to prevent

diffusion and sample leakage and this can be seen in Steps 2 and 3, however in Step 4 the process is not completed because the applied voltage degraded the gel at electrode B and electrical contact was disrupted. The two most probable reasons for the failure of the injection into the separation channel in Step 1 are either a mismatch in the viscosities of the loading and separation gels, or the interface between the two different gel types had a detrimental effect on the electric field strength across the channel.

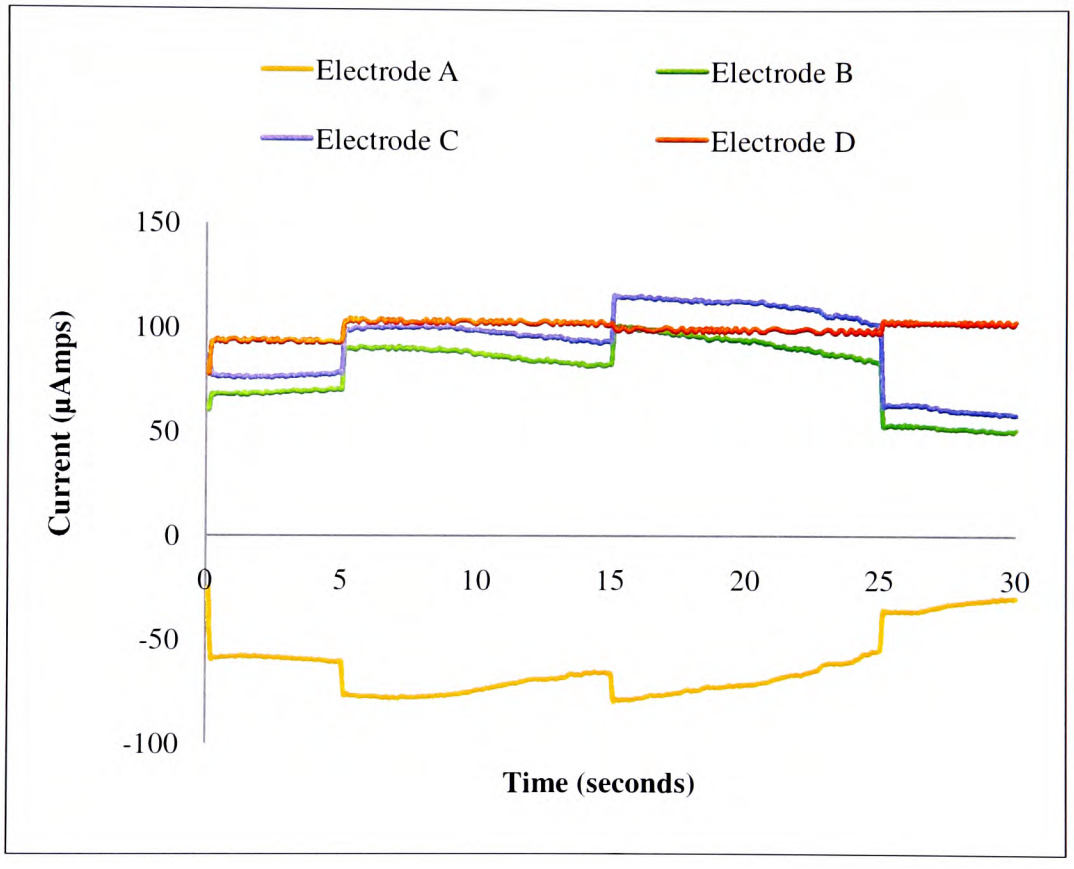

Figure 4-3: The current profile acquired during the electro-kinetic injection from solution into PEO separation gel.

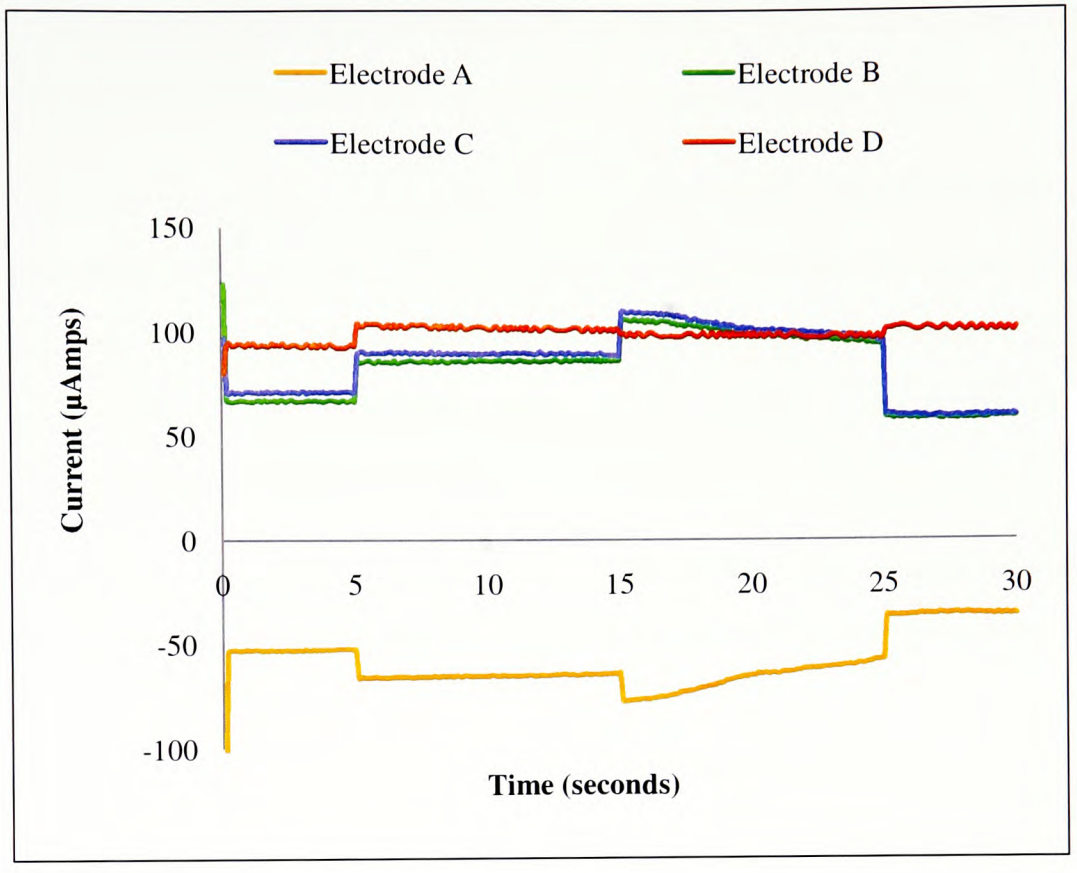

Figure 4-4: The current profile acquired during the electro-kinetic injection from 1.5 % (w/v) agarose gel to PEO separation gel.

Examination of the current profiles acquired for the solution and gel injections (Figure 4-3 and Figure 4-4), however, indicated that the electric currents generated within the system were in fact almost identical, the only difference being the flatter and more even nature of the profile observed for the gel system. This evidence suggested that the increased viscosity of the gel has not influenced the applied electric field, other than a producing a stabilising effect. The observed hindrance to the injection of the PCR products is therefore more likely to be attributable to a physical resistance caused by the higher viscosity agarose gel matrix compared to that of a solution based sample. This would suggest that the same fundamental mechanism of movement would apply in both

the gel and the solution, the only difference being that the physical influence of the gel requires higher voltages and longer time periods for similar movement to occur.

It was therefore necessary to changes the voltage profile for the gel to gel EK injection and as previously, systematic stepwise changes to the voltages at the different electrodes were made and the results inspected visually until a narrow reproducible plug of DNA products was obtained. The optimal voltages are given in Table 4-2 and the successful gel to gel injection is depicted in Figure 4-5.

Table 4-2: The voltages and times required for the optimised electro-kinetic injection of sample contained within a 1.5 % (w/v) agarose gel made with TE buffer, into PEO separation polymer.

	Applied voltage (V)			Applied time (seconds)
	Electrode A	Electrode B and C	Electrode D	
Step 1: Initial injection of sample	1	600	1100	5
Step 2: Concentration of sample and 'pull back' of excess	1	900	825	10
Step 3: Clearance of excess from separation channel opening	1	900	1237.5	30
Step 4: Concentration of sample in separation channel	1	800	1237.5	5

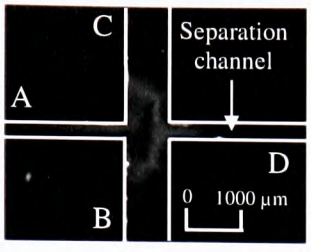

Step 1: Taken 5 seconds after start of injection

After application of the field for 5 seconds, the sample begins to move into the separation channel.

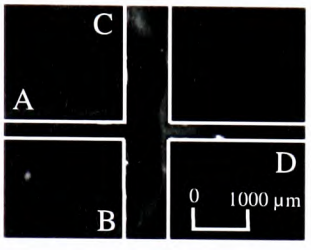

Step 2: Taken 15 seconds after start of injection

After application of the field for 15 seconds, the excess sample is beginning to move away from the entrance of the separation channel.

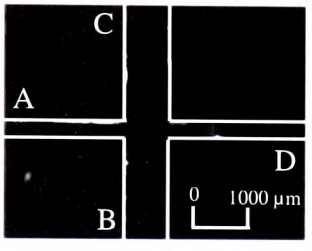

Step 3: Taken 45 seconds after start of injection

After application of the field for 45 seconds, the excess sample is completely clear of the T section, and the sample injected into the separation channel is beginning to focus.

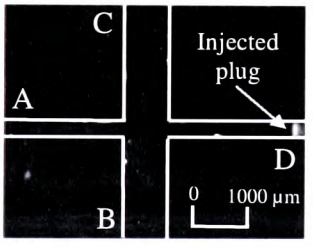

Step 4: Taken 50 seconds after start of injection

At the end of the injection procedure, a focused plug has been successfully injected into the separation channel.

Figure 4-5: Visualisation of the successful electro-kinetic injection of fluorescent PCR product contained within agarose gel, illustrated by a series of fluorescent images taken at recorded times throughout the injection.

This time in Step 1 the PCR products can be seen to be entering the separation channel (towards D) and in Step 4 the sample can be seen to be focussed into a sharp plug. The new voltage profile given in Table 4-2 also indicates a higher field strength was required to move the same sample through the agarose gel matrix.

This increase in field strength can be explained from Equation 4-1 which describes electrophoretic mobility (μ_{ep}) (Where q is the net charge, f is the translational friction

coefficient, v is the migration velocity of the component and E is the electric field) and the Hückel equation[72] (Equation 4-2), which is a modified form of the electrophoretic mobility equation, that takes into account electrophoretic movement of a species in a polymer solution (μ_o), (Where η is the solvent viscosity and q is the polyion's charge and R the polyion's radius).

$$\mu_{ep} = \frac{q}{f} = \frac{v}{E}$$ Equation 4-1

$$\mu_o = \frac{q}{6\pi\eta R}$$ Equation 4-2

The electrophoretic mobility is expressed in terms of charge over the translational friction coefficient; however the additional consideration of a polymer solution necessitates the introduction of not only the viscosity of the solvent but also the radius of the polyions. In both equations whilst the charge could be the same, the added affect of viscosity and the radius of the polyions will alter the electrophoretic mobility within the gel considerably.

4.3 Effect of gel to gel interface on resolution and separation integrity

The process of the electro-kinetic injection was performed in a gel to gel interface; however it was necessary to investigate the effect the change of environment would have on the resolution of the separation and the repeatability of the separation.

4.3.1 Experimental

Micro-fluidic device design 4 (Figure 2-13), was cleaned and prepared as described previously (see Section 4.2). The separation polymer was loaded into the separation channel by pressure injection into port D.

To ascertain the integrity of the injection, and investigate the reproducibility of the gel to gel injection, multiple injections were performed. The injections were monitored at multiple points along the separation channel, including at a 5 mm distance from the entrance to the separation channel and 5 mm distance from the end of the separation channel. The sample was fluorescently labelled and a fluorescent microscope used to capture an image of the injection at multiple timed points throughout the experiment. Electropherograms were also captured and the peak width and resolution measured at different points along the separation channel, and compared to ascertain the repeatability of the injection and its impact on the resolution of the separation.

4.3.2 Results and Discussion

The half peak width for the injected PCR products was measured and found to give 7.7 % RSD (n=3) for the optimal conditions indicated in Table 4-2. (Repeated experiments were performed on the same device, the reagent debris from each experiment was removed and the device was cleaned and reloaded as described.)

As indicated earlier, controlling the injection of a sample into a capillary channel is key to obtaining reproducible electrophoretic separations with reliable detection resolution. In order to improve the resolution of the CE separation, having established the optimal agarose to PEO injection technique, other separation polymers were investigated

including LPA-co-DHA.[101] When the voltage profile given in Table 4-2 was applied for an injection into this matrix, it was found that the difference in viscosity between the separation gels PEO and LPA-co-DHA resulted once again in the optimised voltage profile for the gel to gel injection being no longer valid. When the profile optimised for the PEO was applied to LPA-co-DHA, it was found lower voltages applied to electrodes B and C were satisfactory compared to PEO separations, as seen in . This is thought to occur due to the low resistance afforded by the less viscous PEO separation matrix providing a preferential field for the sample, a higher force is required to alter the direction of the momentum of the sample in PEO, after the initial sample pull down action (Step 1).

Table 4-3: The voltages and times required for the optimised electro-kinetic injection of sample contained within a 1.5 % (w/v) agarose gel made with TE buffer, into LPA-co-DHA separation polymer.

	Applied voltage (V)			Applied time (seconds)
	Electrode A	Electrode B and C	Electrode D	
Step 1: Initial injection of sample	1	600	720	5
Step 2: Concentration of sample and 'pull back' of excess	1	300	400	10
Step 3: Clearance of excess from separation channel opening	1	600	100	30
Step 4: Concentration of sample in separation channel	1	400	2200	5

Once the successful gel to gel injection (LPA-co-DHA) had been obtained with good precision, 2.9 % RSD (n=3), separations of the PCR products could be carried out and an example is in shown in Figure 4-6 in which PCR products vWA and FGA are seen to be separated with a peak resolution of 2.7.

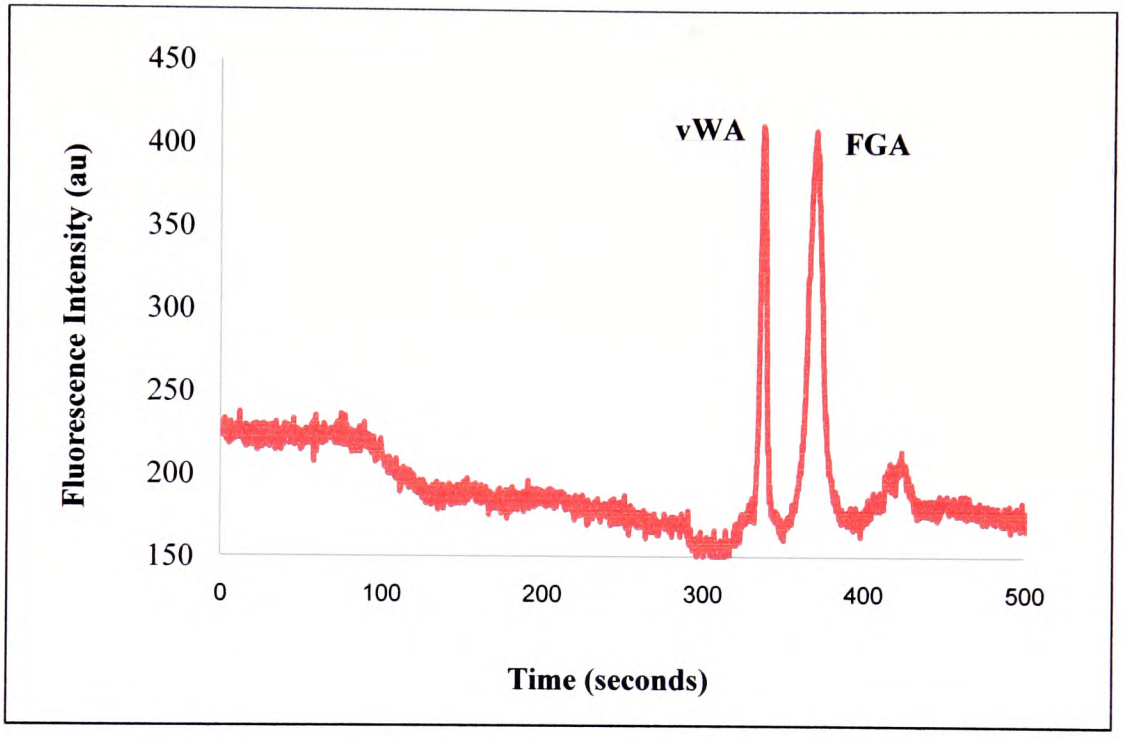

Figure 4-6: Electropherogram, separation of PCR products (vWA and FGA) in 3% LPA-co-DHA, injection field of 90 Vcm^{-1} for 5 seconds, separation field of 275 Vcm^{-1}, FAM florescence label utilised (excitation and emission wavelengths 488 and 522 nm respectively).

4.4 Robustness of gel to gel supported injection

4.4.1 Experimental

During the experimental process described in Section 4.2, there were instances where bubbles or voids were accidently introduced into the micro-fluidic system. Due to the

density of the polymer medium, the gel in the channel held its physical integrity even when the voids were quite large. In order to investigate the robustness of the polymer based system, the experimental procedure was performed as described, to establish the effect of the voids on a polymer based system compared to that of a liquid based system.

4.4.2 Results and Discussion

Figure 4-7 depicts the current profile recorded during an optimised EK gel to gel injection. Analysis of Figure 4-4 and Figure 4-7 indicate that gel to gel injection current profiles are smoother compared to solution to gel injection (Figure 4-3); this suggests a greater degree of electrical stability in the system.

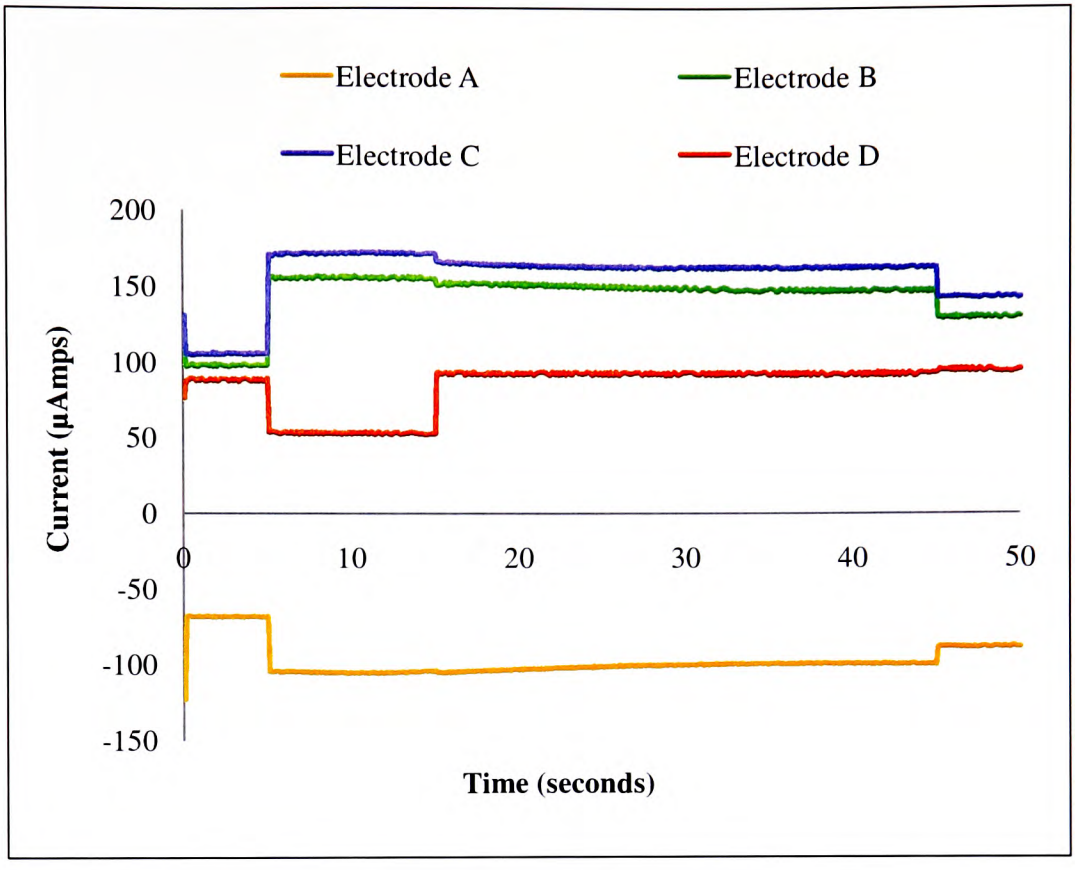

Figure 4-7: The current profile acquired during the optimised EK injection from 1.5% agarose gel to PEO separation gel.

The increased stability of the gel was further displayed when an electro-kinetic injection was successfully carried out with a void or a bubble, introduced into the system as an artefact of reagent introduction (Figure 4-8).

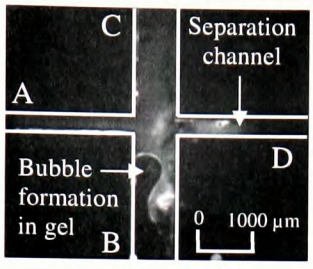

Step 1: Taken 5 seconds after start of injection

After the application of the field for 5 seconds, the sample has entered the separation channel. However the sample is also congregating around the large void.

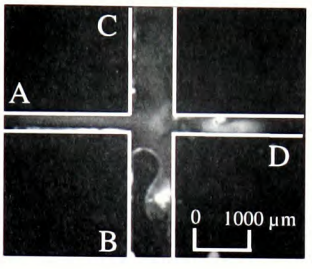

Step 2: Taken 15 seconds after start of injection

After 15 seconds, the sample is beginning to move and form into a plug in the separation channel, some movement of the excess away from the separation channel can also be seen.

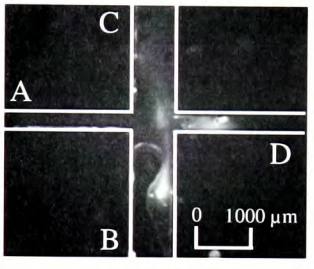

Step 3: Taken 45 seconds after start of injection

After 45 seconds, the T section is beginning to clear apart from around the void, which seems to be distorting the electric field significantly.

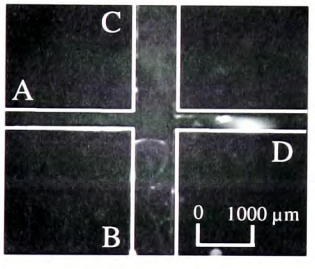

Step 4: Taken 50 seconds after start of injection

After 50 seconds, all excess sample has cleared from the T section, including from around the void. The sample plug has become more defined and has moved further down the separation channel.

Figure 4-8: Visualisation of a successful electro-kinetic injection in agarose gel matrix with a large void present, a bubble.

In the solution based system, a bubble present during the EK injection can severely compromise the fluidic movement and often lead to failure of the process. Figure 4-8 shows a gel to gel EK injection in the presence of a void or a bubble. In Step 1 a large void or bubble can be seen in the channel leading to B; however the PCR products can be seen to have entered the separation channel in the same way as Figure 4-5. In Steps 2 and 3 the excess sample is still cleared away from the separation channel despite

having to move around the bubble. By Step 4 for the excess sample has gone and the sample plug can be seen moving down the separation channel. The sample plug is more diffuse with a wider diameter, however it can clearly be seen that a successful injection of sample can be made, despite the presence of a bubble. The success of an injection with a bubble present was found to be dependent on the placement of the bubble. If a bubble developed either between the interface of the separation matrix and sample containing gel or in the vicinity of the injection point, then this would disrupt the electric field and the injection would be unsuccessful.

4.5 Application of gel to gel electro-kinetic injection to the integrated approach

The next step was to investigate a gel to gel injection of the PCR products from the PCR chamber to the separation channel.

4.5.1 Experimental

In order to establish if the polymer based system could be successfully integrated into the device and to determine if DNA amplified within the micro-fluidic device could be then electro-osmotically pumped into the injection area and then injected into the separation channel. The times and voltages applied to inject the sample into the separation channel can be seen in Table 4-2.

4.5.2 Results and Discussion

The experiment was repeated a number of times and results indicated that the electro-osmotic pumping method was sufficient to move the amplified DNA into position of the injection area. However, results indicated that some degree of size separation was occurring during the pumping mechanism, which was affecting the quality of the injected sample. As the gel in this area had no reactionary purpose, it was feasible that the gel could be made purely of water and to a lower concentration. Investigation was undertaken to ascertain if a reduction in gel concentration in the path towards the injection area would reduce the amount of separation occurring. Results indicated that a gel of 0.75% concentration would reduce the separation affect significantly and still maintain the integrity of the system.

4.6 Electro-kinetic pinched injection into multiple channels

An experiment was then undertaken to investigate the possibility of performing multiple injections into multiple channels within one device. This would allow a number of separation analyses to be performed on the same sample, essentially providing on the spot repeats of the separation under the same conditions, ensuring the accuracy of the analysis.

A number of micro-fluidic device designs were explored as part of this investigation, they included micro-fluidic device design 6 and micro-fluidic device design 7 (Figure 4-9), micro-fluidic device design 8 and micro-fluidic device design 9 (Figure 4-10).

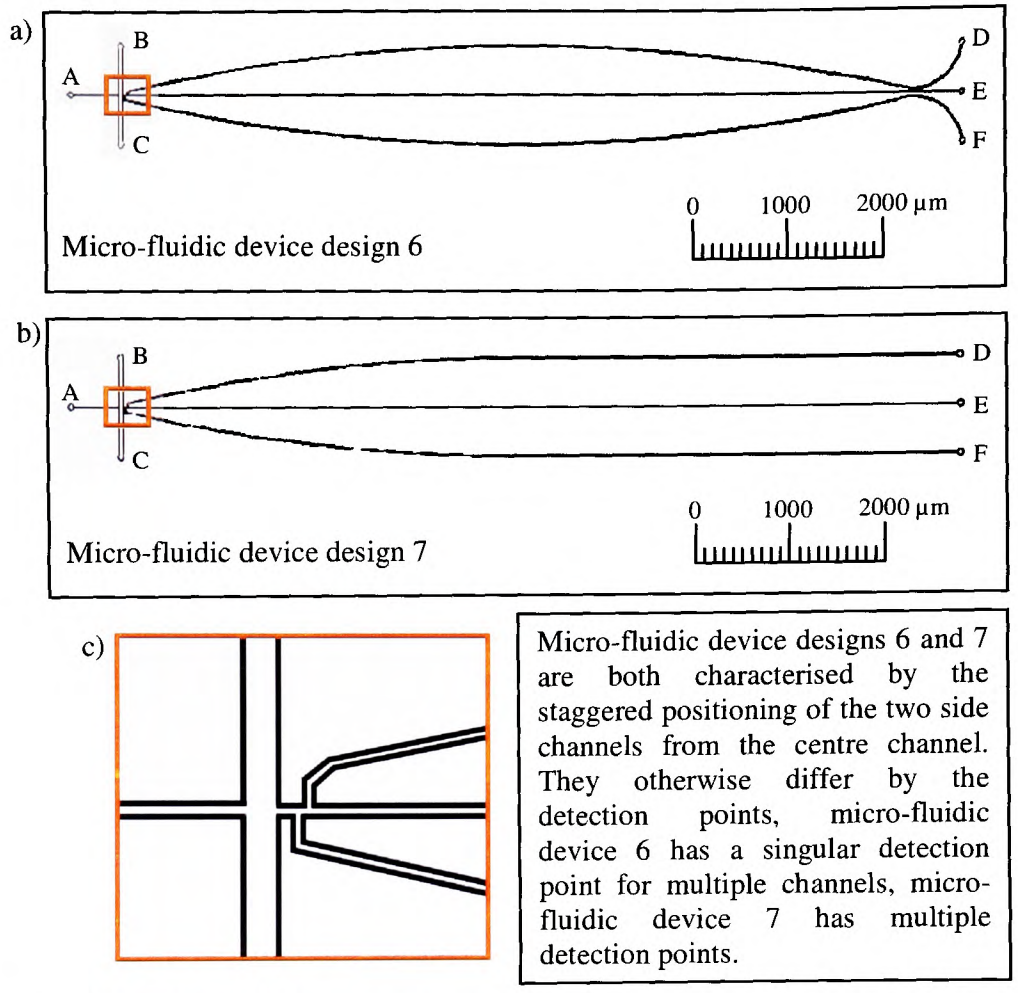

Figure 4-9: a) Micro-fluidic device design 6, b) Micro-fluidic device design 7, c) Close-up of the channel entrance of both Micro-fluidic device designs 6 and 7.

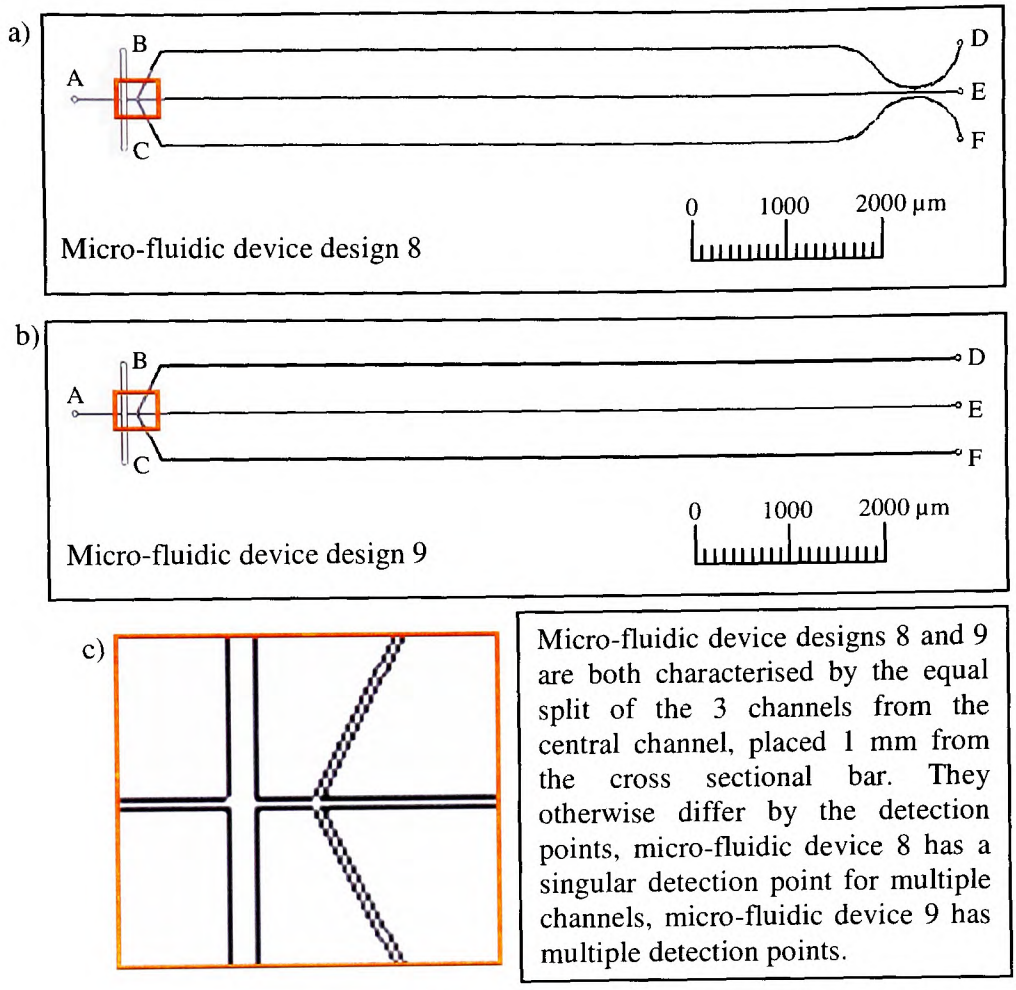

Figure 4-10: a) Micro-fluidic device design 8, b) Micro-fluidic device design 9, c) Close-up of the channel entrance of both Micro-fluidic device designs 8 and 9.

For each experiment, the micro-fluidic device was cleaned and prepared as described in Section 4.2. The separation polymer utilised in the investigation was 4% LPA-co-DHA prepared as described in Section 2.1.2.4. The separation polymer was pressure injected into each of the channels via ports D, E and F, by using a high pressure pump (KDS200 Syringe Infusion Pump). The separation polymer was injected into each channel first into port D, followed by port F, and finally into port E, by injecting the separation polymer in this order we could ensure the 'merge' of the polymer at the point of intersection between the channels.

Experimentation was performed using a 1.5% low melting agarose gel containing the sample; initially the sample was spiked with bromophenol blue in order to better visualise the movement of the sample in the micro-fluidic device, allowing the affects of alterations of the voltage profile to be better assessed.

4.6.1 Investigation of electric-kinetic injection into multiple channels using Micro-fluidic device design 6 and 7

4.6.1.1 Experimental

The investigation began using Micro-fluidic device design 6 (Figure 2-15), a voltage profile was applied similar to that which had already proved successful with a single channel injection but adapted for the multiple channels, as detailed in Table 4-4.

Table 4-4: Starting point for the investigation of the voltages and times to develop an optimised electro-kinetic injection of sample contained within a 1.5 % (w/v) agarose gel into multiple channels.

Port A (V)	Ports B and C (V)	Ports D, E and F (V)	Time (seconds)
1	600	1100	5
1	900	825	10
1	900	1237.5	30
1	800	1237.5	5

A systematic approach was then taken to adjust the profile detailed in Table 4-4 until an optimal arrangement of applied voltages and applied times could be determined that would provide an efficient and even injection into each of the 3 channels.

When a voltage profile was determined to be adequate for further detailed analysis, a sample of fluorescently labelled PCR product was added to the sample and the experiment performed under a fluorescence microscope. Initial experiments had determined that a larger voltage would be required in the centre channel compared to the two side separation channels. This was due to the proximity of the entrance of each of the separation channels to each other; the two side channels were pulling the sample out from the centre channel. Table 4-5 details the changes made to the applied voltage profile:

Table 4-5: The voltages and time applied for the first fluorescent investigation of an optimised electro-kinetic injection of sample into multiple channels.

Port A (V)	Ports B and C (V)	Ports D and F (V)	Port E (V)	Time (seconds)
1	50	850	900	5
1	250	637.5	675	10
1	500	425	450	20
1	600	425	450	30

Further investigation led to the determination of the voltage profile detailed in Table 4-6 and Table 4-7 providing an injection of sample into each of the 3 channels, evidence of which can be seen in Section 4.6.1.2.

Table 4-6: The voltages and time applied for an electro-kinetic injection of sample into multiple channels

Port A (V)	Ports B and C (V)	Ports D and F (V)	Port E (V)	Time (seconds)
1	50	850	900	5
1	350	637.5	675	10
1	600	425	540	20
1	700	425	540	30

Table 4-7: The voltages and time applied for an optimised electro-kinetic injection of sample into multiple channels.

Port A (V)	Ports B and C (V)	Ports D and F (V)	Port E (V)	Time (seconds)
1	50	850	900	5
1	350	637.5	675	10
1	600	425	540	30
1	700	510	540	30
1	400	999	999	10

The investigation was undertaken using Micro-fluidic device design 7 (Figure 2-16), the voltage profile determined to be effective for Micro-fluidic device design 6, detailed in Table 4-7, was applied, and the results of which are detailed in Section 4.6.1.2.

4.6.1.2 Results and Discussion

The application of the voltage profile detailed in Table 4-5 resulted in a successful capture of sample in each of the separation channels, as shown in Figure 4-11. However, the clearance in the T section was ineffective; in addition, the sample was pulled out of the centre separation channel, which is in closest proximity to the entrance of the T section.

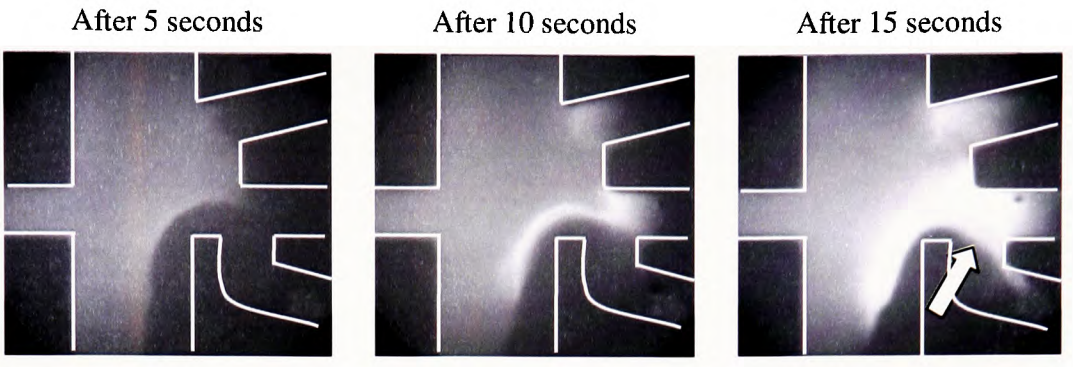

In the first 15 seconds of the injection, the three channels fill as expected, although the sample is pooling on the nearside of the entrance to the three channels (as marked by the arrow).

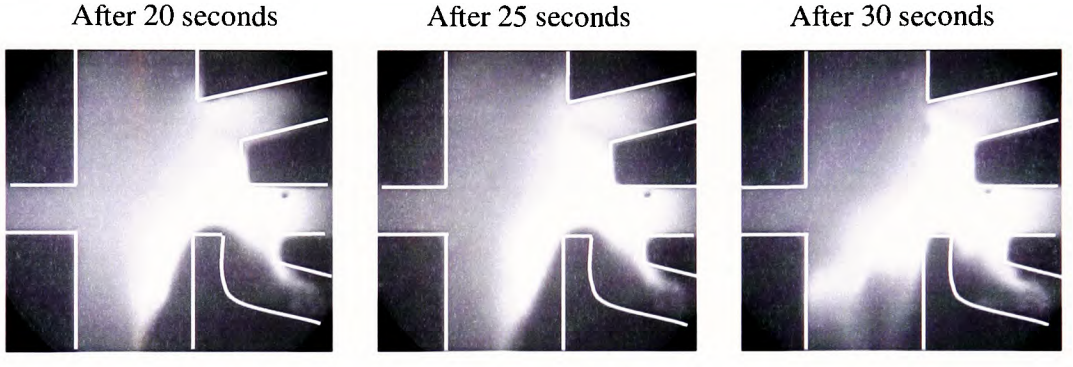

After 20 seconds the introduction of the sample into the centre channels ceases, whilst the two side channels continue to receive from the sample injection process.

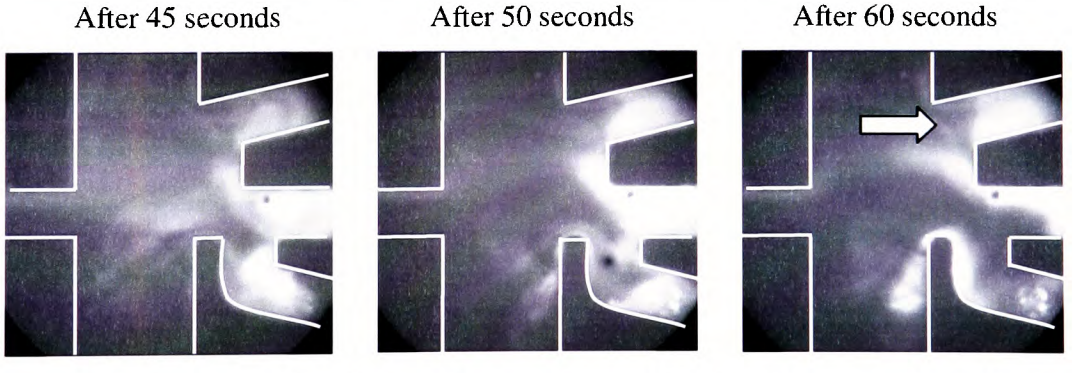

In the last stage of the injection the sample is pulled from the centre channel into the top side channel (as indicated with an arrow).

Figure 4-11: Visualisation of an un-successful electro-kinetic injection into multiple channels, using the voltage profile detailed in Table 4-5.

The application of the voltage profile detailed in Table 4-6 again resulted in an incomplete injection of the sample into each separation channel, as was the removal of the excess sample from the T section. This can be seen in Figure 4-12.

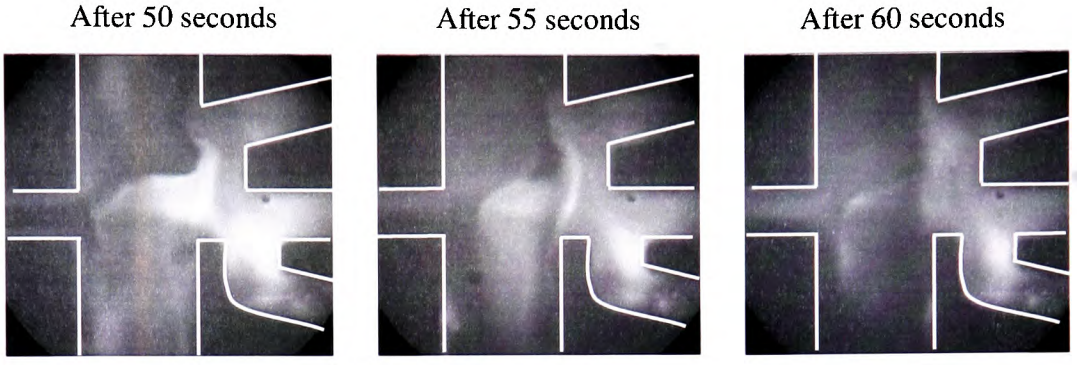

Figure 4-12: Visualisation of an un-successful electro-kinetic injection into multiple channels, as stated the injection process was incomplete, using the voltage profile detailed in Table 4-6.

The timing could be increased slightly to ensure full clearance of the excess sample from channel 2. The voltage increase to 60 Vcm^{-1} in step 4 allowed successful injection into channel 3.

The application of the voltage profile detailed in Table 4-7 resulted in a successful injection into each of the separation channels from the single sample.

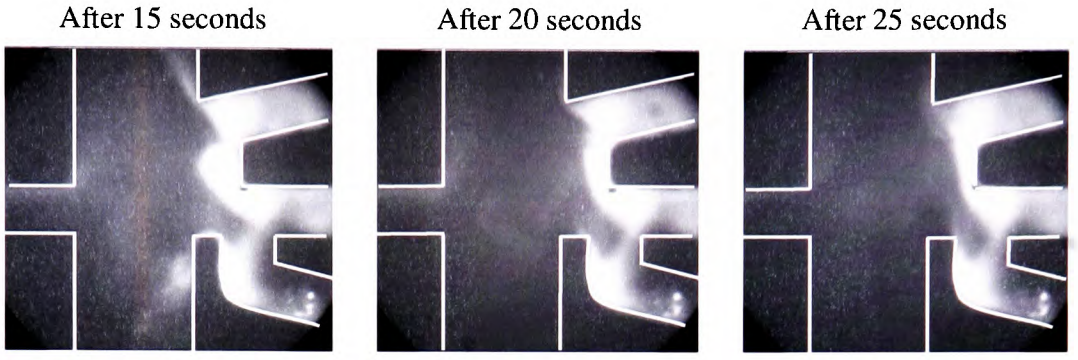

After 15 seconds of the application of the electric field, the second step of the injection process, the sample has been successfully introduced into all three of the channels and excess sample has been removed from the T section.

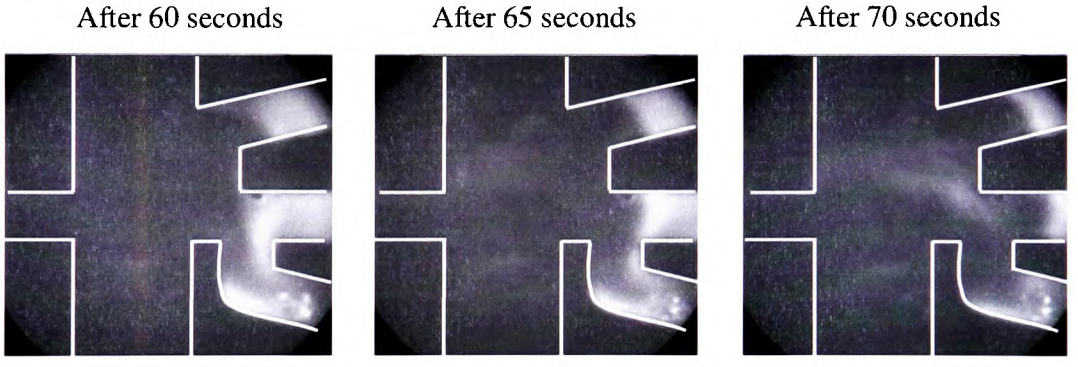

In the latter stages of the injection, the excess sample has cleared from the T section, and after 65 seconds the sample in the separation channels begins to focus into a well contained plug ready for separation.

Figure 4-13: Visualisation of a successful electro-kinetic injection into multiple channels, using the voltage profile detailed in Table 4-7.

During the experimentation it was noticed that the required movement of the sample had been achieved in step 4 prior to the completion of the step, indicating a possible point at which the timing could be reduced if later required. Table 4-8 depicts the re-worked optimised EK injection, reflecting the shorter times and smaller voltages

applicable for a successful EK injection into the multiple channels from one sample source.

Table 4-8 The re-worked voltages and times required for an optimised electro-kinetic injection of sample into multiple channels.

Port A (V)	Ports B and C (V)	Ports D and F (V)	Port E (V)	Time (seconds)
1	50	850	900	5
1	350	637.5	675	10
1	600	425	540	20
1	700	425	540	30

4.6.2 Investigation of electro-kinetic injection into multiple channels using Micro-fluidic device design 8 and 9

4.6.2.1 Experimental

The investigation was undertaken using Micro-fluidic device design 8 (Figure 2-17), followed by Micro-fluidic device design 9 (Figure 2-18), the voltage profile determined to be effective for Micro-fluidic device design 6, detailed in Table 4-7, was applied, and the results of which are detailed in Section 4.2.

4.6.2.2 Results and Discussion

A systematic approach was taken to adjust the profile until an optimal arrangement of applied voltages and applied times could be determined that would provide an efficient

and even injection into each of the 3 channels. However, difficulty was encountered in finding a profile that was sufficient in a providing a clean injection into each of the 3 channels. The geometry of the equal spacing of the side channels, which step directly from the centre channel, proved extremely difficult to implement a successful injection into each of the three channels at the same time. After numerous attempts, no successful injection into each of the three separation channels was achieved, instead manipulation of the applied electric field resulted in a shift in the separation channel favoured, where all sample would move into.

4.7 Conclusions

This chapter has clearly shown the requirements to achieve a successful injection from a gel source, into a gel receiver matrix; in addition experiments have shown that the gel-to-gel injection approach provided stability to the CE pinched injection not seen with the solution approach.

Finally, experimentation has shown that a CE pinched injection into multiple channels can be successfully implemented, this discovery allows for the possibility of further investigation into expanding the device to run multiple separations on the same sample, on the same device, developing an in-built validation system.

Chapter 5: Separation by capillary electrophoresis

5 Aim

This chapter describes the development of the capillary electrophoretic separation process within the micro-fluidic device, including the investigation into appropriate channel widths and channel lengths. A number of different separation polymers were explored, including hydroxyethyl cellulose (HEC), polyethylene oxide (PEO) and linear poly acrylamide (LPA), to name a few. In addition, the experimental design approach taken to optimise the separation performance within the micro-fluidic device system is described.

5.1 Calculating the density of the separation polymers

5.1.1 Experimental

A stoppered flask, which had been cleaned and dried was weighed three times and the average taken (M_f). Deionised water was added to the flask, filled to the rim of the flask and the stopper gently dropped in to place being careful to avoid bubbles, and then secured tightly. The external surface of the flask was dried thoroughly using a clean dry wipe and the flask was re-weighed (M_{fw}).

The temperature of the water was monitored throughout the experiment, and readings taken at the start, during and at the end of the experiment. This was later used to determine the accurate density of the water to be 997.77 kgm^{-3}.

Using Equation 5-1, the volume of the flask (V_f) was accurately determined.

$$V_f = \frac{M_{fw} + M_f}{Density_{water}}$$ **Equation 5-1**

Approximately 1 gram of the polymer was weighed in a cleaned and dried weighing boat, with the actual weight noted accurately (M_p). Deionised water was added to the polymer in the weighing boat, dissolving the polymer so it could easily be transferred into the flask. The weighing boat was rinsed in this fashion several times until the flask was full to the rim, the stopper gently dropped in to place being careful to avoid bubbles, and then secured tightly. The external surface of the flask was dried thoroughly using a clean dry wipe and the flask weighed again, the mass of the flask containing the water and the polymer (M_{fwp}). This was repeated for each polymer concentration. When the polymer was added to the flask it displaced some of the water, the volume of the remaining water (V_w) was then determined using Equation 5-2.

$$V_w = \frac{M_{fwp} - (M_p + M_f)}{Density_{water}}$$ **Equation 5-2**

Therefore, the volume of the polymer was the difference between the volume of the flask and the volume of the water;

$$V_p = V_f - V_w$$ **Equation 5-3**

The density of the polymer (D_p) was then determined using Equation 5-4.

$$D_p = \frac{M_p}{V_p}$$ **Equation 5-4**

Mass of dry stoppered flask was 0.0598 ± 3.0616 x 10^{-6} kg

Mass of flask filled with water was 0.0977 ± 1.7558 x10^{-5} kg

Temperature of the water was 23.2667 ± 0.2082 °C

5.1.2 Results and Discussions

The density of each polymer used throughout this investigation was ascertained, in order to establish the relationship between the density of the separation polymers at different concentrations. The relationship between separation efficiency and the density of the separation polymer was established in Section 1.6.2; however the purpose of this investigation was to gain a better understanding of the relationship between the density of the polymer and the polymers entanglement properties, which is heavily dependent on the concentration of the polymer.

Table 5-1: Calculated density of separation polymers

		Mp (kg)	Mfwp (kg)	VW (m^3)	Vp (m^3)	Dp (kgm^{-3})
LPA-co-DHA	3%	0.98×10^{-3}	9.7706×10^{-2}	3.70×10^{-5}	9.47×10^{-7}	1034.77
	4%	1.09×10^{-3}	9.7732×10^{-2}	3.69×10^{-5}	1.03×10^{-6}	1056.74
	5%	1.05×10^{-3}	9.7775×10^{-2}	3.70×10^{-5}	9.47×10^{-7}	1107.12
LPA	4%	1.45×10^{-3}	9.7743×10^{-2}	3.68×10^{-5}	1.08×10^{-6}	1064.99
	5%	1.18×10^{-3}	9.7777×10^{-2}	3.68×10^{-5}	1.08×10^{-6}	1096.22
	6%	1.19×10^{-3}	9.7764×10^{-2}	3.68×10^{-5}	1.10×10^{-6}	1082.25
PEO	2.0%	1.00×10^{-3}	9.7745×10^{-2}	3.70×10^{-5}	9.25×10^{-7}	1077.30
	2.5%	1.05×10^{-3}	9.7776×10^{-2}	3.70×10^{-5}	9.51×10^{-7}	1107.64
	3.0%	1.05×10^{-3}	9.7795×10^{-2}	3.70×10^{-5}	9.29×10^{-7}	1131.22
POP - 4		0.97×10^{-3}	9.7703×10^{-2}	3.70×10^{-5}	9.37×10^{-7}	1031.85

From the results depicted in Table 5-1, it can be seen that unexpectedly PEO appears to have a higher density than LPA-co-DHA. However, the polymer with the higher density was LPA as expected which has a highly organised cross polymer network, allowing a higher degree of packing. In addition, LPA is characterised by the extremely long lengths the carbon chain can 'grow' to, depending on the initiation procedure employed.

In the case of LPA-co-DHA, the initiation procedure prevents chains above a certain length from forming, capping the possible density the polymer can attain.

PEO and POP-4 are both low density and low viscosity polymers, which gives them the advantage of being easy to load into high pressure environments.

5.2 Determination of the denaturing of DNA

5.2.1 Experimental

An important aspect of DNA size separation is ensuring the DNA is single stranded during the separation process, to ensure the accuracy of the separation. There are numerous methods utilised by which denaturation can be achieved, including thermal denaturation or by additives added to the sample either prior to separation or instead included in the separation matrix.[102-104] Of the different number of additives used, urea is one of the most common, with a number of different concentrations being commonly reported in the literature, 6 M urea was chosen to be investigated as it is also used in the standard capillary electrophoresis the micro-fluidic samples are compared with.

The experiments were performed with the micro-fluidic device placed on a heat plate because a peltier heater of the size required was unavailable. However it was found that controlling the temperature inside the device by this means was extremely difficult, if the temperature was underestimated and actually higher than thought, the separation polymer degraded and the separation was unsuccessful.

Experiments were performed to ensure that the 6 M urea present in the separation matrix was sufficient to denature the DNA and create single strands; this was performed by analysis using the Quant-iT™ PicoGreen® dsDNA assay kit.

A 5 µl aliquot of double stranded DNA and 1 µl of PicoGreen were pipetted on to a microscope slide and the solutions were mixed with the tip of the pipette. The microscope slide was then analysed under a fluorescence microscope (with a 25 times

magnification), and an image captured. The procedure was repeated, with the addition of 6 M urea to the DNA solution.

Further investigation was performed to ensure the same effect was seen when the dsDNA came into contact with the separation matrix containing 6 M urea.

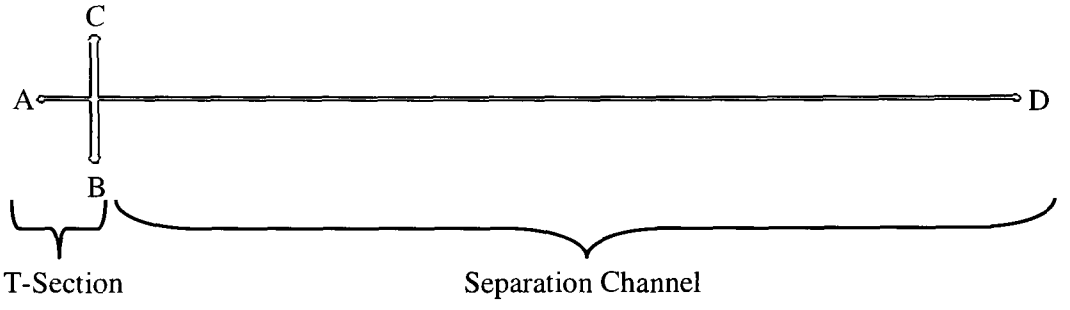

Figure 5-1: Diagram of micro-fluidic device 4 used in this experiment, indicating electrode placement.

Micro-fluidic device design 4 was prepared by flushing the device with 1 M HCl for 5 minutes followed by 1 M NaOH for 5 minutes. 5 % LPA-co-DHA separation matrix containing 6 M urea was introduced into the separation channel by pressure injection via port D. 2 µl of PicoGreen was added to 10 µl of dsDNA solution and mixed, the solution was then introduced into the T-section via port A. The micro-fluidic device was positioned under the fluorescence microscope (with a 10 times magnification), and the platinum electrodes A-D secured into place and the voltage-time profile applied as shown in Table 5-2:

Table 5-2: The voltages and times required for electro-kinetic injection of sample, into 5 % LPA-co-DHA separation polymer.

	Applied electric field strength (Vcm^{-1})			Applied time (seconds)
	Electrode A	Electrodes B and C	Electrode D	
Step 1	1	1	110	5
Step 2	1	300	50	20
Step 3	1	500	15	30
Step 4	1	600	10	30
Step 5	1	400	200	300

The experiment was also repeated with the separation polymer PEO, HEC and LPA.

5.2.2 Results and Discussion

PicoGreen only fluoresces when it comes into contact and binds with double stranded DNA (dsDNA), and will stop fluorescing in the presence of single stranded DNA (ssDNA).

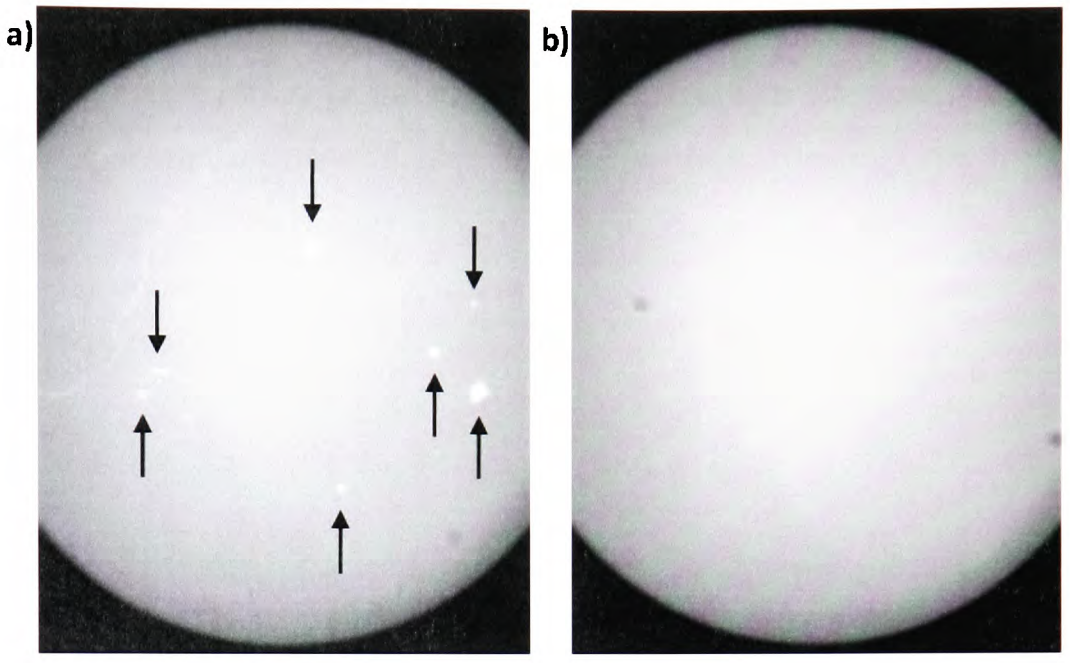

Figure 5-2: Fluorescence image of a) double stranded DNA interaction with PicoGreen, and b) double stranded DNA interaction with PicoGreen in the presence of 6 M urea.

Double stranded DNA can 'clump' when suspended in solution, when PicoGreen was added to the DNA solution it bound to the DNA and fluoresced under a fluorescent microscope, which is clearly indicated by the arrows in Figure 5-2a. However, when the experimented was repeated with the addition of 6M urea, under the same conditions, no evidence of fluorescence was found, as seen in Figure 5-2b. The lack of fluorescence in the presence of the urea supports the theory that 6M urea was successful in denaturing the dsDNA into ssDNA.

The experiment established that 6M urea added to a dsDNA solution was capable of denaturing the DNA to single stranded; further investigation was undertaken to establish if when 6M urea was added to the separation polymer instead of the DNA solution, it would still be as effective at denaturing the DNA. A solution of dsDNA and PicoGreen was electro-kinetically injected into the separation channel containing the separation

polymer formulated to contain the 6M urea. If the urea was effective the fluorescent plug of sample would disappear as it moves further into the separation channel, and the 6M urea acted on the dsDNA.

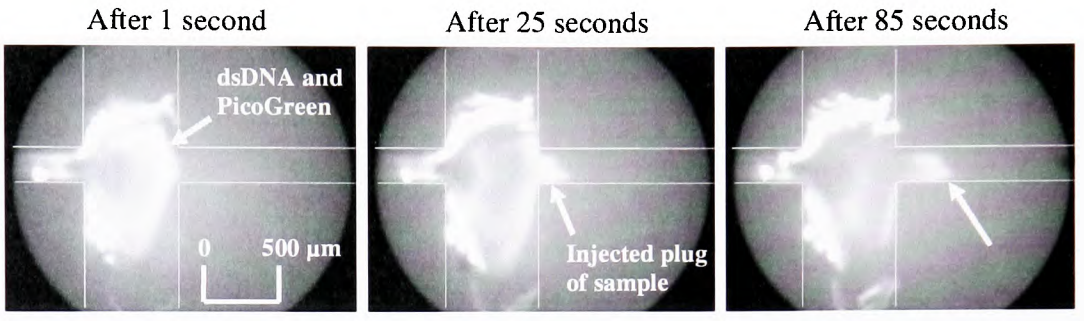

Figure 5-3: Consecutive captures of an electro-kinetically injected plug of sample into urea containing separation matrix

Figure 5-3 shows the dsDNA and PicoGreen complex fluorescing in the T section of the micro-fluidic device at the beginning of the experiment, when the voltage-time profile was applied the complex began to move into the separation channel. After 25 seconds, the sample begins to move into the separation channel, after 85 seconds the plug has moved further into the separation channel. At this point, the DNA was still fluorescing suggesting that the DNA had not yet been denatured to ssDNA.

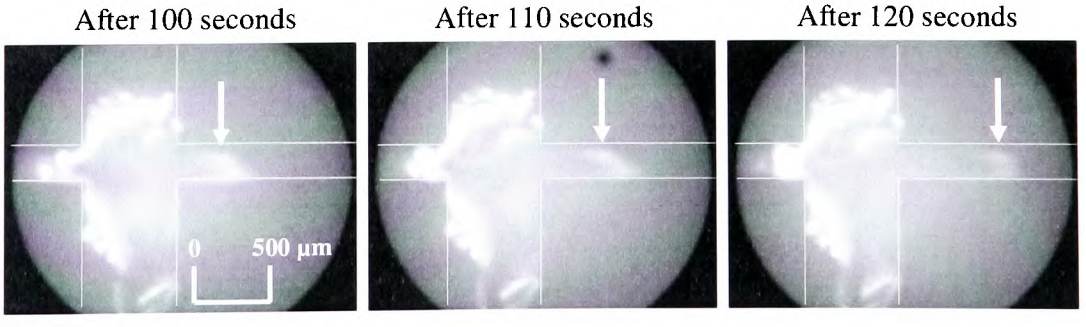

Figure 5-4: Consecutive captures of an electro-kinetically injected plug of sample into urea containing separation matrix

At 100 seconds, as seen in Figure 4-2, the plug has moved into the separation channel by capillary electrophoresis, by 110 seconds the sample plug has began to diminish in fluorescence intensity, by 120 seconds the sample plug is considerably less intense than when the plug was first injected into the separation channel.

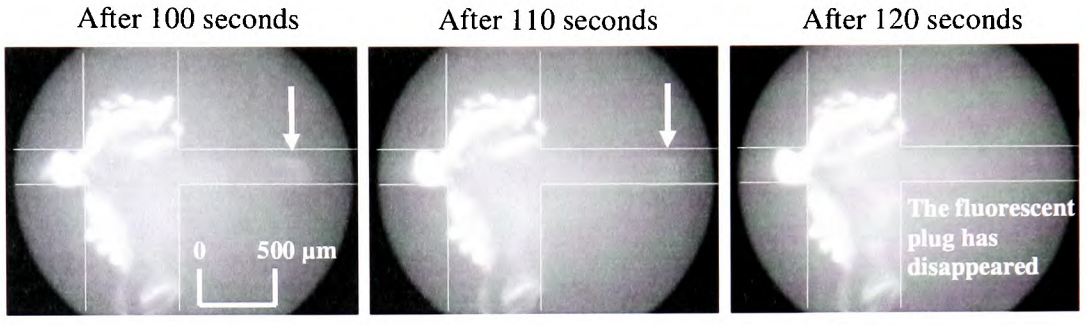

Figure 5-5: Consecutive captures of an electro-kinetically injected plug of sample into urea containing separation matrix

As the sample plug continues to migrate down the separation channel, the fluorescence intensity continued to diminish. After travelling approximately 1000 µm down the separation channel (120 seconds), moving through the separation matrix containing the 6 M urea, the DNA was successfully denatured into the single stranded form, thus no longer fluoresced when in contact with PicoGreen. These results, together with the results presented previously, strongly indicate that the 6 M urea present in the separation matrix is sufficient to denature dsDNA into ssDNA required for successful separation of DNA.

The results indicate that the DNA does not become single stranded immediately; the process can take up to approximately 2 minutes to take effect. Similar results were seen with the other polymer investigated (PEO, HEC and LPA); however the most effective results were seen with the LPA-co-DHA polymer

5.3 Investigation of current production associated with micro-fluidic capillary electrophoresis

5.3.1 Experimental

Following the investigations detailed in Section 5.2, all the separation matrices were made up with 6 M urea, in order to denature the DNA, as single stranded DNA is thought to provide a better resolution during separation as it is more flexible and interacts with the separation matrix more successfully.[105]

Choosing a separation matrix for a micro-fluidic system is dependent on the current generated by the presence of that separation polymer within the system. If the current within the system is too high the integrity of the separation polymer will deteriorate and eventually create a breakage within the system, causing the circuit and therefore the separation to fail. Therefore, ideally we would need a separation polymer with high resistance, resulting in a low current, but with efficient separation properties.

Experiments were undertaken to determine the magnitude of the current generated within the micro-fluidic system depending upon which separation polymer was implemented. In addition, the effect of an increase in the concentration of the polymer, the effect of increased channel length, and the effect of using carbon electrode caps in place of platinum wire electrodes on the magnitude of the current generated within the system was also investigated.

Using micro-fluidic device design 4, 6 and 7, (to investigate channel lengths 8.5, 20 and 22 cm, see Section 2.2.1.2), the separation polymer was pressure injected into the separation channel via port D (see Figure 5-1) and the channel inspected for bubbles. A

5 µl aliquot of bromophenol blue was mixed with 5 µl of 1 x TE buffer, and the solution pressure injected into the T section via port A. The electrodes in use during the experiment were secured into place, and each of the reservoirs filled to the level with the respective solutions. In order for direct comparison of the micro-fluidic system with the capillary system of the 310 ABI PRISM®, a separation voltage of 320 V cm^{-1} was applied. A voltmeter was incorporated into the system, to accurately monitor the current generated, after 60 seconds the experiment was halted and the movement of the bromophenol blue measured. The voltage was then reapplied for another 60 seconds, the current monitored throughout and on completion the movement of the bromophenol blue again measured.

5.3.2 Results and Discussions

As will be further discussed in Section 5.3.2.3, the increased length of the separation channel increases the separation efficiency and the chances of achieving the base pair resolution. However, increasing the length of the separation channel has further implications on the current production within the micro-fluidic system, which could in fact hinder the separation capability of the system. As such an investigation was undertaken to establish the currents produced in the differing micro-fluidic systems.

The results obtained were compared against the known data associated with the ABI PRISM® 310 Genetic Analyzer, and can be found in Table 5-3, Table 5-4, Table 5-5, and Table 5-6.

For each experiment the electric power (Equation 5-5), current using Ohm's law (Equation 5-6), resistance (Equation 5-7), the heat generated was derived from Joules first law (Equation 5-8) and heat energy generated (Equation 5-9) was calculated.

$$Power\ (W) = Voltage\ (V) \times Current\ (A) \rightarrow P = VI$$ **Equation 5-5**

$$Current\ (A) = \frac{Voltage\ (V)}{Resistance(\Omega)} \rightarrow I = \frac{V}{R}$$ **Equation 5-6**

$$Resistance\ (\Omega)$$ **Equation 5-7**

$$= Resistivity\ (\Omega m) \times \left(\frac{Length\ (m)}{Cross\ sectional\ area\ (m^2)}\right) \rightarrow R$$

$$= \rho \times \left(\frac{L}{A}\right)$$

$$Heat\ energy\ generated(J)$$ **Equation 5-8**

$$= Current(A)^2 \times Resistance(\Omega) \times time(secs) \rightarrow Q = I^2 \times R \times t$$

$$Heat\ energy(kJ)$$ **Equation 5-9**

$$= mass(kg) \times specific\ heat\ capacity(kJ\ kg^{-1}\ K^{-1}) \times temperature\ differential(K)$$

$$\rightarrow Q = m \times c \times \Delta\theta$$

Where the specific heat capacity of water is 4.1813 $kJkg^{-1}K^{-1}$, and the density is approximately 1 gml^{-1}.

5.3.2.1 Analysis of current production associated with each polymer

As stated in Section 5.3, the choice of separation polymer in the system is highly dependent on the extent of the current production within the system; measurements of

current production within each of the systems investigated were recorded and are documented in Table 5-3.

Table 5-3: Table of comparable data associated with each type of separation polymer

	310 ABI PRISM	POP-4	PEO	LPA-co-DHA	LPA
Length (m)	0.467	0.085	0.085	0.085	0.085
Cross sectional area (m^2)	$2.0x10^{-09}$	$1.0x10^{-08}$	$1.0x10^{-08}$	$1.0x10^{-08}$	$1.0x10^{-08}$
Volume (m^3)	$9.2x10^{-10}$	$8.5x10^{-10}$	$8.5x10^{-10}$	$8.5x10^{-10}$	$8.5x10^{-10}$
Mass (kg)	$9.2x10^{-7}$	$8.5x10^{-7}$	$8.5x10^{-7}$	$8.5x10^{-7}$	$8.5x10^{-7}$
Field strength (V/m)	32000	32000	32000	32000	32000
Applied voltage (V)	15000	2720	2720	2720	2720
Current recorded (A)	$1.1x10^{-5}$	$7.0x10^{-6}$	$2.2x10^{-5}$	$5.5x10^{-5}$	-
Current density (A/m^2)	5602	700	2200	5500	-
Power (W)	0.165	0.019	0.060	0.150	-
Resistance (Ω)	$1.36x10^{9}$	$3.89x10^{8}$	$1.24x10^{8}$	$4.95x10^{7}$	-
Magnitude related to resistivity, ρ	$2.39x10^{8}$	$8.50x10^{6}$	$8.50x10^{6}$	$8.50x10^{6}$	$8.50x10^{6}$
Heat generated in 60 secs (KJ)	$9.90x10^{-3}$	$1.14x10^{-3}$	$3.59x10^{-3}$	$8.98x10^{-3}$	-
Temperature change	2569.60	321.07	1009.08	2522.70	-
Dye movement in 60 secs (cm)	-	0.9	2.8	2.3	-
Dye movement in 120 secs (cm)	-	2.0	5.0	4.4	-

As can be seen from Table 5-3, the separation matrix used in the standard instrumentation (310 ABI PRISM® Genetic Analyser), POP-4, when implemented in the micro-fluidic system generated the lowest current of each of the separation polymer types. This is as expected, as the polymer was developed for optimum performance in the genetic analyser system. However, the current recorded in the micro-fluidic system is considerably higher than the current stated in the information listed for the 310 ABI PRISM® Genetic Analyser, for the same polymer. This occurs even though the ABI system utilises a longer, narrower capillary than the micro-fluidic system, factors which should suggest a larger current not a smaller one, as shown by the higher current density value calculated for the ABI PRISM system. This would indicate that there is at least one other factor influencing current production within a CE system.

Comparison of the remaining polymers seems to follow the trend of viscosity, the higher the viscosity the higher the current recorded and the lower the resistance. These results are most likely due to the structural properties of the polymers; the more structured the polymer, the higher the viscosity of the polymer. Results indicate that an increased current is produced within the systems of the higher viscosity polymers; the higher current would suggest the higher viscosity polymer systems experienced a decreased resistance.

It was observed during the experiment, that for lower viscosity polymers, there was a greater loss of the separation polymer as noted in the reservoir. This affect was most noticeable with the least viscous polymer, POP-4, which after the 60 seconds experiment time period was almost completely depleted. These findings suggested that although the lowest current was recorded for this polymer, this polymer was unsuitable for use in a micro-fluidic system if a suitable supply of matrix cannot be maintained

throughout the time required for a separation, which could be anything in the order of 10 to 60 minutes depending on the length of the separation column.

5.3.2.2 Polymer concentration affect on current production

As the concentration of the polymer can be highly effective in achieving the desired separation efficiency, as such the current production within the micro-fluidic device system in relation to the concentration of the polymer was recorded and documented in Table 5-4.

Table 5-4: Table of comparable data associated with different concentrations of the separation polymer PEO

	310 ABI PRISM	2.0 % PEO	2.5 % PEO	3.0 % PEO
Length (m)	0.469	0.085	0.085	0.085
Cross sectional area (m^2)	$1.96x10^{-9}$	$1.00x10^{-8}$	$1.00x10^{-8}$	$1.00x10^{-8}$
Volume (m^3)	$9.2x10^{-10}$	$8.5x10^{-10}$	$8.5x10^{-10}$	$8.5x10^{-10}$
Mass (Kg)	$9.2x10^{-7}$	$8.5x10^{-7}$	$8.5x10^{-7}$	$8.5x10^{-7}$
Field strength (V/m)	32000	32000	32000	32000
Applied voltage (V)	15000	2720	2720	2720
Current recorded (A)	$1.1x10^{-5}$	$2.0x10^{-5}$	$2.0x10^{-5}$	$2.2x10^{-5}$
Current density (A/m^2)	5602	2000	2000	2000
Power (W)	$1.65x10^{-1}$	$5.44x10^{-2}$	$5.44x10^{-2}$	$5.98x10^{-2}$
Resistance (Ω)	$1.36x10^{9}$	$1.40x10^{8}$	$1.40x10^{8}$	$1.20x10^{8}$
Magnitude related to resistivity, ρ	$2.39x10^{8}$	$8.50x10^{6}$	$8.50x10^{6}$	$8.50x10^{6}$
Heat generated in 60 secs (KJ)	$9.90x10^{-3}$	$3.26x10^{-3}$	$3.26x10^{-3}$	$3.59x10^{-3}$
Temperature change (K)	2569.60	917.34	917.34	1009.08
Dye movement in 60 secs (cm)	-	3.5	3.1	2.8
Dye movement in 120 secs (cm)	-	6.7	6.1	5.0

The results in Table 5-4 indicate that the lower current was recorded in the system of the separation matrix used in the standard instrumentation (310 ABI PRISM® Genetic

Analyser), POP-4. Of the separation polymers investigated in the micro-fluidic system, the lower concentrations of 2 and 2.5 % were recorded to have approximately the same current, with very little difference recorded in the current produced for the higher concentration of 3 %. These results would indicate that the concentration of the polymer, in this instance, had very little effect on the current recorded for each system.

5.3.2.3 The effect of channel length on current production

The affect of the channel length on the separation efficiency was briefly investigated in Section 5.3.2, however these investigations were also substantiated by the investigation of the current production detailed in Table 5-5.

Table 5-5: Table of comparable data associated with different channel lengths, with additional data comparing affects of increase of channel length between two polymer types.

	310 ABI PRISM	POP-4			3 % PEO		
Length (m)	0.469	0.085	0.2	0.22	0.085	0.2	0.22
Cross sectional area (m^2)	$1.96x10^{-9}$	$1.00x10^{-8}$	$1.00x10^{-8}$	$1.00x10^{-8}$	$1.00x10^{-8}$	$1.00x10^{-8}$	$1.00x10^{-8}$
Volume (m^3)	$9.2\text{-}10^{-10}$	$8.5x10^{-10}$	$2.0x10^{-9}$	$2.2x10^{-9}$	$8.5x10^{-10}$	$2.0x10^{-9}$	$2.2x10^{-9}$
Mass (Kg)	$9.2x10^{-7}$	$8.5x10^{-7}$	$2.0x10^{-6}$	$2.2x10^{-6}$	$8.5x10^{-7}$	$2.0x10^{-6}$	$2.2x10^{-6}$
Field strength (V/m)	32000	32000	32000	32000	32000	32000	32000
Applied voltage (V)	15000	2720	6400	7040	2720	6400	7040
Current recorded (A)	$1.1x10^{-5}$	$7.0x10^{-6}$	$3.3x10^{-5}$	$7.0x10^{-5}$	$2.2x10^{-5}$	$3.0x10^{-5}$	$4.2x10^{-5}$
Current density (A/m^2)	5602	700	3300	7000	2200	3000	4200
Power (W)	0.165	0.019	0.211	0.493	0.060	0.192	0.296
Resistance (Ω)	$1.36x10^{9}$	$3.90x10^{8}$	$1.90x10^{8}$	$1.00x10^{8}$	$1.20x10^{8}$	$2.10x10^{8}$	$1.70x10^{8}$
Magnitude related to resistivity, ρ	$2.39x10^{8}$	$8.50x10^{6}$	$2.00x10^{7}$	$2.20x10^{7}$	$8.50x10^{6}$	$2.00x10^{7}$	$2.20x10^{7}$
Heat generated in 60 secs (KJ)	$9.90x10^{-3}$	$1.14x10^{-3}$	$1.27x10^{-2}$	$2.96x10^{-2}$	$3.59x10^{-3}$	$1.15x10^{-2}$	$1.77x10^{-2}$
Temperature change (K)	2569.60	321.07	1513.62	3210.70	1009.08	1376.02	1926.42
Dye movement in 60 secs (cm)	-	0.9	1.3	2.0	2.8	3.1	3.8
Dye movement in 120 secs (cm)	-	2.0	2.9	4.4	5.0	4.7	5.9

As can be seen from Table 5-5, POP-4 implemented in the micro-fluidic system with the shortest channel length, generated the lowest current of each of the separation polymer types. Again, this is as expected, as the polymer was developed for optimum performance in the genetic analyser system. Comparison of the remaining polymers seems to follow obvious trend, the higher current was produced in the micro-fluidic systems with the longer channel lengths.

5.3.2.4 Affect of carbon electrode on current production

Table 5-6: Repeat of Table 5-5, with the addition of carbon electrodes placed in the separation channel reservoirs in place of the standard platinum wire electrodes.

	310 ABI PRISM	POP-4			3 % PEO		
Length (m)	0.469	0.085	0.2	0.22	0.085	0.2	0.22
Cross sectional area (m^2)	$1.96x10^{-9}$	$1.00x10^{-8}$	$1.00x10^{-8}$	$1.00x10^{-8}$	$1.00x10^{-8}$	$1.00x10^{-8}$	$1.00x10^{-8}$
Volume (m^3)	$9.2\text{-}10^{-10}$	$8.5x10^{-10}$	$2.0x10^{-9}$	$2.2x10^{-9}$	$8.5x10^{-10}$	$2.0x10^{-9}$	$2.2x10^{-9}$
Mass (Kg)	$9.2x10^{-7}$	$8.5x10^{-7}$	$2.0x10^{-6}$	$2.2x10^{-6}$	$8.5x10^{-7}$	$2.0x10^{-6}$	$2.2x10^{-6}$
Field strength (V/m)	32000	32000	32000	32000	32000	32000	32000
Applied voltage (V)	15000	2720	6400	7040	2720	6400	7040
Current recorded (A)	$1.1x10^{-5}$	$2.9x10^{-5}$	$2.8x10^{-5}$	$1.1x10^{-4}$	$3.4x10^{-5}$	$3.5x10^{-5}$	$4.0x10^{-5}$
Current density (A/m^2)	5602	2900	2800	11000	3400	3500	4000
Power (W)	0.165	0.079	0.179	0.774	0.092	0.224	0.282
Resistance (Ω)	$1.36x10^{9}$	$9.38x10^{7}$	$2.29x10^{8}$	$6.40x10^{7}$	$8.00x10^{7}$	$1.83x10^{8}$	$1.76x10^{8}$
Magnitude related to resistivity, ρ	$2.39x10^{8}$	$8.50x10^{6}$	$2.00x10^{7}$	$2.20x10^{7}$	$8.50x10^{6}$	$2.00x10^{7}$	$2.20x10^{7}$
Heat generated in 60 secs (KJ)	$9.90x10^{-3}$	$4.73x10^{-3}$	$1.08x10^{-2}$	$4.65x10^{-2}$	$5.55x10^{-3}$	$1.34x10^{-2}$	$1.69x10^{-2}$
Temperature change (K)	2569.60	1330.15	1284.28	5045.39	1559.48	1605.35	1834.69
Dye movement in 60 secs (cm)	-	1.1	1.7	3.2	3.0	3.4	4.1
Dye movement in 120 secs (cm)	-	2.5	3.2	4.5	4.8	6.1	7.2

The results seen in Table 5-6 vary little from that of Table 5-5, in the way that the currents recorded are within a similar range compared to those recorded with the platinum electrodes. However, a rather unusual effect happened when the carbon electrodes were used in the micro-fluidic device system that contained POP-4, instead of the current produced increasing with channel length, it actually decreased. This further substantiates the argument that the polymer POP-4 has been successfully engineered for optimum separation resolution in the longer length capillary systems that are implemented within the 310 ABI PRISM® Genetic Analyser systems. However this also indicates why POP-4 proves so unsuccessful in a micro-fluidic device, as a micro-fluidic device cannot provide the larger sample vessels needed to sustain the higher voltages required for a longer channel length like those used within the 310 ABI PRISM® Genetic Analyser systems (see Section 5.4).

5.4 Investigation of effect of increasing channel length on separation efficiency

The effect of increasing the length of the channel on the separation efficiency was investigated; the theory was discussed previously in Section 1.6.2.5.

5.4.1 Experimental

A number of micro-fluidic devices were designed, firstly Micro-fluidic device design 10 (Figure 2-19) which had a channel length of 20 cm, secondly a Micro-fluidic device design 11 (Figure 2-20) which had a channel length of 22 cm. The width of the bend in the channel was designed in order to overcome factors, such as the train track effect, which could distort the separation across the channel. This would have a large effect on

the separations performed within this system, due to the difficulty in accomplishing the base pair resolution.[106]

For each experiment the micro-fluidic device was prepared and loaded as described previously in Section 5.2.1.

5.4.2 Results and Discussions

Introduction of the separation polymer was achieved using the mechanical syringe infusion pump (KDS200, *Kd Scientific*), which allowed for a very slow injection rate to be applied in order to ensure the separation polymer filled the channel without voids or air bubbles being introduced. However, the procedure was still quite difficult to achieve, due to the large amount of back pressure that results from the longer channel lengths.

Numerous attempts to fill the separation channels with either LPA or the LPA-co-DHA polymers proved unsuccessful with many of the channels blocking completely, this was most likely due to the density of the polymers. The separation polymer PEO was successfully introduced into the micro-fluidic device; however, experiments performed using these devices yielded very few useful results. After many repeated attempts, the higher applied voltages required for the longer length channels destroyed the integrity of the separation polymer, stopping the experiment before the sample reached the end of the channel. When the voltage was reduced, to accommodate this problem, the extended lengths of time the voltages were applied to the channels resulted in the degradation of the separation polymer at the point of the contact with the electrode and separation polymer, to a point where connection was lost and the experiment was stopped.

A successful separation from the longer channel lengths was not achieved; the most likely reason for this is the width of the channels, which were designed to be a specific width to allow for detection of the florescence signal. In addition, the capillary systems have a large well either end of the capillary, to which the electrode is introduced. This allows for a lot of the heat generated from the experiment to dissipate, there is no such feature in the micro-fluidic system that would allow the heat to dissipate, which explains the excessive damage to the separation polymer when a high voltage is applied for extended periods of time.

5.5 Experimental design approach to optimisation of separation

5.5.1 Experimental

In order to establish if there was a set of optimum parameters to apply within the micro-fluidic system that would ensure the maximum resolution could be achieved, an experimental design plan was implemented. There were three main factors considered within the experimental design plan, the concentration of the polymer, the volume of sample injected for separation and the field strength applied across the separation column, see Table 5-7.

Table 5-7: The factors investigated as part of the experimental design

Polymer Concentration		Injection Time (seconds)	Field Strength (Vcm^{-1})
PEO (%)	LPA (%)		
2	3	5	200
2.5	4	6	225
3	5	7	250
			275
			300

A design for the experimentation that would adequately test the desired parameters was produced by a response surface approach using the software *Design Expert 7.1.6*. This approach was taken in order to accommodate the most possible variation and interaction between the variables selected to be investigated, in the least possible number of experiments. Thus increasing the efficiency of the experiments and reducing the overall experiment time length. Response surface methodology however only accommodates a certain number of variables before the number of experiments required to test them sufficiently begins to increase exponentially, as such LPA-co-DHA and PEO were investigated separately, see Table 5-8 and Table 5-9)

Table 5-8: Experimental design plan for LPA-co-DHA

Std	Run	Polymer Concentration (%)	Injection Time (seconds)	Field Strength (Vcm^{-1})
9	1	3	5	200
4	2	4	7	250
5	3	5	6	275
1	4	5	5	250
6	5	3	6	225
8	6	4	6	300
7	7	3	7	300
3	8	5	7	225
2	9	4	5	275

Table 5-9: Experimental design plan for PEO

Std	Run	Polymer Concentration (%)	Injection Time (seconds)	Field Strength (Vcm^{-1})
9	1	2	5	200
4	2	2.5	7	250
5	3	3	6	275
1	4	3	5	250
6	5	2	6	225
8	6	2.5	6	300
7	7	2	7	300
3	8	3	7	225
2	9	2.5	5	275

5.5.2 Results and Discussions

5.5.2.1 Optimisation of CE separation in LPA-co-DHA

Based on the experimental design plan, the experiments were performed in run order. Figure 5-6 shows an example of an electropherogram obtained using laser induced fluorescent detection.

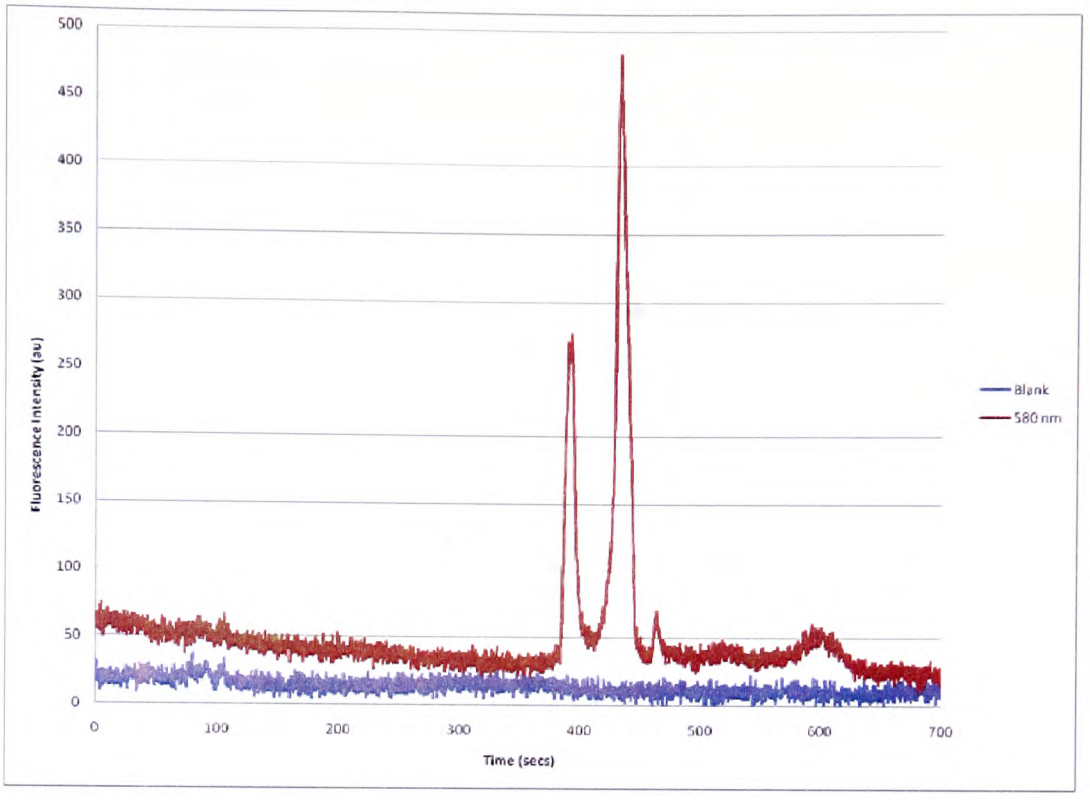

Figure 5-6: Electropherogram of the separation of the PCR products vWA and FGA, an example of an electropherogram from one of the experiments designed by the experimental design plan.

The velocity ratio (γ) is the ratio of migration times of the two components and increasing this ratio should increase the separation between the peaks.

The velocity ratio is concurrent with the migration time of each of the components, i.e. the migration time of peak 2: migration time of peak 1.

The resolution was calculated as follows;

$$Resolution = \frac{\Delta t_r}{W_{av}}$$ **Equation 5-10**

The theoretical number of plates (N) of the column was calculated based on the relationship between resolution, number of plates of the column and the velocity ratio or ratio of migration times;

$$Resolution = \frac{\sqrt{N}}{4} \times (\gamma - 1)$$ **Equation 5-11**

$$rearranged\ to\ \rightarrow N = \left(\frac{Resolution}{(\gamma - 1)} \times 4\right)^2$$

Resolution is generally defined as the relationship between the separation of the peaks and the peak widths, in the equation (γ-1) measures the separation and $\sqrt{N}/4$ measures the peak width. Therefore, increasing γ will result in an increase in the separation of the peaks, and increasing N decreases the width of the peaks.

Table 5-10: Results obtained from experimental design plan applied to LPA-co-DHA separation matrix.

Run	Polymer Concentration (%)	Injection Time (seconds)	Field Strength (Vcm^{-1})	Velocity ratio	Number of plates	Resolution
1	3	5	200	1.1401	2758.61	1.8396
2	4	7	250	1.1589	1085.80	1.3090
3	5	6	275	1.0355	26019.96	1.4316
4	5	5	250	1.1036	7341.64	2.2192
5	3	6	225	1.1242	2097.37	1.4220
6	4	6	300	1.0866	2633.85	1.1111
7	3	7	300	1.1294	812.12	0.9219
8	5	7	225	1.1309	2707.81	1.7029
9	4	5	275	1.1789	1823.94	1.9101

Results indicate that the optimum separation parameters are an electro-kinetic injection of 5 seconds into the 5 % concentration of LPA-co-DHA, and separation field strength of 250 Vcm^{-1} applied, as identified by the highest resolution factor.

Field strength of 250 Vcm^{-1} appears to be the best separation field rather than 200 Vcm^{-1}. At 200 Vcm^{-1}, the greatest distance between the two peaks could be achieved, however there was a greater likelihood of band broadening occurring, which decreased the resolution between the two peaks.

The resolution and number of plates calculated for each experiment was entered into the experimental design model, the model extrapolated the data to create a surface model predicting the behaviour of the system when the variables are changed.

5.5.2.1.1 Analysis and optimisation of results

The *'Fit Summary'* is a feature of the design expert, which compares the values for the probability of the fit, the standard deviation, the adjusted R-Squared values (a measure of the amount of variation around the mean explained by the model, adjusted for the number of terms in the model) and the PRESS values (Predicted Residual Sum of Squares) for each model type. The purpose is to compare and contrast these values in order to establish the model that 'best fits' the data accumulated.

The criterion by which the 'best fit' model is chosen is as follows; a low probability of seeing the observed F value (if the null hypothesis is true), a low standard deviation, and a high adjusted 'R-Squared' value and a low PRESS value.

A quadratic and cubic model were immediately discounted due to the obvious unsuitability stated in the initial summary, analysis of the *'Fit Summary'* indicated that the 'Linear' model (which highlights how the significance of adding the linear terms to the mean and blocks contributes to the model) was the most suitable fit for the data, analysis of the '2FI' model (which highlights how the significance of adding the two factor interaction terms to the mean, block and linear terms already in the model will contribute to the model) also indicated it would be a suitable choice.

Table 5-11: Comparison of relevant data required to choose the best fit model

	Linear	2FI
Prob-F	0.0109	0.2354
Standard Deviation	0.18	0.12
Adjustable R-Squared	0.7989	0.9176
PRESS	0.55	1.59

Examination of Table 5-11 indicates a linear model would provide the lower probability and PRESS value; however the 2FI model would provide the more suitable standard deviation and R-Squared values. Therefore further investigation was required to assess which was the more suitable model.

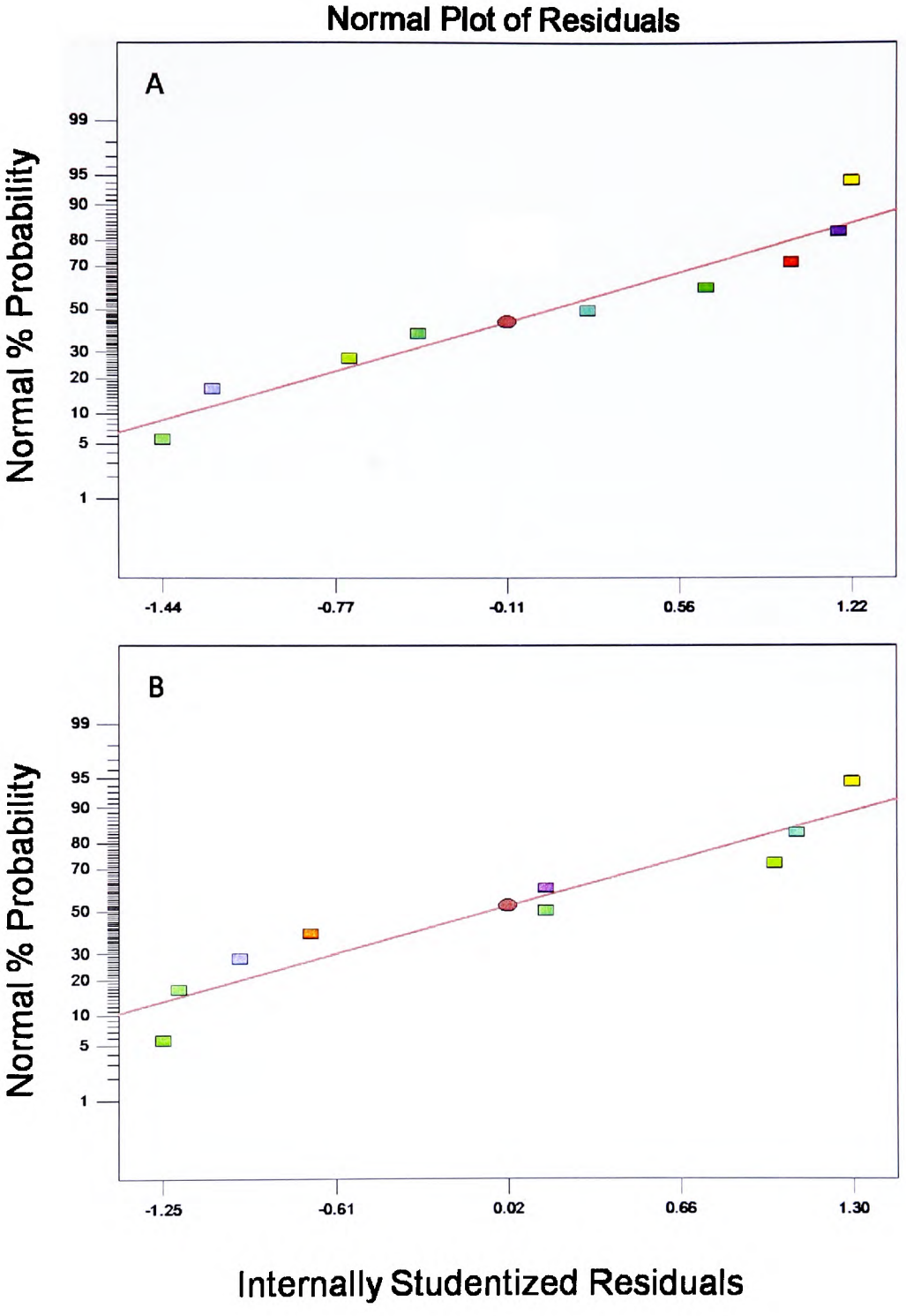

Figure 5-7: Analysis of the normal probability of studentised residuals for A; the linear model, and B; the 2FI model

The normal plot of residuals should ideally be a straight line, indicating no abnormalities. Both plots, as shown in Figure 5-7, follow this trend well, with no significant outliers in either.

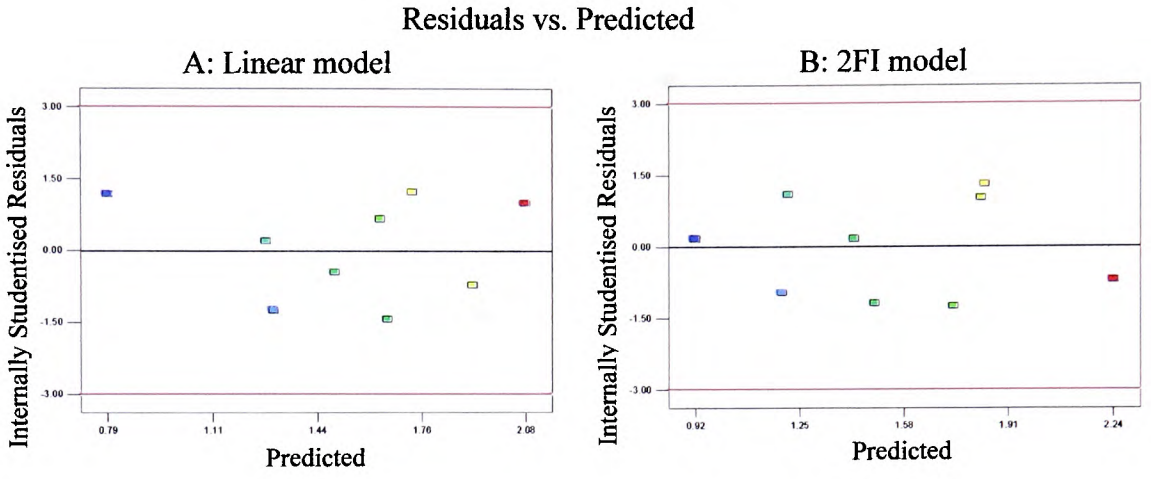

Figure 5-8: Analysis of the studentised residuals versus predicted values for A; the linear model, and B; the 2FI model

When analysing the studentised residuals versus predicted value plots, there should be an approximate even spread of the studentised residuals values across the plot, indicating an independence to the corresponding predicted values. Again both plots, as seen in Figure 5-9, fulfil these criteria well, indicating both model types are performing within necessary parameters.

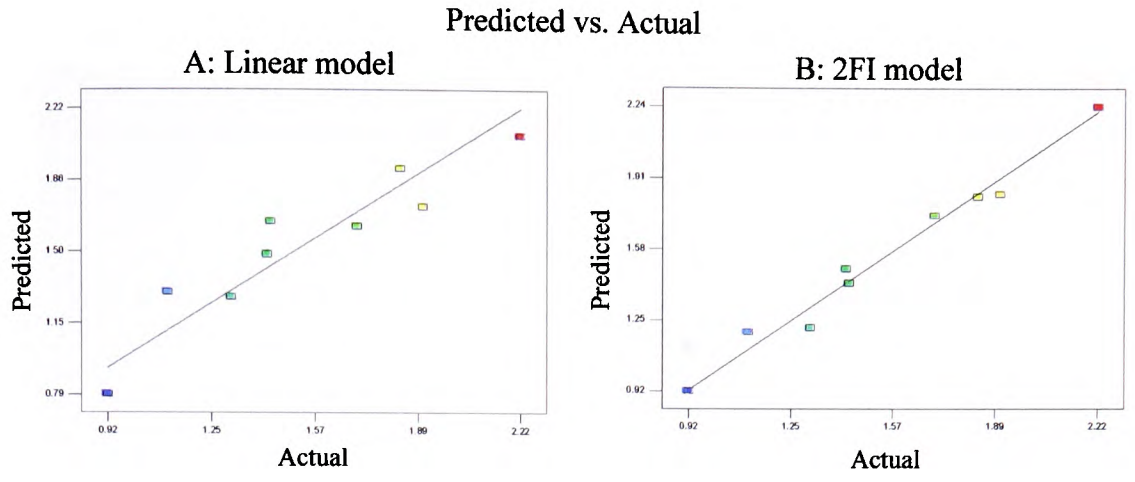

Figure 5-9: Analysis of the predicted versus actual results for A; the linear model, and B; the 2FI model

In the predicted versus actual plot for each model, the values should follow the trend line to indicate a good fit, as can be seen in Figure 5-9 that both data sets follow the trend, however, a better correlation is indicated in the 2FI model.

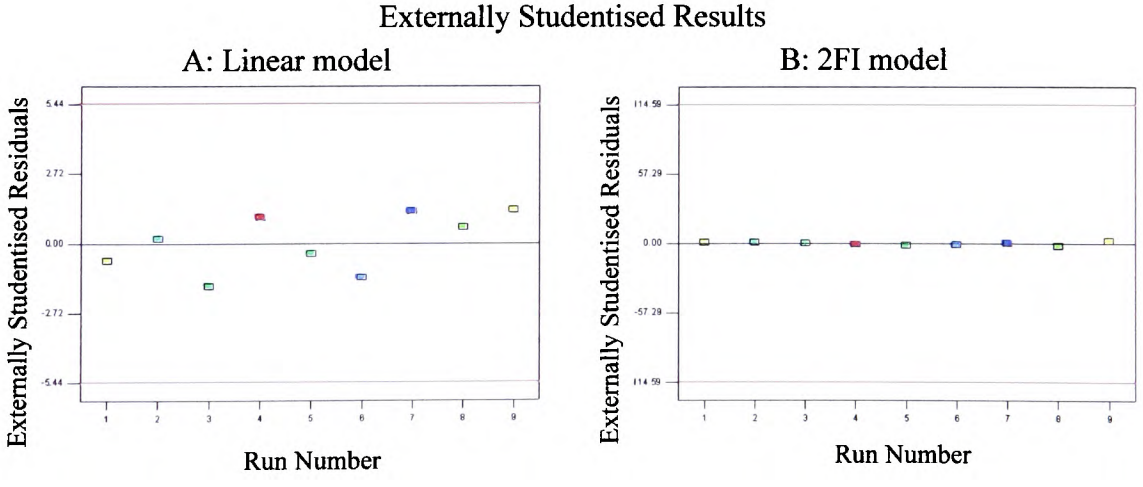

Figure 5-10: Analysis of the externally studentised residuals, otherwise known as the outlier T plot, for A; the linear model, and B; the 2FI model

When analysing the externally studentised residuals plot, we are looking for points that fall outside the plus and minus 3.5 standard deviation limits, which are placed as red

lines on the graphs. Figure 5-10 indicates there are no outliers present in either model, suggesting both are suitable, although the 2FI model shows a very high correlation to the trend line.

After consideration, it was decided that the 2FI model provided the better fit for the data, and was the model chosen to proceed with for further analysis. The final choice was based on the better fit of predicted versus actual plots of both models, which highlighted a greater degree of fit in the 2FI model.

The F Value is a ratio of the sum of the squared residuals for terms in the model divided by the sum of the squares for the residuals; it shows the relative contribution of the model variance to the residual variance. A large number indicates more of the variance being explained by the model; a small number says the variance may be more due to noise. In the model, injection time has the highest F Value of 34.54, indicating that altering the parameters of this factor will have the highest impact on the resolution. The factor that had the lowest F Value of 7.37 was polymer concentration, indicating the factor has a smaller impact on the resolution. These results were further substantiated by analysis of the Prob>F value, which states the probability of getting an F Value of a certain size if the term did not have an effect on the resolution of the separation. In general, a term that has a probability value less than 0.05 would be considered a significant effect, both injection time and field strength fall within these criteria, and therefore are deemed significant. As a probability value greater than 0.10 is generally regarded as not significant, polymer concentration was thus considered an insignificant factor.

The equation, the model determined would accurately predict the resolution of a separation at specific parameters is shown in Equation 5-12;

$$Resolution = -4.10073 + (2.06476 \times polymer\ conc.) + (0.13434 \times injection\ time) + (0.024628 \times field\ strength) - (0.052171 \times polymer\ conc. \times injection\ time) - (6.30052 \times 10^{-3} \times polymer\ conc. \times field\ strength) - (1.3044 \times 10^{-3} \times injection\ time \times field\ strength)$$

Equation 5-12

Injection time was the factor that produced the largest variation in resolution, after further analysis of the resulting model; it was also found that the variation was entirely predictable.

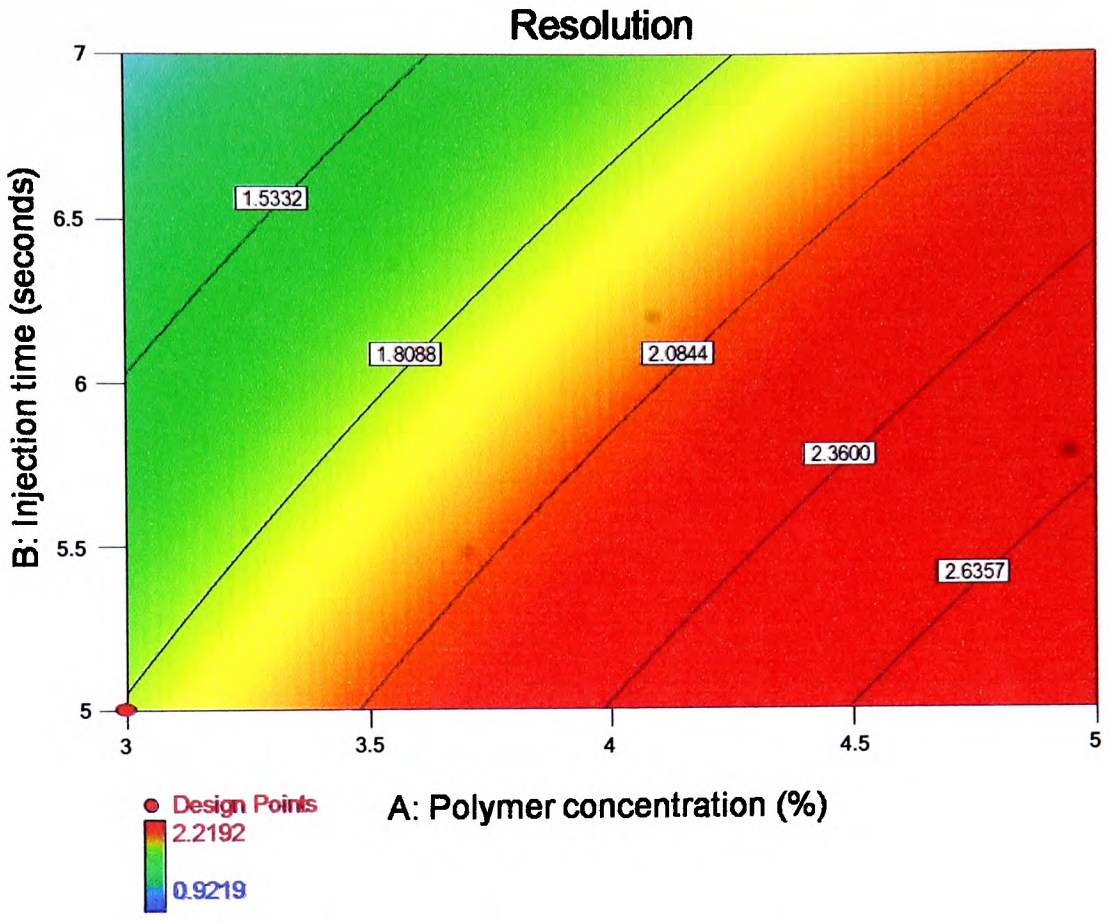

Figure 5-11: Contour plot displaying the impact on resolution with changing injection time and polymer concentration, at fixed field strength of 200 Vcm-1. (Red indicates high resolution to blue indicating low resolution).

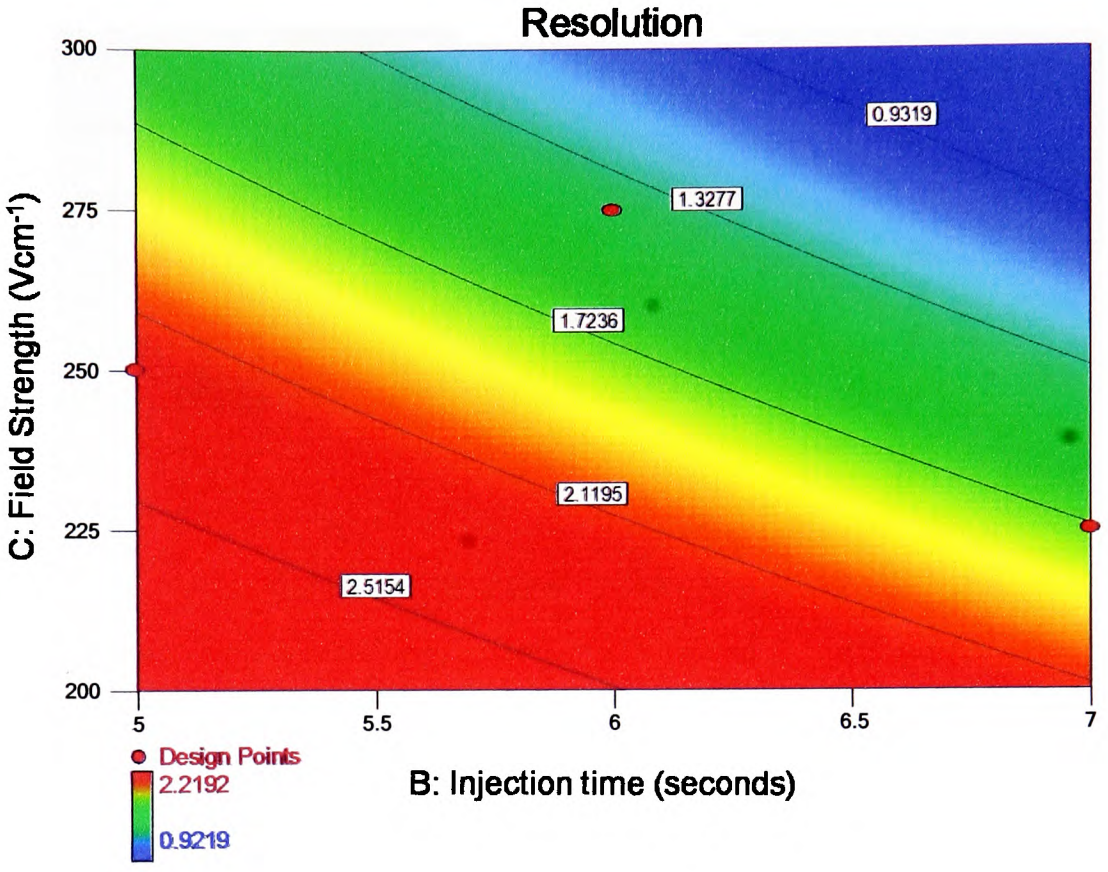

Figure 5-12: Contour plot displaying the impact on resolution with changing injection time and field strength, at a fixed polymer concentration of 5%. (Red indicates high resolution to blue indicating low resolution).

As displayed in Figure 5-11 and Figure 5-12, no matter the values implemented for the other two factors, an increase in the injection time always resulted in a decrease in the resolution, without exception.

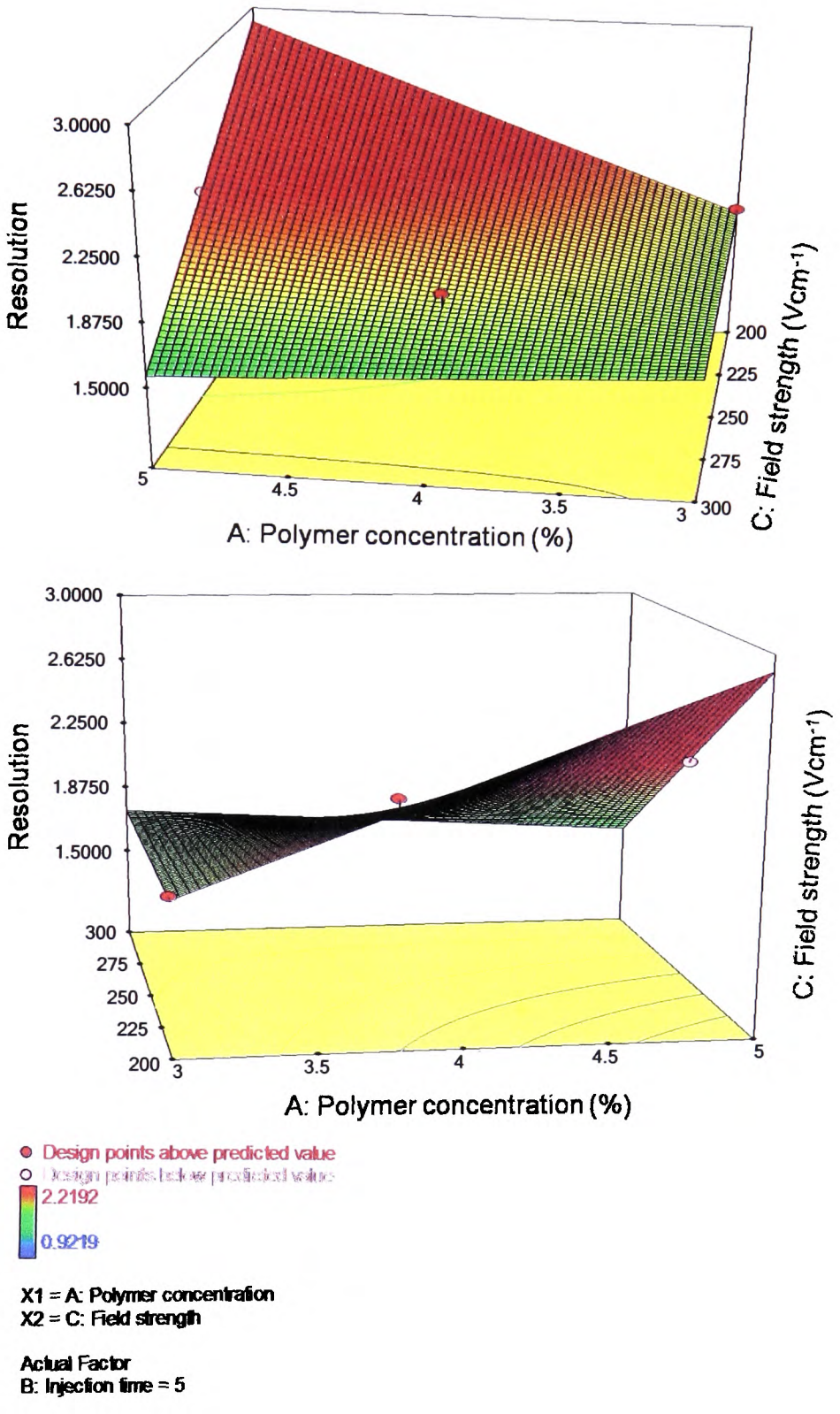

Figure 5-13: 3D contour plot (shown at 2 angles) displaying the interaction between polymer concentration and field strength, at a fixed injection time of 5 seconds. (Red indicates high resolution to blue indicating low resolution).

Figure 5-13 depicts the model produced as a result of the experimental design approach to optimisation, Figure 5-12 proved that an injection time of 5 seconds was un-arguably the optimum time for injection as indicated by the very clear gradient towards red in the bottom left hand corner, and was therefore selected as the fixed variable throughout the rest of the analysis. The first perspective of the graph shows that the best resolution achievable will be obtained from a separation performed in the higher concentration polymer, 5 %, and with the lowest separation field of 200 Vcm^{-1}. This would contradict the thought that a high concentration of polymer and low separation field would possibly create a large peak width that would prevent the possibility of obtaining a one base pair resolution separation. The second perspective of the graph, however, does indicate that the interaction of the concentration of the separation polymer and the strength of the separation field does in fact interact as was predicted; high field strength and high concentration separation polymer, and low field strength and a low concentration separation polymer both result in the lowest resolutions achieved.

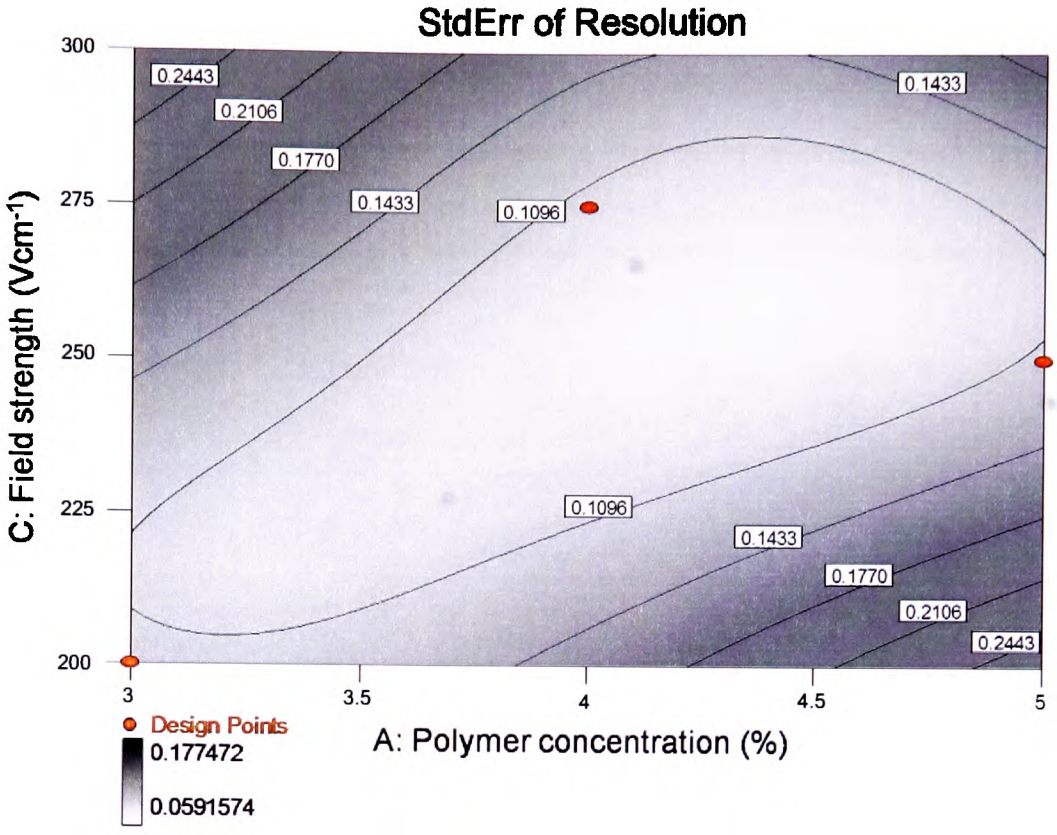

Figure 5-14: Contour plot displaying the values of the standard error in resolution as a respondent to interaction between polymer concentration and field strength, at a fixed injection time of 5 seconds.

Figure 5-14 depicts the standard error of resolution, derived from the difference between the measured values and the expected values. An increase of standard error in the resolution at the periphery of the experimental parameters is to be expected, however instead of the concentric circular pattern that would be expected, the graph displays a diagonal oblong shape. The greatest error is seen when the parameters are set to the highest field strength and the weakest polymer concentration, and the weakest field strength and the highest polymer concentration, which are the parameters that provide the fastest and slowest separation times respectively.

5.5.2.2 Optimisation of CE separation in PEO

The same experiments as described for LPA-co-DHA were then repeated for PEO to see as we are able to compare the results. The results obtained are shown in Table 5-12.

Table 5-12 Results obtained from experimental design plan applied to PEO separation matrix.

Run	Polymer Concentration (%)	Injection Time (seconds)	Field Strength (Vcm^{-1})	Velocity ratio	Number of plates	Resolution
1	2.0	5	200	1.2083	287.13	0.8824
2	2.5	7	250	1.0273	25628.14	1.0926
3	3.0	6	275	1.1093	911.56	0.8250
4	3.0	5	250	1.1009	1084.75	0.8308
5	2.0	6	225	1.0699	2466.64	0.8679
6	2.5	6	300	1.1071	1746.32	1.1189
7	2.0	7	300	1.2455	273.44	1.0149
8	3.0	7	225	1.0365	25428.45	1.4551
9	2.5	5	275	1.1148	929.51	0.8750

The results are more complicated than seen previously with the LPA-co-DHA polymer. The best resolution was seen when the experimental parameters of a 7 second injection time, a polymer concentration of 3.0 % and an applied separation field of 225 Vcm^{-1} were implemented. Unlike the LPA-co-DHA model, which determined a field strength of 250 Vcm^{-1} was the most efficient separation field for separation. As described in Section 1.6, separation theory would suggest that a low electric field over a high electric field would provide the best separation. The results obtained would contradict this

theory, suggesting, like the LPA-co-DHA model, that the interaction between each of the variables significantly affects the separation capabilities.

Another anomaly seen with these results was that the larger injection time produced the better resolution, in the previous model it was determined that maintaining a low injection time was critical to producing a good resolution; however this was not seen with this model. The results in general seem to be unpredictable, with no discerning pattern forming after further analysis of the model.

5.5.2.2.1 Analysis and optimisation of results

As discussed with the LPA-co-DHA model in Section 5.5.2.1.1, a quadratic and cubic model were immediately discounted due to the obvious unsuitability stated in the initial summary. Analysis of the *Fit Summary* indicated that the 'Linear' model was the most suitable fit for the data, analysis of the '2FI' model also indicated it would be a suitable choice.

Table 5-13: Comparison of relevant data required to choose the best fit model.

	Linear	2FI
Prob-F	0.0496	0.8526
Standard Deviation	6613.87	8879.65
Adjustable R-Squared	0.6245	0.3232
PRESS	5.6470	1.4220

A linear model provides the lower probability of errors and PRESS values, although the standard deviation values for both models are extremely high, a further example of the unexpected nature of the results obtained. Further analysis of the model proved that the

2FI model was in fact unfeasible; due to the nature of the data certain analyses could not be performed, forcing the decision towards a linear model.

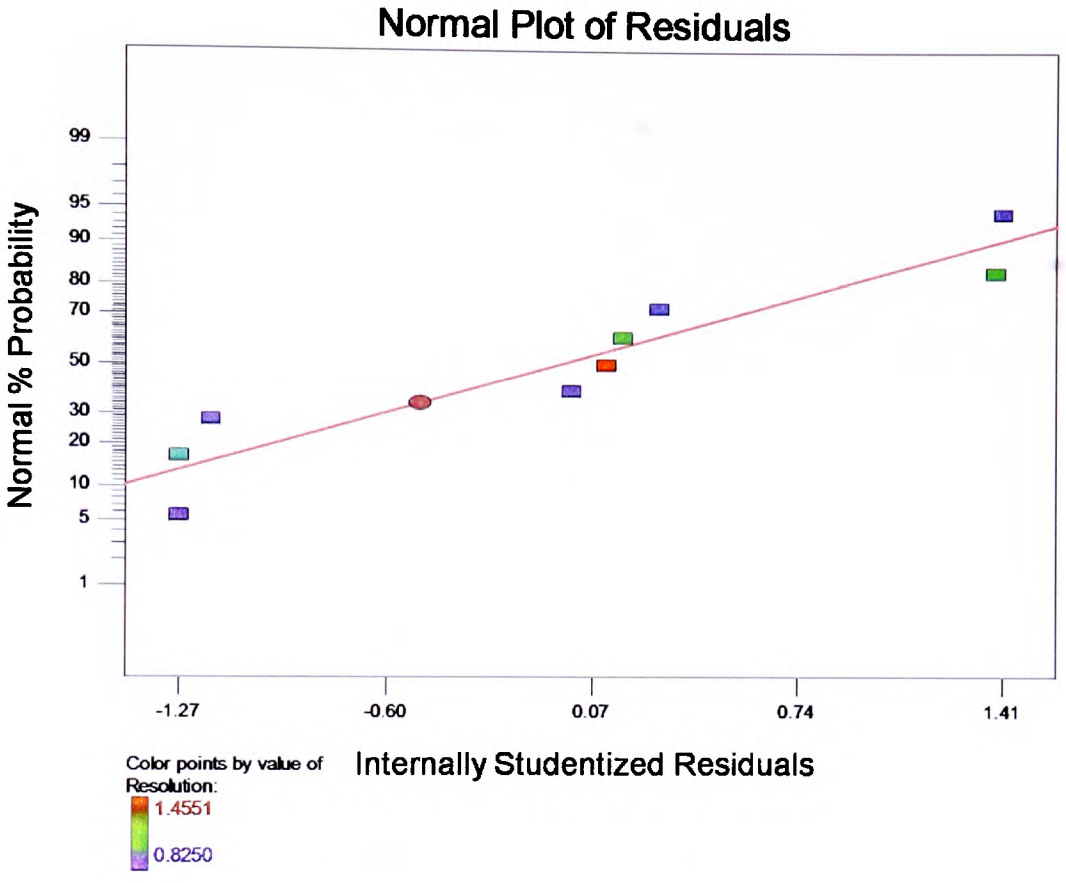

Figure 5-15 Analysis of the normal probability of studentised residuals for the linear model

The normal plot of residuals should ideally be a straight line, indicating no abnormalities, as is shown in Figure 5-15.

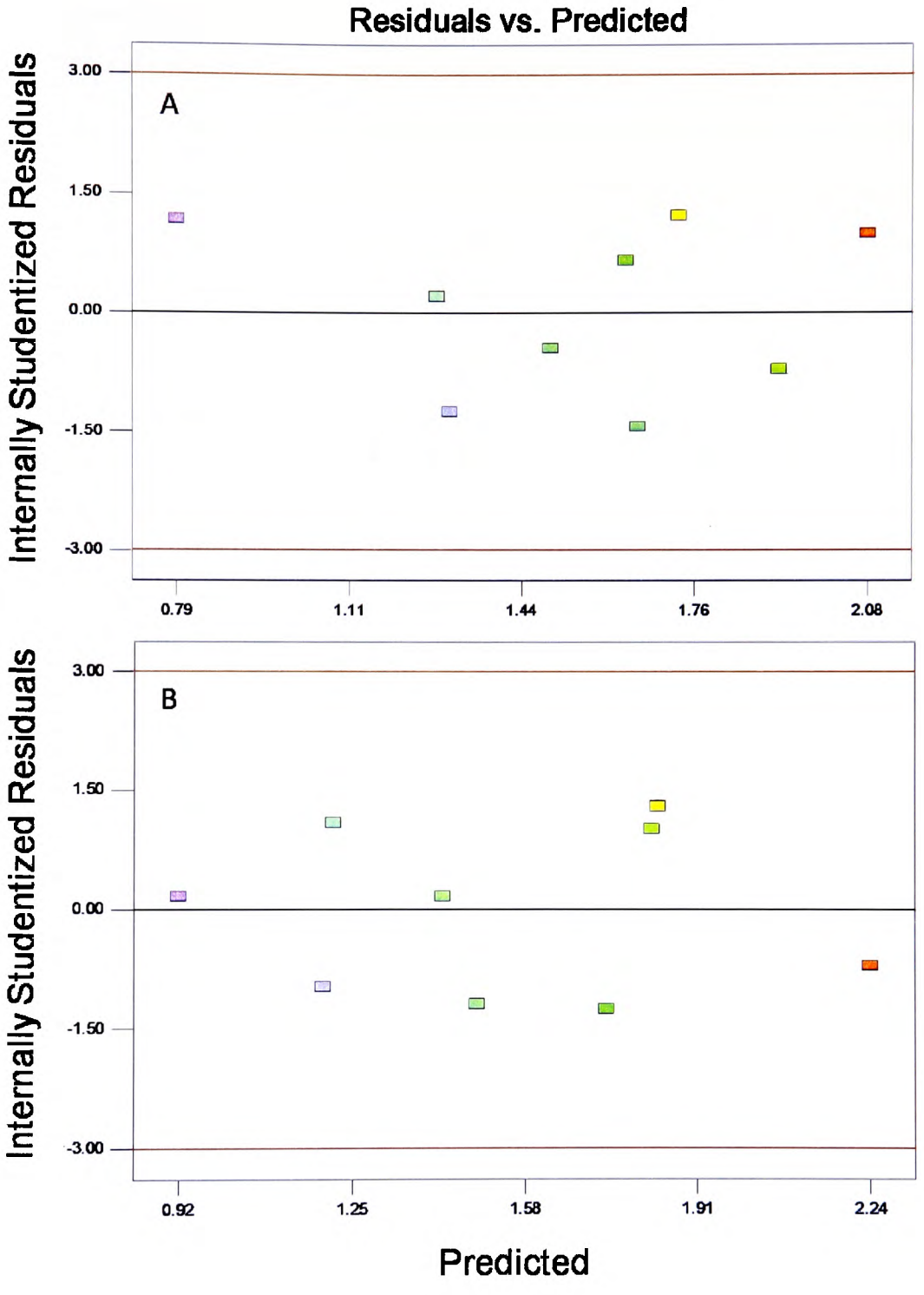

Figure 5-16: Analysis of the studentised residuals versus predicted values for A; the linear model, and B; the 2FI model

As explained previously, when analysing the studentised residuals versus predicted value plots, there should be an approximate even spread of the studentised residuals values across the plot, indicating independence to the corresponding predicted values. Again Figure 5-16 indicates both plots fulfil these criteria well, indicating both model types are performing within necessary parameters.

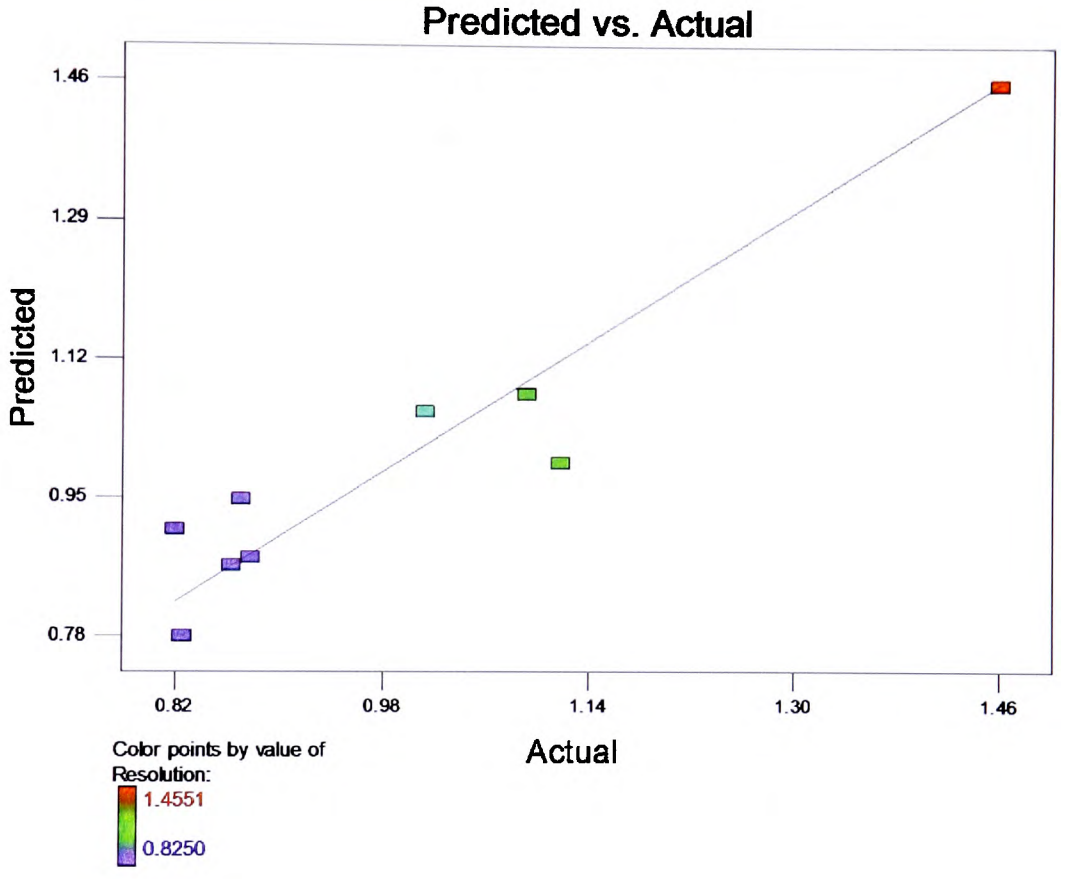

Figure 5-17 Analysis of the predicted versus actual results for the linear model

Figure 5-17 shows that the predicted versus actual plot does not follow the trend line well, with some points experiencing noticeable distance from the trend line. This model is the best option available; however, it is important to treat the results obtained carefully.

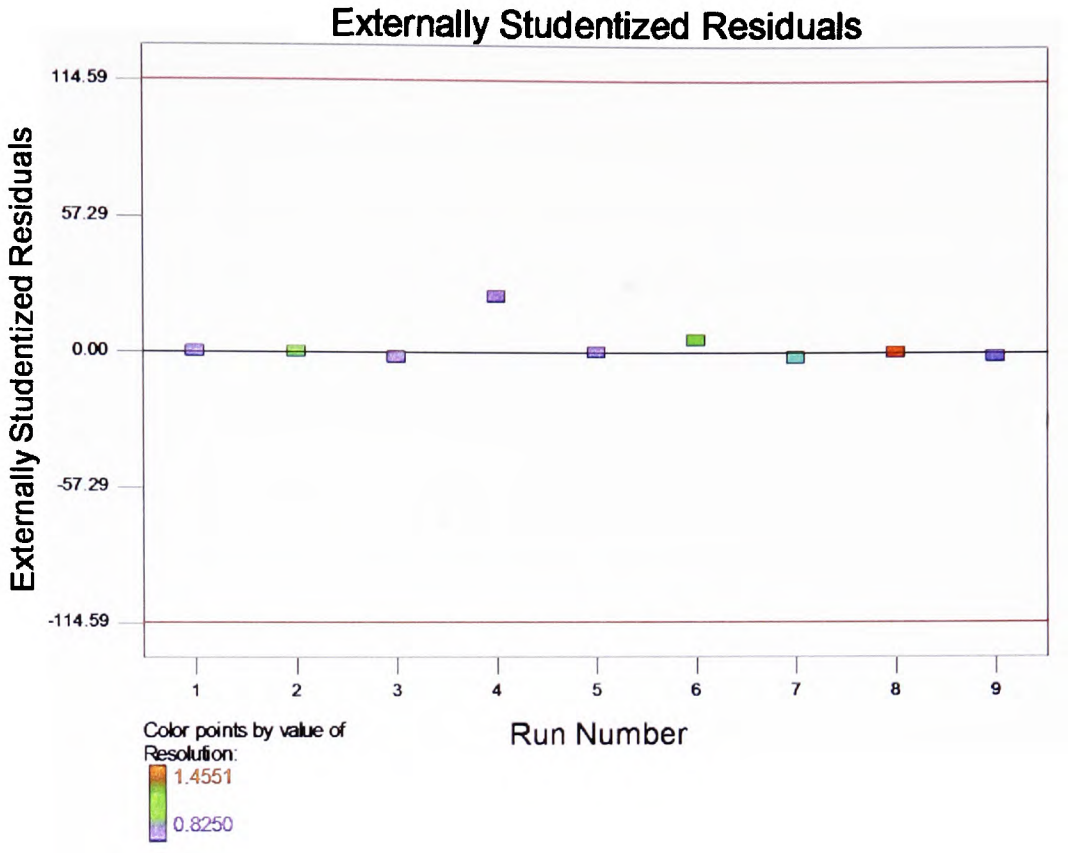

Figure 5-18 Analysis of the externally studentised residuals, otherwise known as the outlier T plot, for the linear model.

When analysing the externally studentised residuals plot, we are looking for points that fall outside the plus and minus 3.5 standard deviation limits, which are placed as red lines on the graphs. In this case, there are no outliers present identified, as seen in Figure 5-18, suggesting the model is suitable.

As stated previously, the F Value is a ratio of the sum of the squared residuals for terms in the model/ sum of the squares for the residuals, and is important for showing the relative contribution of the model variance to the residual variance. A large number indicates more of the variance being explained by the model; a small number says the variance may be more due to noise. In the model, Injection time has the highest F Value

of 0.71, indicating that altering the parameters of this factor will have the highest impact on the resolution. The factor that had the lowest F Value of 0.21 was polymer concentration, indicating the factor has a smaller impact on the resolution. However, these values are incredibly small, much smaller than seen with the previous model indicating the effect of each variable was difficult to determine due to the large variance seen in the data. This theory is further supported by analysis of the Prob>F values, as stated previously, a term that has a probability value less than 0.05 would be considered a significant effect, where as a value greater than 0.10 is generally regarded as not significant. For this model, each of the Prob>F values were significantly above 0.10, thus considered insignificant factors.

The equation, the model determined would predict the resolution of a separation at specific parameters is shown below;

$$\begin{aligned} Resolution = {} & -0.051009 + (0.13563 \times polymer\ conc.) \\ & - (0.86606 \times injection\ time) \\ & + (0.026222 \times field\ strength) \\ & + (0.40184 \times polymer\ conc. \times injection\ time) \\ & - (9.92779 \times 10^{-3} \times polymer\ conc. \\ & \times field\ strength) \\ & - (3.04128 \times 10^{-4} \times injection\ time \\ & \times field\ strength) \end{aligned} \qquad \textbf{Equation 5-13}$$

Injection time was the factor that produced the largest variation in resolution, after further analysis of the resulting model; however, it was found that the variation followed no discernable pattern. As can be seen in Figure 5-19, with increasing applied

field strength the positioning of the higher resolution alters dramatically, and not in a manner that can be easily predicted or explained.

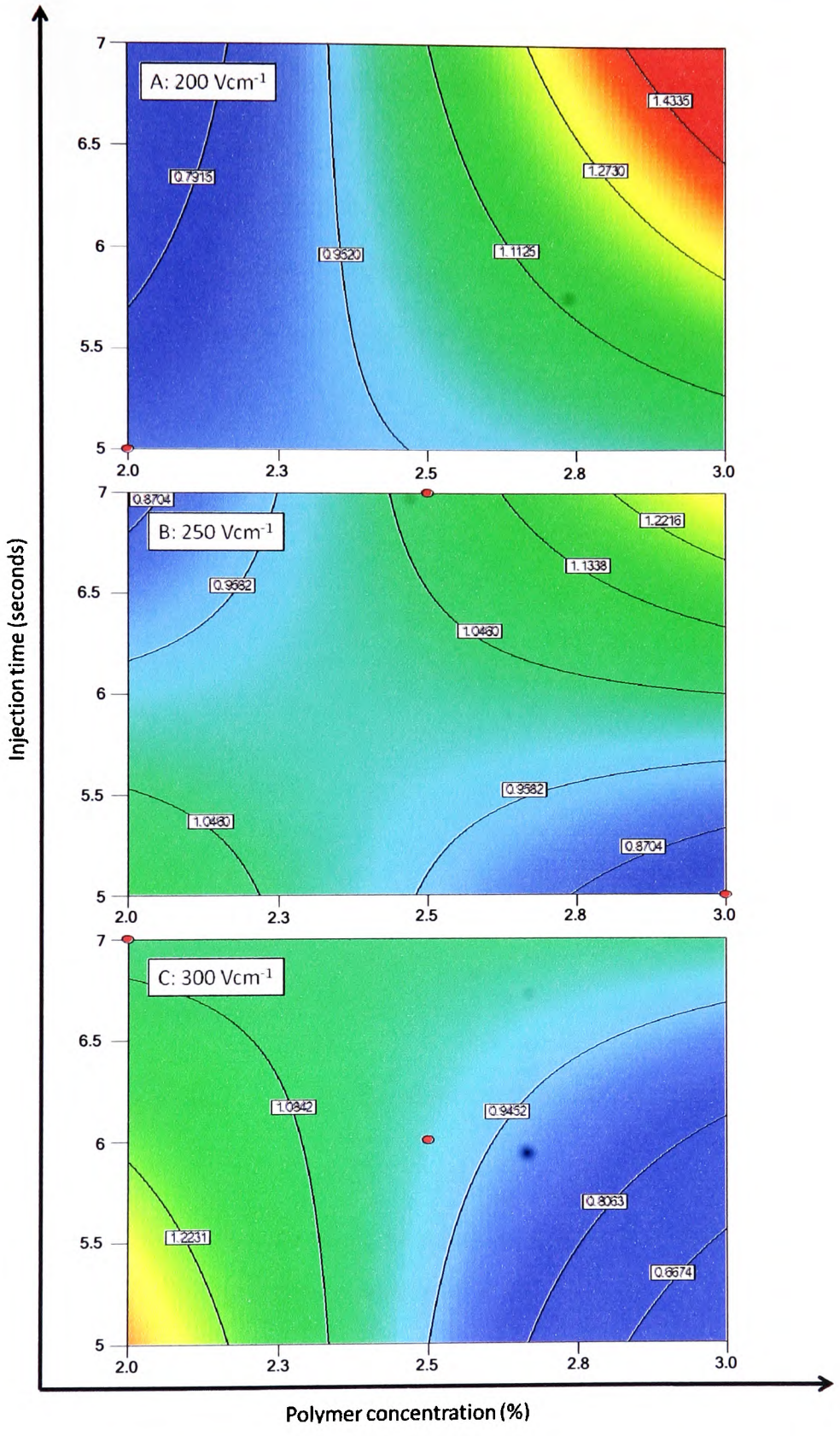

Figure 5-19 Contour plot displaying the impact on resolution with changing injection time and polymer concentration, at fixed field strengths of A; 200 Vcm^{-1}, B; 250 Vcm^{-1} and C; 300 Vcm^{-1}.

It can be seen in Figure 5-19, at 200 Vcm^{-1} a higher resolution is apparent at the higher injection time and higher polymer concentrations, at 250 Vcm^{-1} the higher resolution is seen in this range *as well* as at the opposite range of lowest injection time and lower polymer concentrations. At 300 Vcm^{-1} the last range provides the better resolution again, of lowest polymer concentration and injection time. These results are very contradictory to what you would expect and also in relation to each other.

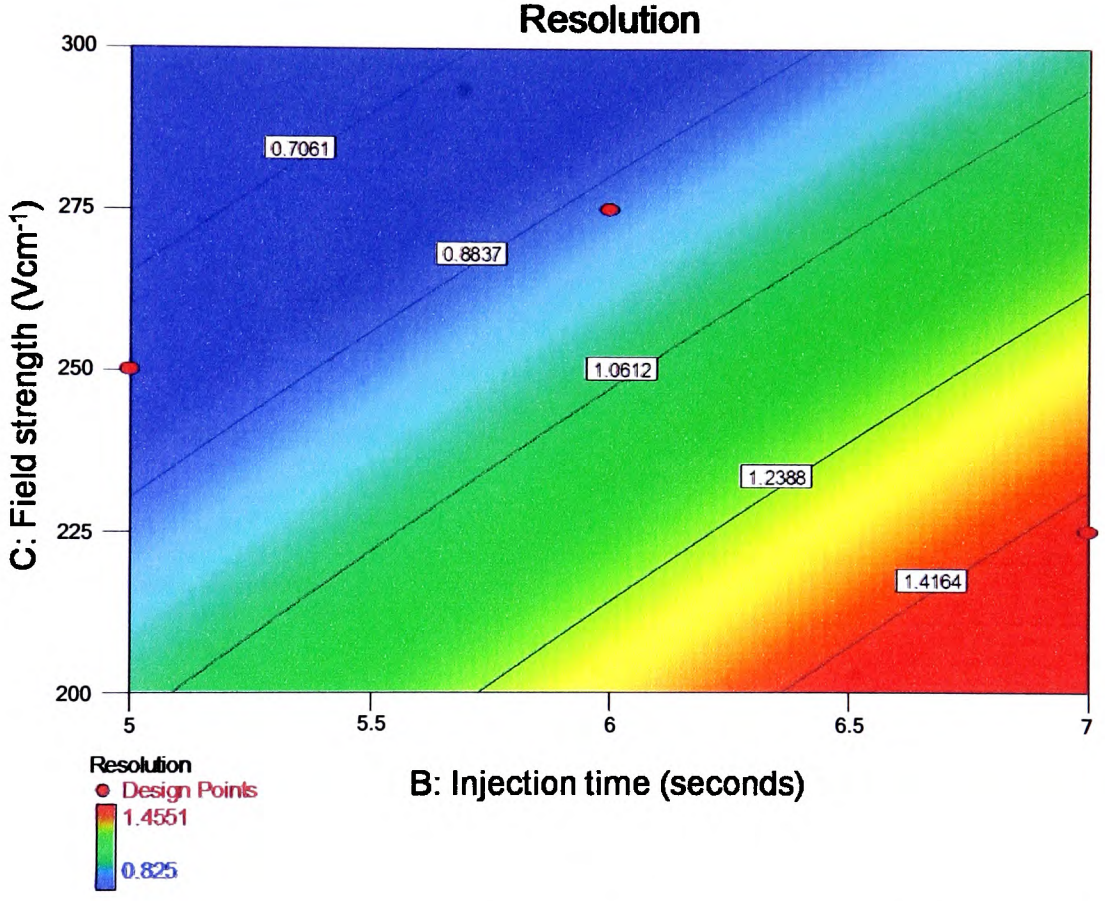

Figure 5-20: Contour plot displaying the impact on resolution with changing injection time and field strength, at a fixed polymer concentration of 3%

Again, a large degree of variation in optimum resolution was seen when comparing the injection time against field strengths at varying polymer concentrations, an example of which can be seen in Figure 5-20. The inconsistency in the data recorded makes

analysing the model effectively difficult, we cannot simply make the statement that one variable is the grater contributor and therefore should be fixed to a certain position as with the previous model.

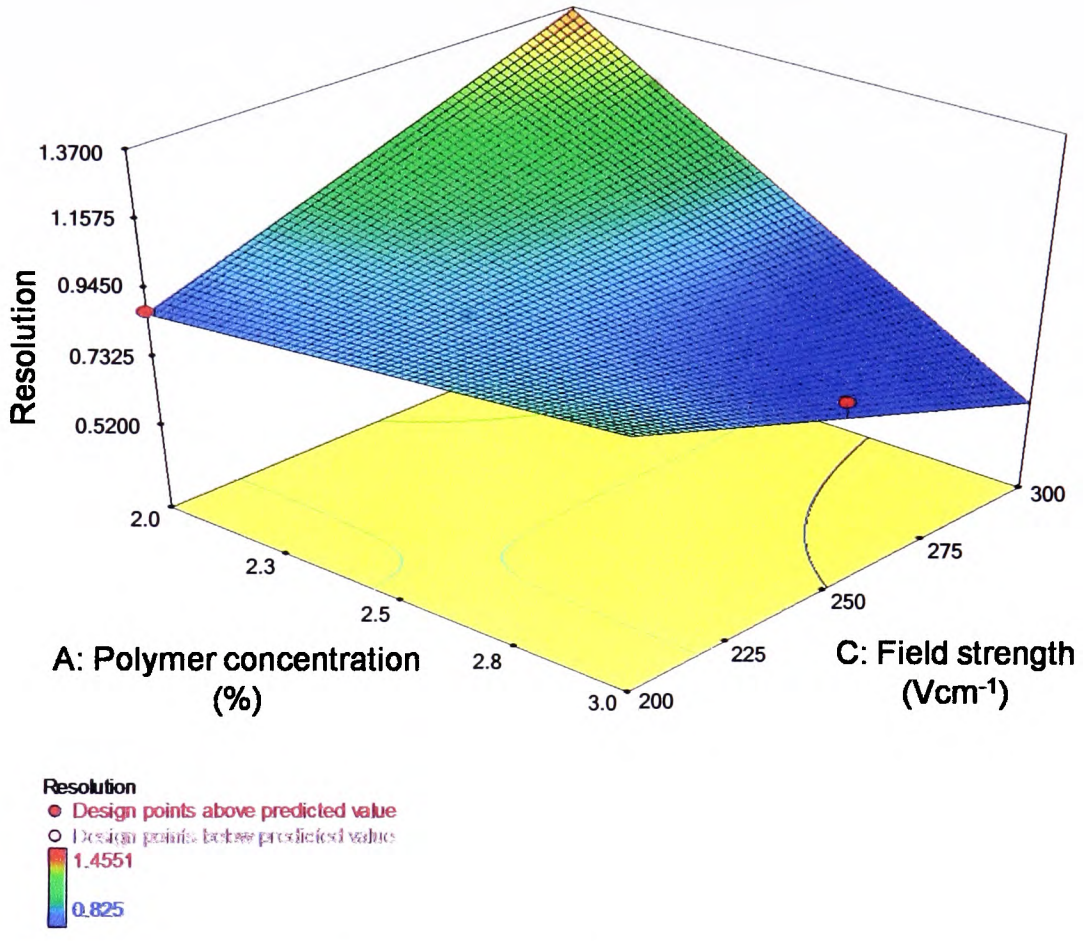

Figure 5-21: 3D contour plot displaying the interaction between polymer concentration and field strength, at a fixed injection time of 5 seconds.

Figure 5-21 depicts the resolution contour plot for varying polymer concentration and field strengths at a fixed injection time of 5 seconds; the graph indicates that the better resolution could be attained from the parameters of a polymer concentration of 2% and a field strength of 300 Vcm^{-1}.

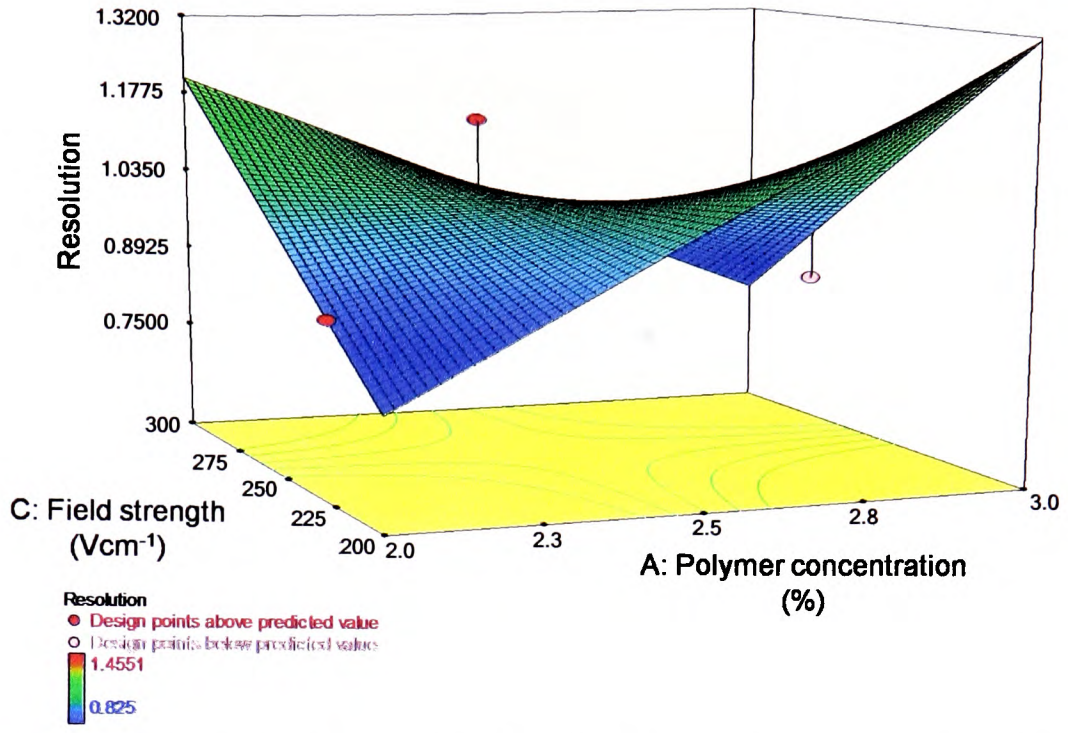

Figure 5-22: 3D contour plot displaying the interaction between polymer concentration and field strength, at a fixed injection time of 6 seconds.

Figure 5-22 depicts the resolution contour plot for varying polymer concentration and field strengths at a fixed injection time of 6 seconds; unlike for a 5 second injection (Figure 5-21) the graph indicates that the better resolution could be attained from the parameters of a polymer concentration of 3% and a field strength of 200 Vcm^{-1}. Although a good resolution could also be obtained from the optimum parameters identified in Figure 5-21, the difference in the contour plots would indicate a degree of uncertainty within the results.

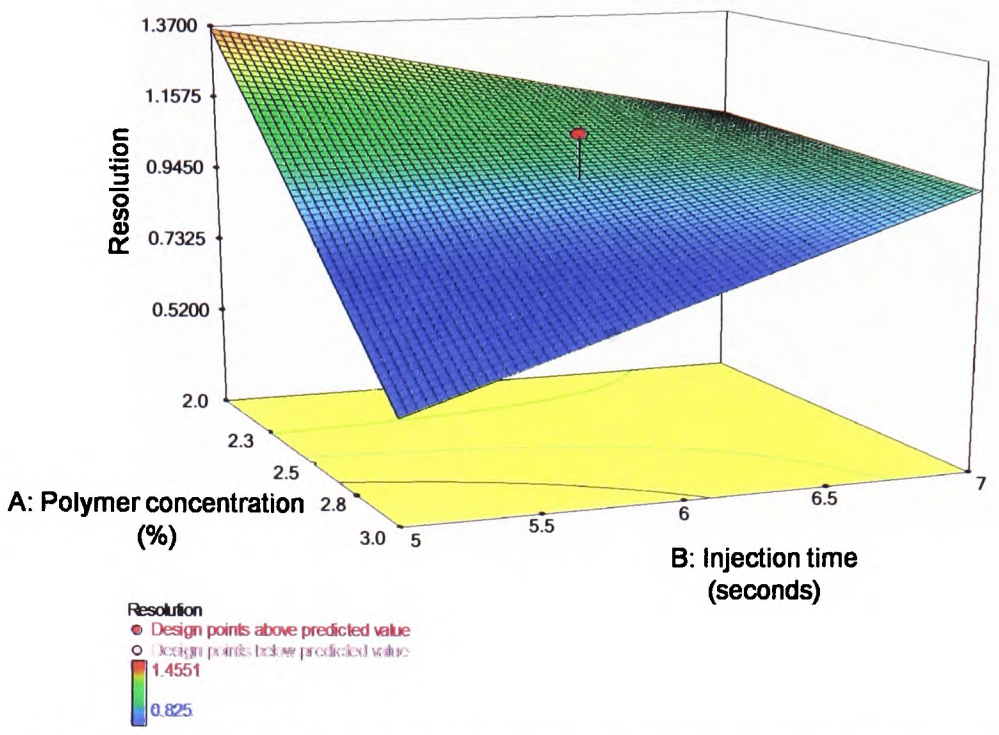

Figure 5-23: 3D contour plot displaying the interaction between polymer concentration and injection time, at fixed field strength of 300 Vcm^{-1}.

Figure 5-23 depicts the resolution contour plot for varying polymer concentration and injection times at a fixed field strength of 300Vcm^{-1}; the graph indicates that the better resolution could be attained from the parameters of a polymer concentration of 2% and an injection time of 5 seconds, contradicting the previous experiments (Figure 5-19 and Figure 5-20) which indicated an injection time of 7 seconds was preferential.

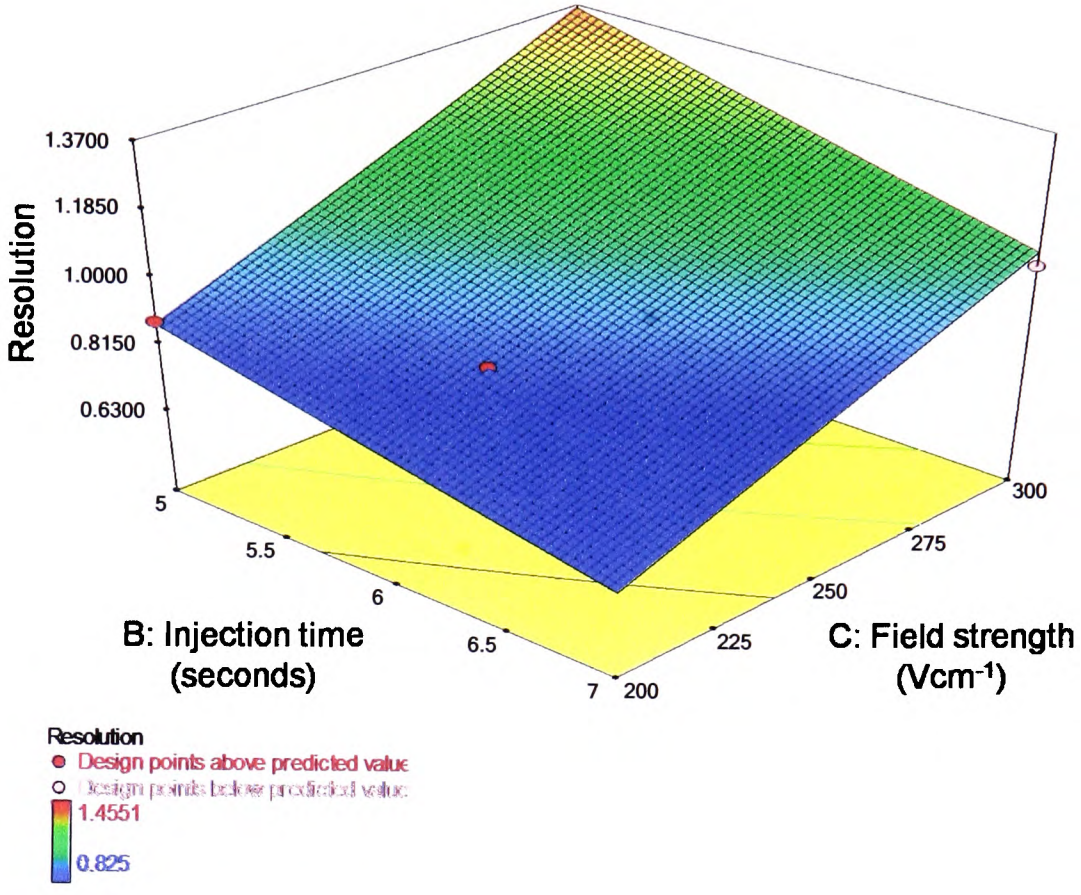

Figure 5-24: 3D contour plot displaying the interaction between injection time and field strength, at fixed polymer concentration of 2%.

Figure 5-24 depicts the resolution contour plot for varying injection time and field strength at a fixed polymer concentration of 2%; the graph indicates that the better resolution could be attained from the parameters of an injection time of 5 seconds and a field strength of 300 Vcm^{-1}.

In summary, the results displayed in Figure 5-19 to Figure 5-24, show very little consistency in indicating the optimum parameters suitable for a separation in a PEO polymer, indicating the unsuitability of a PEO polymer when trying to attain a reproducible and accurate separation of amplified DNA.

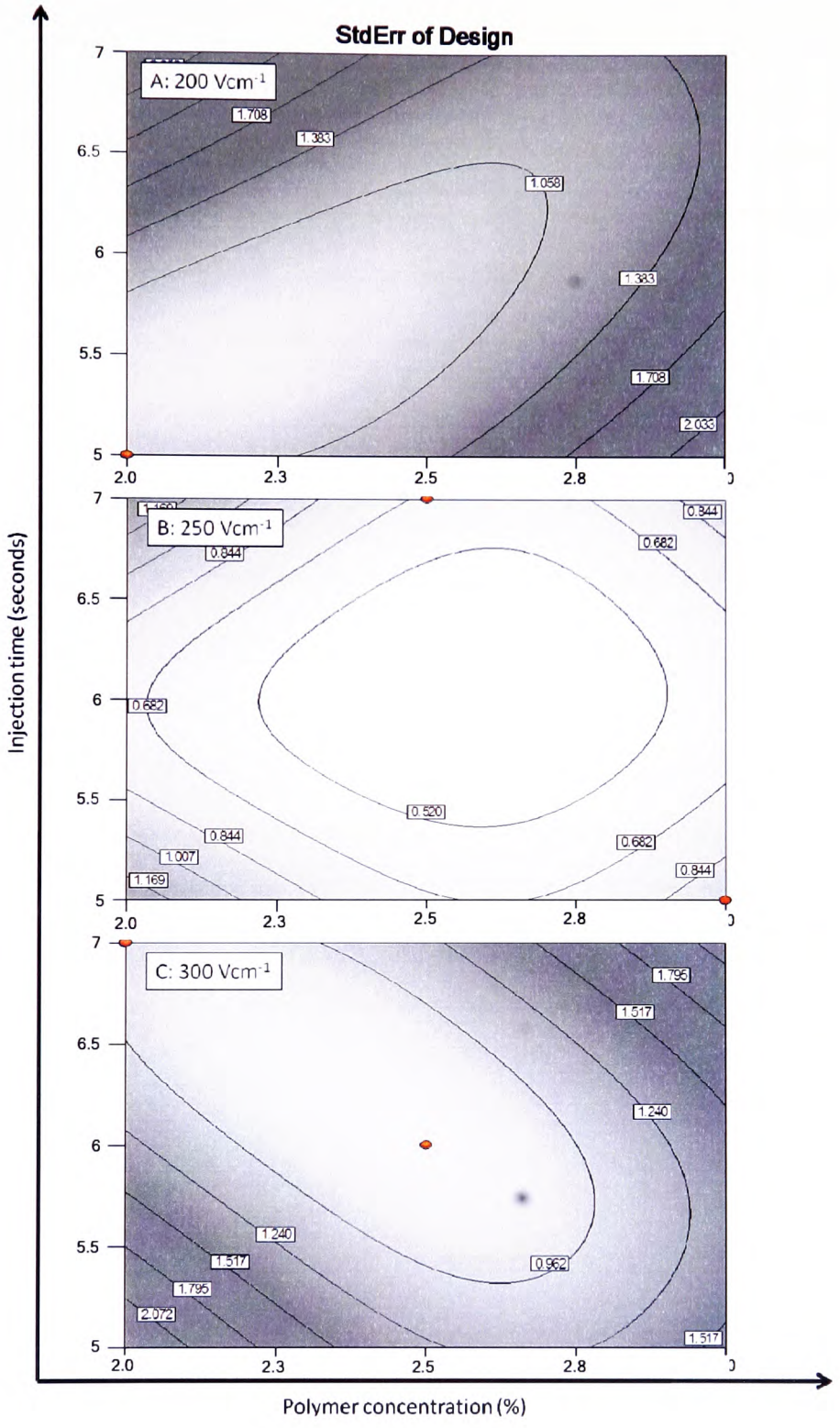

Figure 5-25: Contour plot displaying the values of the standard error in resolution as a respondent to interaction between polymer concentration and injection time, at a fixed field strength of A; 200 Vcm^{-1}, B; 250 Vcm^{-1} and C; 300 Vcm^{-1}.

The standard error contour plots displayed in Figure 5-25 would indicate that a mid range parameter set of a 250 Vcm^{-1} field strength, a 2.5% polymer concentration and an injection time of 6 seconds provides the lowest standard error in the experiment. Again these results are not conducive with the results provided by the contour plots, further highlighting how the separations performed in a PEO separation polymer do not provide consistent results and therefore it's the unsuitability.

5.6 Conclusions

This chapter has described the experimental design approach to optimisation of DNA separation by capillary electrophoresis. Of the many separation polymers investigated evidence has indicated that the LPA-co-DHA copolymer is the most effective at a achieving a good resolution, however, experiments indicate that single base pair resolution was not achieved and a further investigation is required.

Chapter 6: Conclusions

This thesis discusses the successful application of EOP through a gel supported reagent matrix, supported by a silica monolith which additionally acted as the extraction surface for DNA clean up and elution prior to PCR amplification. It was determined that PCR could successfully be performed in the specifically designed PCR reagent agarose gel, even after the application of an electric field of 100 Vcm^{-1}. Stability testing indicated that the agarose gel containing all the reagents necessary for PCR was stable for up to four weeks, when stored at 4°C.

Also discussed was the successful optimisation and application of a gel to gel electro-kinetic injection of a sample from a gel supported matrix into a polymer gel separation matrix. The work has identified the importance viscosity plays on a gel to gel system for electro-kinetic injections, compared to a solution injection, indicating much higher electric fields were required to achieve identical movement within a sample gel matrix. Interestingly, the opposite effect was noted when the viscosity of the separation gel was increased, the electric field required to clear excess sample from separation channel entrance was found to be much lower with the higher viscosity separation gel than the low viscosity separation gel.

Evidence of an increase in control and robustness for a gel supported injection over solution based introduction has been demonstrated. In addition, an interesting aspect of this work was that the presence of a bubble in the sample gel did not cause the problems of excess joule heating observed in sample solution based systems. Although bubbles did alter the pathway of the injection mechanism substantially, the robustness of the system allowed the current to still be maintained and an injection achieved. It is important to remember that if this disruption occurred in a solution only fluidic system, a break in the electric field would have severely compromised the injection process.

These results will support the development of a fully integrated portable gel based DNA analyser on a micro-fluidic device. The use of both applied voltages and gels leads to several advantages for integration including simplification of instrumentation with no need for moving parts and reduction of macro to micro interfacing and power requirements. The gels allow allows the storage of the reactants at the time of manufacture along with increasing the robustness of the EK injection.

Investigations undertaken indicate that the LPA-co-DHA copolymer is the separation matrix that would provide the best resolution, however the separation polymer is still highly viscous and the introduction into the micro-fluidic device difficult to achieve.

Future work

The results from this thesis are being combined with the other work on the project to develop a fully integrated system using follow on funding.

As discussed in this thesis, a successful integration of the sample introduction, clean up and PCR amplification was described, however a fully integrated process including injection, separation and detection was not achieved in the time allowed for this project. I would have liked to have completed the overall aim of the project which was to perform all processes on a single device, in a single experiment.

The preliminary research undertaken in the area of electro-kinetic injection into multiple channels demonstrated interesting and promising results. I would have liked to develop the preliminary research further, to gain better control of the injection volume and ensuring the quality of the injection by more accurately measuring the delivered samples in each channel. I would have also liked to complete the multi-channel

injection work process regarding the injection and separation of a known PCR product sample, completing the injection and separation process and producing parallel electropherograms for comparison. The possibility of developing in built repeats and validation into single use device's, reducing the volume of sample required, and also the preparation time and resources required to perform multiple analyses. The ability to run multiple analyses on one sample would provide the opportunity to expand the functionality of micro-fluidic devices extensively.

Another direction I would have liked to take the multi-channel electro-kinetic injection research in would be to investigate the possibility of performing a parallel injection from multiple sources into a single channel, in order to investigate the possibility of injecting the sizing ladder required during the separation process separately. As the introduction of the sizing ladder at the injection stage was a problem we never found a workable solution for, as it had to be introduced to the sample, and mixed prior to the injection stage. This work could have be expanded further to develop a series of injections between different processes and the sequential addition of different reagents as needed, such as a mixing stage that allowed you to inject the PCR product and inject the size ladder and the same time, mix it, and then inject the mixture into the separation channel or channels. Keeping the sizing ladder separately would be a huge benefit to the validity of the analysis, but was never fully considered during this project.

During the investigation of the optimisation of separation, the separation polymer was prepared and polymerised in a syringe, then pressure injected into the separation channel. Introducing the separation polymer into the separation channel by pressure injection increases the risk of fractures and density changes being introduced into the separation polymer. These inconsistencies and anomalies could alter or delay the natural

path of the PCR product, disrupting or distorting the actual separation and therefore the electropherogram. I would have liked to have explored the difference in separation efficiency and accuracy that could have been achieved using higher density separation media's, polymerised in the channel. It is thought that if the separation polymer had been polymerised inside the channel it would have reduced the risk of the described imperfections, and improve the quality and accuracy of the separations performed. Removing separation polymer that has been polymerised inside the channel is extremely difficult, and therefore is only really suitable for plastic single use chips, which was unavailable during this investigation.

1. Woodsand, R.; Foggo, D., Should Britain have a compulsory DNA database? The Sunday Times February 24, 2008.

2. Gill, P.; Jeffreys, A. J.; Werrett, D. J., Forensic Application of DNA Fingerprints. Nature 1985, 318, (6046), 577-579.

3. Butler, J. M., Genetics and genomics of core short tandem repeat loci used in human identity testing. Journal Of Forensic Sciences 2006, 51, (2), 253-265.

4. Saiki, R. K.; Gelfand, D. H.; Stoffel, S. J.; Higuchi, R.; Horn, G. T.; Mullis, K. B.; Erlich, H. A., Science 1988, 239, 487-491.

5. Moretti, T. R.; Baumstark, A. L.; Defenbaugh, D. A.; Keys, K. M.; Brown, A. L.; Budowle, B., Validation of STR typing by capillary electrophoresis. Journal of Forensic Sciences 2001, 46, (3), 661-676.

6. Bienvenue, J. M.; Duncalf, N.; Marchiarullo, D.; Ferrance, J. P.; Landers, J. P., Microchip-based cell lysis and DNA extraction from sperm cells for application to forensic analysis. Journal Of Forensic Sciences 2006, 51, (2), 266-273.

7. Obeid, P. J.; Christopoulos, T. K., Continuous-flow DNA and RNA amplification chip combined with laser-induced fluorescence detection. Analytica Chimica Acta 2003, 494, (1-2), 1-9.

8. Dittrich, P. S.; Manz, A., Single-molecule fluorescence detection in microfluidic channels - the Holy Grail in mu TAS? Analytical And Bioanalytical Chemistry 2005, 382, (8), 1771-1782.

9. Erickson, D.; Sinton, D.; Li, D. Q., A miniaturized high-voltage integrated power supply for portable microfluidic applications. Lab On A Chip 2004, 4, (2), 87-90.

10. Loughran, M.; Cretich, M.; Chiari, M.; Suzuki, H., Separation of DNA in a versatile microchip. Sensors And Actuators B-Chemical 2005, 107, (2), 975-979.

11. Grover, W. H.; Skelley, A. M.; Liu, C. N.; Lagally, E. T.; Mathies, R. A., Monolithic membrane valves and diaphragm pumps for practical large-scale integration into glass microfluidic devices. Sensors And Actuators B-Chemical 2003, 89, (3), 315-323.

12. Du, X. G.; Fang, Z. L., Static adsorptive coating of poly(methyl methacrylate) microfluidic chips for extended usage in DNA separations. Electrophoresis 2005, 26, (24), 4625-4631.

13. Huang, F. C.; Liao, C. S.; Lee, G. B., An integrated microfluidic chip for DNA/RNA amplification, electrophoresis separation and on-line optical detection. Electrophoresis 2006, 27, (16), 3297-3305.

14. Lagally, E. T.; Emrich, C. A.; Mathies, R. A., Fully integrated PCR-capillary electrophoresis microsystem for DNA analysis. Lab On A Chip 2001, 1, (2), 102-107.

15. Lagally, E. T.; Mathies, R. A., Integrated genetic analysis microsystems. Journal Of Physics D-Applied Physics 2004, 37, (23), R245-R261.

16. Vilkner, T.; Janasek, D.; Manz, A., Micro total analysis systems. Recent developments. Analytical Chemistry 2004, 76, (12), 3373-3385.

17. Zhang, C. S.; Xu, J. L.; Ma, W. L.; Zheng, W. L., PCR microfluidic devices for DNA amplification. Biotechnology Advances 2006, 24, (3), 243-284.

18. Zhang, C. S.; Xing, D.; Li, Y. Y., Micropumps, microvalves, and micromixers within PCR microfluidic chips: Advances and trends. Biotechnology Advances 2007, 25, (5), 483-514.

19. Truong, T. Q.; Nguyen, N. T., A polymeric piezoelectric micropump based on lamination technology. Journal of Micromechanics and Microengineering 2004, 14, (4), 632-638.

20. Jeong, O. C.; Konishi, S., Fabrication of a peristaltic micro pump with novel cascaded actuators. Journal of Micromechanics and Microengineering 2008, 18, (2).

21. Vandepol, F. C. M.; Vanlintel, H. T. G.; Elwenspoek, M.; Fluitman, J. H. J., A THERMOPNEUMATIC MICROPUMP BASED ON MICRO-ENGINEERING TECHNIQUES. Sensors and Actuators a-Physical 1990, 21, (1-3), 198-202.

22. Liu, R. H.; Bonanno, J.; Yang, J. N.; Lenigk, R.; Grodzinski, P., Single-use, thermally actuated paraffin valves for microfluidic applications. Sensors And Actuators B-Chemical 2004, 98, (2-3), 328-336.

23. West, J.; Karamata, B.; Lillis, B.; Gleeson, J. P.; Alderman, J.; Collins, J. K.; Lane, W.; Mathewson, A.; Berney, H., Application of magnetohydrodynamic actuation to continuous flow chemistry. Lab on a Chip 2002, 2, (4), 224-230.

24. Liu, R. H.; Yang, J. N.; Lenigk, R.; Bonanno, J.; Grodzinski, P., Self-contained, fully integrated biochip for sample preparation, polymerase chain reaction amplification, and DNA microarray detection. Analytical Chemistry 2004, 76, (7), 1824-1831.

25. Guttenberg, Z.; Muller, H.; Habermuller, H.; Geisbauer, A.; Pipper, J.; Felbel, J.; Kielpinski, M.; Scriba, J.; Wixforth, A., Planar chip device for PCR and hybridization with surface acoustic wave pump. Lab on a Chip 2005, 5, (3), 308-317.

26. Nie, F. Q.; Macka, M.; Barron, L.; Connolly, D.; Kent, N.; Paull, B., Robust monolithic silica-based on-chip electro-osmotic micro-pump. Analyst 2007, 132, (5), 417-424.

27. Gui, L.; Ren, C. L., Numeric simulation of heat transfer and electrokinetic flow in an electroosmosis-based continuous flow PCR chip. Analytical Chemistry 2006, 78, (17), 6215-6222.

28. Reichmuth, D. S.; Chirica, G. S.; Kirby, B. J., Increasing the performance of high-pressure, high-efficiency electrokinetic micropumps using zwitterionic solute additives. Sensors and Actuators B-Chemical 2003, 92, (1-2), 37-43.

29. Kuo, C. T.; Liu, C., A novel microfluidic driver via AC electrokinetics. Lab on a Chip 2008, 8, 725-733.

30. Grossman, P. D.; Colburn, J. C., Capillary Electrophoresis Theory and practice, Academic Press, Inc. 1992 112.

31. Revermann, T.; Gotz, S.; Kunnemeyer, J.; Karst, U., Quantitative analysis by microchip capillary electrophoresis - current limitations and problem-solving strategies. Analyst 2008, 133, (2), 167-174.

32. Baba, Y.; Tsuhako, M., Gel-Filled Capillaries for Nucleic-Acid Separations in Capillary Electrophoresis. Trac-Trends in Analytical Chemistry 1992, 11, (8), 280-287.

33. Gui, L.; Ren, C. L., Analytical and numerical study of joule heating effects on electrokinetically pumped continuous flow PCR chips. Langmuir 2008, 24, (6), 2938-2946.

34. Hu, G. Q.; Xiang, Q.; Fu, R.; Xu, B.; Venditti, R.; Li, D. Q., Electrokinetically controlled real-time polymerase chain reaction in microchannel using Joule heating effect. Analytica Chimica Acta 2006, 557, (1-2), 146-151.

35. Belder, D.; Ludwig, M.; Wang, L. W.; Reetz, M. T., Enantioselective catalysis and analysis on a chip. Angewandte Chemie-International Edition 2006, 45, (15), 2463-2466.

36. Kim, D. K.; Kang, S. H., On-channel base stacking in microchip capillary gel electrophoresis for high-sensitivity DNA fragment analysis. Journal Of Chromatography A 2005, 1064, (1), 121-127.

37. Blaze, R. G.; Kumaresan, P.; Mathies, R. A., Microfabricated bioprocessor for integrated nanoliter-scale Sanger DNA sequencing. Proceedings Of The National Academy Of Sciences Of The United States Of America 2006, 103, (19), 7240-7245.

38. Cruces-Blanco, C.; Gamiz-Gracia, L.; Garcia-Campana, A. M., Applications of capillary electrophoresis in forensic analytical chemistry. Trac-Trends in Analytical Chemistry 2007, 26, (3), 215-226.

39. Easley, C. J.; Karlinsey, J. M.; Bienvenue, J. M.; Legendre, L. A.; Roper, M. G.; Feldman, S. H.; Hughes, M. A.; Hewlett, E. L.; Merkel, T. J.; Ferrance, J. P.; Landers, J. P., A fully integrated microfluidic genetic analysis system with sample-in-answer-out

capability. Proceedings of the National Academy of Sciences of the United States of America 2006, 103, (51), 19272-19277.

40. Leach, A. M.; Wheeler, A. R.; Zare, R. N., Flow injection analysis in a microfluidic format. Analytical Chemistry 2003, 75, (4), 967-972.

41. Zhang, L.; Yin, X. F.; Fang, Z. L., Negative pressure pinched sample injection for microchip-based electrophoresis. Lab On A Chip 2006, 6, (2), 258-264.

42. Leong, J. C.; Tsai, C. H.; Fu, L. M., Design of high resolution analysis technique for capillary electrophoresis microchip. Japanese Journal of Applied Physics 2007, 46, (10A), 6865-6870.

43. Heller, C., Principles of DNA separation with capillary electrophoresis. Electrophoresis 2001, 22, (4), 629-643.

44. Woolley, A. T.; Mathies, R. A., Ultra-High-Speed Dna Fragment Separations Using Microfabricated Capillary Array Electrophoresis Chips. Proceedings Of The National Academy Of Sciences Of The United States Of America 1994, 91, (24), 11348-11352.

45. Woolley, A. T.; Mathies, R. A., Ultra-High-Speed Dna-Sequencing Using Capillary Electrophoresis Chips. Analytical Chemistry 1995, 67, (20), 3676-3680.

46. Schmalzing, D.; Koutny, L.; Adourian, A.; Belgrader, P.; Matsudaira, P.; Ehrlich, D., DNA typing in thirty seconds with a microfabricated device. Proceedings Of The National Academy Of Sciences Of The United States Of America 1997, 94, (19), 10273-10278.

47. Wu, D. P.; Qin, J. H.; Lin, B. C., Electrophoretic separations on microfluidic chips. Journal of Chromatography A 2008, 1184, (1-2), 542-559.

48. Wenclawiak, B. W.; Puschl, R., Sample injection for capillary electrophoresis on a micro fabricated device/on chip CE injection. Analytical Letters 2006, 39, (1), 3-16.

49. Tsai, C. H.; Yang, R. J.; Tai, C. H.; Fu, L. M., Numerical simulation of electrokinetic injection techniques in capillary electrophoresis microchips. Electrophoresis 2005, 26, (3), 674-686.

50. Breadmore, M., Recent advances in enhancing the sensitivity of electrophoresis and electrochromatography in capillaries and microchips. Electrophoresis 2007, 28, (1-2), 254-281.

51. Xu, Y.; Zhang, C. X.; Janasek, D.; Manz, A., Sub-second isoelectric focusing in free flow using a microfluidic device. Lab On A Chip 2003, 3, (4), 224-227.

52. Prest, J. E.; Baldock, S. J.; Day, P. J. R.; Fielden, P. R.; Goddard, N. J.; Brown, B. J. T., Miniaturised isotachophoresis of DNA. Journal of Chromatography A 2007, 1156, 154-159.

53. Zalewski, D. R.; Schlautmann, S.; Schasfoort, R. B. M.; Gardeniers, J. G. E., Electrokinetic sorting and collection of fractions for preparative capillary electrophoresis on a chip. Lab on a Chip 2008, 8, (5), 801-809.

54. Lee, C. H.; Hsiung, S. K.; Lee, G. B., A tunable microflow focusing device utilizing controllable moving walls and its applications for formation of micro-droplets in liquids. Journal of Micromechanics and Microengineering 2007, 17, (6), 1121-1129.

55. Goedecke, N.; McKenna, B.; El-Difrawy, S.; Gismondi, E.; Swenson, A.; Carey, L.; Matsudaira, P.; Ehrlich, D. J., Microdevice DNA forensics by the simple tandem repeat method. Journal Of Chromatography A 2006, 1111, (2), 206-213.

56. Kang, K. H.; Kang, Y. J.; Xuan, X. C.; Li, D. Q., Continuous separation of microparticies by size with direct current-dielectrophoresis. Electrophoresis 2006, 27, (3), 694-702.

57. Soper, S. A.; Stryjewski, W.; Zhu, L.; Xu, Y.; Wabuyele, M.; Chen, H. W.; Galloway, M.; McCarley, R. L., Polymer-based modular microsystems for DNA sequencing. Conference on Miniaturized Chemical and Biochemical Analysis Systems 2003, 717-720.

58. Janasek, D.; Schilling, M.; Franzke, J.; Manz, A., Isotachophoresis in free-flow using a miniaturized device. Analytical Chemistry 2006, 78, (11), 3815-3819.

59. Chen, R.; Luo, X.; Di, X.; Li, Y.; Sun, Y.; Hu, Y., Single-based resolution for oligodeoxynucleotides and their phosphorothioate modifications by replaceable capillary gel electrophoresis. Journal of Chromatography B 2006, 843, 334-338.

60. Viovy, J. L., Electrophoresis of DNA and other polyelectrolytes: Physical mechanisms. Reviews of Modern Physics 2000, 72, (3), 813-872.

61. Slater, G. W.; Kenward, M.; McCormick, L. C.; Gauthier, M. G., The theory of DNA separation by capillary electrophoresis. Current Opinion in Biotechnology 2003, 14, (1), 58-64.

62. Duong, T. T.; Kim, G.; Ros, R.; Streek, M.; Schmid, F.; Brugger, J.; Anselmetti, D.; Ros, A., Size-dependent free solution DNA electrophoresis in structured microfluidic systems. Microelectronic Engineering 2003, 67-8, 905-912.

63. Minc, N.; Futterer, C.; Gosse, C.; Dorfman, K. D.; Viovy, J. L., Fast separation of long DNA in a microchip. Conference on Miniaturized Chemical and Biochemical Analysis Systems 2003, 1311-1314.

64. Doyle, P. S.; Bibette, J.; Bancaud, A.; Viovy, J. L., Self-assembled magnetic matrices for DNA separation chips. Science 2002, 295, (5563), 2237-2237.

65. Buel, E.; LaFountain, M.; Schwartz, M.; Walkinshaw, M., Evaluation of capillary electrophoresis performance through resolution measurements. Journal of Forensic Sciences 2001, 46, (2), 341-345.

66. Ekstrom, P. O.; Bjorheim, J., Evaluation of sieving matrices used to separate alleles by cycling temperature capillary electrophoresis. Electrophoresis 2006, 27, (10), 1878-1885.

67. Paegel, B. M.; Emrich, C. A.; Weyemayer, G. J.; Scherer, J. R.; Mathies, R. A., High throughput DNA sequencing with a microfabricated 96-lane capillary array electrophoresis bioprocessor. Proceedings Of The National Academy Of Sciences Of The United States Of America 2002, 99, (2), 574-579.

68. Liang, D. H.; Song, L. G.; Zhou, S. Q.; Zaitsev, V. S.; Chu, B., Poly(N-isopropylacrylamide)-g-poly(ethyleneoxide) for high resolution and high speed separation of DNA by capillary electrophoresis. Electrophoresis 1999, 20, (14), 2856-2863.

69. Zhou, P.; Yu, S. B.; Liu, Z. H.; Hu, J. M.; Deng, Y. Z., Electrophoretic separation of DNA using a new matrix in uncoated capillaries. Journal Of Chromatography A 2005, 1083, (1-2), 173-178.

70. Fung, E. N.; Pang, H. M.; Yeung, E. S., Fast DNA separations using poly(ethylene oxide) in non-denaturing medium with temperature programming. Journal of Chromatography A 1998, 806, (1), 157-164.

71. Wu, C. H.; Liu, T. B.; Chu, B., Viscosity-adjustable block copolymer for DNA separation by capillary electrophoresis. Electrophoresis 1998, 19, (2), 231-241.

72. Zhang, J.; Wang, Y. M.; Liang, D. H.; Ying, Q. C.; Chu, B., Association behavior of PDMA-g-PMMA in mixed solvents and its application as a DNA separation medium. Macromolecules 2005, 38, (5), 1936-1943.

73. Zhang, J.; He, W. D.; Liang, D. H.; Fang, D. F.; Chu, B.; Gassmann, M., Designing polymer matrix for microchip-based double-stranded DNA capillary electrophoresis. Journal Of Chromatography A 2006, 1117, (2), 219-227.

74. Hjerten, S., High-Performance Electrophoresis - Elimination of Electroendosmosis and Solute Adsorption. Journal of Chromatography 1985, 347, (2), 191-198.

75. Handique, K.; Burke, D. T.; Mastrangelo, C. H.; Burns, M. A., Nanoliter Liquid Metering in Microchannels Using Hydrophobic Patterns. Analytical Chemistry 2000, 72, (17), 4100-4109.

76. Gillmor, D. S., 2nd Annual IEEE-EMBS Special Topic Conf. on Microtechnologies in Medicine and Biology (Madison, WI, USA) 2002, 51-56.

77. Badal, M. Y.; Wong, M.; Chiem, N.; Salimi-Moosavi, H.; Harrison, D. J., Protein separation and surfactant control of electroosmotic flow in poly(dimethylsiloxane)-coated capillaries and microchips. Journal of Chromatography A 2002, 947, (2), 277-286.

78. Ertl, P.; Emrich, C. A.; Singhal, P.; Mathies, R. A., Capillary electrophoresis chips with a sheath-flow supported electrochemical detection system. Analytical Chemistry 2004, 76, (13), 3749-3755.

79. Chen, H.; Zhou, M.; Jin, X. Y.; Song, Y. M.; Zhang, Z. Y.; Ma, Y. J., Chemiluminescence determination of ultramicro DNA with a flow-injection method. Analytica Chimica Acta 2003, 478, (1), 31-36.

80. Butler, J. M., FORENSIC DNA TYPING, Elsevier (USA). 2005; p 329.

81. Zhu, L.; Stryjewski, W.; Lassiter, S.; Soper, S. A., Fluorescence multiplexing with time-resolved and spectral discrimination using a near-IR detector. Analytical Chemistry 2003, 75, (10), 2280-2291.

82. Zhu, L.; Stryjewski, W. J.; Soper, S. A., Multiplexed fluorescence detection in microfabricated devices with both time-resolved and spectral-discrimination capabilities using near-infrared fluorescence. Analytical Biochemistry 2004, 330, (2), 206-218.

83. Gotz, S.; Karst, U., Recent developments in optical detection methods for microchip separations. Analytical and Bioanalytical Chemistry 2007, 387, (1), 183-192.

84. Wang, S. L.; Fan, X. F.; Xu, Z. R.; Fang, Z. L., A simple microfluidic system for efficient capillary electrophoretic separation and sensitive fluorimetric detection of

DNA fragments using light-emitting diode and liquid-core waveguide techniques. Electrophoresis 2005, 26, (19), 3602-3608.

85. Yao, B.; Yang, H.; Liang, Q.; Ren, K.; Gao, Y.; Wang, Y.; Qiu, Y., High-Speed, Whole-Column Fluorescence Imaging, Detection for Isoelectric Focusing on a Microchip, Using an Organic Light Emitting Diode as Light Source. Analytical Chemistry 2006, 78, (16), 5845-5850.

86. Hanning, A.; Lindberg, P.; Westberg, J.; Roeraade, J., Laser induced fluorescence detection by liquid core waveguiding applied to DNA sequencing by capillary electrophoresis. Analytical Chemistry 2000, 72, (15), 3423-3430.

87. Karger, A. E.; Harris, J. M.; Gesteland, R. F., Multiwavelength Fluorescence Detection for DNA Sequencing Using Capillary Electrophoresis. Nucleic Acids Research 1991, 19, (18), 4955-4962.

88. Lee, D. S.; Chang, B. H.; Chen, P. H., Development of a CCD-based fluorimeter for real-time PCR machine. Sensors And Actuators B-Chemical 2005, 107, (2), 872-881.

89. Invitrogen Quant-iT™ PicoGreen ® dsDNA Reagent and Kits; June 2008.

90. Xu, F.; Jabasini, M.; Baba, Y., Screening of mixed poly(ethylene oxide) solutions for microchip separation of double-stranded DNA using an orthogonal design approach. Electrophoresis 2005, 26, (15), 3013-3020.

91. Chiesl, T. N.; Putz, K. W.; Babu, M.; Mathias, P.; Shaikh, K. A.; Goluch, E. D.; Liu, C.; Barron, A. E., Self-associating block copolymer networks for microchip

electrophoresis provide enhanced DNA separation via "inchworm" chain dynamics. Analytical Chemistry 2006, 78, (13), 4409-4415.

92. Young, R. J.; Lovell, P. A., Introduction to polymers. Second ed.; Chapman and Hall: 1991.

93. Haswell, S. J., Development and operating characteristics of micro flow injection analyisis systems based on electroosmotic flow. Analyst 1997, 122, 1R-10R.

94. Haswell, S. J., Development and Operating Characteristics of Micro Flow Injection Analysis Systems Based on Electroosomotic Flow. Analyst 1997, 122, 1R-10R.

95. Qu, Q. S.; Tang, X. Q.; Wang, C. Y.; Yang, G. J.; Hu, X. Y.; Lu, X.; Liu, Y.; Yan, C., Preparation of particle-fixed silica monoliths used in capillary electrochromatography. Journal Of Separation Science 2006, 29, (13), 2098-2102.

96. Al-Lawati, H.; Watts, P.; Welham, K. J., Efficient protein digestion with peptide separation in a micro-device interfaced to electrospray mass spectrometry. Analyst 2006, 131, (5), 656-663.

97. Shaw, K. J.; Joyce, D. A.; Docker, P. T.; Dyer, C. E.; Greenman, J.; Greenway, G. M.; Haswell, S. J., Simple practical approach for sample loading prior to DNA extraction using a silica monolith in a microfluidic device. Lab On A Chip 2009, 9, (23), 3430-3432.

98. http://www1.gelifesciences.com/. (Date accessed August 2009)

99. http://www.spartanbio.com. (Date accessed August 2009)

100. Butler, J. M.; Ruitberg, C. M.; Vallone, P. M., Capillary electrophoresis as a tool for optimization of multiplex PCR reactions. Fresenius Journal of Analytical Chemistry 2001, 369, (3-4), 200-205.

101. Fredlake, C. P.; Hert, D. G.; Kan, C. W.; Chiesl, T. N.; Root, B. E.; Forster, R. E.; Barron, A. E., Ultrafast DNA sequencing on a microchip by a hybrid separation mechanism that gives 600 bases in 6.5 minutes. Proceedings of the National Academy of Sciences of the United States of America 2008, 105, (2), 476-481.

102. Liu, Y.; Kuhr, W. G., Separation of Double- and Single-Stranded DNA Restriction Fragments: Capillary Electrophoresis with Polymer Solutions under Alkaline Conditions. Analytical Chemistry 1999, 71, (9), 1668-1672.

103. Heller, C., Separation of double-stranded and single-stranded DNA in polymer solutions: I. Mobility and separation mechanism. Electrophoresis 1999, 20, (10), 1962-1977.

104. Heller, C., Separation of double-stranded and single-stranded DNA in polymer solutions: II. Separation, peak width and resolution. Electrophoresis 1999, 20, (10), 1978-1986.

105. Butler, J. M., Forensic DNA Typing. Elsevier 2005, Page 318.

106. Paegel, B. M.; Hutt, L. D.; Simpson, P. C.; Mathies, R. A., Turn geometry for minimizing band broadening in microfabricated capillary electrophoresis channels. Analytical Chemistry 2000, 72, (14), 3030-3037.